

Integrated optics and new wave phenomena in optical waveguides

P. K. Tien

Bell Telephone Laboratories, Holmdel, New Jersey 07733

Research in integrated optics has two goals: One is to apply thin-film technology to the formation of optical devices and circuits. The other is the integration of a large number of optical devices on a small substrate, so forming an optical circuit reminiscent of the integrated circuit in microelectronics. The result is a new breed of optical devices in the form of miniature optical waveguides. They include lasers, modulators, switches, detectors, prisms, lenses, and polarizers, and many of them have efficiencies better than their bulk counterparts. Simple integrated optical circuits have also been constructed, and rapidly advancing semiconductor technology indicates that monolithic integrated optical circuits can readily be developed using GaAs-related compounds. In this paper, we review the state-of-the-art of integrated optics and explore new wave phenomena in optical circuits. The specific topics to be discussed are: light-wave couplers and m -line spectroscopy, refraction and reflection of light in thin films, normal modes of the uniform, the graded and the metal-clad waveguides, optics in tapered films, theory of corrugated waveguides, and more importantly, physics of various thin-film optical devices and the method of the circuit formation.

CONTENTS

I. Introduction and Historical Development	361
A. Historical development	361
B. Research in integrated optics	364
II. Optics in Waveguides and Couplers	365
A. Waveguides and the rule of refractive index	365
B. Waveguide and radiation modes	366
C. Ray optics and zigzag waves	368
D. Prism couplers and m -line spectroscopy	371
E. Grating coupler and corrugated waveguides	373
F. Uniform and graded waveguides	374
G. The potential-well model of the waveguide and WKB method	375
III. Tapered-Film Waveguides and Research in Thin-Film Prisms, Lenses, and Circuit Formation	377
A. Tapered-film waveguides and tapered transitions	377
B. Two-dimensional optics and the Goos-Haenchen shift	378
C. Two-layered construction, light-guiding interconnections in optical circuits, and the potential-well model of the composite waveguides	379
D. Thin-film prisms, lenses, and other passive optical components	381
E. Directional couplers and branching waveguides	382
F. Tapered-film light wave couplers and the cutoff property of the waveguide	384
G. Metal-clad waveguides and method of isolating high-index substrates	386
IV. Periodic Waveguides, Monolithic Integrated Optical Circuits, and Research in Thin-Film Lasers, Modulators, and Switches	387
A. Periodic structures in optical waveguides	387
B. Bragg-reflector lasers and distributed feedback lasers	391
C. Al-Ga-As DFB and BR laser diodes	395
D. Thin-film optical modulators, switches, and beam deflectors	397
E. (Al,Ga)As technology and monolithic integrated optical circuits	401
V. Conclusions and Remarks	407
Acknowledgments	408
References	408

I. INTRODUCTION AND HISTORICAL DEVELOPMENT

A. Historical development

For hundreds of years, the basic design of optical systems has not been changed; they have consisted of bulky

and heavy components which required careful alignment and protection against vibration, moisture, and temperature drift. In an effort to make them more compatible with modern technology, *integrated optics* came into being in the early 1970's (Tien *et al.*, 1969; Miller, 1969; Tien, 1971, 1974; Miller, Marcatili and Li, 1973; Taylor and Yariv, 1974; Chang *et al.*, 1974; Kogelnik, 1975; Suematsu, 1975; Blum, 1975; Conwell, 1976). At that time, the availability of low-loss optical fibers had already brought new dimensions to optical communication (Kapron *et al.*, 1970; Keck *et al.*, 1973), and there was a surge of interest in compact optical systems. One started the research in integrated optics by exploring a series of new ideas. The first idea was to apply thin-film technology to form optical devices and circuits. The idea is attractive, since thin-film technology has already dominated the electronics industry. It was found that a thin layer of dielectric film which has a refractive index larger than that of the surroundings is a perfect optical waveguide. The next idea was then the use of such waveguides as the basic structures of all the optical components including lasers, modulators, detectors, prisms, lenses, polarizers, and couplers. The transmission of a light wave from one optical component to another becomes a problem of interconnecting two waveguides. The use of guided light waves in thin films instead of Gaussian beams in space has placed integrated optics closer to microwave technology than to geometrical optics. The third idea, which naturally followed, was to deposit many thin-film optical components on a common substrate to form a complete integrated optical circuit. With all of the components solidly bonded to the substrate, the problems of vibration and alignment are minimized. Moreover, the vision of a medium-scale or even a large-scale integration of an optical system is definitely inspiring.

Guided-wave optics and thin-film technology are, therefore, the two basic elements of integrated optics. Initially, one thought of forming optical circuits by simply extending the technology of microelectronics. However, optical wavelengths are on the order of 10^6 times smaller than uhf (ultra high frequency) radio waves, and

it soon became obvious that new materials and new methods of construction are needed for optical circuits. Fortunately, light-wave couplers (Tien *et al.*, 1969, 1970, 1975; Harris and Shubert, 1969, 1971; Ulrich, 1970, 1971, 1973; Harris *et al.*, 1970, 1971; Midwinter, 1970; Iogansen, 1962; Dakss *et al.*, 1970; Kogelnik and Sosnowski, 1970; Hope, 1972; Dalgoutte, 1973; Tien and Martin, 1971) were invented; and by means of them, one can couple a laser beam efficiently into a thin film for studying waveguide modes and testing new optical materials. At the beginning, even the simple experiment of propagating a light wave in a thin film was not easy. Because of the roughness of the film surface, the light wave did not propagate very far in the film before it was completely scattered. We remember when a sputtered ZnO film was first used as an optical waveguide (Tien *et al.*, 1969); it had a loss of more than 60 dB/cm and we only observed a light path less than 1-mm long in the film. Soon, waveguides made of glass (Goell and Standley, 1969, 1970; Goell *et al.*, 1970) and those of polymerized organosilicon films (Tien *et al.*, 1972) had losses less than 1 dB/cm (Fig. 1). In the past six years waveguides have been formed in various materials by different processes (Tien and Ballman, 1975) which include reactive sputtering (Tien *et al.*, 1969; Hensler *et al.*, 1971; Gia Russo and Kumar, 1973; Takada *et al.*, 1974; Westwood and Ingrey, 1975; Quinn *et al.*, 1975; Shuskus *et al.*, 1974), vacuum evaporation (Tien, 1971), ion implantation (Wei *et al.*, 1973, 1975; Barnoski *et al.*, 1974), proton bombardment (Schineller *et al.*, 1968; Standley *et al.*, 1972; Garmire *et al.*, 1972; Barnoski *et al.*, 1973; Somekh *et al.*, 1973; Stoll *et al.*, 1973), ion migration (Izawa and Nakagome, 1972; Shah, 1975), solution deposition (Shubert and Harris, 1968; Ulrich and Weber, 1972), polymerization by gas discharge (Tien *et al.*, 1972), and by exposure in uv light (Ostrowsky and Jacques, 1971; Weber *et al.*, 1972; Tomlinson and Weber, 1975), and more importantly, diffusion (Taylor *et al.*, 1972; Martin and Hall, 1972; Kaminow and Carruthers, 1973; Carruthers *et al.*, 1974; Hammer and Philips, 1974; Schmidt and Kaminow, 1974; Noda *et al.*, 1974; Standley and Ramaswamy, 1974; Garmire, 1975; Chinn *et al.*, 1975; Minakata *et al.*, 1975; Ramaswamy and Standley, 1975), and various methods of epitaxy (Hall *et al.*, 1970; Tien *et al.*, 1972; Cho and Reinhart, 1972; Ballman *et al.*, 1973, 1975; Rand and Standley, 1972; Hammer *et al.*, 1972; Goell, 1973; Garmire, 1973; Tracy *et al.*, 1973; Logan and Reinhart, 1973; Tien *et al.*, 1974; Miyazawa, 1973; Wolfe *et al.*, 1974; Reinhart *et al.*, 1974; Miyazawa *et al.*, 1975; Kondo *et al.*, 1975; Ralston *et al.*, 1975; Fox *et al.*, 1975; Kahn, 1970; Ramaswamy, 1972; Chang, 1971; Kleinknecht, 1974; Tsand and Wang, 1976; Boetz *et al.*, 1976; Merz and Cho, 1976; Merz *et al.*, 1976; Tensen *et al.*, 1975).

Imagine an integrated optical circuit such as the one illustrated in Fig. 2. It consists of many optical components which are themselves waveguides and are interconnected by waveguides. The light wave in the circuit may be visualized as a surface wave which propagates along the two-dimensional plane of the film. Since the fields in each waveguide must satisfy the boundary conditions, there is a set of the normal modes that a wave-

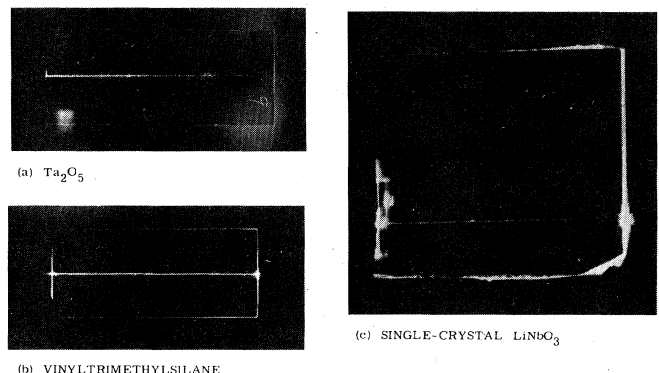


FIG. 1. Photographs (a), (b), and (c) show light wave propagation observed in a Ta_2O_5 , a vinyltrimethylsilane, and a single-crystal LiNbO_3 film waveguide. The losses in these waveguides are 1, 0.1, and 1 dB/cm, respectively.

guide can accommodate and the light wave can propagate in any of those normal modes. By assigning one channel of the information to each normal mode, an integrated optical circuit has the capability of carrying many channels of the information simultaneously. Each normal mode will be represented by an eigenvector in the plane of the film with an eigenvalue β .

The essence of integrated optics is that we deal with surface waves and their optics in the two-dimensional plane of the film. Early in 1969, a modified Snell's law was formulated to explain refraction of light observed between waveguides (Tien and Ulrich, 1970; Tien and Martin, 1971), and by applying this law, thin-film prisms, lenses, and other passive optical components were invented (Ulrich and Tien, 1969; Shubert and Harris, 1970; Ulrich and Martin, 1971; Righini *et al.*, 1972; Tien *et al.*, 1974, 1975; Harper and Spiller, 1974, 1975; Verber *et al.*, 1976). Another impor-

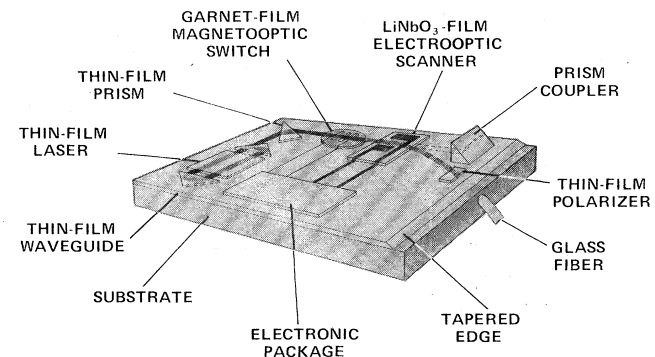


FIG. 2. Historically, we thought an integrated optical circuit should contain all sorts of optical devices such as the one shown above. The devices are made of thin films and they are interconnected by thin-film waveguides. However, as integrated optics developed, we realized that such circuits are difficult to fabricate. We now believe that a circuit should have only two or three different kinds of devices, although we can have a large number of them in each kind. For example, a circuit containing a large number of laser diodes and waveguides can satisfy most of our needs.

tant development also started at that time was the use of diffraction gratings in various optical components. A grating is simply a corrugated surface which may be formed either on the top surface or at the film-substrate interface of a waveguide. The waveguides containing gratings are called corrugated waveguides, or simply, periodic structures. The use of gratings for reflecting light in waveguides was first proposed by Miller (1969). Soon, one found the possibility of using gratings for coupling light waves into waveguides (Dakss *et al.*, 1970; Kogelnik and Sosnowski, 1970). Then in 1971, Kogelnik and Shank proposed the use of corrugated waveguides as laser cavities, and they demonstrated a dye laser based on this principle. They called this type of laser *distributed feedback laser*. Their idea was immediately extended to form Bragg-reflector lasers (Kaminow *et al.*, 1971; Wang, 1974). Lately, diffraction gratings are also used to form band rejection filters, electro-optic deflectors and mode-order converters. The initial success of these thin-film devices set integrated optics on a solid foundation.

The use of semiconductor *p-n* junction diodes for modulation of light dates back to the early sixties. For example, Nelson and Reinhart reported light modulation in reversely biased GaP junctions in 1964. Recently, Reinhart and Miller (1973) have built efficient modulators in AlGaAs/GaAs/AlGaAs double heterostructures. In addition to the activities in AlGaAs alloy compounds, Tien *et al.* (1972, 1974) reported a magneto-optic switch which involved an iron-garnet film as the optical waveguide. The film they used was originally developed for magnetic bubble devices. Between 1972 and 1975, single-crystal LiNbO₃ films which have large electro-optic and acousto-optic constants were formed by eight different methods. Never before has a single material obtained so much attention from material scientists. Those methods include out-diffusion of Li (Kaminow and Carruthers, 1973; Carruthers *et al.*, 1974); in-diffusion of Nb (Hammer and Philips, 1974; Ramaswamy and Standley, 1975), Cu (Noda *et al.*, 1974), and transition metals (Schmidt and Kaminow, 1974); epitaxial growth by melting (Ballman *et al.*, 1975; Tien *et al.*, 1974; Miyazawa, 1973) and that through flux (Ballman *et al.*, 1975; Miyazawa *et al.*, 1975; Kondo *et al.*, 1975); reactive sputtering (Gia Russo *et al.*, 1973; Takada *et al.*, 1974); ion exchange (Shah, 1975), and ion implantation (Wei *et al.*, 1975). More importantly, intensive research has produced thin-film magneto-optic, electro-optic, and acousto-optic devices (Tien *et al.*, 1972, 1974; Schmidt and Kaminow, 1975; Kogelnik and Schmidt, 1976; Noda *et al.*, 1975; Kaminow *et al.*, 1974, 1975; Tien *et al.*, 1974) which are simple to construct, convenient to operate, and in most cases, more efficient than their bulk counterparts.

At present, research in integrated optics is geared to optical communication. So far, there are three semiconductor diode lasers which can be operated in continuous wave at room temperature, and naturally, these are candidates for light sources in future optical communication systems. One is the well-known AlGaAs/GaAs/AlGaAs double heterostructure laser which radiates near 0.89 μm, in the near infrared (Alferov *et al.*, 1970; Pansh *et al.*, 1969). The other two are still in

the research stage involving AlGaAsSb/GaAsSb/AlGaAsSb (Nahory *et al.*, 1976) and InP/GaInPAs/InP (Hsieh, 1976) heterostructures, respectively. They radiate between 1.0 and 1.3 μm in the wavelength region where glass fibers used for optical communication have a minimum of dispersion and transmission losses (for a comprehensive review of semiconductor laser studies, see Panish, 1976). Because of this advanced semiconductor technology developed in laser research, one naturally thought of forming monolithic integrated optical circuits including waveguides, detectors, modulators, and lasers using Al-Ga-As or other III-V alloy compounds. In such semiconductor circuits, *p-n* junctions and heterostructures are often used as waveguides to construct modulators and lasers. It was discovered in the early sixties, that a *p-n* junction can guide a light wave quite efficiently (Bond *et al.*, 1963; Yariv and Leite, 1963; Kressel and Nelson, 1969). The plasma contribution to the refractive index of a semiconductor, such as GaAs, decreases with increasing electron concentration. When a *p-n* junction is reversely biased, electrons are swept out of the depletion region, which becomes a high refractive index waveguiding layer. Since the refractive index also decreases with increasing Al concentration in the Al-Ga-As system, a better waveguide can be formed by using a heterostructure which consists of a GaAs *p-n* junction sandwiched between two layers of the low-index Al-Ga-As. As of today, these *p-n* junction and heterostructure waveguides have been formed by epitaxial growth, diffusion, doping, and ion-implantation. Modulators made of AlGaAs heterostructures have efficiencies comparable to the LiNbO₃ devices (Reinhart and Miller, 1972; McKenna and Reinhart, 1976). Distributed feedback lasers built in the similar heterostructures have recently been demonstrated for room-temperature and continuous-wave operation (Nakamura *et al.*, 1975; Casey, Jr. *et al.*, 1975).

In spite of the intensive research in GaAs and related alloy compounds since the sixties, new technological advancement continues to emerge. First, as mentioned previously, the work of Nakamura *et al.* (1975) and that of Casey, Jr. *et al.* (1975) has demonstrated that efficient DFB lasers can be formed in the AlGaAs system. Next, the method of preferential etching has been applied by Logan and Reinhart (1973) to form channel waveguides, and by Comerford and Zory (1974) to form corrugated waveguides in GaAs. Following their work, one discovered that waveguides and lasers could be grown inside the preferentially etched channels by liquid phase epitaxy. The technique is called "embedded epitaxy" by Lee *et al.* (1976), "etched buried structure" by Burnham and Scifres (1975), and "etch and fill" by Boetz *et al.* and by Tsang and Wang (1975). Since then, preferential etching and selective growth have become important techniques in integrated optics (see discussion in Sec. IV. E. Third, Tsukada (1974) demonstrated the possibility of confining the light wave and the carriers both vertically and laterally by using a buried heterostructure, thus improving efficiency of the diode laser. Fourth, the pioneering work of Arthur and Cho (Arthur, 1968; Cho, 1971; Cho and Arthur, 1975) has made molecular beam epitaxy competitive to the liquid phase

epitaxy. Finally, by introducing a wedge in the well which contains the GaAs melt, R. A. Logan developed a new technique in the liquid phase epitaxy to form films with tapered edges and those of variable compositions (Reinhart and Logan, 1975; Merz *et al.*, 1975; Logan and Reinhart, 1975). Mainly because of these activities in semiconductor technology and the continued improvement in photolithographic technique to form submicron structures, we are convinced more than ever that a medium-scale integration of optical circuit is possible.

We should also point out several new techniques which can be used to assemble thin-film components into an optical circuit. It was discovered in 1973 that it is possible to interconnect two waveguides by simply tapering the edges of the films and overlapping them to form a smooth junction. Tapered films or tapered edges of waveguides have since played an important role in various forms of circuit construction (Tien and Martin, 1971; Tien *et al.*, 1973, 1974, 1975; Reinhart and Logan, 1974, 1975; Logan and Reinhart, 1975; Merz *et al.*, 1975). Another important technique is the isolation of low-index devices from a high-index substrate (Ostrowsky *et al.*, 1973; Tien *et al.*, 1975). Active devices such as lasers and modulators are made of epitaxial or diffused layers which require single-crystal substrates. These substrates have high refractive indices ranging from $n=2.0$ to 3.6, and are not suitable for forming low-index passive devices, typically with $n=1.49-1.9$. The idea is to cover a part of the substrate surface by an isolating layer of metallic or low-index dielectric film so that the active devices are formed directly on the substrate, while the passive devices are formed on the isolating layer.

Some simple integrated optical circuits have also been constructed. For example: in 1973 Ostrowsky *et al.* formed a circuit on a silicon substrate, which contains a glass waveguide and a silicon photodetector; Martin (1975) formed an optical switch coupled to a branching waveguide by diffusing Cd into a ZnSe substrate; Reinhart and Logan (1975) reported a monolithic AlGaAs circuit which involves a laser coupled to a modulator through a tapered-film coupler. Very recently, Schmidt (1976) described a 4×4 switching network formed by diffusing Ti into LiNbO₃ substrate. Finally, Aiki *et al.* reported an excellent AlGaAs circuit for frequency multiplexing which contains six diode lasers and waveguides (1976).

B. Research in integrated optics

The purpose of this paper is tutorial; it reviews the present status of integrated optics. For problems involving dielectric waveguides, a direct application of Maxwell's equations is often cumbersome. For example, a simple thin-film waveguide involves two interfaces and coupled waveguides involve four interfaces; a large number of simultaneous equations are thus required to describe the boundary conditions. To simplify the calculation, several models of guided-wave optics have been developed, such as the lenslike medium (for example, Tien *et al.*, 1956), the zigzag waves (Tien

et al., 1969; Tien and Ulrich, 1970; Tien, 1971), and the analogy between light waves in waveguides and electrons trapped in potential wells (Tien, 1974). Those models are by no means rigorous, but they do provide an insight into a complex problem, and, more importantly, many of the important inventions in integrated optics were developed from those models.

Most of the discussion in this paper deals with inventions that restructure bulk optical devices into thin-film components. The possibility of forming those familiar optical devices, such as prisms, lenses, modulators, and lasers, in thin films, has fascinated many. Moreover, the thin-film geodesic lenses recently reported by Verber (1976) are capable of focusing a light beam to the diffraction limit and of resolving light beams with an angular separation as small as 3.3 mrad. The strip-waveguide modulator built by Kaminow, *et al.*, (1975) has a merit constant, $1.7 \mu\text{W}/\text{MHz}$, which is several orders of magnitude better than those of the earlier bulk devices.

We have shown earlier that devices used in integrated optics are made of waveguides, *p-n* junctions and heterostructures. In those structures, the film, which is used to carry the light wave, has a thickness on the order of one optical wavelength; the waveguides have thus the usual *transverse electric* (TE) and *transverse magnetic* (TM) modes with discrete eigenvalues. The waveguides used in integrated optics appear in two basic forms: channel waveguides and film-waveguides. In the channel waveguides, light wave propagation is confined within the channel and the wave phenomenon resembles that in microwave circuits. The channel waveguides are typically a few microns wide. The film-waveguides are much wider. A device made of a film-waveguide could cover an area, thousands of optical wavelengths long and wide. In that case, the light path in the plane of the waveguide will follow closely geometric optics which is significantly different from the wave optics observed in microwave circuits. *The main purpose of this paper is, therefore, to explore new wave phenomena arising from the use of the waveguides to form optical components and circuits.*

With the existing GaAs technology, a chip which contains a large number of diode lasers can be developed readily (see discussion in Sec. IV.E). Diode lasers and light emitting diodes (LEDs) can be directly modulated and they are, themselves, optical switches and nonlinear elements. Since gratings have to be used to form distributed feedback and Bragg reflector lasers, circuits containing lasers, LEDs, waveguides, and gratings will not be difficult to fabricate. Such circuits can perform a variety of the functions in optical communication. *The basic philosophy of the integrated circuit is that we should have few kinds of components, but have a large number of the same kind. In the past, lasers have always been used as individual light sources. We have yet to learn how to design a circuit involving many lasers, especially if light from one laser can be injected into another laser. Would such circuits be stable? Can we design efficient optical logic circuits? Would the lasers used as the active elements in switching operation be different from those designed primarily as light sources? These questions*

and others have to be answered in order to utilize fully the capability of integrated optical circuits. Therefore, to develop integrated optics to its full potential, we are concerned not only with the formation of thin-film optical devices and circuits, but also with the exploration of new ideas in device physics as well as in circuit design.

II. OPTICS IN WAVEGUIDES AND COUPLERS

A. Waveguides and the rule of refractive index

The use of dielectric waveguides for conducting electromagnetic waves was discussed as early as 1910 by Hondros and Debye. The field distributions in film waveguides were analyzed by Carcuvitz (1948) and also by Collin (1960). Their solutions were subsequently used to study light-guiding phenomena observed in $p-n$ junctions (Yariv and Leite, 1963). Various aspects of the film waveguides were not, however, exhaustively investigated until the inception of integrated optics in the early 1970's.

It is possible to analyze the wave propagation in waveguides from several different points of view. The waveguide is itself a lenslike medium and the waves in it may be considered as though they were focused continuously by a sequence of lenses (see for example, Tien *et al.*, 1956). Of course, one may also set up an eigenvalue problem from Maxwell's equations, and proceed to solve normal modes in the waveguide and the field distribution associated with each normal mode (Collin, 1960). Still another approach is the use of ray optics, where we consider a ray of light which is reflected back and forth between the top and bottom surfaces of the film, following a zigzag path in the waveguide (Tien *et al.*, 1969; Tien and Ulrich, 1970; Tien, 1971). Because of the importance of the waveguides in integrated optics, we shall study all these approaches. During the discussion, we shall introduce an important rule, known as the rule of refractive index. This rule has far-reaching consequences in all the wave phenomena to be discussed later in this paper.

Figure 3 shows various forms of optical waveguides used in integrated optics (McKenna, 1967; Nelson and McKenna, 1967; Marcuse, 1969, 1972; Marcatili, 1969; Goell, 1969; Tien *et al.*, 1969; Tien and Ulrich, 1970; Tien, 1971; Kappeny and Burke, 1973; Reisinger, 1973; Kaminow *et al.*, 1974; Reinhart *et al.*, 1974; Furuta *et al.*, 1974; Lotspeich, 1975; McLevige *et al.*, 1975; Blum *et al.*, 1975; Yamamoto *et al.*, 1975; Kuester and Chang, 1975). Among them, the simplest one is the film waveguide which consists of a layer of dielectric film deposited on a substrate. A film waveguide thus involves three media: an airspace, a film, and a substrate; their interfaces are parallel to one another and unless otherwise specified, they are parallel to the $x-y$ plane. The thickness of the film ranges from a fraction of one micron to several microns and, more importantly, the film has a refractive index which is larger than those of the substrate and the airspace. To show that the waveguide is a lenslike medium, consider in Fig. 4(a), a plane wave which starts from the left of the figure and propagates toward the right. The solid and dashed lines represent, respectively, the wave fronts and the lines of energy flow. Since the refrac-

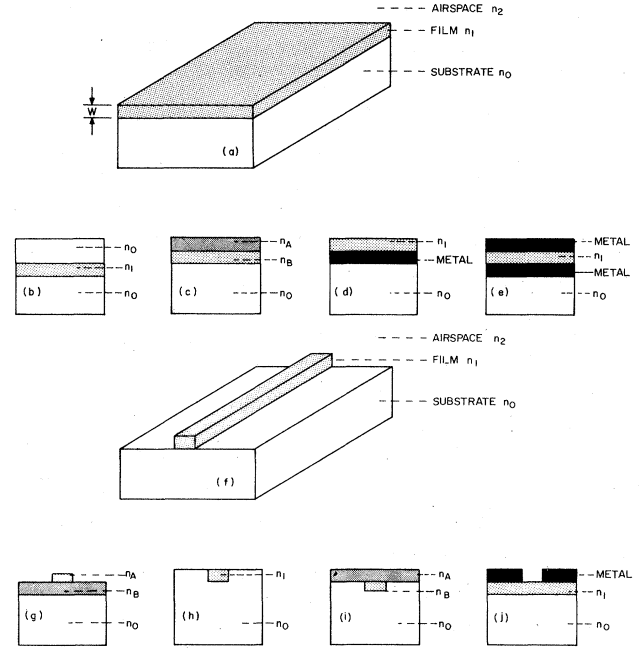


FIG. 3. Figures (a), (b), (c), (d), and (e) illustrate various film waveguides: (a) asymmetric film-waveguide, $n_1 > n_0 > n_2$; (b) symmetric film-waveguide, $n_1 > n_0$; (c) composite waveguide, $n_A, n_B > n_0$; (d) metal-clad waveguide, $n_1 > 1.0$; (e) optical strip-line, $n_1 > 1.0$. Figures (f), (g), (h), (i), and (j) illustrate various channel waveguides: (f) and (g) ridge waveguides, $n_A, n_B > n_0$; (h) embedded waveguide, $n_1 > n_0$; (i) inverted ridge waveguide, $n_A, n_B > n_0$; (j) metal-slot-waveguide, $n_1 > n_0$.

tive index is larger and the wave propagates slower in the film than in the air-space and the substrate, the wave front is distorted and it gradually becomes concave toward the right as the wave progresses [Fig. 4(a)]. Consequently, there is a natural tendency towards focusing the light wave into the film. Any structure which

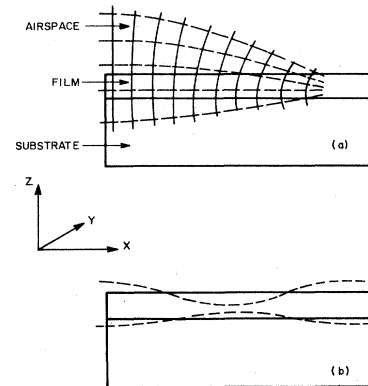


FIG. 4. (a) A waveguide may be considered as a lenslike medium which tends to focus a light beam into the waveguide. Consider a plane wave starting from the left of the figure. The solid and dashed lines represent, respectively, wave fronts and lines of the energy flow, as the wave propagates from left to right along the waveguide. (b) Exact calculation including diffraction shows that the cross section of the light beam in a lenslike medium varies periodically in space.

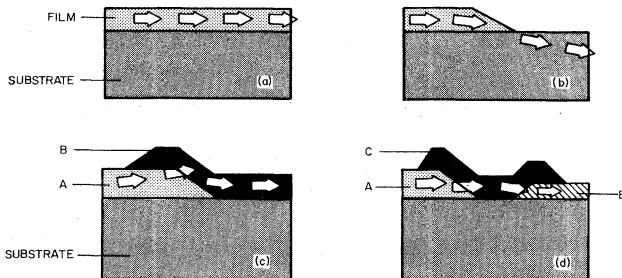


FIG. 5. It is possible to explain light wave propagation in (a) a film waveguide; (b) a tapered-film light-wave coupler; (c) a junction between two waveguides and (d) an interconnection C between devices A and B by a simple rule of refractive index.

has a refractive-index distribution peaked in the middle has the same focusing property and is a lenslike medium. Exact calculations including diffraction show that the outer boundary of the light beam oscillates (for example, Tien *et al.*, 1956) [Fig. 4(b)]. These calculations are, however, rarely used in integrated optics, since it is difficult to identify various forms of the beam trajectory with the normal modes of the waveguide. Nevertheless, the concept of the lenslike medium is important; it emphasizes the role played by the refractive index in wave propagation. It also leads to an important rule of waveguide optics—the rule of refractive index: *In a multilayer structure parallel to the light wave propagation such as the waveguide, light tends to propagate in the region where the refractive index is the largest, or, the wave velocity is the slowest.* This rule, in spite of its simplicity, explains many important inventions in integrated optics: Fig. 5(a) shows an optical waveguide, in which the wave propagates in the film because the film has a larger refractive index than those of the substrate and the airspace. By the same token, *p-n* junctions and heterostructures are also waveguides. Figure 5(b) is a tapered-film coupler. In this case, a film is terminated on a substrate. Near the end of the film, the light wave in the film enters into the substrate instead of the airspace because the refractive index of the substrate is larger than that of the airspace. Figure 5(c) illustrates a junction between two waveguides. A light wave in film A will enter into film B only if both A and B have refractive indices larger than those of the substrate and the airspace. Finally, Fig. 5(d) is a method of interconnection. A light wave starting from device A can be channeled through the interconnection C into another device B only because A, B, and C have larger indices than those in the rest of the structure. In all the above examples, if the structure of the waveguide varies in space, we assume that it varies slowly compared with the optical wavelength. Stated more specifically, in an integrated optical circuit, many different waveguide structures are interconnected together, but the transitions between them are always gradual so that in each transition, the wave is able to adjust itself adapting to the new surroundings. What we have implied in the

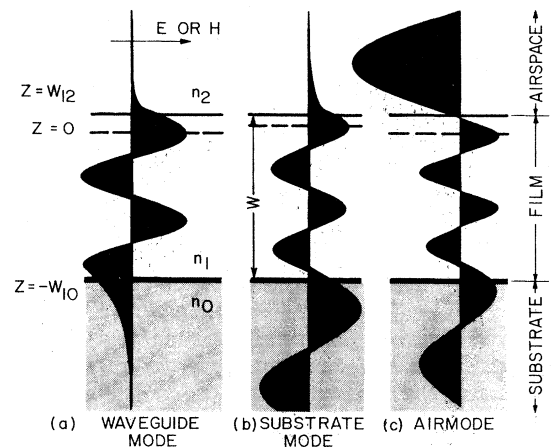


FIG. 6. Electric field distribution of a TE wave in (a) a "waveguide" mode; (b) a "substrate" mode; and (c) an "airspace" mode.

above rule of refractive index, is the provision that the wave maintains a normal mode of propagation in various waveguide structures which form the optical circuit.

B. Waveguide and radiation modes

The waveguides shown in Fig. 3 and the optical components formed by those waveguides will be the main subjects of this paper. Although most of our discussion will be confined to film waveguides, it applies equally well to channel waveguides. In any case, the important quantities which enter into the discussion are the eigenvalues, β 's, of the normal modes which we shall discuss fully below.

The light wave propagates in a waveguide in the form of normal modes. They are eigensolutions of the wave equation, obtained by solving the boundary conditions of the waveguide. There are three types of normal modes: As shown in Fig. 6, the waves are bounded (a) in the film in "waveguide" modes, and (b) in the film and the substrate in "substrate" modes; (c) the waves fill all three spaces (airspace, film, and substrate) in the "air" modes (Tien *et al.*, 1971). The "substrate" and "air" modes are also called radiation modes and they have been discussed in detail by Marcuse (1969). The field distributions in "waveguide" and "radiation" modes are given in Table I and illustrated in Fig. 6. The "waveguide," "substrate," and "air" modes form a complete set of the eigensolutions and they have nondegenerate eigenvalues. All the normal modes are orthogonal to one another. Let us use the letter n for refractive index; the subscripts $j=0, 1$, and 2 to denote the substrate, film, and airspace, respectively; $k = \omega/c$, where ω is the angular frequency of the light wave and c is the velocity of light in vacuum. The eigenvalues of the "waveguide" modes are discrete, ranging from kn_0 to kn_1 . Those of the "substrate" and "air" modes are continuous ranging from kn_2 to kn_0 and 0 to kn_2 , respectively. In integrated optics, a light wave in the

TABLE I. Electric field distribution in (a) a waveguide mode, (b) a substrate mode, and (c) the even and odd air modes.^a

A. Waveguide mode $\sin^{-1}(n_0/n_1) < \theta_1 < \pi/2; kn_0 < \beta < kn_1$			
Medium	k_{xj}	k_{zj}	E_y (TE wave)
Film	$=\beta$	$=b_1$	$A \cos b_1 z$
Substrate	$=\beta$	$=ip_0$	$A \cos(\Phi_{10} + m\pi) \exp[-p_0(z - W_{10})]$
Air-space	$=\beta$	$=ip_2$	$A \cos\Phi_{12} \exp[-p_2(z - W_{12})]$

B. Substrate mode $\sin^{-1}(n_2/n_1) < \theta_1 < \sin^{-1}(n_0/n_1); \sin^{-1}(n_2/n_0) < \theta_0 < \pi/2; kn_2 < \beta < kn_0$			
Medium	k_{xj}	k_{zj}	E_y (TE wave)
Film	$=\beta$	$=b_1$	$A \cos b_1 z$
Substrate	$=\beta$	$=b_0$	$\frac{1}{2}A[\cos(b_1 W_{10}) - i(b_1/b_0) \sin(b_1 W_{10})] \exp[-ib_0(z - W_{10})] + c.c.$
Air space	$=\beta$	$=ip_2$	$A \cos\Phi_{12} \exp[-p_2(z - W_{12})]$

C. Even and odd air modes $0 < \theta_1 < \sin^{-1}(n_2/n_1); 0 < \theta_0 < \sin^{-1}(n_2/n_0); 0 < \theta_2 < \pi/2; 0 < \beta < kn_2$			
Medium	k_{xj}	k_{zj}	
Film	$=\beta$	$=b_1$	{ Even $A \cos b_1 z$ Odd $A \sin b_1 z$
Substrate	$=\beta$	$=b_0$	{ Even $\frac{1}{2}A[\cos(b_1 W_{10}) - i(b_1/b_0) \sin(b_1 W_{10})] \exp[-ib_0(z - W_{10})] + c.c.$ Odd $-\frac{1}{2}A[\sin(b_1 W_{10}) + i(b_1/b_0) \cos(b_1 W_{10})] \exp[-ib_0(z - W_{10})] + c.c.$
Air space	$=\beta$	$=b_2$	{ Even $\frac{1}{2}A[\cos(b_1 W_{12}) - i(b_1/b_2) \sin(b_1 W_{12})] \exp[-ib_2(z - W_{12})] + c.c.$ Odd $\frac{1}{2}A[\sin(b_1 W_{12}) + i(b_1/b_2) \cos(b_1 W_{12})] \exp[-ib_2(z - W_{12})] + c.c.$

^aIn deriving these expressions, we have chosen $z=0$ at the position where E_y is either zero or maximum. These positions of $z=0$ are therefore different for different modes.

waveguide is considered as a surface wave. The eigenvalue of a normal mode is defined as the phase constant of this surface wave, or ω/v , where v is the phase velocity measured along the two-dimensional plane of the waveguide. The letter β is customarily used to denote the eigenvalue of the normal mode. The physical meaning of these normal modes will be discussed in Sec. II C. Here, we only show how eigenvalues of the "waveguide" modes can be solved from Maxwell's equations.

Since a waveguide consists of three media—airspace, film, and substrate—we shall consider waves in each medium separately. In rectangular coordinates, the waves propagate as

$$\exp[i\omega t \mp ik_{xj}x \mp ik_{yj}y \mp ik_{zj}z],$$

where $j=0, 1, 2$ denotes substrate, film, airspace as defined earlier, and k_x , k_y , and k_z are the wave numbers (phase constants) along x , y , and z , respectively. It is obvious that the components of the wave vector along x , y , z should add to the wave vector itself such that

$$k_{xj}^2 + k_{yj}^2 + k_{zj}^2 = k^2 n_j^2. \quad (1)$$

By identifying $k_{xj}^2 = -\partial^2/\partial x^2$, $k_{yj}^2 = -\partial^2/\partial y^2$, and $k_{zj}^2 = -\partial^2/\partial z^2$, we recognize immediately that Eq. (1) is the wave equation in an isotropic dielectric medium of refractive index n_j , which is

$$\left(\frac{\partial^2}{\partial x^2} + \frac{\partial^2}{\partial y^2} + \frac{\partial^2}{\partial z^2} \right) E_j = -k^2 n_j^2 E_j, \quad (1a)$$

where E_j is the electric field. An identical equation can be written for the magnetic field H_j . Of course, we could derive (1a) from the Maxwell equations.

Imagine a light beam in a film waveguide. The thickness of the light beam should be equal to that of the film, which is on the order of 1 μm . The width of the light beam is, however, arbitrary. As long as the beam is more than 50 μm wide, which amounts to about 100 optical wavelengths in the visible spectrum, it should not expand significantly by diffraction, particularly when the optical circuit considered is only several centimeters long. Therefore, the light beam in the film waveguide has the shape of a very thin flat ribbon which is about 1 μm thick and 50 μm wide. With that thickness-to-width ratio, we are justified in assuming a sheet of the light beam which is infinitely wide, so that the fields may be considered to be uniform along the width of the beam. Let the film be in the $x-y$ plane. Unless otherwise specified, we will always assume in this paper that the light path projected to the film surface is along x . We have then $\partial/\partial y = \mp ik_{yj} = \mp ik_{y1} = \mp ik_{y2} = 0$. In addition, since the waves in the film, substrate, and airspace are matched along their interfaces, the components of the wave vectors parallel to the $x-y$ plane must be the same in all three media. It is convenient to put $k_{x0} = k_{x1} = k_{x2} = \beta$, and here, β is the eigenvalue of the normal mode which we are going to solve from Maxwell's equations. Customarily, we take $k_{zj} = b_j$ if it is real and $k_{zj} = ip_j$ if it is imaginary. Note that

β , b_j , and p_j are always real and positive. As shown in Fig. 6(a), we expect, in "waveguide" modes, that the fields are sinusoidal in z inside the film and decrease exponentially outside. The wave number k_{z1} is then real and may be denoted by b_1 . The wave numbers k_{z0} and k_{z2} are imaginary and may be denoted by $i p_0$ and $i p_2$. From (1a), we have

$$b_1^2 + \beta^2 = k^2 n_j^2; \quad p_{0,2}^2 = \beta^2 - k^2 n_{0,2}^2. \quad (1b)$$

It turns out that by assuming $\partial/\partial y = 0$, the Maxwell equations can be separated into two independent sets. One set, which involves the field components E_{yj} , H_{zj} , and H_{xj} only, is called the TE (transverse electric) wave and the other set, which involves H_{yj} , E_{zj} and E_{xj} only, is called the TM (transverse magnetic) wave. By expressing the field in (1a) in its x , y , and z components, we have for TE waves

$$\partial^2 E_{yj} / \partial z^2 = -(k^2 n_j^2 - \beta^2) E_{yj}; \quad (2)$$

$$H_{xj} = -(i/k)(\partial/\partial z) E_{yj}; \quad (3)$$

$$H_{zj} = (i/k)(\partial/\partial x) E_{yj}. \quad (4)$$

The corresponding equations for TM waves are

$$\partial^2 H_{yj} / \partial z^2 = -(k^2 n_j^2 - \beta^2) H_{yj}; \quad (5)$$

$$E_{xy} = (i/k n_j^2)(\partial/\partial z) H_{yj}; \quad (6)$$

$$E_{xz} = -(i/k n_j^2)(\partial/\partial x) H_{yj}. \quad (7)$$

For "waveguide" modes, there must be at least one maximum in the field distribution inside the film (see Fig. 6a). It is convenient to take $z=0$ as that maximum and to specify $z=W_{12}$ and $z=-W_{10}$ as the upper and lower boundaries of the film. The total thickness of the film is then $W=W_{10}+W_{12}$. We have

$$\begin{aligned} E_{y1} \text{ (or } H_{y1}) &= A \cos b_1 z, \quad -W_{10} < z < W_{12}, \\ E_{y2} \text{ (or } H_{y2}) &= C \exp(-p_2 |z - W_2|), \quad z > W_{12}, \\ E_{y0} \text{ (or } H_{y0}) &= D \exp(-p_0 |z - W_{10}|), \quad z < -W_{10}, \end{aligned} \quad (8)$$

where A , C , and D are the amplitudes of E_y for the TE wave and those of H_y for the TM wave. The other field components may be found from Eqs. (3) and (4), or (6) and (7). The fields E_{yj} and H_{xj} (or H_{yj} and E_{xj}) must be matched at the air-film and film-substrate interfaces, giving us a total of four boundary conditions. We have also the four unknowns C/A , D/A , W_{12} , and β . The eigenvalue problem described is therefore solvable. By eliminating all the unknowns except β , we obtain mode equations

$$\tan(b_1 W) = b_1(p_0 + p_2)/(b_1^2 - p_0 p_2)$$

and

$$\tan(b_1 W) = b_1[(n_1/n_0)^2 p_0 + (n_1/n_2)^2 p_2]/[b_1^2 - (n_1^2/n_0 n_2)^2 p_0 p_2]$$

for TE and TM waveguide modes, respectively. Similar equations have been derived by Collin (1970) for the case of the symmetric waveguides where $n_0=n_2$ and $p_0=p_2$. The above equations together with (1b) may be used to determine eigenvalue β . The solution thus obtained is multivalued and each value of β represents one waveguide mode. The number of possible modes depends on the thickness of the film and the refractive indices. Different waveguide modes are identified by

the mode order, $m=0, 1, 2, \dots$, respectively. The field distributions (E_y for the TE wave, and H_y for the TM wave) of the $m=0, 1, 2, \dots$ mode have 1, 2, 3, ... maxima inside the film. Note that m starts from 0. The quantity β/k is called the mode index. It specifies the ratio of the wave velocity in a vacuum to that in the waveguide and thus plays the role of the refractive index. For this reason, the mode index is also called the effective refractive index. In the literature, we frequently use the letter N for the mode index in order to distinguish it from the real refractive index n .

C. Ray optics and zigzag waves

It turns out that the eigenvalue problem considered above can also be solved by ray optics. Due to the fact that the waveguide involves plane geometry, the field distribution in it can be analyzed as a superposition of two plane waves. Representing each plane wave by an optical ray, or a wave vector, normal to the wave front, we have converted a field problem to that of geometric optics.

Consider, in Fig. 7(a), a ray of light B which propagates toward the upper surface of the film. If the incident angle θ_1 is larger than the critical angle $\sin^{-1}(n_2/n_1)$, the ray B will be totally reflected at the surface. During this total internal reflection, a part of the field called an "evanescent wave" will penetrate into the air space. This evanescent wave decreases exponentially outside the film in the same manner as is shown in Fig. 6. In addition, as the ray B is totally reflected into ray A at the film surface, the phase of the reflected light wave is advanced by $2\Phi_{12}$ at the point of reflection, where

$$\Phi_{12} = \tan^{-1}(p_2/b_1) \quad (9a)$$

for the TE wave and

$$\Phi_{12} = \tan^{-1}(n_1^2 p_2/n_2^2 b_1) \quad (9b)$$

for the TM wave. Here, $0 \leq \Phi_{12} \leq \pi/2$, and p_2 and b_1 have been defined earlier in (1b). This phenomenon of total

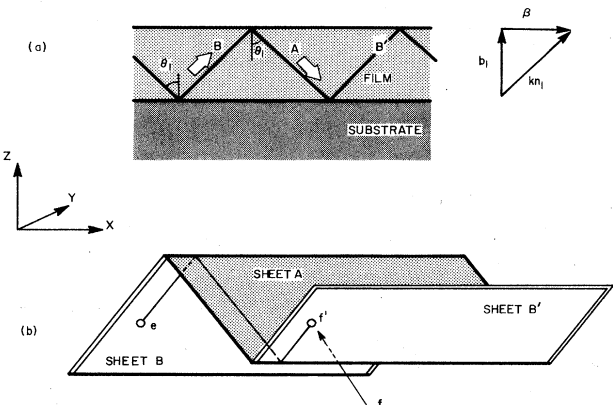


FIG. 7. In the zigzag-wave model, we use rays B, A, B', \dots , to represent waves in a waveguide. Hence, the zigzag ray shown in (a) is equivalent to the plane wave shown in (b). We can visualize, in this model, a sheet of the plane wave B which folds into sheet A at the upper film boundary, then into sheet B' at the lower film boundary and so on.

internal reflection is discussed in Born and Wolf (1970). Similarly, if $\theta_1 > \sin^{-1}(n_0/n_1)$, ray A will be totally reflected into ray B' at the lower surface of the film; in this case,

$$\Phi_{10} = \tan^{-1}(p_0/b_1)$$

and

(10)

$$\Phi_{10} = \tan^{-1}(n_1^2 p_0/n_0^2 b_1),$$

respectively, for TE and TM waves. Here again, $0 \leq \Phi_{10} \leq \pi/2$. Therefore, light waves propagate in the film-waveguide in a zigzag manner and they are called zigzag waves.

We have explained earlier that rays B, A, and B' are plane waves which have wave vectors in the directions of the rays and wave numbers equal to kn_1 . If these plane waves were narrow beams, rays B and A, or rays A and B', would not meet exactly at the same spot on the film boundary but rather would be displaced slightly from one another in the lateral direction. This phenomenon is called the Goos-Haenchen shift (Lotsch, 1968). However, as long as the rays represent plane waves or wide beams, as they do in the waveguide, Eqs. (9) and (10) are correct. According to the vector diagram in Fig. 7(a), we have

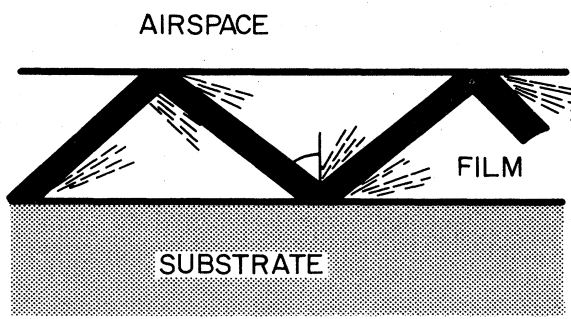
$$\beta = kn_1 \sin \theta_1 \quad \text{and} \quad b_1 = kn_1 \cos \theta_1 \quad (1c)$$

which, of course, agrees with (1b). Note that there is a value of θ_1 corresponding to each value of β . Different waveguide modes may thus be considered as zigzag waves of different θ_1 's. We will use a similar concept later on for the "substrate" and "air" modes.

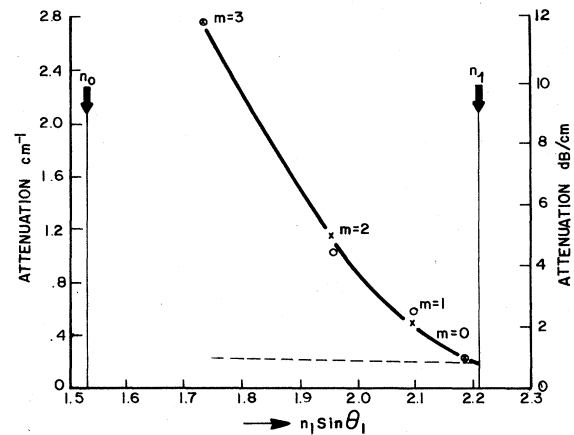
The use of the zigzag-wave model often simplifies the problem: First, by introducing the phase angles $2\Phi_{12}$ and $2\Phi_{10}$ at the interfaces, one isolates the waves in the film from those in the airspace and the substrate, and thus eliminates the necessity of matching the fields at

the film boundary, a task which normally would involve four simultaneous equations. Moreover, by taking $\partial\Phi_{10}/\partial\omega$ and $\partial\Phi_{12}/\partial\omega$ into account, the zigzag-wave model predicts correctly the group velocity of the wave including the Goos-Haenchen shift. Second, if the film is coupled to a bulk medium as in the case of the light-wave couplers, it is only necessary to consider the coupling at those points where the zigzag wave strikes the film surface, and at these points, simple ray optics can be used. Third, the zigzag-wave model predicts correctly the large scattering losses observed in the waveguide. Consider a film 1-μm thick; for the light wave to travel a distance of 1 cm in x , there are about 1000 zigzag bounces [Fig. 8(a)]. If the scattering loss is 0.5% for each reflection at the film surface, the loss in the waveguide can be as large as 10 cm⁻¹. Indeed, in spite of intensive research efforts directed at forming smooth surfaces, the major loss in the waveguide is still the scattering loss from the surfaces. Finally, it is also important that in this model one can visualize physically a light wave which zigzags down the waveguide.

To fully understand the zigzag-wave model, one needs to combine ray optics with wave optics. We have mentioned that rays B, A, and B' are truly plane waves. What we really have is a sheet of infinitely wide plane wave B which propagates along the wave vector B in the film [(Fig. 7(b))]. The wave folds into sheet A in the first total reflection, then into sheet B' in another total reflection and so on. The sheets A, A', A'', ..., and B, B', and B'' therefore overlap one another in the physical space. If a , a' , and a'' are points on the sheets A, A', and A'', respectively, which are superposed upon one another in the physical space, the phases of the waves at a , a' , and a'' must be equal or differ by a multiple of 2π . Otherwise, the waves in different sheets would not add in phase and they cannot be built up con-



(a)



(b)

FIG. 8. In (a), we show that the zigzag-wave model explains well the large scattering loss observed in the film waveguide. Light is scattered each time the zigzag ray hits the film surface. Since there are about 1000 such zigzag bounces in 1-cm distance, the total loss can be large even though the loss per bounce is small. According to the Rayleigh criterion, scattering loss decreases with increasing incident angle θ_1 . In (b), we plot losses of different waveguide modes versus $n_1 \sin \theta_1$. The $m=0$ mode which has the largest θ_1 has thus the lowest scattering loss. In this figure, the dashed line indicates the loss due to volume absorption in the film, and the vertical distance between the solid and dashed lines is that due to scattering at the surfaces.

structively in the waveguide. The same requirement applies to the waves in sheets B, B', B'', \dots . The condition that the waves in different sheets of reflection must add in phase in the physical space provides us with an equation from which the eigenvalues β 's of the waveguide modes can readily be derived. We will show the calculation involved below.

Let the light wave travel a distance Δx in a time Δt in one zigzag. Consider two points, e and f , both on sheet B but spaced by the distance Δx [Fig. 7(b)]. The coordinates of e and f are, respectively, (x_1, z_1) and $(x_1 + \Delta x, z_1)$. Assume at time t_1 , that the phase of the wave at e is zero. The phase of the wave at point f and at $t = t_1 + \Delta t$ will then be $(\omega \Delta t - \beta \Delta x)$. If, on the other hand, we follow the reflections of the wave through a complete zigzag, the wave at e on sheet B will, after a time Δt , land on sheet B' at the point f' and will have a phase at that point

$$\omega t - \beta \Delta x - 2b_1 W + 2\Phi_{10} + 2\Phi_{12}.$$

Since the points f and f' in sheets B and B' actually coincide in the physical space and we require the phases at these points to either be equal or differ by a multiple of 2π , we thus obtain an important relation

$$b_1 W = \Phi_{10} + \Phi_{12} + 2m\pi. \quad (11)$$

where $m = 0, 1, 2, \dots$. In addition, we have from (1b) that

$$\beta^2 = k^2 n_1^2 - b_1^2. \quad (12)$$

Equations (11) and (12) may be used to calculate the eigenvalues β . Here m indicates the order of the waveguide mode. Equation (12) is the mode equation derived by Tien et al. (1969) in the zigzag-wave model. The equation is mathematically equivalent to the mode equation given earlier in Sec. II. B, but appears in a form which is more convenient to use. Not only does it contain the mode order m explicitly, but also each term in the equation acquires a specific meaning in the zigzag-wave model.

Consider, as a specific example, a waveguide formed by depositing a 1.5- μm thick ZnS film on a glass substrate. We have $n_1 = 2.2899$, $n_0 = 1.5040$, $n_2 = 1.0$, and $k = 5.927 \times 10^4 \text{ cm}^{-1}$ at the wavelength of the YAG:Nd laser, 1.06 μm . There are five TE waveguide modes in this film, and the mode indices are 2.264, 2.201, 2.086, 1.916, and 1.685 for the mode orders, $m = 0, 1, 2, 3$, and 4, respectively. These mode indices correspond to the incident angles $\theta_1 = 81.4^\circ, 74.0^\circ, 65.6^\circ, 56.8^\circ$, and 47.4° , in that order. Note that the mode index and the incident angle of the $m=0$ mode approach n_1 and 90° , respectively, while those of the $m=4$ mode approach n_0 and the critical angle ($\sin^{-1}(n_0/n_1)$) as the limits.

It is easy to plot mode curves as those shown in Fig. 9a. Here, the solid and dotted curves are for the TE and TM modes, respectively. Each curve represents one "waveguide" mode. Let us examine these mode curves closely. First, one can draw a horizontal line from any given value of the film thickness W . The intercepts on this horizontal line by the mode curves give the values of mode indices, N 's, and those of the incident angles, θ_1 's. We see that the $m=0$ mode has the largest N and θ_1 , and N and θ_1 become increasingly

smaller for the higher-order modes. Second, as W increases, we move up the horizontal line. More mode curves will be intercepted by the horizontal line and more "waveguide" modes will be admitted to the waveguide. Third, all mode curves start, at the left, from $N=n_0$, and end, at the right, to $N=n_1$, and they are monotonically increasing functions from left to right. The film thickness indicated by a mode curve at $N=n_0$, is thus the minimum thickness that a waveguide must acquire in order to allow this "waveguide" mode to propagate. This thickness is called "cutoff" thickness. For example, in the above example, we have taken $W=1.5 \mu\text{m}$. The $m=5$ mode has a "cutoff" thickness $1.60 \mu\text{m}$, which is larger than $1.5 \mu\text{m}$, and thus, this mode is "cutoff" in this waveguide. All lower-order modes have cutoff thicknesses less than $1.5 \mu\text{m}$ and they are the modes allowed in this waveguide. Finally, at $N_1=n_0$, θ_1 is $\sin^{-1}(n_0/n_1)$, or the critical angle of the film-substrate interface. The figure shows that, for θ_1 less than this critical angle, or $N < n_0$, all waveguide modes are cutoff. It is the region where only "substrate" and "air" modes can exist.

We have interpreted earlier that a wave in a "waveguide" mode of mode index N , is a zigzag wave with $\theta_1 = \sin^{-1}(N/n_1)$ [See Eq. (1c)]. Figure 9(b) shows the zigzag waves corresponding to the waveguide modes discussed in the above example. Again, we see the zigzag rays are almost parallel to the interface for the $m=0$ mode, and the zigzag angle θ_1 becomes smaller and smaller for the higher-order modes, approaching the critical angle as the limit.

With this zigzag-wave model in mind, we may now present a clearer view of the "waveguide", "substrate", and "air" modes discussed in Sec. II B. Consider, in Fig. 9(c), a plane wave which propagates in the film with an incident angle θ_1 , and let this incident angle decrease gradually from 90° . Starting from the lower diagram of this figure, in the range of $\sin^{-1}(n_0/n_1) < \theta_1 < 90^\circ$, this plane wave is totally reflected at the two film surfaces. It is a zigzag wave shown in Fig. 9(b) and thus represents a "waveguide" mode. As θ_1 decreases further into the range of $\sin^{-1}(n_2/n_1) < \theta_1 < \sin^{-1}(n_0/n_1)$, the middle diagram shows a plane wave totally reflected at the upper film surface, but no longer so at the lower film surface. In fact, the light wave is refracted into the substrate as it should in a "substrate" mode. The dividing line between the "waveguide" and "substrate" mode is thus the critical angle, $\sin^{-1}(n_0/n_1)$, of the film-substrate interface. At this critical angle, both modes share the same mode index, $N=n_0$, and the refracted wave in the substrate is directed parallel to the interface. Finally, in the range of $0 < \theta_1 < \sin^{-1}(n_2/n_0)$, the top diagram shows a light wave refracted into both the air space and the substrate representing an "air" mode. In this case, the dividing line between the "substrate" and "air" modes is the critical angle at the film-air interface, and at this critical angle, the light beam is refracted into the air space in the direction parallel to the interface. It is now clear that the total reflection phenomenon plays an essential role in dielectric waveguides. It divides the normal mode spectrum into "waveguide," "substrate," and "air" modes. According to the way that we have looked at this problem, these

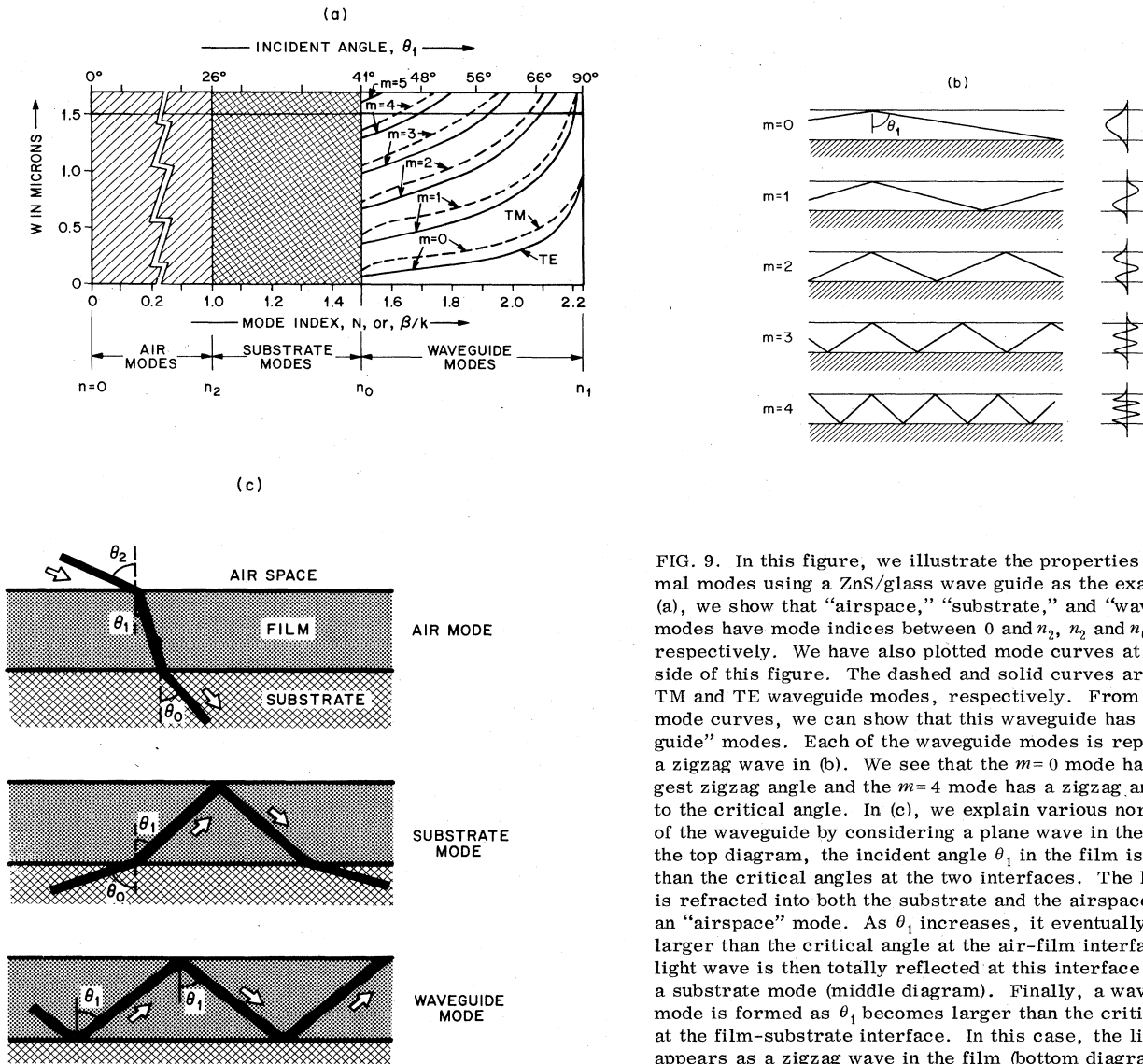


FIG. 9. In this figure, we illustrate the properties of the normal modes using a ZnS/glass wave guide as the example. In (a), we show that "airspace," "substrate," and "waveguide" modes have mode indices between 0 and n_2 , n_2 and n_0 , n_0 and n_1 , respectively. We have also plotted mode curves at the right side of this figure. The dashed and solid curves are for the TM and TE waveguide modes, respectively. From the TE mode curves, we can show that this waveguide has 5 TE "waveguide" modes. Each of the waveguide modes is represented by a zigzag wave in (b). We see that the $m=0$ mode has the largest zigzag angle and the $m=4$ mode has a zigzag angle close to the critical angle. In (c), we explain various normal modes of the waveguide by considering a plane wave in the film. In the top diagram, the incident angle θ_1 in the film is smaller than the critical angles at the two interfaces. The light beam is refracted into both the substrate and the airspace forming an "airspace" mode. As θ_1 increases, it eventually becomes larger than the critical angle at the air-film interface. The light wave is then totally reflected at this interface forming a substrate mode (middle diagram). Finally, a waveguide mode is formed as θ_1 becomes larger than the critical angle at the film-substrate interface. In this case, the light beam appears as a zigzag wave in the film (bottom diagram).

modes describe simply a plane wave which propagates in various possible directions in a space occupied by film, substrate, and airspace.

According to the Rayleigh criterion (Rayleigh, 1896, 1907; Beckmann and Spizzichino, 1963; Tien, 1971), the scattering loss suffered in a reflection from a plane surface varies as $(1-K^2 \cos^2 \theta_1)$, where K^2 specifies the roughness of the surface and θ_1 is the incident angle. For the $m=0$ mode, $\theta_1 \approx 90^\circ$ and $\cos^2 \theta_1 \approx 0$, its scattering loss should be the smallest as compared with the other waveguide modes. Careful measurement of the losses in the waveguide has shown that this is indeed true [see Fig. 8(b)]. Moreover, the above formula enables one to separate the scattering loss from the absorption loss and thus to gain invaluable information concerning the optical quality of the material used in the waveguide (Tien, 1971).

D. Prism couplers and m -line spectroscopy

In the early waveguide experiments, the problem of coupling a light beam from a laser into a thin-film waveguide was a serious one. It is very difficult to focus a light beam into a waveguide through the edge of the film. Not only is the film very thin, which requires a tightly focused and carefully positioned light beam, but also the edge is rough, causing excessive scattering of the light. Fortunately, one soon discovered that it is possible to couple a light beam through the top surface of the film. Prism (for example, Tien *et al.*, 1969) and grating (for example, Dakss *et al.*, 1970) couplers are constructed from this principle and will be discussed in this section. Tapered-film (Tien and Martin, 1971) couplers are constructed according to a different principle and will be discussed in Sec.

III. F.

In the past, prisms have been used for coupling in various ways. For example: In the sixties, Iogansen (1962) analyzed the coupling mechanism in connection with his work on the resonance filter. Osterberg and Smith (1964) reported the transmission of an image between two prisms along the surface of a sheet of Pilkington float glass. Otto (1968) started a series of experiments involving the excitation of plasmons in a sheet of metallic film. When the research in integrated optics had just begun, Tien *et al.* (1969) and Harris and Shubert (1969) studied the use of the prism for excitation of waveguide modes. Figure 10 illustrates the prism coupler used by Tien *et al.* A rectangular prism was pressed against a thin-film waveguide leaving a small air gap between the base of the prism and the top surface of the film. The air gap was on the order of 0.1 μm . A light beam from a laser entered the prism and was totally reflected at the base of the prism. The total reflection left only evanescent fields in the air gap. It was these evanescent fields which coupled the light wave in the prism into the waveguide. By mounting the prism-film assemblage on a turntable, they were able to vary the direction of the incident beam with respect to the film. Interestingly, they found that in order to excite a particular waveguide mode, the light beam must be oriented in a certain direction. By properly changing that direction, any waveguide mode can be excited. This possibility of selective excitation of the waveguide modes is very important in integrated optics. *In addition, Tien *et al.* (1969) also discovered m-line spectroscopy, by means of which one can determine wave velocities of the normal modes, refractive indices of the film and the substrate, thicknesses of the film and the substrate, and loss in the waveguide. The prism coupler has since become an indispensable tool in waveguide experiments.*

The physics of the prism coupler can easily be explained using the zigzag-wave model described in Sec. II. C. *In general, for effectively coupling a light wave from one medium to another, two conditions must be met. First, the wave velocities in the two coupled media must be the same, and second, the length along*

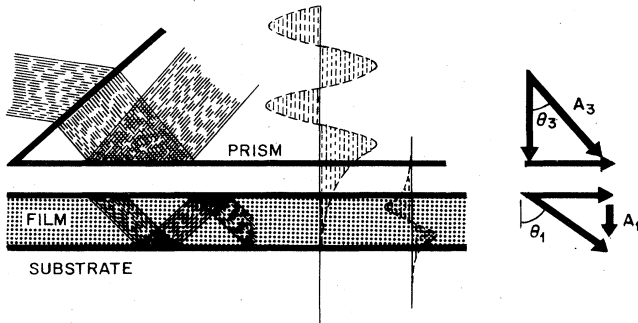


FIG. 10. In a prism coupler, the incoming laser beam is totally reflected at the base of the prism and the light wave in the prism is coupled into the waveguide through the evanescent fields. The direction of the laser beam in the prism must be such that the synchronous condition indicated by the vector diagram shown at the right is satisfied.

the coupled boundary must be adjusted according to the strength of the coupling. Referring to the vector diagram in Fig. 10, if the refractive index of the prism is n_3 and the incident angle of the light wave in the prism is θ_3 , the wave in the prism will have the x component of its wave vector equal to $k_{x3} = kn_3 \sin\theta_3$. On the other hand, a light wave in the waveguide, being a zigzag wave, will have the x component of its wave vector equal to $kn_1 \sin\theta_1$, which we recognize is the eigenvalue β of the waveguide mode. When these two x components of the wave vectors are equal, the light wave in the prism, will have the same wave velocity as that in the waveguide and the first condition for effective coupling is satisfied. For the second condition, it is easy to see that the coupling length depends upon the width of the light beam, and that the coupling strength varies with the spacing of the air gap; both of these quantities can be easily adjusted in the prism coupler.

A direct calculation of the fields in the air gap indicates that the coupling strength between the prism and the waveguide is very small. In spite of this, an overall coupling efficiency of more than 90% has been observed (Ulrich, 1971). To explain this, consider, in Fig. 11, a zigzag wave in the waveguide which strikes the upper surface of the film at points 1, 2, 3, and 4. In the same figure, we represent the light beam in the prism by four parallel rays which hit the prism base at points 1', 2', 3', and 4' directly opposite to points 1, 2, 3, and 4 across the gap. Draw a dashed line starting from point 1', normal to the direction of wave propagation. This dashed line is a wave front of the laser beam in the sense that the light wave reaches points 1', 2'', 3'', and 4'' at the same time and has the same phase at those points. Let the light wave at point 1' excite a small wave A_1 in the film at $t=0$. After a definite time interval, the A_1 wave has executed a complete zigzag and reaches point 2 in the waveguide. Precisely during the same time interval, ray 2''-2' in the prism travels from point 2'' to point 2' and excites another small wave A_2 in the film. The waves A_1 and A_2 are in phase at point 2, and they add constructively. The resultant wave amplitude in the waveguide at point 2 is therefore twice

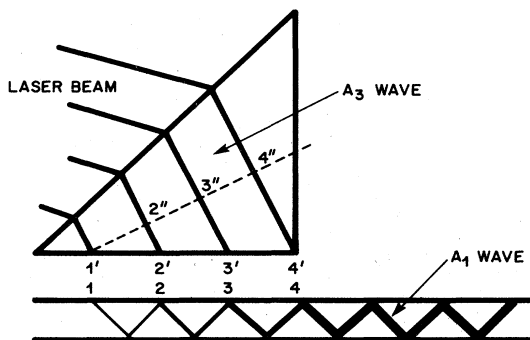


FIG. 11. In a prism coupler, we can show that the light energy in the prism is continuously fed into the waveguide at the points 1, 2, 3, 4, ... However, the coupling is effective only if the fields excited at these points are in phase with a zigzag wave in the waveguide. When this condition is satisfied, the amplitude of the zigzag wave in the coupling region increases roughly as the number of zigzags.

and the wave intensity is four times those at point 1. Similarly, the wave amplitude at point 3 is three times and the wave intensity is nine times those at point 1. Normally, there are about 100 such zigzags in the prism coupler, and the wave intensity in the waveguide can be built up very quickly even though only a very small wave is excited at each point. The condition that all of the small waves add in phase is, of course, precisely the same condition described earlier for matching the wave velocity in the prism to that in the waveguide. For this reason, it is also called the synchronous condition. The incident angles θ_3 used to excite various waveguide modes are called synchronous angles.

Figure 12(a) is an experimental arrangement used by Tien *et al.* (1969) to observe m lines. In this experiment, two prism couplers spaced apart by a distance d , were used to couple a laser beam into and out of a thin-film waveguide. A screen at the right was used to display the light emerging from the output prism. The experimenters oriented the incoming laser beam so that a single waveguide mode was excited in the film. As the light wave in this mode propagated from the input

prism to the output prism, part of the light was scattered into other waveguide modes. The scattered light also propagated in the film, and, as it reached the output prism, it was coupled out of the prism into many different directions. That occurred because the scattered light involved many waveguide modes and each of them had its own output angle satisfying the synchronous condition. We thus observed a bright spot on the screen which represented the light in the main waveguide mode excited at the input, and in addition, a set of bright lines representing the light that has been scattered into the other waveguide modes. There was one line for each waveguide mode. Figure 12(b) is a photograph of the m lines; it is a beautiful display of the waveguide modes. The angular positions of those lines may be used to calculate wave velocities of the normal modes as well as refractive index and thickness of the film. Using this method, it is possible to determine wave velocity and refractive index accurate to 1 part in 10 000 (Tien *et al.*, 1973). It is also possible to determine loss in the waveguide from the widths of the m -lines. This technique is called the m -line spectroscopy.

E. Grating coupler and corrugated waveguides

We have mentioned earlier, in Sec. I. A, that a grating is a corrugated surface, and that a waveguide containing a corrugated surface is a corrugated waveguide. In spite of numerous published calculations, the problem of blazed gratings and that of gratings with deep grooves have not been completely solved (Harris *et al.*, 1972; Ogawa *et al.*, 1973; Dalgoutte, 1973; Neviere *et al.*, 1973; Rigrod, 1974; Peng *et al.*, 1974, 1975; Handa *et al.*, 1975; Ghizoni *et al.*, 1976; Rigrod and Marcuse, 1976; Streifer *et al.*, 1976). For tutorial purposes, we will review the Rayleigh method (Rayleigh, 1907). It is based on an elegant hypothesis that the diffracted waves are simply a set of outgoing plane waves.

To illustrate this method, let the corrugated surface be situated at the top surface of the film, $z=0$, and the corrugation has the form

$$z = \frac{1}{2} h \sin(2\pi/d)x, \quad (13)$$

where $\frac{1}{2} h$ and d are, respectively, the amplitude and the period of the corrugation. Consider an incoming laser beam which is incident on the grating from the airspace at an angle θ_i such that

$$E_{yt}(x, z, t) = A \exp\{i[\omega t + (k \cos\theta_i)z - (k \sin\theta_i)x]\}.$$

Substituting Eq. (13) into this expression and expanding the result in terms of Bessel functions, we find for the field at the grating boundary

$$E_{yt} = A \sum_m J_m\left(\frac{hk \cos\theta_i}{2}\right) \exp i\left[\omega t - \left(k \sin\theta_i + m \frac{2\pi}{d}\right)x\right].$$

This field distribution in x at the grating surface must, according to the Rayleigh method, be matched by that of a set of outgoing plane waves. These outgoing waves are the waves diffracted by the grating and, according to the above equation, should vary in x as

$$k_{xd} = k \sin\theta_i + m(2\pi/d), \quad (14)$$

where $m = 0, \pm 1, \pm 2, \dots$ gives the order of the diffraction.

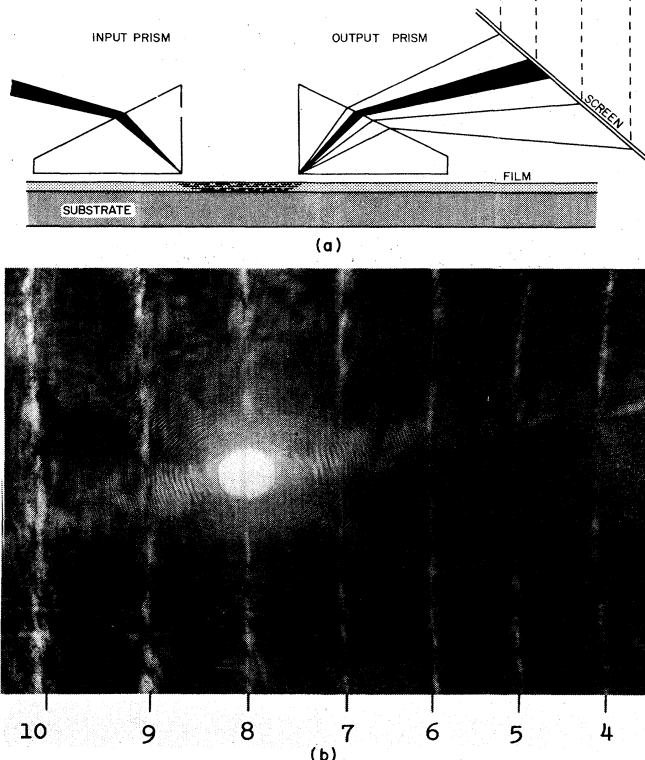


FIG. 12. (a) illustrates the experimental arrangement used in observing m lines, and (b) is a photograph of the m lines observed in a ZnO/glass waveguide. Each m line shown in this photograph represents one waveguide mode. The numbers at the bottom of this photograph indicate the orders of the modes (Tien, Ulrich, and Martin, 1969).

According to Eq. (14), the x components of the wave vectors for the diffracted waves have two terms: One is the x component of the original wave vector \mathbf{k} of the incident wave. The other is a component provided by the grating and has a magnitude $m(2\pi/d)$, in accordance with the order of the diffraction m . For this reason, the component $m(2\pi/d)$ in (14) is called a grating vector. Note that the grating vector is in the plane of the film and normal to the corrugated lines.

According to Fig. 13, we could design a grating so that one of the k_{xd} 's in Eq. (14) equals to one of the eigenvalues of the waveguide modes. In this case, one of the diffracted waves will propagate in the waveguide and the grating serves as a coupler which couples the incident light beam into the waveguide. Experimentally, the grating coupler has rarely had a coupling efficiency better than 20%, since other orders of diffraction may match the eigenvalues of the radiation modes and they create losses by exciting waves in the airspace and the substrate. However, efficient coupling can be achieved if the laser beam is launched through the substrate in a way that none of the radiation modes are excited. Furthermore, one could blaze the grating for the best excitation of the waveguide modes (Dakss *et al.*, 1970; Kogelnik and Sosnowski, 1970; Harris *et al.*, 1972; Hope, 1972; Ogawa *et al.*, 1973; Dalgoutte, 1973; Turner *et al.*, 1973; Neviere, 1973; Ulrich, 1973; Tomlinson, 1975; Aoyagi *et al.*, 1976).

To form a corrugated surface on a substrate or on a film, we first spin coat the surface with a positive photoresist such as Az-1350J. The photoresist coating is then exposed to two oblique beams of uv light which interfere to form alternating dark and bright fringes. In the areas of the surface exposed to the bright fringes, the uv light acts to break down some of the bonds between the polymer molecules, thus reducing the average molecular weight of the resist. The coating in these areas

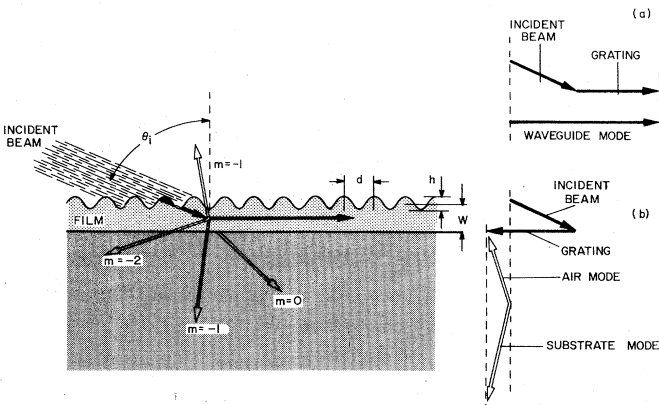


FIG. 13. The figure at the left shows how a grating can diffract an incident wave into many orders. A zigzag wave and thus a "waveguide" mode is excited in a waveguide only if one of the diffraction orders is in phase with the zigzag wave. The diagram in (a) shows the vector relation required for such a grating coupler. On the other hand, other diffraction orders of the grating could match the phases of the "substrate" or "airspace" modes and thus introduce losses to the coupling by diverting part of the incident energy into radiations in substrate or airspace.

is then removed by using an AZ developer. The photoresist mask thus formed has openings corresponding to the exposed pattern of the fringes. Finally, by ion-milling or chemical etching through these openings, a corrugated surface is formed on the substrate. Several interesting techniques have been developed for the fabrication of the gratings, particularly, on the GaAs surface. For example: By forming interference patterns in an oil bath, Shank and Schmidt (1973) produced $0.1-\mu$ periodic surface structures. In order to form wide grooves in a photoresist coating, Tsang and Wang developed a technique of "simultaneous exposure and development" (1974, 1975, 1976). Mollenauer *et al.* (1976) developed an ingenious method of translating the light beam in order to form large-area gratings. Recently, Austin and Stone (1976) were able to control the profiles of the gratings by exposing the resist simultaneously under interfered and uniform light beams. For GaAs surfaces, $H_2SO_4-H_2O_2-H_2O$ and Br_2-CH_3OH are common etchants. Preferential etching in GaAs has been discussed by Iida and Ito (1971), Tarui *et al.* (1971), and Comerford and Zory (1974).

F. Uniform and graded waveguides

All waveguides formed by vacuum deposition or sputtering have a very sharp interface between the film and the substrate; the refractive index is uniform throughout the film and it varies abruptly at the interface. Those waveguides are called *uniform waveguides* [Fig. 14(a)]. Waveguides formed by diffusion and those made of solid solutions have, however, gradual index profiles [Figs. 14(b) and (c)] and they are called *graded waveguides*.

In the waveguides formed by diffusion, the index decreases exponentially from the top surface as

$$n(z) = n_0 + \Delta n \exp(-|z|/d), \quad (15)$$

where Δn is the difference in refractive index between the top surface of the film and the substrate, and z is measured from the top film surface toward the substrate. Diffused waveguides were first formed by Taylor *et al.* (1972), and by Martin and Hall (1972) by dif-

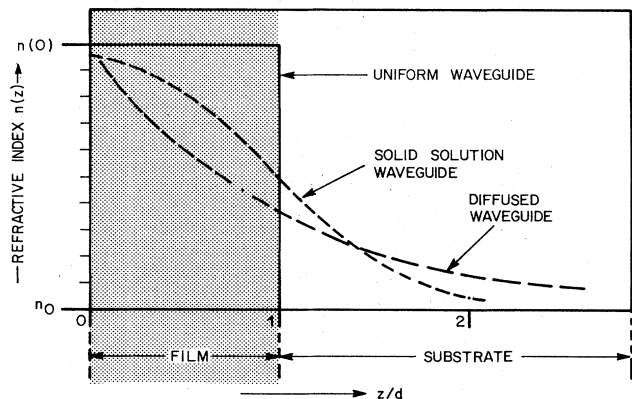


FIG. 14. We call "uniform waveguides" for those the refractive index distributions are step functions, and "graded waveguides" for those the refractive index profiles vary gradually from the film to the substrate.

fusing Se into CdS or ZnS crystals. They obtained $\Delta n/n_0$ ratios of typically several percent with values of d ranging from 2 to 10 μ . Later, LiNbO₃ waveguides were formed by Kamino and Carruthers (1973, 1974) by outdiffusing Li from LiNbO₃ and by Hammer and Philips (1974) by diffusing Nb into LiTaO₃. Excellent waveguides have also been obtained by diffusing Ti, V, Ni, and Cu into LiNbO₃, and LiNbO₃ into LiTaO₃ (Schmidt and Kamino, 1974; Noda *et al.*, 1974). Graded index distributions have also been observed in waveguides formed by melt-phase epitaxy (Miyazawa, 1973; Tien *et al.*, 1974; Ballman *et al.*, 1975). They have index profiles (Tien *et al.*, 1974) of

$$n(z) = n_0 + \Delta n \left[1 + \exp \left(\frac{z - d}{a} \right) \right]^{-1}. \quad (16)$$

Graded waveguides made by melt-phase epitaxy and by diffusion have been extensively used in forming light switches, modulators, and scanners.

Rather interestingly, the m lines observed from a uniform waveguide and a graded waveguide are strikingly different (Tien *et al.*, 1974). The photographs in Fig. 15 show that the spacing between two neighboring m lines increases with m in uniform waveguides, but decreases with m in graded waveguides. To explain this, we will use below WKB method to solve for the mode indices of the graded waveguides.

G. The potential-well model of the waveguide and WKB method

We can construct another model of the waveguide by considering the light waves in it as though they were electrons trapped in a potential well. This analogy allows the direct application of the WKB method to the calculation of the mode indices. The Schrödinger equation for an electron in a square-wave potential well [Fig. 16(a)] is

$$\frac{d^2\psi}{dz^2} + \frac{8\pi^2 m}{h^2} (E - V_j) \psi_j = 0, \quad j = 0, 1, 2, \quad (17)$$

where $V_2 > V_0 > V_1$. In the case of the waveguide, we add and subtract $k^2 n_1^2$ in (1a). Remember that $\partial^2/\partial y^2 = 0$ and $\partial^2/\partial x^2 = -\beta^2$; we obtain a wave equation of a uniform waveguide as

$$\frac{d^2 E_j}{dz^2} + [(k^2 n_1^2 - \beta^2) - (k^2 n_1^2 - k^2 n_j^2)] E_j = 0. \quad (18)$$

If we make then the associations

$$E \rightarrow \frac{k^2 k^2}{8\pi^2 m} (n_1^2 - \beta^2/k^2), \quad (19)$$

and

$$V_j \rightarrow \frac{h^2 k^2}{8\pi^2 m} (n_1^2 - n_j^2), \quad (19)$$

the Eqs. (17) and (18) will be identical. Here, in this model, we compare the bound state of an electron in a potential well with the waveguide mode in a film. It follows then that we may represent a uniform waveguide by the square potential well as shown in Fig. 16(b). In this figure, the proportionality constant $h^2/8\pi^2 m$ in Eq. (19) is omitted for purposes of simplification. We can

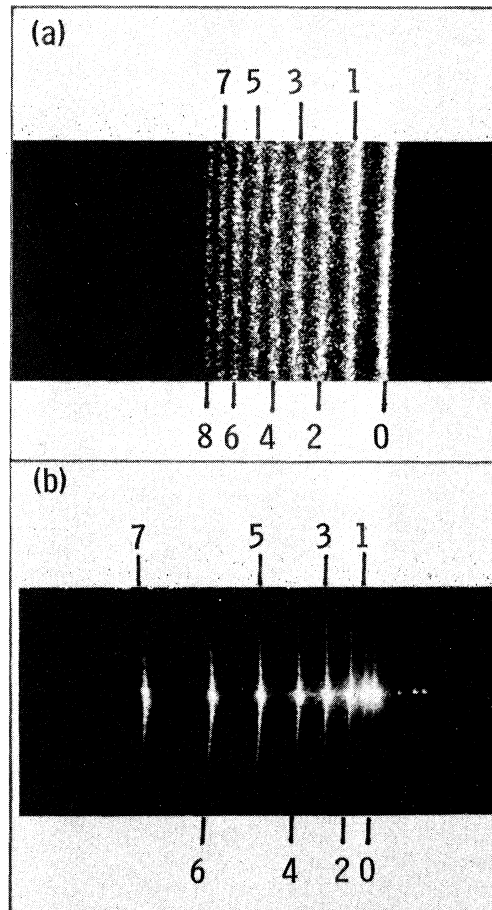


FIG. 15. The photographs in this figure show the m lines observed in (a) a "graded" waveguide, and (b) a "uniform" waveguide, and the numbers indicate orders of the waveguide modes. Interestingly, the spacings of the m lines in a "graded" waveguide decrease with the mode order, m , whereas those of a "uniform" waveguide increase with m . (Tien, Riva-Sanseverino, Martin, Ballman, and Brown, 1974).

easily justify Fig. 16(b) as follows: Imagine a plane wave, a TE wave for example, to initially be in the film. This plane wave has a kinetic energy $(kn_1)^2$ and a wave vector kn_1 which is its momentum. Consider, hypothetically, that the wave leaves the film and enters the substrate. In the substrate, the wave vector assumes a new value kn_0 and the wave has a new kinetic energy $(kn_0)^2$. This reduction in the total kinetic energy from $(kn_1)^2$ to $(kn_0)^2$ must be compensated for by an increase in the potential energy across the film-substrate boundary. Consequently, the potential of the well representing the waveguide [Fig. 16(b)] must rise by the amount $k^2(n_1^2 - n_0^2)$ at the film-substrate interface. We also observe that in this model, the energy level E of the electron corresponds to $(kn_1)^2 - \beta^2$ of the waveguide mode, which is simply b_1^2 . Had we started waveguide theory from the potential-well model, we would have used b_1^2 instead of β as the eigenvalue of the waveguide mode.

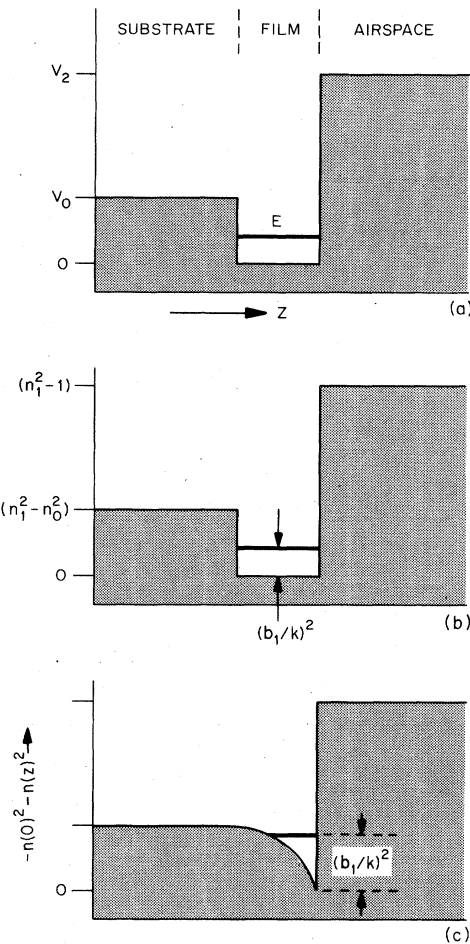


FIG. 16. As far as the field distribution is considered, a light wave in a waveguide may be analyzed as an electron trapped in a potential well. The diagram in (a) shows the usual potential energy distribution and an energy level E of an electron in a square potential well. The diagrams in (b) and (c) show, respectively, the similar distributions of $n^2(0) - n^2(z)$ in a "uniform" and a "graded" waveguide. Using this model, the eigenvalue of the waveguide mode corresponds to the energy level of the electron.

It is difficult to calculate mode indices of a graded waveguide. Conwell (1973) developed a theory which applies only to the case in which $n_1(z)$ varies exponentially. For an arbitrary index distribution, we naturally thought of using the WKB method. We proceed as follows: First, in a graded waveguide, b_1 is no longer a constant; it varies with $n(z)$ as

$$b_1^2(z) + \beta^2 = k^2 n_1^2(z), \quad (20)$$

which obviously follows from Eq. (12). Then, in the spirit of the WKB approximation, the mode Eq. (11) becomes (Tien *et al.*, 1974)

$$\int_0^{z_t} b_1(z) dz = \Phi_{10} + \Phi_{12} + m\pi, \quad (21)$$

where the limits of the integral $z=0$ and $z=z_t$ are the classical turning points of the wave function in the po-

tential well. The turning point z_t obviously satisfies the condition

$$b_1(z_t) = 0, \quad (22)$$

implying that at this turning point, we will have $\beta = kn_1(z_t)$. Since most graded waveguides are made of single crystal films, they will have refractive indices near or greater than 2.0, a value which is substantially larger than that of the airspace, 1.0. We thus can take $\Phi_{12} = \pi/2$ for all practical purposes. Since the quantity $(-2\Phi_{10})$ is the phase change which occurred in the wave function at the turning point z_t , making a standard linear approximation, Φ_{10} will then be given by $(\pi/4)$. Knowing Φ_{12} and Φ_{10} , equations (20), (21), and (22) can be used to solve for the mode indices. The WKB approximation used here turns out to be remarkably accurate. In Table II, the mode indices of a diffused waveguide calculated by the WKB method are compared with those from the exact theory of Conwell (1973). Surprisingly, the agreement between the two methods is better than 2 parts in 10 000.

Using the potential-well model, it is now easy to explain why the distribution of m lines (see Fig. 15) should differ between graded and uniform waveguides. In this model, waveguide modes are the bound states of an electron, and higher-order modes correspond to the higher energy levels. The area enclosed between each energy level and the bottom of the well in Fig. 16(c) is an integral of $b_1^2 dx$, while Eq. (21) involves an integral of $b dx$. Note that the potential well of the graded waveguide has a sloping bottom [Fig. 16(c)]. For maintaining the integral of $b_1 dx$ equal to a certain definite quantity as indicated in Eq. (21), the sloping bottom of the potential well has the effect of narrowing the spacings between the levels in the higher energy states and widening those in the lower energy states. Consequently, the spacing of the m lines of a graded waveguide appears to be gradually narrowing from the $m=0$ mode toward the higher-order modes.

TABLE II. The mode indices computed by the WKB method are compared with those computed by the exact theory of Conwell. Case 1 is calculated for a diffused waveguide in which $d = 2.23 \mu\text{m}$, $\Delta n = 0.0987$, and $n_0 = 2.177$. Case 2 is for another diffused waveguide in which $d = 0.931 \mu\text{m}$, $\Delta n = 0.043$, and $n_0 = 2.177$.

m	Conwell's theory	WKB method
A. Case 1: 9 modes		
0	2.2400	2.2399
1	2.2196	2.2192
2	2.2059	2.2057
3	2.1961	2.1959
4	2.1889	2.1888
5	2.1838	2.1835
6	2.1802	2.1800
7	2.1781	2.1778
8	2.1771	2.1771
B. Case 2: 2 modes		
0	2.1897	2.1898
1	2.1789	2.1790

III. TAPERED-FILM WAVEGUIDES AND RESEARCH IN THIN-FILM PRISMS, LENSES, AND CIRCUIT FORMATION

A. Tapered-film waveguides and tapered transitions

We shall discuss various wave phenomena associated with *tapered-film waveguides* and *tapered-edges* of the waveguides; these thin-film structures may be used to form *tapered transitions* between any two optical components and thus play an essential role in circuit formation in integrated optics. We define the term *tapered-film waveguide* in a rather broad sense. It could be a waveguide in which the thickness of the film increases or decreases gradually forming a long taper, or it could mean a waveguide in which the composition of the film varies. *Tapered transitions* also appear in various forms. For example, Fig. 17(a) illustrates a tapered transition which is simply a tapered-film waveguide joining smoothly two waveguides made of a same material but of different thicknesses. Figure 17(b) illustrates another typical tapered transition used to join two waveguides made of different materials. It involves a tapered edge of one film deposited on top of another film. As of today, *tapered transitions* are used extensively in forming thin-film prisms, lenses, and other passive optical components; they are also used as light wave couplers, as junctions between waveguides and as interconnections in optical circuits. Indeed, in order for a light wave to propagate continuously

in an optical circuit without disturbances, all optical devices should have tapered edges and be interconnected by tapered transitions.

Wave phenomena in tapered films were first investigated by Tien and Martin (1971). At that time, we were still searching for better materials to form optical waveguides, and in these early experiments, films were deposited by vacuum evaporation or by reactive sputtering. In order to measure thickness of the film, an edge of the film was routinely formed on the substrate; that was done by covering part of the substrate with a sheet of metal or plastic during the deposition process. We found, curiously, that the edges of the films thus formed were always gently tapered, and they have a slope varying from 1:10 to 1:1000 depending upon the way that the substrate was masked. For example, a film 1- μm thick, could taper to nothing over a distance of 10 to 1000 μm , corresponding roughly to 10–1000 optical wavelengths. These tapered edges were thus perfect tapered-film waveguides. It was in these waveguide experiments that we observed refraction and total internal reflection of light discussed later. We also observed, at that time, that a light beam propagating in a thin film could mysteriously disappear in a tapered edge of the film. Based on those wave phenomena, Tien and Ulrich formulated a modified Snell's law (Tien and Ulrich, 1970; Tien and Martin, 1971), Tien and Martin formed tapered-film couplers (Tien and Martin, 1971; Tien et al., 1975) and Tien et al., developed methods of forming light-guiding interconnections in optical circuits (Tien et al., 1973). Tapered-film waveguides and tapered transitions have been formed by vacuum evaporation, reactive sputtering, gas-discharge polymerization, liquid-phase epitaxy, and molecular-beam epitaxy (Tien and Martin, 1970; Tien et al., 1973, 1975; Logan and Reinhart, 1975; Reinhart and Logan, 1974, 1975; Merz, et al., 1975; Logan, 1976).

One requirement of the tapered transition is, of course, that its thickness or composition vary only slightly in one optical wavelength. Since the optical wavelength is small, tapered transitions can easily be formed and they are, in fact, formed naturally in most waveguide structures. Mainly because of these tapered transitions, the optical systems which we are going to discuss differ considerably with the microwave and the bulk optical systems. In an optical system made of bulk components, each time a light wave passes through an optical element, it will suffer a 6% reflection. These small reflections from a large number of optical elements can degrade the system. Similarly, in microwave systems, small reflections from junctions of the waveguides and those between the components pose a serious problem. In integrated optical circuits, however, thin-film devices are interconnected by tapered transitions; such reflections between optical elements simply do not occur. We may look at this problem in two different ways: First, as will be discussed in great detail later, to reflect effectively a light wave in a waveguide, the waveguide must have a corrugation with a period equal to half the optical wavelength. A tapered transition simply does not have such a corrugation. Secondly, if we divide a tapered transition into many small sections, the reflections from the different sec-

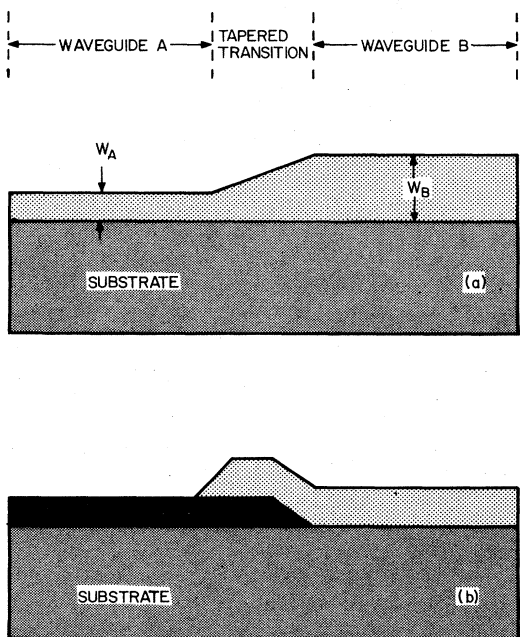


FIG. 17. The schematic drawings in this figure show examples of tapered transitions: In (a), a tapered transition joins smoothly two waveguides of different thicknesses, and in (b), the transition is formed by overlapping the ends of two waveguides. A tapered transition should have a structure which varies slowly in space as compared with the optical wavelength, and which must have a refractive index larger than the substrate.

tions will be small and furthermore be out of phase with one another, thus adding to zero.

Another unique property of the optical waveguides is that light scattered from a rough surface or a rough spot does not form a reflected wave in the waveguide. Measurement of the scattered light from a film waveguide shows that most of the scattering is in the forward direction. Even if the light were isotropically scattered, the film is so thin and the solid angle subtended by the thickness of the film is so small that any light scattered backward into that solid angle is negligible. Because of this property and the one discussed earlier, reflections from scattering or from different optical components are seldom observed. Consequently, circulators and nonreciprocal devices, which play an important role in microwave systems, are not needed in optical circuits.

More importantly, in an optical circuit formed by smooth waveguides and tapered transitions, conversion between different waveguide modes does not occur; the light wave thus maintains itself in a single normal mode of propagation and the power in that waveguide mode is conserved throughout the circuit. We call this an adiabatic process. If the optical circuit is going to carry different channels of information in different waveguide modes, it will be of prime importance that one is able to design a circuit in which a light wave can propagate "adiabatically". Let us approximate the taper of the waveguide by a large number of small flat steps. Across each step, conversion between two waveguide modes is small since their respective fields are orthogonal to one another. Moreover, the waves converted in the successive steps do not add constructively, since the conversion considered here takes place between two waveguide modes which have different wave velocities. To summarize, we may conclude that a light wave is neither partially reflected nor subjected to mode conversion in a tapered transition.

B. Two-dimensional optics and the Goos-Haenchen shift

We have described previously waves and optics in waveguides as "surface waves" and "two-dimensional optics." To show such "surface waves" and "two-dimensional optics" analytically, let us decompose the three-dimensional wave equation (1a) into two separate equations given by

$$\left(\frac{\partial^2}{\partial x^2} + \frac{\partial^2}{\partial y^2} \right) \mathbf{E} = -\beta^2 \mathbf{E}; \quad (23)$$

and

$$\frac{\partial^2}{\partial z^2} \mathbf{E} = -b^2 \mathbf{E}, \quad (24)$$

where, in these equations, we recall $\beta^2 + b_1^2 = k^2 n_1^2$ in waveguides. Equation (23) describes a wave in the two-dimensional plane of the waveguide ($x-y$ plane). This wave has a wave vector and a phase constant equal to, respectively, the eigenvector and the eigenvalue of the "waveguide" mode discussed in Sec. II. B. It has, therefore, all the properties of the "surface wave" that we are looking for. In fact, what we have done above is to separate the horizontal motion of a zigzag wave in

Eq. (23) from its up-down motion in Eq. (24), and thus to show that the "surface wave" has to follow the horizontal motion of the zigzag wave. This horizontal wave motion is the "two-dimensional optics."

We notice that Eq. (23) is the usual wave equation in two-dimensional space, provided we replace the refractive index of the space by the mode index. Therefore, in two-dimensional optics that we shall consider, the mode index plays the role of the refractive index. In principle, the mode index can be made to vary in the $x-y$ plane by varying the thickness or the composition of the film. The problem to be considered in this section is then simply geometric optics in a space of variable refractive index, where the Fermat's principle and Snell's law, in terms of wave velocity, must hold.

Consider now specifically two film waveguides A and B with mode indices (β_A/k) and (β_B/k) , respectively and assume $\beta_A > \beta_B$. The two waveguides are joined by a tapered transition along the boundary $x-x'$ [Fig. 18(a)]. Since the mode index plays the role of the refractive index in two-dimensional optics, we may rewrite Snell's law as follows

$$\beta_A \sin \alpha_A = \beta_B \sin \alpha_B, \quad (25)$$

where α_A is the incident angle in waveguide A , and α_B is the angle of refraction in waveguide B . Both angles lie in the plane of the film (the $x-y$ plane according to our notation). Thus, if $\alpha < \sin^{-1}(\beta_B/\beta_A)$, refraction will

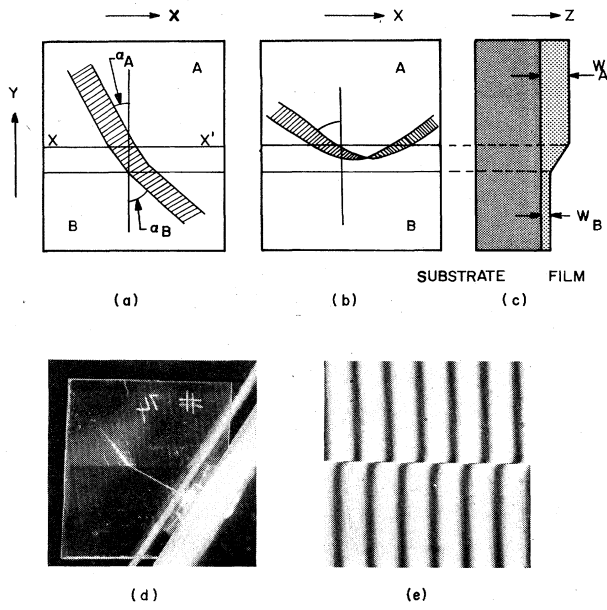


FIG. 18. The diagrams (a) and (b) illustrate refraction and total reflection of light observed between two film-waveguides, A and B . The side view of the waveguides used in this observation is shown in (c). In the experiment discussed in the text, a ZnS/glass waveguide was used for A and a polystyrene/glass waveguide for B . A photograph of the experimental observation is shown in (d). The photograph in (e) was taken under a Leitz interference microscope. The large shift in the interference fringes observed in this photograph at the junction of the waveguides A and B indicates that the two waveguides have widely different mode indices (P. K. Tien, and R. J. Martin, unpublished work).

occur at the boundary $x-x'$, and a light wave originated in waveguide A will be refracted into waveguide B according to the above equation.

Besides the use of mode indices instead of refractive indices in Eq. (25), refraction phenomenon in waveguides is somewhat different from that commonly recognized in bulk media. When a light wave is refracted in bulk media, part of the wave is reflected at the boundary, and in fact, Fresnel's formulae are commonly used to calculate the intensity of the reflection. This partial reflection may be attributed to a mismatch in wave impedance caused by the abrupt change in refractive index at the boundary, and can be eliminated entirely if the index varies gradually as in the case of the tapered transition. Such a possibility is well known in microwave theory and was discussed previously in Sec. III. A. It is thus important to note that, although we still can write Snell's law in two-dimensional optics, Fresnel's law of refraction no longer applies due to the tapered transition.

It is now clear that the refraction phenomenon is not due to the mismatch in wave impedance. Refraction can occur when the wave impedances of the two bulk media are not matched at the sharp boundary. It can also occur when the wave impedances of the waveguides are matched as in the tapered transition. We recall that Snell's law of refraction may be derived from Fermat's principle. Imagine a light wave propagating toward the boundary $x-x'$. Let us divide its wave front into small segments. Since different segments of the wave front cross the boundary at different times, a tilt in the wave front is necessary to render equal optical paths to all the segments. Since an optical path is defined as an integral of the product of the refractive index (or mode index) and the light path in physical space, the light beam will be tilted in a same manner, and thus the refraction will be the same, whether the index varies abruptly or gradually.

Another wave phenomenon which also is not related to the mismatch in wave impedance is the total internal reflection. One should not confuse the total reflection with the partial reflection discussed earlier. To show that total reflection can occur also in a tapered transition, we divide, this time hypothetically, the transition into small sections parallel to the $x-x'$ boundary [Fig. 18(b)], and calculate the optics occurring in the successive sections by repeatedly applying Snell's law. We find that, if $\alpha_A > \sin^{-1}(\beta_B/\beta_A)$, the light beam continuously changes its direction as it approaches the boundary until it completely turns around forming a total reflection. This concept that a light beam physically turns around in total reflection agrees well with a calculation of the group wave velocity and is also consistent with the Goos-Haenchen shift. Since we have used only Snell's law in the above, it is easy to show that total reflection phenomenon depends only upon the final values β_A and β_B of the two waveguides, irrespective of how the index is varied in the transition.

When a very narrow light beam is used to observe total internal reflection, the reflected beam is displayed slightly from the incident beam along the $x-x'$ boundary. This lateral displacement is called the Goos-Haenchen shift. Since optics occurring in waveguides may be

easily photographed under a microscope, the waveguide thus provides a unique opportunity to study closely this phenomenon, which in the past, has aroused considerable interest (Lotsch, 1968; Tamir and Oliner, 1969; Horowitz and Tamir, 1971; Renard, 1964; Kozaki and Mushike, 1975). Figure 19 is a photograph displaying, rather remarkably, an unusually large Goos-Haenchen shift observed at the tapered edge of a film waveguide. Such photographs have not been possible in bulk media.

To recapitulate, in bulk media separated by a sharp boundary, as a light wave is refracted at the boundary, part of the wave is reflected. The intensity of the reflection increases gradually as the incident angle approaches the critical angle until the light wave is totally reflected at the critical angle. For the waveguides joined by a tapered transition, however, the entire light beam is refracted into waveguide B (Fig. 18) as long as the condition $\alpha_A < \sin^{-1}(\beta_B/\beta_A)$ holds, and then, the total reflection appears suddenly at, and remains beyond, the critical angle, $\sin^{-1}(\beta_B/\beta_A)$. Refraction and total internal reflection discussed above are the two most important phenomena in two-dimensional optics, and the recognition of these wave phenomena in waveguides have made thin-film prisms, lenses, and other passive optical components possible.

C. Two-layered construction, light-guiding interconnections in optical circuits, and the potential-well model of the composite waveguides

One interesting method of circuit formation is the "two-layered construction". It requires two different films; the refractive index of one film should be significantly larger than that of the other. At visible and near-infrared wavelengths, III-V semiconductor compounds such as GaAs, AlAs, and GaP have refractive indices near or above 3.0. Other commonly used high-index materials such as ZnS, ZnO, Ta₂O₅, Nb₂O₅, LiNbO₃, and LiTaO₃ have indices between 1.9 and 2.4. Low-index materials are glass, SiO₂, and solution-deposited or gas-discharge-polymerized polymers; they have indices ranging from 1.4 to 1.7.

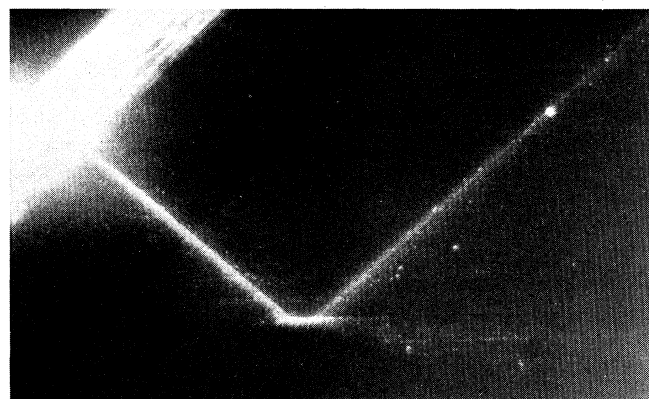


FIG. 19. The photograph shows an unusually large Goos-Häenchen's shift observed at the tapered edge of a film waveguide. In this photograph, the fine dark horizontal line is the tapered edge of the film, at which, the light wave shown is totally reflected (P. K. Tien and R. J. Martin, unpublished work).

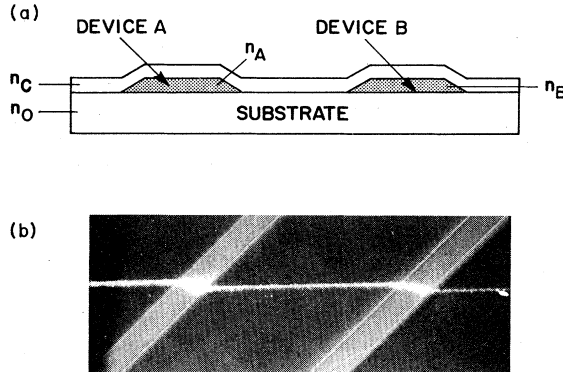


FIG. 20. The diagram in (a) illustrates two-layered construction. In this method, one first forms devices *A* and *B* on a substrate, which are then covered by film *C*. In the experiment described in the text, devices *A* and *B* are the two diagonal ZnS strips shown in the photograph in (b). The light wave propagated, from left to right, in the following order: first in film *C*, next in ZnS strip, then in film *C* again, in the second ZnS strip, and finally in Film *C*. In this case, film *C* is used for the interconnection between *A* and *B* as well as their input and output terminals (Tien, Riva-Sanseverino, Martin, and Smolinsky, 1974).

Figure 20(a) illustrates a typical arrangement of the "two-layered construction" (Tien *et al.*, 1974). Here, two thin-film high-index devices, *A* and *B*, each with tapered edges, are first formed on a substrate. The devices and the rest of the substrate are then covered by film *C* which has a refractive index considerably lower than the indices of the devices, but still larger than the index of the substrate. In the area that is not occupied by the devices, a light wave in the circuit will propagate in film *C*, since this is the only film present on the substrate. In the area occupied by either *A* or *B*, the light wave will enter and propagate in the device according to the rule of refractive index discussed in Sec. II. A. The light beam will thus be kicked up and down between the top film *C* and the lower film *A* or *B* which forms the device. It is evident from the above discussion that film *C* serves as the interconnection between *A* and *B*, and also as their input and output terminals in the circuit.

Let devices *A* and *B* discussed above be two ZnS strips deposited diagonally on the surface of a glass substrate as they are shown in Fig. 20(b). A plasma polymerized vinyltrimethylsilane (VTMS) film may be used as film *C*. The refractive indices of ZnS, VTMS, and glass are 2.3423, 1.5327, and 1.5125, respectively, at the 0.6328- μm line of the helium-neon laser. The photograph in Fig. 21(b) was taken by Tien *et al.* (1974) under the above experimental circumstances. It shows a light beam in the circuit, which was refracted each time it crossed a boundary of the ZnS strips. These refractions indicate that the light beam was truly in the VTMS film in the areas not occupied by the ZnS strips and that it propagated in the strips in the areas occupied by them. Since the mode index of the ZnS waveguide is quite different from that of the VTMS waveguide, such refractions should occur according to two-dimensional optics discussed in Sec. III. B.

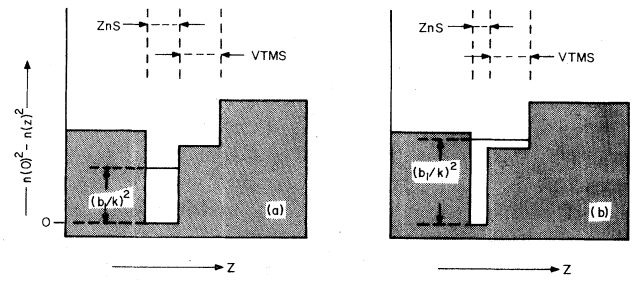


FIG. 21. The composite waveguide discussed in the text has two light-guiding films, a VTMS film and a ZnS film. Such a waveguide may be analyzed as two potential wells standing side by side. The diagram in (a) shows the case that the light wave is completely trapped in the ZnS film, whereas the diagram in (b) corresponds to the case that the light energy spreads over evenly in both films.

The phenomenon described above is readily explained by the potential-well model discussed in Sec. II. G. In the areas occupied by ZnS strips, the waveguide is made of two layers of the films, ZnS and VTMS. This composite waveguide (Tien *et al.*, 1973) can be represented by two potential wells standing side by side as shown in Fig. 21. Because of the large refractive index of ZnS, the potential well representing the ZnS film has a very deep bottom and the energy level for the TE $m=0$ mode is located below the bottom of the well representing the VTMS film. Consequently, the light wave is trapped in the ZnS potential well, leaving only evanescent fields in VTMS. On the other hand, if the ZnS layer were to be very thin, the energy level of the TE $m=0$ mode would be raised above the bottom of the potential well representing the VTMS film. In this case, the light wave would spread over both films. The "two-layered construction," therefore, works only if the mode index of the ZnS waveguide is sufficiently large for the light wave to be completely trapped in it. This is, of course, the limitation of this type of construction.

To overcome the above limitation of the "two-layered construction," we shall discuss another method of circuit formation, which applies to all possible cases (Tien *et al.*, 1973). Here again, we first form devices *L* and *M* on a substrate as shown in Fig. 22. In this method, however, the interconnecting film *G* does not cover devices *L* and *M* entirely. Of course, the edges of *L*, *M*, and *G* are tapered. Now consider Fig. 22 from left to right. In the part of device *L* that is not covered by film *G*, a light wave has to propagate in *L* alone. As the wave reaches the tapered edge of *L*, it is forced to propagate in film *G*. We can explain this using the potential-well model by computing the energy level in potential wells representing films *L* and *G*. In a similar manner, the light wave is forced to pass from *G* to *M* and then to propagate in *M* alone. In this method of interconnection, the refractive indices, the thicknesses and the relative positions of *L*, *M*, and *G* are not important. The only requirements are: that their refractive indices be larger than the index of the substrate and that their edges be gently tapered. Indeed, the light-guiding interconnections considered here for optical circuits are as simple as the formation of conducting paths in electronics.

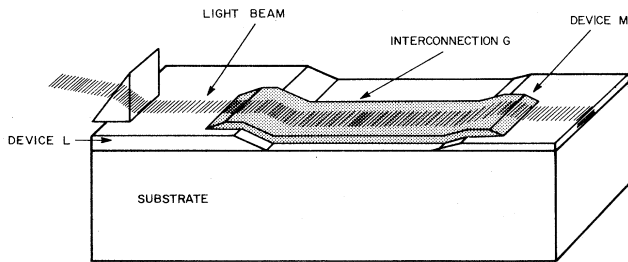


FIG. 22. The diagram illustrates another method to form a light-guiding interconnection. In this case, a light wave in device L is shown to enter film G through its left tapered edge, and then to leave film G into device M at the other tapered edge.

An interesting experiment (Tien *et al.*, 1973) to demonstrate the above method of interconnection is illustrated in Fig. 23. In this experiment, devices L and M are two VTMS films, both $1.17 \mu\text{m}$ thick ($n=1.539$). They are capable of carrying TE $m=0$ and $m=1$ waveguide modes with mode indices $N=1.5277$ and 1.4853 , respectively. The interconnection G is made of trimethylsilane ($n=1.567$) and is only $0.408 \mu\text{m}$ thick so that it will carry only TE $m=0$ mode. That is, TE $m=1$ mode is cut off in film G . The substrate is Corning 744 pyrex ($n_0=1.4704$). In the upper photograph of Fig. 23, a light beam launched in the TE $m=0$ mode in film L , at the left of the photograph, is observed to propagate freely from L to G and from G to M . There is no scattering of light at the tapered transitions, indicating that this method of interconnection works properly. In the lower photograph of the same figure, a light wave launched in the TE $m=1$ mode is observed to stop abruptly at interconnection G as it should, since the TE $m=1$ mode is cut off in the interconnection. This experiment also indicates that there is no conversion from the $m=1$ to the $m=0$ mode in the tapered transition as discussed in Sec. III.A; otherwise, the converted light would have gone through the interconnection and we would have observed a faint light beam in G and M .

D. Thin-film prisms, lenses, and other passive optical components

After having observed refraction and total reflection of light as discussed in Sec. III.B, the idea of forming thin-film prisms, lenses, and corner reflectors came naturally. Photographs of these basic waveguide components (Tien *et al.*, 1974, 1975) are shown in Fig. 24. These photographs were taken by facing the camera squarely at the film (the $x-y$ plane in our notation) and they show light paths traced by the surface waves in the waveguides. The sizes of these devices are roughly 1 mm along both the x and y directions. Consider, specifically, the thin-film prism in Fig. 24(b) as an example. The mode index of the waveguide inside the triangular area of the prism is 2.170, and that of the waveguide outside this area is 1.525. Of course, the above high-index and low-index waveguides are joined by tapered transitions. According to two-dimensional optics discussed in Sec. III.B, a light wave will be refracted as it enters the high-index waveguide inside the triangular area from the low-index waveguide outside this area. The light wave will be refracted again as it leaves the

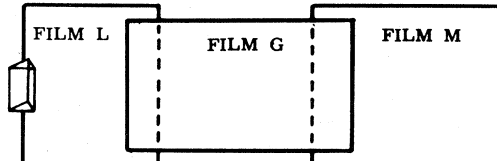
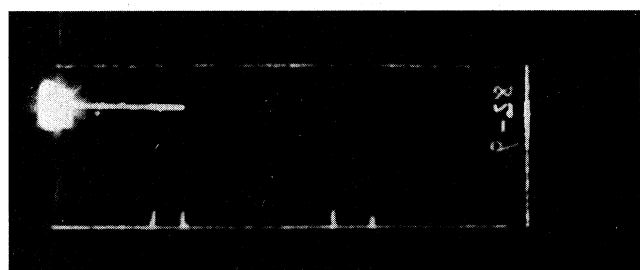
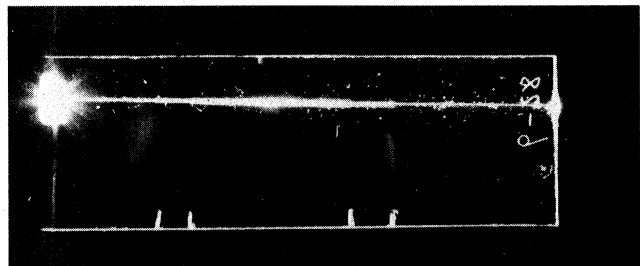


FIG. 23. The two top photographs were taken in an experiment used to demonstrate the interconnection method illustrated in Fig. 22. The bottom diagram shows the arrangement of films L , G , and M used in this experiment. Both films L and M can carry TE $m=0$ and $m=1$ modes, but the TE $m=1$ mode is cut-off in film G . The top photograph shows that a light wave excited in film L in the TE $m=0$ mode proceeded smoothly from L to G and to M indicating that this method of interconnection worked perfectly. In the lower photograph, the light beam stopped abruptly at film G , indicating that there was no mode conversion in the tapered transition. Otherwise, the converted light would have gone through and would have appeared as a faint beam in G and M . (Tien, Martin, and Smolinsky, 1973).

triangular area and reenters the low-index waveguide outside. These refractions are fully demonstrated in the above photograph and they cause the deflection of light in the prism. Figures 24(a) and (c) are, respectively, photographs of a thin-film lens and a thin-film polarizer, constructed based on the same basic principle. Figure 25 is a photograph of a thin-film corner reflector which is a direct application of the total reflection phenomenon discussed in Sec. III.B (Tien *et al.*, 1975).

Of course, the efficiencies of these thin-film passive optical components depend critically upon our ability to form two waveguides of widely different mode indices. Thin-film prisms and lenses were first reported by Ulrich and Tien at the Electron Device Research Conference in Rochester in 1969. They used two ZnS films of thicknesses 2400 \AA and 700 \AA , respectively, to form high-index and low-index waveguides. A glass substrate was used in their experiments (Ulrich and Martin,

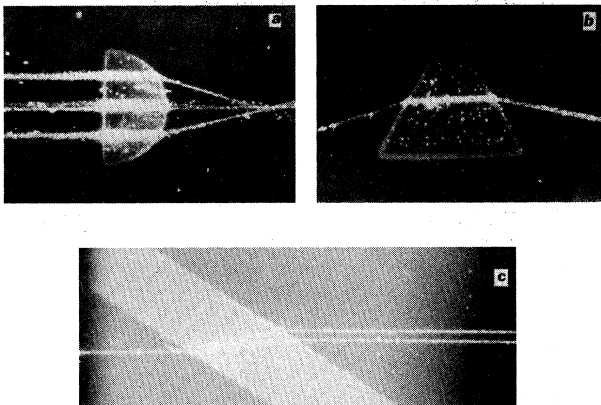


FIG. 24. Photographs in (a), (b), and (c) show, respectively, a thin-film lens, a thin-film prism, and a thin-film polarizer made in two-layered construction (Tien, Riva-Sanseverino, Martin, and Smolinsky, 1974).

1971). Subsequently, Shubert and Harris (1970) and Tien *et al.* (1974) formed prisms and lenses using the "two-layered construction" described in Sec. III. C. To form a thin-film prism by this method, one first deposits a high-index film, such as ZnS, in the triangular area only, and then covers the ZnS film and the rest of the substrate area by a layer of low-index film such as polystyrene. All devices shown in Fig. 24 were made by this method. Lately, Righini *et al.* (1972), Spiller and Harper (1975), and Verber *et al.* (1976) reported geodesic waveguide lenses. The geodesic lens is formed by first grinding a spherical depression into the surface of a glass substrate using a steel ball. A waveguide

layer is then formed in the glass by ion exchange in molten AgNO_3 salt for about 15 hours at 250°C .

Much can be said for the thin-film optical components described above. First, they are small and many of them can be formed simultaneously on a common substrate. Second, in a bulk optical system, the light beam always starts from a low-index medium, air, then goes through a high index optical element usually made of glass, and finally returns to the low-index medium of air. Such a system is called a "positive" optical system. In an integrated optical circuit, however, the optical element can be a waveguide with a mode index either larger or smaller than that outside the element. We may thus form either a "positive" or a "negative" optical system. It should be noted that a "negative" convex lens is a divergent lens. Finally, by properly choosing thicknesses of the films and waveguide mode, one can control the dispersion of the device. Furthermore, by shaping the thickness-profile of the optical element, one can correct for aberration. Because of these new capabilities, the design of a waveguide circuit is very different from that of a bulk optical system.

E. Directional couplers and branching waveguides

Directional couplers and branching waveguides are important components in microwave systems. They have been studied extensively in integrated optics for coupling a light wave from one waveguide to another, for switching and modulation of light, as frequency selective couplers, and as mode order converters (Marcatili, 1969; Kurazono *et al.*, 1972; Ihaya *et al.*, 1972; Yajima, 1973; Taylor, 1973; Wilson and Teh, 1973; Goell, 1973; Somekh *et al.*, 1973; Zernik, 1974; Schmidt and Kaminow, 1974; Auracher, 1974; Gedeon, 1974; Chandross *et al.*, 1974; Furuta *et al.*, 1974; Webster and Zernik, 1975; Hammer, 1975; Papuchon *et al.*, 1975; Campbell, 1975; Martin, 1975; Milton and Burns, 1975; Burns and Milton, 1975; Smith, 1975; Dalgoutte *et al.*, 1975; Burns *et al.*, 1976; Hsu and Milton, 1976; Standley and Ramaswamy, 1976; Schmidt and Kogelnik, 1976; Auracher *et al.*, 1976). In the tapered transitions discussed in Secs. III. A to III. C, light waves are transferred from one waveguide to another through a transition region in which the two waveguides are in mutual contact forming a composite waveguide. In the directional couplers shown in Figs. 26(a) and (b), however, two films (or two channel waveguides) *A* and *B* are separated by a small gap. The gap is filled with a material of low refractive index so that the coupling between *A* and *B* is through evanescent fields only. We call this type of coupling "optical tunneling". Figure 26(e) is a photograph of the directional coupler made by Standley and Ramaswamy (1976).

If the waves in *A* and *B* both propagate forward, the coupling is called *codirectional*. It is easy to show that, if the mode indices of *A* and *B* are exactly equal, the wave intensity in *A* will decrease as $\cos^2(\kappa x)$ and that in *B* will increase as $\sin^2(\kappa x)$, where κ and x are, respectively, the coupling constant and the coupling distance. A complete transfer of light energy between *A* and *B* will thus occur when $\kappa x = \pi/2, 3\pi/2, \dots$. On the other hand, if the mode indices of *A* and *B* are not

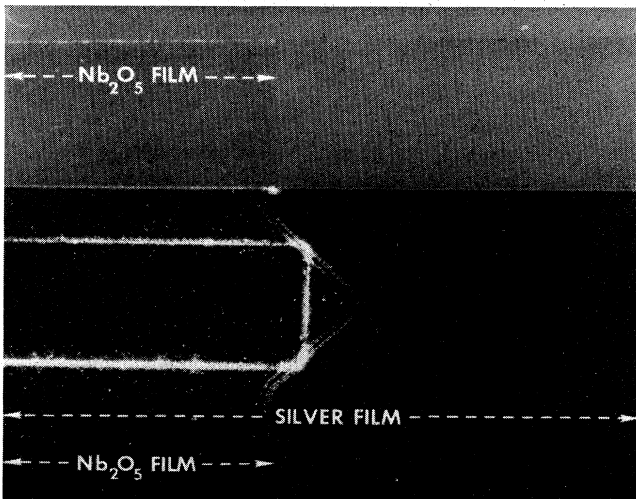


FIG. 25. The advantage of the metal-clad optical components is that they can be formed on any substrate. The above photograph shows a thin-film corner-reflector which has the structure of a silver-clad Nb_2O_5 waveguide (Tien, Martin, and Riva-Sanseverino, 1975).

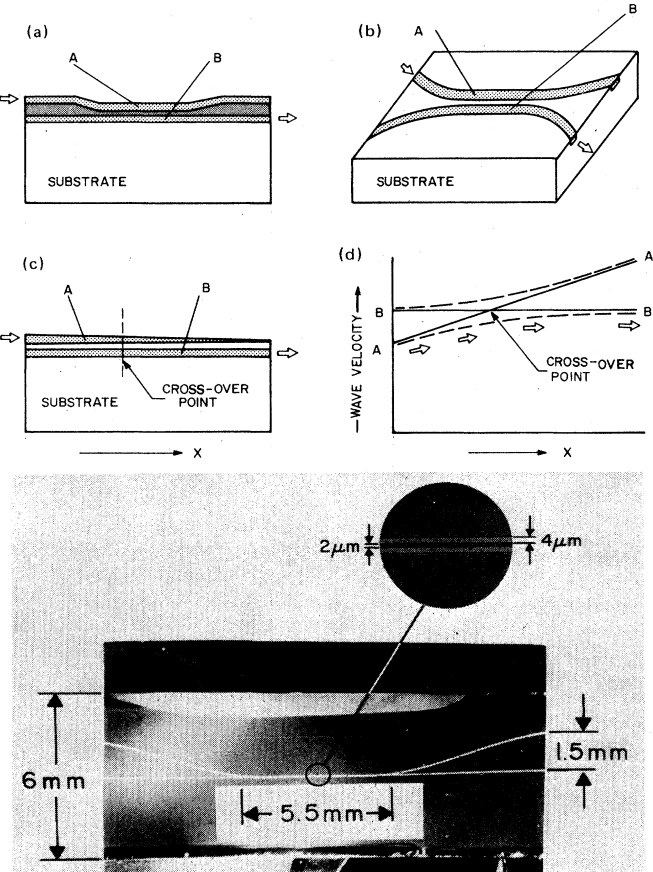


FIG. 26. Figures (a) and (b) illustrate directional couplers made from film-waveguides and from channel waveguides. Figures (c) and (d) show the tapered-velocity coupler discussed in the text. We have plotted, in (d), wave velocities of the two waveguides A and B , versus distance, x , along the waveguides. The dashed curves are the true velocities in the coupler, and the solid curves are the wave velocities, if the two waveguides are not coupled. The arrows indicate that a wave fed into waveguide A will be coupled to waveguide B in this coupler. Figure (e) is a photograph of a directional coupler made of two channel waveguides, each $4\text{-}\mu\text{m}$ wide. In the coupling region, the spacing between the two waveguides is $2\text{ }\mu\text{m}$. This directional coupler was made by R. D. Standley and V. Ramaswamy by diffusing Ti into LiNbO_3 (1976).

equal, the intensity in B will vary as

$$E_B^2(x) = E_A^2(0) \left(\frac{4\kappa^2}{\Delta\beta^2 + 4\kappa^2} \right) \sin^2 \left[\left(\frac{\Delta\beta^2 + 4\kappa^2}{4\kappa^2} \right)^{1/2} \kappa x \right].$$

Here $\Delta\beta = k\Delta N$, where $k = \omega/c$ as defined in Sec. II. B and ΔN is the difference in the mode indices of A and B . $E_B^2(x)/E_A^2(0)$ is reduced to $\frac{1}{2}$ when $\Delta\beta = 2\kappa$. Using the $0.6328\text{ }\mu\text{m}$ line of the helium-neon laser and assuming that the coupled region x is 2 mm long, it follows $\Delta N = 1.12 \times 10^{-4}$. Therefore, a very small difference in the mode indices of A and B can sufficiently decouple the two waveguides.

It is now evident that for a complete transfer of light energy from one waveguide to another waveguide via "optical tunneling," one has to control precisely the thicknesses of films A and B , or both thicknesses and widths if channel waveguides are used, so that their

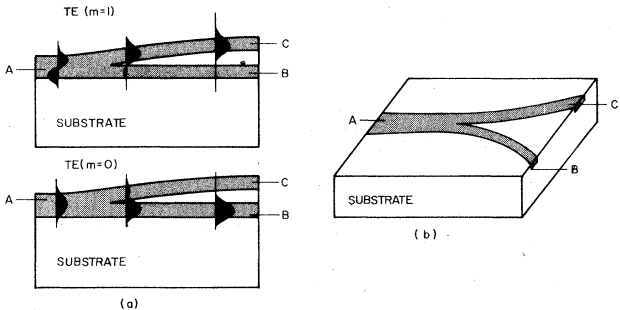


FIG. 27. The figures (a) and (b) illustrate a branching waveguide made from film waveguides, and from channel waveguides, respectively. In (a), we show that a TE $m=1$ mode excited at the input terminal A will be directed to the upper branch C , while a TE $m=0$ mode will be directed to the lower branch B . The operation of the branching waveguide depends upon the field distribution and the wave velocities of the input and branch waveguides at the branching point.

mode indices will be exactly equal. In addition, one must also control κx to be equal to an odd multiple of $\pi/2$, where κ depends on the gap between A and B , and x is the length of the coupling region. It is extremely difficult to meet all these conditions in practice. For this reason, "optical tunneling" is rarely used in integrated optics to form junctions between waveguides or interconnections in optical circuits. To perform these functions, the methods described earlier in Sec. III. B to III. C involving tapered transitions are far superior.

An ingenious method to relax the above stringent conditions of "optical tunneling" is to use a scheme called "tapered velocity coupler." This scheme is reminiscent of the "adiabatic fast passage of the magnetization reversal" used in the early MASER experiments of the 1950's. In the "tapered velocity coupler," the thickness of the film used for waveguide A , decreases gradually in x as shown in Figs. 26(c) and (d), so that the thicknesses of films A and B are exactly equal at only one point. This point is called the cross-over point and its location is arbitrary. It is easy to show that, with this arrangement, a complete power transfer between A and B is always possible regardless of the value of κx provided it is sufficiently large (Wilson and Teh, 1973; Milton and Burns, 1975).

Branching waveguides are commonly known as "T" or "Y" junctions in microwave systems. A branching waveguide could be a film, A , which splits into two films, B and C , as shown in Fig. 27(a). It could also be a channel waveguide forming a Y in the plane of the film as shown in Fig. 27(b). The branching waveguide, shown in Fig. 27(a), was first studied by Yajima (1973). He showed that, if the thicknesses of the films used to form arms B and C are equal, the branching waveguide acts as a "mode separator" in the sense that an input wave in the TE $m=0$ mode will be directed only to the arm B and that in the TE $m=1$ mode will be directed only to the arm C . He explained this by showing that TE $m=0$ (TE $m=1$ mode) has nearly the same mode indices in the input arm and arm B (arm C). If the thicknesses of the films used for B and C are not equal, there will be mode conversion at the branching point. This problem has been studied in detail by Burns and

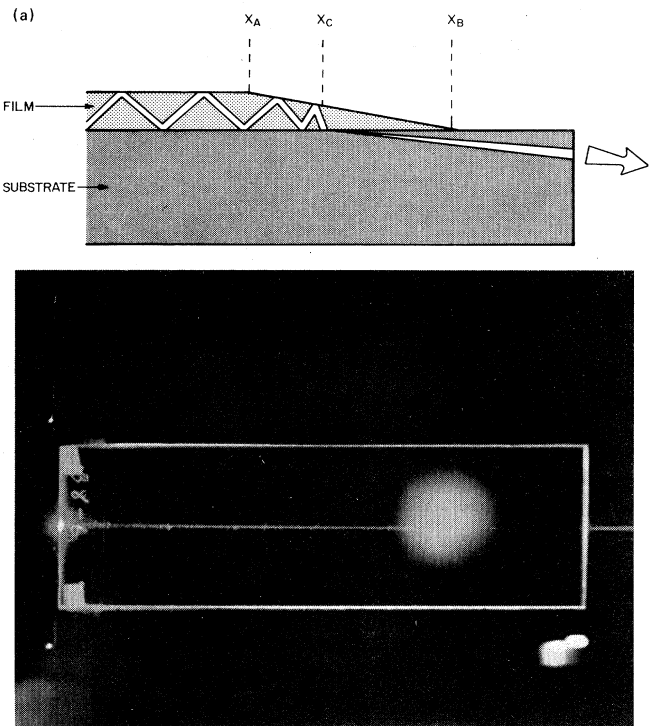


FIG. 28. To explain physics of the tapered film coupler, we should look at the up-down motion of the zigzag wave in the x - z plane of the coupler. In (a), we show that a zigzag wave enters into the tapered edge of the film ($X_A \rightarrow X_B$). The zigzag angle of the wave becomes smaller and smaller, and eventually, at point X_c , the angle becomes smaller than the critical angle at the film-substrate interface. The light wave then can no longer be totally reflected at the interface, and instead, enters into the substrate. The photograph in (b) shows an experimental demonstration of the coupler. A light beam in a ZnS film was coupled into a glass substrate at a tapered edge and then through the substrate entered into outside space. Note that the glass substrate did not scatter the light; the light beam became totally invisible, once it entered into the substrate. The circular spot light shown near the center of this photograph was used in order to make the tapered edge of the film visible (Tien and Martin, 1970).

Milton (1975). In any case, one must examine indices of waveguide modes in each arm and field distribution at the branching point in order to determine if there is a mode conversion, a mode splitting, or simply a power division. Often, one has to control minute details of the structure in order to duplicate the performance of a branching waveguide.

Returning to the directional coupler, we have shown that the intensity of the light wave coupled into waveguide B can be cut to a half by varying ΔN from 0 to 1.12×10^{-4} . Such a small amount of ΔN can easily be produced by an electric field in an electro-optic material such as LiNbO_3 . Directional couplers and branching waveguides made in electro-optic material are therefore excellent optical switches and modulators. These applications will be discussed in detail later in Sec. IV. D.

F. Tapered-film light wave couplers and the cutoff property of the waveguide

We have discussed the use of tapered transitions for coupling between two waveguides. It turns out that they can also be used for coupling between a waveguide and a semi-infinite space such as the substrate. Undoubtedly, the coupling now concerns waveguide and radiation modes (see Sec. II. B). We shall also show that refraction and total reflection between two waveguides, which have been discussed previously in Sec. III. B, will also occur between a waveguide and a semi-infinite space.

The problem to be considered is illustrated in Fig. 28(a). We have, at the left, a uniform film deposited on a substrate forming an optical waveguide. The thickness of the film is then tapered to nothing in a tapered edge which leaves a bare substrate surface at the right. Assume a light wave propagating in the waveguide toward this tapered edge. We let the direction of the wave propagation be normal to the edge in *Case I*, and then let this direction vary in *Case II*. The angle between the wave propagation and the normal of the edge will be denoted as incident angle α_i . Of course, this angle is in the plane of the film, and according to our notation, the film is parallel to the x - y plane. In *Case I*, $\alpha_i = 0$.

Figure 28(b) is a photograph taken under the conditions described for *Case I*. In this experiment (Tien and Martin, 1970), a ZnS film ($n = 2.342$) deposited on a glass substrate ($n = 1.512$) formed the waveguide, and the film had a tapered edge which was made visible in this photograph by projecting a condensed spot light to the film. Light from a helium-neon laser ($\lambda = 0.6328 \mu\text{m}$) was used to excite a wave which propagated from left to right in the TE $m = 0$ mode ($N = 1.984$) of the waveguide. This light beam was clearly visible in the waveguide at the left of the tapered edge, but disappeared completely in the space at the right of this edge. We have mentioned earlier in Sec. III. A that experiments of this sort have led us to investigate wave phenomena in tapered transitions.

The light beam which disappeared in the space at the right of the tapered film edge, actually went into the substrate. Since the glass substrate does not scatter light, the light beam in it became totally invisible. We have explained this phenomenon in Sec. II. A by the rule of refractive index. We shall now consider this problem in more detail using the zigzag-wave model. Figure 28(a) illustrates the optics in the x - z plane. As the zigzag wave in the waveguide enters into the tapered section, the zigzag angle θ_1 becomes smaller and smaller, and eventually, at the point X_c , becomes smaller than the critical angle, $\sin^{-1}(n_0/n_1)$, of the film-substrate interface. The light will then no longer be totally reflected at the interface, but instead, will be refracted into the substrate. Indeed, in the experiment, we did observe a light beam emerging from the substrate exactly as it is shown in Fig. 28(a). In wave theory, the waveguide mode becomes cut off beyond the point X_c (see discussion in Secs. II. B and II. C), and there, the solution of the wave equation must be "substrate" modes. Thus, the wave theory also predicts that the light wave will

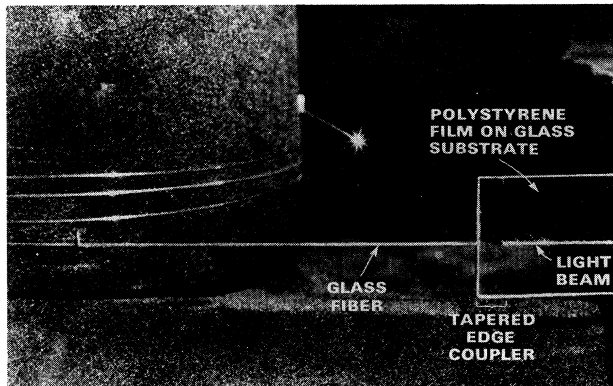


FIG. 29. In the experiment shown in the above photograph, a light beam in a polystyrene/glass waveguide was coupled into the substrate through a tapered edge of the film. The radiation in the substrate was then intercepted by a glass fiber. This film to fiber coupler had a coupling efficiency better than 90% (Tien, Smolinsky, and Martin, 1975).

enter the substrate beyond the point X_c .

Interestingly, the light radiated into the substrate forms a thin pencil beam and this beam is projected at an angle of about 4° below the film-substrate interface. These experimental observations have been verified by a detailed calculation based on ray optics and also by a wave theory involving the coupling between "waveguide" and "substrate" modes (Tien et al., 1975). These calculations additionally show that light energy in the waveguide is completely transferred into the substrate within a distance of merely 10 optical wavelengths from the cutoff point X_c . It is thus possible to couple a light wave in the waveguide into a space outside the waveguide via the substrate, or vice versa since optics is reciprocal. It is also possible to intercept the radiation in the substrate by an optical fiber as in the experiment (Tien et al., 1975) illustrated in Fig. 29. A tapered edge of the film used for such purposes is called a tapered-film light wave coupler (Tien and Martin, 1970; Tien et al., 1975; Reinhart and Logan, 1975; Merz et al., 1975; Logan, 1976).

Next, we shall consider Case II, as the incident angle α_i varies. We recall that α_i is the angle in the plane of the waveguide and is measured between the light path and the normal of the tapered film edge. In Case I ($\alpha_i = 0$), we have studied the up-down motion of the zigzag wave in the vertical $x-z$ plane [Fig. 28(a)]. Now that $\alpha_i \neq 0$ in Case II, it is necessary to study wave motion in the horizontal $x-y$ plane as well as in the vertical plane. In Sec. III. B, we have expressed wave motion in three-dimensional space by two-dimensional wave equations (23) and (24), in horizontal and vertical planes, respectively. We should expect the wave motion in the vertical plane to be the same for both Cases I and II, since, when Eq. (24) is considered, the angle α_i does not enter into the picture. We also recall in the discussion of Secs. II. B and II. C., that the mode index is n_0 for the substrate mode representing a plane wave which propagates in the substrate along the film-substrate interface, and is n_2 for a plane wave directed at an angle, $\sin^{-1}(n_2/n_0)$, below the interface. Since the

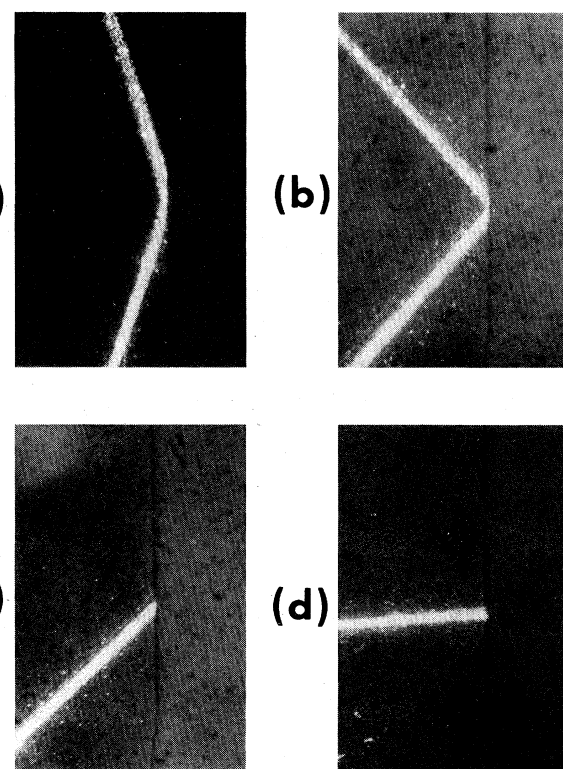


FIG. 30. A series of photographs shows experiments of refraction and reflection of light at a tapered edge of a ZnS/glass waveguide. The tapered edge appears in these photographs as a dark vertical line. In the area at the left of this edge, there was a uniform ZnS film, and at the right of this edge, it was a bare glass substrate surface. We are showing here the light paths in the $x-y$ plane of the film. The light wave was launched in the waveguide from left to right toward the tapered edge. It may be seen that the light beam was either totally reflected as in (a) and (b) or refracted into the substrate as in (c) and (d). Of course, the light beam became invisible inside the substrate which did not scatter the light. The incident angle α_i in the plane of the film was 75° , 53° , 47° , and 3° , respectively, in (a), (b), (c), and (d). The critical angle at the ZnS/glass interface was 49.5° (Tien and Martin, 1970).

wave refracted into the substrate, discussed for Case I, is only 4° below the interface, we may take the index of the substrate mode equal to n_0 for all practical purposes.

We now consider wave motion in the horizontal $x-y$ plane for Case II. The $x-y$ plane is divided into two halves by the tapered edge of the film (see Fig. 30). For the left half of the plane, we use the index of the waveguide mode N_1 in the wave equation (23). For the right half plane, we use in (23) the index of the substrate mode, which we argued above to be equal to n_0 . The solution of the problem is then simply Snell's law in the form

$$N_1 \sin \alpha_i = n_0 \sin \alpha_r,$$

where α_r is the angle of refraction in the $x-y$ plane. We may now conclude that, if $\alpha_i < \sin^{-1}(n_0/N_1)$, the light beam in the waveguide will be refracted into the substrate. The light path in the $x-y$ plane follows the

above equation and the zigzag wave in the vertical plane is identical to that shown for Case I. If, however, $\alpha \geq \sin^{-1}(n_0/N_1)$, the light beam in the waveguide will be totally reflected at the film edge. As usual, the reflected beam has the same mode index N_1 , and the angle of the reflection is equal to the angle of incidence in the $x-y$ plane.

Figure 30 shows a series of photographs taken under the conditions described in Case II (Tien and Martin, 1970). The vertical dark line in each photograph is the tapered edge of the film, and a ZnS/glass waveguide occupies the space at the left of this edge. Photographs from (a) to (d) correspond to $\alpha_i = 75^\circ, 53^\circ, 47^\circ$, and 3° , respectively. The mode index N_1 is 1.984, and n_0 is 1.512. The critical angle α_i which determines the refraction or total reflection of the light beam is $\alpha_i = 49.5^\circ$. Similar to the photograph shown in Fig. 28(b), when the light beam is refracted into the substrate, the beam disappears in the space at the right of the film edge. A close examination of these photographs shows that there is no partial reflection associated with the refraction of the light. We have discussed this thoroughly in Sec. III.B. In fact, our earlier discussion explains all the observations made in these experiments.

G. Metal-clad waveguides and method of isolating high-index substrates

For a lossy medium, we commonly use a complex refractive index $\hat{n} = n(1 + ik)$. Here, the real component n is the true refractive index and the imaginary component nk expresses loss in the medium. The quantity k is called the attenuation index or extinction coefficient and should not be confused with the coupling constant used in Sec. III.E. At the wavelength of 0.6328 μm , the complex refractive indices of silver, gold, and aluminum are, respectively, $\hat{n} = 0.065 + i40$, $0.15 + i3.2$, and $1.2 + i7.0$. They all have very large imaginary components and one would then assume that the metals are extremely lossy media for light wave propagation. What was not expected was the discovery of low-loss metal-clad waveguides and optical striplines (Otto and Sohler, 1971; Takamo and Hamasaki, 1972; Reisinger, 1973; Kaminow *et al.*, 1974; Tien *et al.*, 1975, 1976; Yamamoto *et al.*, 1975; Batchman and Rashleigh, 1975).

A metal-clad waveguide is formed [Fig. 3(d)] by depositing a light-guiding dielectric film on a metallic film (typically about 1000 Å thick) which serves as a substrate. An optical stripline is a light-guiding dielectric film sandwiched between two metallic films [Fig. 3(e)]. Since the fields in the waveguides penetrate into metallic films, why do these waveguides have low losses? For TE waves, the fields are very small at the metallic boundary, and thus Ohmic loss should be small in spite of the large extinction coefficient. This is not true, however, in the case of TM waves. We can explain this by showing that the wave equation and its solutions contain only \hat{n}^2 but not \hat{n} explicitly. Hence, in the waveguides of complex indices, the real and imaginary components of \hat{n}^2 (or dielectric constant) determine, respectively, the optics and the loss in light wave propagation. For silver, copper, and aluminum, $\hat{n}^2 = -15.996 + i0.520$, $-10.218 + i0.96$, and -47.56

TABLE III. Mode indices of an air-polystyrene-silver waveguide using a 1.81- μm -thick polystyrene film; and losses in air-polystyrene-silver waveguides.

Modes	Mode indices		Mode indices		
	Measured	Calculated	Modes	Measured	Calculated
TE ₀	1.582	1.574	TM ₀	1.577	1.571
TE ₁	1.547	1.547	TM ₁	1.543	1.538
TE ₂	1.503	1.502	TM ₂	1.484	1.484
TE ₃	1.438	1.438	TM ₃	1.407	1.406
TE ₄	1.349	1.351	TM ₄	1.304	1.302
TE ₅	1.238	1.238	TM ₅	1.169	1.168
TE ₆	1.092	1.095	TM ₆	1.004	1.014
Losses (dB/cm)					
Thickness of the polystyrene film (μm)		TE ₀	TE ₁	TM ₀	TM ₁
1		13.609	51.77	136.46	313.92
2		1.85	7.60	19.03	62.94
2.5		1.03	4.03	9.92	33.58
3		0.63	2.32	5.91	20.21

+i16.8, respectively. Judging from the imaginary components of \hat{n}^2 , the loss is small in silver, slightly larger in gold, and still larger in aluminum. Indeed, a detailed calculation based on wave theory shows the above concept is correct and aluminum-clad waveguides are far more lossy than silver-clad waveguides. In general, TM modes are more lossy than TE modes and, in all cases, the loss is higher in higher-order waveguide modes. Moreover, for a loss less than 1 dB/cm, the thickness of the dielectric film should be larger than 1 μm . The results of the calculation for silver-clad polystyrene waveguides are listed in Table III. In addition, light wave propagation in a silver-clad polystyrene waveguide and that in an aluminum-clad polystyrene waveguide are shown, respectively, in Figs. 31(a) and (b). Since a shorter light path indicates a larger loss in the waveguide, these photographs also indicate that aluminum is more lossy than silver.

The fact that the real component of \hat{n}^2 is negative is also interesting, especially since we have stated that this quantity determines the optics in waveguides. In fact, we may state the condition for waveguiding, as to have a larger real component of \hat{n}^2 in the film than in the substrate. Since the metallic substrate has a negative real component, we may use a dielectric film of arbitrarily low refractive index for the light-guiding layer and still satisfy the condition of waveguiding. Moreover, now that the real component of \hat{n}^2 is positive for the film, and negative for the substrate, the index of the waveguide mode may have any value between 1 and n_1 , a range much wider than that available to the usual dielectric waveguide. Because of this, metal-clad waveguides usually accommodate a large number of waveguide modes.

Figure 25 is a photograph of a corner reflector made of a silver-clad Nb_2O_5 waveguide (Tien *et al.*, 1975). Metal-clad devices such as this have many advantages: They are protected against stray light from the substrate beneath the metallic film, particularly since the

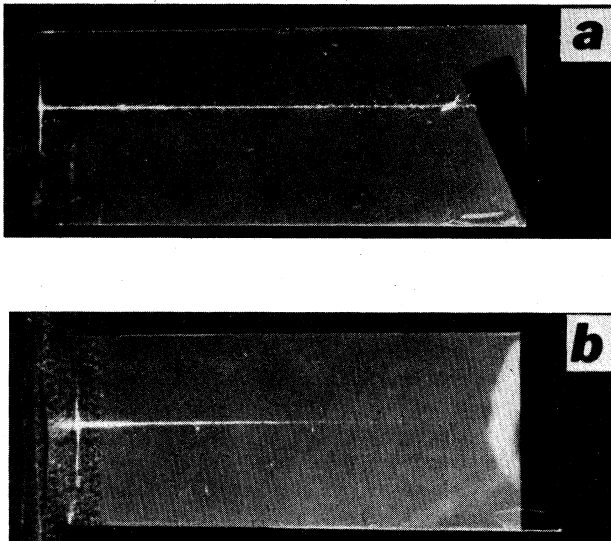


FIG. 31. Photographs (a) and (b) show light wave propagation in a silver-clad and in an aluminum-clad polystyrene waveguide. In such photographs, a short light path means a large loss in the waveguide (Tien, Martin, and Riva-Sanseverino, 1975).

substrate normally traps a large amount of light energy and is a source of interference. The metal-cladding can be used as an electrode and assists to dissipate the heat. More importantly, metal-clad components can be formed on any substrates regardless of its refractive index, and even on a lossy substrate.

High-index GaAs ($n \approx 3.6$), LiNbO₃ ($n \approx 2.29$), and silicon ($n \approx 4.0$) substrates are needed, respectively, for forming heterostructure lasers, diffused electro-optic modulators, and silicon photodetectors. On the other hand, passive optical components are better made by low-index materials such as glass ($n \approx 1.6$) or organic compounds ($n = 1.5$ to 1.7). To form a hybrid integrated optical circuit, therefore, one covers part of the high-index substrate by a layer of silver so that active devices are directly grown on the substrate and low-index passive components are formed on the silver layer. The high-index and low-index devices are then interconnected to form a circuit. Of course, one may also use SiO₂ instead of silver, since SiO₂ has a very small refractive index, $n = 1.47$.

Field distributions in metal-clad waveguides have been calculated by Reisinger (1973) and Kaminow *et al.*, (1974). Indices of the waveguide modes may be calculated from the mode equation (11) (see Sec. II. C) using complex refractive indices. Methods of forming junctions between the metal-clad waveguides and the usual dielectric waveguides have also been discussed (Tien *et al.*, 1976). Evaporated silver films could be patchy; the dielectric property of such patchy films may be analyzed using the Maxwell-Garnett theory (Maxwell-Garnett, 1904, 1906). The TM $m = -1$ mode of the metal-clad waveguide is the plasmon discussed by Otto (1971).

IV. PERIODIC WAVEGUIDES, MONOLITHIC INTEGRATED OPTICAL CIRCUITS, AND RESEARCH IN THIN-FILM LASERS, MODULATORS, AND SWITCHES

A. Periodic structures in optical waveguides

Theories of the diffraction grating are well-documented in optics. Periodic waveguides are also familiar to those who have worked with microwave traveling-wave tubes. These early studies have profound effects in integrated optics, and it is not accidental that the corrugated waveguide has become an important thin-film optical component. We have already discussed Rayleigh's grating theory in Sec. II. E. We will use frequently, below, the coupled mode theory which was first introduced by Pierce in the studies of microwave devices (Pierce, 1954; Tien, 1958; Louisell, 1960). The purpose of this section is to provide a broad theoretical background for the later discussion on laser structures. First, we will continue the discussion of the corrugated waveguide given in Sec. II. E, and show that the effect of the corrugated surface is to vary the mode index of the waveguide periodically in space. The result is a wave equation of periodic coefficient in the form of the Mathieu or Hill equation. We will then solve this wave equation by the coupled mode theory and discuss the solutions in terms of the "stop" and "pass" bands of wave propagation. Finally, in order to gain proper perspective on the problem, we will rederive wave solutions in the form of normal modes and discuss the group velocity and space harmonics of normal modes based on the Floquet theorem.

Consider now a light wave propagating in a corrugated waveguide, which is partly diffracted into another di-

rection. The problem we have here is to find a corrugation which allows both the incident and diffracted waves to propagate in the same waveguide mode. We have shown in Sec. II. E that we may consider a corrugated surface as the source of a wave vector mG in the plane of the film and oriented in the direction normal to the corrugated lines. Here, $m = -2, -1, 0, 1, 2, \dots$ gives the order of diffraction and $|G| = 2\pi/d$, where d is the period of the corrugation. Now, let β_i and β_d be the wave vectors of the incident and diffracted waves. These three wave vectors, β_i , β_d , and G , lie in the plane of the film and should satisfy the vectorial relation

$$\beta_d = \beta_i + mG; \quad |G| = 2\pi/d \quad (27)$$

which is, of course, the condition for Bragg diffraction. In integrated optics, we are particularly interested in the case where $m = -1$ and $\beta_d = -\beta_i$ (Fig. 32). Under these conditions, the diffracted wave will simply be a reflection of the incident wave. Let $|\beta_i| = |\beta_d| = 2\pi/\lambda$, where λ is the optical wavelength in the waveguide. We have from Eq. (27)

$$|\beta_i| = |\beta_d| = |G|/2; \quad \lambda = 2d.$$

Therefore, when the period of the grating is equal to half the optical wavelength in the waveguide, the diffracted wave of the $m = \pm 1$ order will be a reflection of the incident wave. A corrugated waveguide in this form may thus be used as a reflector in two-dimensional optics, and is called a Bragg reflector. Note that β_i , here, is an eigenvalue of the waveguide without the corrugated surface. The effect of the corrugated surface is just then the diffraction of the wave described above.

We can easily see what is happening in a Bragg reflector. As an incident wave travels forward in the waveguide, it passes by the many fringes of the corrugated surface. Each fringe reflects a small fraction of the incident wave; thus, we have many small reflected waves distributed over the surface of the corrugation. For this reason, the corrugated waveguide is also

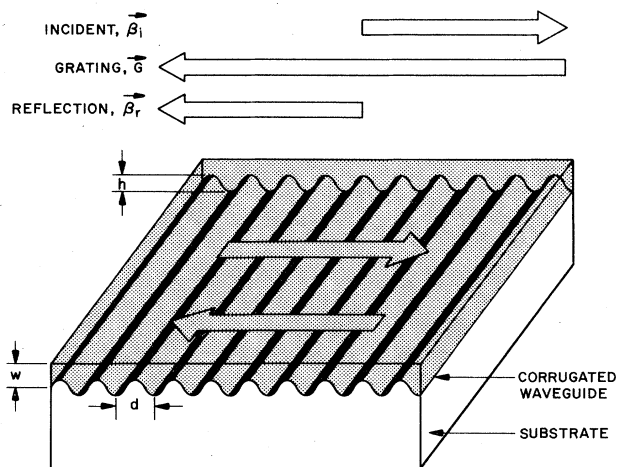


FIG. 32. The figure illustrates a corrugated waveguide which has a corrugated surface at the film-substrate interface. The vector diagram on the top shows the condition required to form a Bragg reflector.

called a distributed feedback circuit. Let us take the phase of the wave reflected at the first fringe as our reference. The wave reflected at the second fringe will then be excited half a period later. This wave travels backward a half-wavelength, reaching the first fringe, with exactly the same phase as that of the wave reflected from the first fringe. These two reflections thus add in phase. Similarly, the waves reflected from the third, fourth, ..., fringes also add constructively, all combining to form the largest possible reflection. Hence, Eq. (28) gives the condition for optimum reflection. Since β varies with the frequency ω of the light wave, only waves of one frequency will satisfy Eq. (28). The frequency ω and the phase constant β which satisfy this condition are called the Bragg frequency and the Bragg phase constant, and are customarily denoted by ω_0 and β_0 , respectively. Note that $\beta_0 = |G|/2 = \pi/d$.

As we stated earlier, the film lies in the $x-y$ plane and the waves propagate in the $\pm x$ directions. Unless otherwise specified, we shall, in future discussions, consider only the TE wave. As the thickness of the film varies periodically with the corrugation, the electric energy and magnetic energy stored in the waveguide also vary periodically along x . According to microwave theory, we may draw an equivalent circuit for the corrugated waveguide. Such a circuit would be in the form of a smooth waveguide loaded periodically with lumped capacitors or inductors. In a Bragg reflector, these capacitors or inductors would be spaced a half-wavelength apart and would act as the small obstacles producing the local reflections. Since we are dealing with distributed capacitors and inductors, the wave reflected at each obstacle will be 90° out of phase with the wave exciting it. The exact theory of the corrugated waveguide is difficult, but the concept of the equivalent circuit and the fact that we are dealing with an infinitely wide sheet of the surface wave in a waveguide (see discussion in Secs. II. B and III. B), allow us to represent the three-dimensional electromagnetic field problem by a one-dimensional wave equation which assumes that the mode index of the waveguide varies periodically in space.

Let us consider a perfectly sinusoidal corrugation with a period d and a peak-to-peak depth h (Fig. 32). Note that $\beta_0 = \pi/d$. If the thickness of the waveguide without the corrugation is W_0 , then the thickness with the corrugation will vary as

$$W(x) = W_0 + \frac{1}{2} h \cos 2\beta_0 x. \quad (29)$$

Since the mode index of the waveguide depends on the thickness of the film (see Sec. II. C), we may define $\beta(x)$ as the "local eigenvalue" which will vary in x in accordance with the change in $W(x)$. Strictly speaking, this quasistationary approach should not be used here, since $W(x)$ does not vary slowly with x . However, in practice, it is still a good approximation. We next proceed to calculate $\beta(x)$ by expressing it in the form of a Taylor series in h . For the first order approximation, we have

$$\beta(x) = \beta|_{W=W_0} + \left. \frac{d\beta}{dW} \right|_{W=W_0} \times \frac{h}{2} \cos 2\beta_0 x. \quad (30a)$$

The value of $d\beta/dW$ at $W = W_0$ may be computed by differentiating the mode equation (11) with respect to β :

we find immediately,

$$\beta(x) = \beta|_{W=W_0} + 2\kappa \cos 2\beta_0 x, \quad (30b)$$

and

$$\kappa = \frac{1}{4} (b_1^2/\beta) h (W_0 + 1/p_0 + 1/p_2)^{-1}, \quad (31)$$

where b_1 , p_0 , and p_2 are those values of a smooth waveguide of thickness $W = W_0$. It is important to realize in this formula that the coupling constant κ is the same regardless of whether the grating is formed on the top surface of the film or whether it is formed at the film-substrate interface. Using the $\beta(x)$ given by Eq. (30b) as the β in (23) and taking $\partial/\partial y = 0$, we obtain the wave equation for this type of corrugated waveguide, namely

$$(d^2/dx^2)E + (\beta^2 + 4\kappa\beta \cos 2\beta_0 x)E = 0. \quad (32)$$

In this equation, β is one of the eigenvalues of a smooth waveguide having thickness $W = W_0$, and $\beta_0 = \pi/d$ as determined by the period d of the corrugation. When the waveguide is designed such that $\beta = \beta_0$, (32) describes a Bragg reflector. We are interested in the solutions of this equation when β departs from β_0 by a small quantity δ given by

$$\delta = \beta - \beta_0; \quad \delta \ll \beta_0. \quad (33)$$

We can solve Eq. (32) exactly; the solutions are those of Mathieu's equation, and they represent the normal modes in a corrugated waveguide. Alternatively, since we know the eigensolutions of the smooth waveguide, we may construct from them the wave solutions of the corrugated waveguide. This type of the perturbation theory is called coupled mode theory and is only applicable if the periodic coefficient in (32) is small. It is instructive to discuss first the exact solutions of the Mathieu equation and then to proceed with the coupled mode theory which is usually adequate in integrated optics.

Denoting $X = \beta_0 x$, $a = \beta^2/\beta_0^2$, and $2q = -4\kappa\beta/\beta_0^2$, Eq. (32) becomes

$$d^2E/dX^2 + (a - 2q \cos 2X)E = 0 \quad (33)$$

which is, of course, Mathieu's equation. This equation has been discussed extensively in a book by McLachlan (1947). The solutions of the equation can be represented by a butterfly diagram (see Fig. 33). In this diagram, a and q are assigned to the vertical and horizontal axes, respectively. When $a (= \beta^2/\beta_0^2) = 1, 4, 9, \dots$, the Bragg conditions (27) for the orders $m = \pm 1, \pm 2, \pm 3, \dots$ are satisfied. The parameter $q (= -2\kappa\beta/\beta_0^2)$ gives the degree of perturbation caused by the corrugated surface. The shaded areas in the diagram indicate the stop-bands and the unshaded areas the pass-bands. We notice that the Bragg conditions $a = 1, 4, 9, \dots$, are located in the stop-bands. The waves in the stop-bands are exponentially increasing or decreasing functions. This is to be expected since in the Bragg reflector, the incident wave decreases exponentially as it converts itself into the reflected wave. In the pass-bands, the normal modes of the wave equation in the form of the periodic functions may be found since they represent the free running waves in the corrugated waveguide. At the boundaries between the stop- and pass-bands the solutions are Ce_n and Se_n functions; i.e., they are periodic functions formed from a

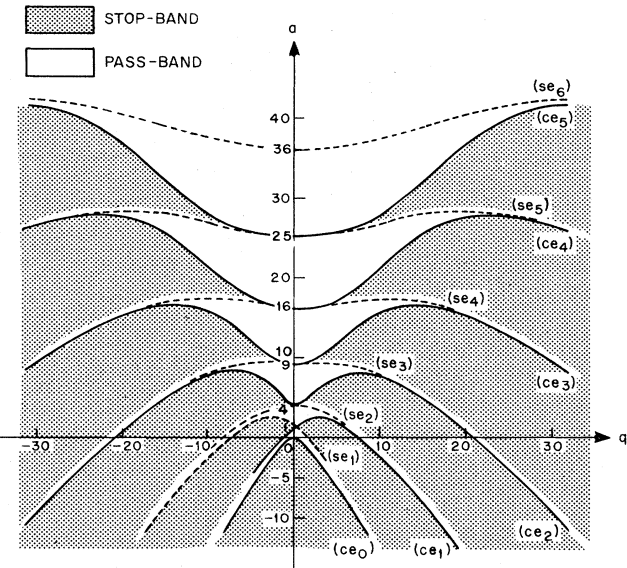


FIG. 33. Waves in a corrugated waveguide are solutions of the Mathieu equation. The above figure is the butterfly diagram of the Mathieu equation. The shaded areas are the stop bands. The Bragg conditions are located at $a = 1, 4, 9, \dots$, in this diagram.

series of terms involving $\sin(rX)$ and $\cos(rX)$, where $r = 1, 2, 3, \dots$. Since we are particularly interested in the case where q is small and $m = \pm 1$, the problem that we shall consider belongs to that area of the butterfly diagram in the vicinity of the point $a = 1$.

The exact solutions of the Mathieu equation are difficult to manipulate, since they involve a series of the terms which converge rather slowly. As long as we restrict ourselves to the case that the periodic coefficient in (32) is small, which is usually the case, we may proceed with the coupled mode theory below. By setting $\kappa = 0$ in (32), we find that the solutions are $B \exp[i\omega t - i\beta x]$ and $A \exp[i\omega t + i\beta x]$, representing, respectively, the forward and backward traveling waves in a smooth waveguide. It is easy to see that the corrugated surface introduces a coupling between the forward and backward waves, and we can describe this coupling effect by allowing the amplitudes, A and B , of the above waves to vary in x . Replacing A and B in the above solutions by $A(x)$ and $B(x)$, we put the true solutions of Eq. (32) in the form

$$\begin{aligned} a(x, t) &= A(x) \exp[i\omega t + i\beta x], \\ b(x, t) &= B(x) \exp[i\omega t - i\beta x]. \end{aligned} \quad (34)$$

Remember from (33) that $(\beta - \beta_0) = \delta$, where $\delta = 0$ is the Bragg condition. For small coupling, we expect $A(x)$ and $B(x)$ to vary slowly; if this is the case, $d^2A(x)/dx^2$ and $d^2B(x)/dx^2$ may be neglected. With this approximation, and with substitution of $a(x, t) + b(x, t)$ for E in Eq. (32), we find

$$\begin{aligned} dA(x)/dx &= -i\kappa B(x) e^{-i2\delta x}, \\ dB(x)/dx &= i\kappa A(x) e^{i2\delta x}. \end{aligned} \quad (35)$$

These equations are the coupled mode equations. We

notice that the coupling coefficients ($-i\kappa$) and ($i\kappa$) in these two equations are imaginary, agreeing with the concept of a smooth waveguide being loaded periodically with capacitors or inductors. Moreover, the two coefficients are opposite in sign. This is due to the fact that $a(x, t)$ and $b(x, t)$ travel in opposite directions. We call this type of coupling "contradirectional." We next note that the power carried by the $a(x, t)$ wave is $-|A(x)|^2$ and that by the $b(x, t)$ wave is $|B(x)|^2$. We may easily show from Eq. (35) that

$$(d/dx)[|B(x)|^2 - |A(x)|^2] = 0.$$

Thus the total power carried by the two waves is conserved. The solutions which satisfy (35) have the following forms

$$B(x) = R(x)e^{-i\delta x} = (r_1 e^{rx} + r_2 e^{-rx})e^{-i\delta x}, \quad (36)$$

$$A(x) = S(x)e^{i\delta x} = (s_1 e^{rx} + s_2 e^{-rx})e^{i\delta x},$$

where

$$r_1 = \frac{(-i\gamma - \delta)}{\kappa} s_1; \quad r_2 = \frac{(i\gamma - \delta)}{\kappa} s_2, \quad (37)$$

and

$$\gamma^2 = \kappa^2 - \delta^2. \quad (38)$$

Here, s_1 and s_2 are arbitrary constants which must be determined from the boundary conditions. When $\kappa > \delta$, γ is real and each term in $A(x)$ and $B(x)$ is an exponentially increasing or decreasing function. Solutions falling into this category are in the stop-band. When $\kappa < \delta$, we have an imaginary γ and the solutions which are periodic functions are in the pass-band. By our neglect of $d^2A(x)/dx^2$ and $d^2B(x)/dx^2$ earlier in the derivation, we have ignored here all the higher orders of diffraction other than $m = \pm 1$. By combining Eqs. (32), (34), (36), and (37), we have finally

$$a(x, t) = [s_1 e^{rx} + s_2 e^{-rx}] e^{i(\omega t + \beta_0 x)},$$

$$b(x, t) = \left[\frac{(-i\gamma - \delta)}{\kappa} s_1 e^{rx} + \frac{(i\gamma - \delta)}{\kappa} s_2 e^{-rx} \right] e^{i(\omega t - \beta_0 x)},$$

$$E(x, t) = a(x, t) + b(x, t). \quad (39)$$

Equations (36)–(39) are the basic equations which we will discuss below in detail.

Consider a corrugated waveguide located between $x=0$ and $x=L$. This corrugated waveguide is connected to a smooth waveguide at $x=L$ such that $a(x, t)=0$ at the point $x=L$. Let a wave incident at $x=0$ with an amplitude $B(0)$, we have then

$$a(L, t) = 0$$

and

$$b(0, t) = B(0) e^{i\omega t}.$$

Combining Eqs. (39) and (40), we find

$$a(x, t) = \left\{ \frac{-\kappa \sinh \gamma (x-L)}{i\gamma \cosh \gamma L - \delta \sinh \gamma L} \right\} B(0) e^{i(\omega t + \beta_0 x)}, \quad (41a)$$

$$b(x, t) = \left\{ \frac{i\gamma \cosh \gamma (x-L) + \delta \sinh \gamma (x-L)}{i\gamma \cosh \gamma L - \delta \sinh \gamma L} \right\} B(0) e^{i(\omega t - \beta_0 x)} \quad (41b)$$

$$\frac{a(0, t)a^*(0, t)}{b(0, t)b^*(0, t)} = \frac{\kappa^2 \sinh^2 \gamma L}{\gamma^2 \cosh^2 \gamma L + \delta^2 \sinh^2 \gamma L}, \quad (42a)$$

$$\frac{a(0, t)}{b(0, t)} = \left\{ \frac{\sinh \gamma L}{[\gamma^2 \cosh^2 \gamma L + \delta^2 \sinh^2 \gamma L^{1/2}]} \right\} e^{i\phi}, \quad (42b)$$

where

$$\phi = \arctan[(\gamma/\delta) \coth(\gamma L)]. \quad (42c)$$

Equations (42a) and (42b) give, respectively, the reflectivities in intensity and in amplitude at $x=0$. The former is plotted in Fig. 34 for several values of κ . Here, again, the shaded area indicates the stop-band. Note that the reflectivity is the largest at the Bragg condition $\delta=0$. It then slowly decreases in the stop-band and finally follows a curve roughly of the form $[\kappa \sin(\delta/\kappa)/(\delta/\kappa)]^2$ in the pass-band. The fact that the reflectivity is not always small in the pass-band is an important observation. Under the Bragg condition, $\delta=0$, we have $\gamma=\kappa$; (41) and (42a) then become

$$a(x, t) = \frac{i \sinh \kappa (x-L)}{\cosh \kappa L} B(0) e^{i(\omega t + \beta_0 x)},$$

$$b(x, t) = \frac{\cosh \kappa (x-L)}{\cosh \kappa L} B(0) e^{i(\omega t - \beta_0 x)},$$

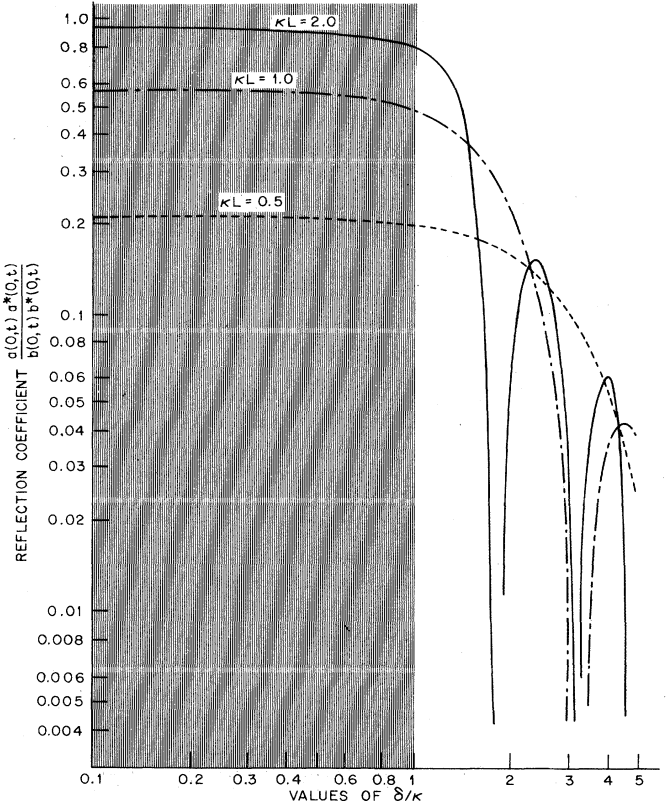


FIG. 34. In a corrugated waveguide, the reflection is maximum at the Bragg condition. The above diagram shows how the reflection coefficient varies as we move away from this condition. The curves are plotted versus δ/κ for $\kappa L = 0.5, 1.0$, and 2.0 , where κ is the coupling constant, and δ is the deviation (in phase constant) from the Bragg condition. The shaded area is the stop band.

$$\frac{a(0, t)}{b(0, t)} \frac{a^*(0, t)}{b^*(0, t)} = \tanh^2 \kappa L, \quad (44a)$$

$$\frac{a(0, t)}{b(0, t)} = -i \tanh \kappa L. \quad (44b)$$

It is important to note that, at $x=0$, $a(0, t)$, and $b(0, t)$ in Eq. (43) are 90° out of phase. This again confirms our earlier supposition that the waveguide is periodically loaded by capacitances or inductances.

Within a limited range of frequencies, δ is linearly proportional to $(\omega - \omega_0)$, where ω is the actual laser frequency used in the experiment, and ω_0 is the Bragg frequency satisfying Eq. (28). Figure 33 may then be interpreted as a reflectivity versus frequency plot. Thus, as we vary the frequency of the light wave in a corrugated waveguide, the reflectivity will be large in a band of frequencies centered at $\omega = \omega_0$ and will diminish beyond. The use of corrugated waveguides as band rejection filters has been studied by Kermisch (1969), Dabby *et al.* (1972, 1973), Uchida (1973), Flanders *et al.* (1974), Matshuhara and Hill (1974), Schmidt *et al.* (1974), and Hill (1974). In general, one can broaden the response of the filter by introducing a chirp in the corrugation. Additionally, one can reduce the side lobes by varying the depth of the corrugation.

In the coupled mode theory described above, we have assumed that $\beta \approx \beta_0$ so that only the $m=\pm 1$ order of diffraction would be important and all the other orders might be neglected. Similarly, if we may choose the period of corrugation so that $\beta \approx 3\beta_0$, the $m=\pm 3$ order would stand out as the important one. In fact, this third-order grating is commonly used in the laser diode experiments. In this case, we would need to replace the $\cos 2\beta_0 x$ in Eq. (32) by $\cos 6\beta_0 x$ and redefine $\delta = \beta - 3\beta_0$. All other results of the theory would be the same. Of course, the coupling constant κ for third-order diffraction would be much smaller than that of first-order. Various profiles of the corrugation have been investigated to enhance third-order diffraction.

Although solution $a(x, t)$ and $b(x, t)$ derived above are complete solutions of the wave equation, they are not the normal modes of a corrugated waveguide. The normal modes must satisfy the following conditions: First, a normal mode may be expressed in terms of a fundamental and many space harmonics. According to the Floquet theorem, these components have phase constants which can differ from one another only by a multiple of $2\pi/d$ or $2\beta_0$, where d is the period of the corrugation. Second, the fundamental and space harmonics must have a same group velocity so that they propagate together as a single unit. Finally, a corrugated waveguide, itself standing alone, is symmetric with respect to $\pm x$; the normal modes representing the forward and backward waves should contain identical amounts of the space harmonics. We shall now derive these normal modes below. Using relation (37), we rewrite Eq. (39) in terms of the constants s_1 and r_2 . The result is

$$a(x, t) = s_1 \exp\{i[\omega t + (|\gamma| + \beta_0)x]\} + \xi r_2 \exp\{i[\omega t - (|\gamma| + \beta_0)x + 2\beta_0 x]\}, \quad (45)$$

$$b(x, t) = r_2 \exp\{i[\omega t - (|\gamma| + \beta_0)x]\} + \xi s_1 \exp\{i[\omega t + (|\gamma| + \beta_0)x - 2\beta_0 x]\}, \quad (46)$$

where

$$\xi = \kappa / (|\gamma| + \delta). \quad (47)$$

Remembering that normal modes exist only in the passband, we have accordingly $\gamma = i|\gamma|$. We now group the first term in $b(x, t)$ and the second term in $a(x, t)$ as $F(x, t)$, and the remaining terms in Eq. (45) and Eq. (46) as $G(x, t)$. We find

$$\begin{aligned} F(x, t) &= r_2 \exp\{i[\omega t - (|\gamma| + \beta_0)x]\} \\ &\quad + \xi r_2 \exp\{i[\omega t - (|\gamma| + \beta_0)x + 2\beta_0 x]\}, \\ G(x, t) &= s_1 \exp\{i[\omega t + (|\gamma| + \beta_0)x]\} \\ &\quad + \xi s_1 \exp\{i[\omega t + (|\gamma| + \beta_0)x - 2\beta_0 x]\}. \end{aligned} \quad (48)$$

Solutions $F(x, t)$ and $G(x, t)$ in the above equations are the normal modes that we are looking for. They represent the forward and backward waves, respectively in the corrugated waveguide, reminiscent of the Bloch waves in a lattice structure. Here, r_2 and s_1 are the arbitrary constants to be determined by the boundary conditions at the two ends of the waveguide. We shall now show that $F(x, t)$ and $G(x, t)$ indeed satisfy the three conditions we imposed earlier for the normal modes. First, in $F(x, t)$, the first term is the fundamental and the second term, its $m=-1$ space harmonic. Their phase constants differ by $2\beta_0$ in accordance with Floquet's theorem. Next, since $d\omega/d(|\gamma| + \beta_0) = d\omega/d(|\gamma| - \beta_0)$, where $(|\gamma| + \beta_0)$ and $(|\gamma| - \beta_0)$ are, respectively, the phase constants of the first and second terms in $F(x, t)$, the fundamental and the harmonic have the same group velocity which is positive. Similarly, the two terms in $G(x, t)$ are, respectively, the fundamental wave and the $m=-1$ harmonic of the second normal mode. They too, have the same group velocity, this time, however, being negative. Finally, the quantity ξ which represents the ratio of the harmonic to the fundamental is the same in both $F(x, t)$ and $G(x, t)$. What is surprising, here, is that although $|\gamma|$ is a small quantity when compared to β_0 in the phase constants of the waves, it nonetheless determines the group velocity. It is also interesting to note that in coupled mode theory, waves of similar phase constants are grouped together whereas in the normal modes, waves are grouped according to their group velocities.

In the stop-band, γ is real and $F(x, t)$ and $G(x, t)$ in Eq. (48) give imaginary group velocities. We may thus define the stop bands as those regions in which the group velocities have imaginary values, and the passbands as those regions in which the group velocities are real. If $\kappa=0$, we have $\xi=0$ and $\gamma=\delta$. In this case, the harmonics in Eq. (48) disappear and $F(x, t)$ and $G(x, t)$ become, respectively, $\exp(i\omega t - i\beta x)$ and $\exp(i\omega t + i\beta x)$. The eigensolutions of a corrugated waveguide thus reduce to those of a smooth waveguide, as expected.

B. Bragg-reflector lasers and distributed feedback lasers

We shall discuss two important laser structures: Bragg-reflector (BR) lasers and distributed feedback (DFB) lasers; both involve corrugated waveguides (Kogelnik and Shank, 1971, 1972; Shank *et al.*, 1971;

Hill and Watanabe, 1972, 1973, 1975; Bjorkholm and Shank, 1972; Marcuse, 1972; Wittke, 1972; Zory, 1972; Wang and Sheem, 1973; Shubert, 1974; Nakamura, 1974; Wang, 1973, 1974; Aoyagi and Namba, 1974, 1975; Chinn, 1973; DeWames and Hall, 1973; Bjorkholm *et al.*, 1973; Elachi and Yeh, 1973; Chinn and Kelley, 1974; Haus and Shank, 1976; Haus, 1976; Yariv, 1973; Stoll and Yariv, 1973; Chang, 1973; Yariv and Yen, 1974; Cordero and Wang, 1974; Yariv and Gover, 1975; Nakamura and Yariv, 1974). The papers published on these subjects can be divided into three groups: The first group discusses the coupled mode theory of the DFB laser, including the papers by Kogelnik and Shank (1971, 1972), and Hill and Watanabe (1972, 1973, 1975). The second group of papers is by Yariv and Yen (1974) and Chinn and Kelley, dealing with the subject of a Bragg reflector in an active medium which is capable of amplifying light. The third group of papers (Wang and Sheem, 1973; Wang, 1973, 1974; Cordero and Wang, 1974; Yariv and Gover, 1975) treats the expansion of waves in normal modes, which has already been discussed in Sec. IV. A. A BR laser consists of three sections connected in cascade. The middle section is a smooth waveguide which contains the active medium capable of generating light. The two end sections are corrugated waveguides serving as the Bragg reflectors. The optical cavity used in the BR laser is thus not much different from a Fabry-Perot interferometer and the theory involved is straight forward. A DFB laser has only one section—a corrugated waveguide which is, itself, an amplifying medium. The laser is able to retain the optical energy generated by the amplifying medium, simply because the normal mode that carries the optical energy forward in the waveguide is coupled through its space harmonic to the normal mode that carries the optical energy in the opposite direction, and vice versa. Interestingly, the DFB laser cannot be operated at the Bragg condition. Several questions now arise: Why does the DFB laser have to be operated in the pass band? Will it be able to retain all the energy generated by the active medium? Will the operation of the DFB laser be affected by the way the corrugated waveguide is terminated at the two ends? We will discuss these questions and their answers.

Figure 35 shows several simplified laser structures. In all these structures, an active medium formed on a substrate serves as the optical waveguide. Either through electric excitation or by optical pumping, light is generated in the waveguide. In Fig. 35(a), the two ends of the structure are cleaved, providing mirrorlike surfaces from which an incident light wave may be reflected. The light wave will thus be reflected back and forth between the two cleaved surfaces, which, together with the waveguide, form a Fabry-Perot cavity. When the waveguide is pumped, the wave energy in the cavity will grow and oscillations will occur if the net gain in the medium is larger than the reflections loss at the two ends. The condition required for the onset of oscillation is called threshold. A laser is usually operated well above threshold. In this case, the wave intensity in the waveguide continues to rise after oscillation begins, until it is finally limited by some nonlinear

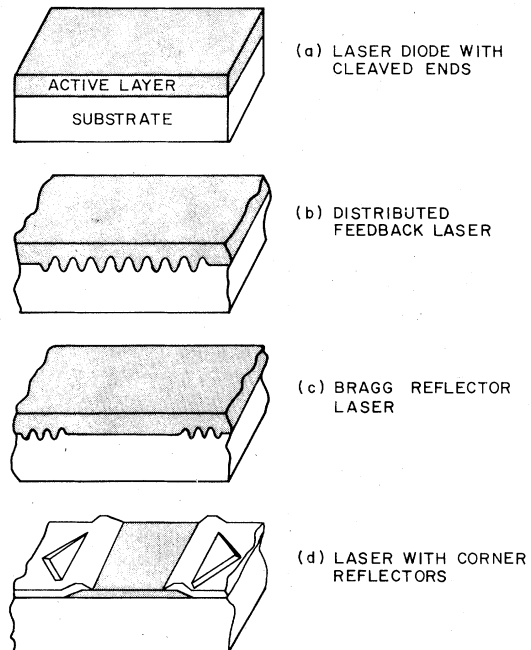


FIG. 35. Different laser structures considered in integrated optics.

process in the laser. Actually, without pumping, the waveguide (active film) in the GaAs injection laser diode is quite lossy, and a loss of 30 to 70 cm^{-1} is, in fact, common. The reflectivity at either cleaved end would be about 30% if light were directed normal toward the surface. Since a zigzag ray in the waveguide is not normal to the end surface, the reflectivity can be much higher depending on the waveguide mode in operation (see Reinhart *et al.*, 1971). The laser with a stripe geometry is typically 380 μm long and 13- μm wide. It is necessary to excite this laser with an electric current density on the order of 1000 A/cm^2 in order to provide sufficient gain to allow oscillation at room temperature.

Let the optical gain and absorption loss in the waveguide, in field amplitude per centimeter, be, respectively, α_g and α_i . If the reflectivity, in wave intensity, from either cleaved end is R , and the laser is $L \text{ cm}$ long, the threshold condition may be written as

$$R^{*2} \exp\{2(\alpha_g - \alpha_i)L\} = 1 \quad (49)$$

which is, of course, the basic equation governing any oscillator.

Once the two ends of a laser are cleaved, it is difficult to connect the laser to an optical circuit. For this reason, it is of interest to look for a method of reflecting light without physically interrupting the active film, thus enabling the active film to be a continuous part of the circuit. The Bragg reflector seems to be the natural candidate for this purpose. In Fig. 35(c), two Bragg reflectors are used in place of the cleaved ends of the laser discussed above. The resulting structure is called the Bragg-reflector laser (BRL) and will be discussed in detail below.

Bragg reflections can be very efficient. For example,

in a GaAs injection laser, the active waveguide has $n_0 = n_2 = 3.48$ and $n_1 = 3.60$. In the case of a grating 100- μm long with $h = 500 \text{ \AA}$ (see notation used in Sec. IV. A) and if the film thickness $W_0 = 0.40 \mu\text{m}$, one obtains, at the Bragg condition, $\kappa = 0.023$ and a reflectivity R , close to 96%. If, however, we increase the thickness of the active film, W_0 , to 1.0 μm , κ and R decrease to 0.0027 and 7.2%, respectively. In the Bragg reflector laser, only the space between the Bragg reflectors is pumped, providing gain [see Fig. 35(c)]. We thus protect the gain region of the laser from possible damages caused by the chemical or ion etching used to fabricate the gratings. On the other hand, we then need to add an extra length to the active waveguide in order to make room for the Bragg reflectors. This extra space is not pumped and can add a significant amount of loss to the semiconductor laser.

We next ask: why should we not place the Bragg reflectors inside the gain region and combine the left and right reflectors into a single corrugated waveguide? The result of this arrangement is the DFB laser shown in Fig. 35(b). Unfortunately, the DFB laser can only be operated in the pass-band. We thus cannot take advantage of the large reflectivity value obtainable under the Bragg condition. To put it in proper perspective, we assume for the moment that the gain in the waveguide is zero. We draw a line dividing the grating into two equal halves and locate this line at $x = 0$ (Fig. 36). Consider a light wave A launched at $x = 0$, propagating towards the right. Part of this light is reflected back by the corrugations in the waveguide. According to (44b), at $x = 0$, the reflected wave A' will have a phase 90° out from that of wave A , under the Bragg condition. This A' wave then continues to travel into the left half of the waveguide. Similarly, the light wave A'' reflected in

the left half of the waveguide will be 90° out of phase with the A' wave, and thus be opposite in phase with the A wave launched, originally, at $x = 0$. Therefore, under the Bragg condition, the light wave cancels itself in each round trip and wave energy in the laser can never be built up. By moving away from the Bragg condition, however, we introduce an additional phase shift between the A and A'' waves in the factor $\exp(\pm i2\delta x)$ in Eq. (35). In fact, it is necessary to move the operating condition actually into the pass band in order to have an added phase of π or some odd multiple of π . With this additional phase shift, the A'' and A wave indeed add in phase at $x = 0$, and the waves grow as they feed one another in each round trip. The added phase shifts of different odd multiples of π result in different frequencies of oscillation, which correspond to the different longitudinal modes of the laser.

We have shown in Fig. 34 that even in the pass band, the reflectivity can still be significant. Nakamura and Yariv (1974) have made calculations to compare the performance of DFB lasers with that of cleaved lasers. Their results are shown in Fig. 37. Here, the net gain $\alpha = \alpha_g - \alpha_i$ required for the laser to oscillate is plotted versus the length L of the laser for: (a) $h = 500 \text{ \AA}$ and $W_0 = 2, 1.5, 1.075$, and $0.5 \mu\text{m}$ and, (b) $W_0 = 1 \mu\text{m}$ and $h = 100, 250, 500, 750$, and 1000 \AA . The solid curves are for the DFB lasers and the dotted one for the cleaved lasers. In principle, for a given AlGaAs heterostructure, the DFB laser performs better than the cleaved laser if $(h/\mu\text{m}) \times L(\mu\text{m})/W_0(\mu\text{m}) > 20$. Thus, for $L = 400 \mu\text{m}$, the grating should be designed so that $(h/W_0) > 0.05$. In practice, however, the etched grating is far from perfect, introducing scattering loss in the cavity. The threshold of the DFB laser, at its best, only approaches that of the cleaved laser.

In the presence of the gain $\alpha (= \alpha_g - \alpha_i)$, the quantity β in Eqs. (30b) and (32), and δ in (33), Eqs. (35)–(42c) should be replaced, respectively, by $(\beta + i\alpha)$ and $(\delta + i\alpha)$.

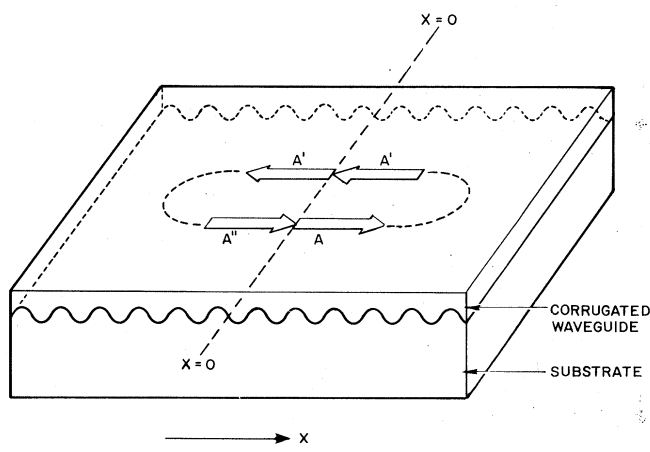


FIG. 36. The figure illustrates why a DFB laser cannot be operated in the stop band. We divide the corrugated waveguide into two halves at $x = 0$. Given the Bragg condition in the stop band, the phase of the A' wave will be 90° out of phase with the A wave. Similarly, that of the A'' wave will be 90° out of phase with the A' wave. The A and A'' waves are therefore opposite in phase at $x = 0$ and they cancel one another in a round trip. Hence, the energy in the DFB structure will not grow under the Bragg condition.

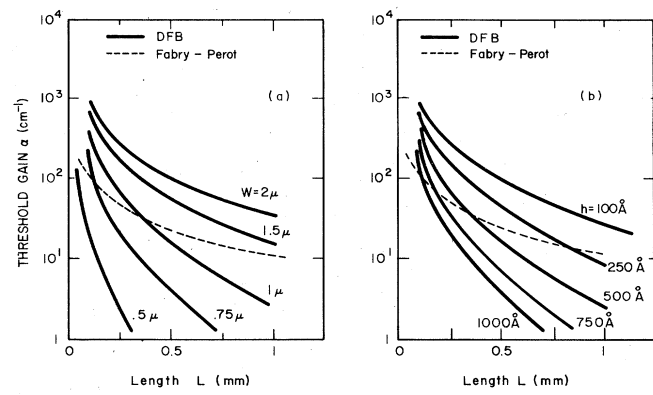


FIG. 37. In this figure, the solid curves are the threshold gains $\alpha (\text{cm}^{-1})$ required for a DFB laser and the dashed curves are those for a cleaved (Fabry-Perot) laser. The calculation was made for an (Al, Ga)As double heterostructure in which $n_0 = n_2 = 3.48$ and $n_1 = 3.60$. The laser wavelength considered is 0.9 μm . In the above figures, h and d are, respectively, the depth and the period of the corrugation, and W is the thickness of the active layer (Nakamura and Yariv, 1974).

We thus have the following:

$$\beta(x) = \beta + i\alpha + 2\kappa \cos 2\beta_0 x, \quad (50)$$

$$d^2/dx^2 E + (\beta^2 + 2i\alpha\beta + 4\kappa\beta \cos 2\beta_0 x)E = 0, \quad (51)$$

$$dA(x)/dx = -i\kappa\beta(x)e^{2(\alpha-i\delta)x}, \quad (52a)$$

$$d\beta(x)/dx = i\kappa A(x)e^{-2(\alpha-i\delta)x}, \quad (52b)$$

$$\gamma^2 = \kappa^2 + (\alpha - i\delta)^2, \quad (53)$$

$$\frac{a(0, t)}{b(0, t)} = \frac{i\kappa \sinh \gamma L}{(\alpha - i\delta) \sinh \gamma L - \gamma \cosh \gamma L}. \quad (54)$$

Here, we have assumed again that the corrugated waveguide is located between $x=0$ and $x=L$. Without gain, the reflectivity $a(0, t)/b(0, t)$ in (54) will always be less than unity. With gain, when

$$\gamma \coth \gamma L = (\alpha - i\delta) \quad (55)$$

the denominator of (54) will vanish, resulting in an infinite reflectivity. This, of course, indicates the onset of oscillation. In fact, Eq. (55) is the threshold condition for the DFB laser. We recall that, if we let the laser frequency, ω , vary, we will have $\delta = \beta - \beta_0 \approx N(\omega - \omega_0)/c$, where N is the mode index. The quantities α and δ in Eq. (55) therefore determine, respectively, the threshold gain and the frequency of laser oscillation. In Fig. 38 (Yariv and Yen, 1974), the contours of constant reflectivity, $|a(0, t)/b(0, t)|^2$, are plotted in a two-dimensional plane of αL versus δL . We see that the reflectivity rises sharply when the threshold condition (55) is approached.

In the coupled mode theory of DFB lasers discussed by Kogelnik and Shank (1971, 1972), they argued that, as an oscillator, the wave energy is generated inside the laser. Since the oscillation is self-sustaining and does not require any input, the forward wave $b(x, t)$ in Eq. (34) at $x=0$ and the backward wave $a(x, t)$ at $x=L$ can be set equal to zero. Using these boundary conditions, these authors obtained exactly the same threshold condition (55) given above.

Kogelnik and Shank (1971, 1972) have also considered the case where the gain of the medium varies periodically along x . This situation can easily be achieved in a dye laser operated by optical pumping. One can vary

FIG. 38. If a corrugated waveguide is formed in a medium which is able to amplify the light, the reflectivity $a(0, t)a^*(0, t)/b(0, t)b^*(0, t)$ in the waveguide may be larger than one. In fact, an infinite reflectivity marks the threshold condition of the DFB laser. In the above figure, the contours of the constant reflectivity are plotted using αL as the vertical axis and δL as the horizontal axis, where α is the gain constant of the medium and δ is the deviation (in phase constant) from the Bragg condition. The curves are for the case $\kappa L = 0.4$, where κ is the coupling constant (Yariv and Yen, 1974).

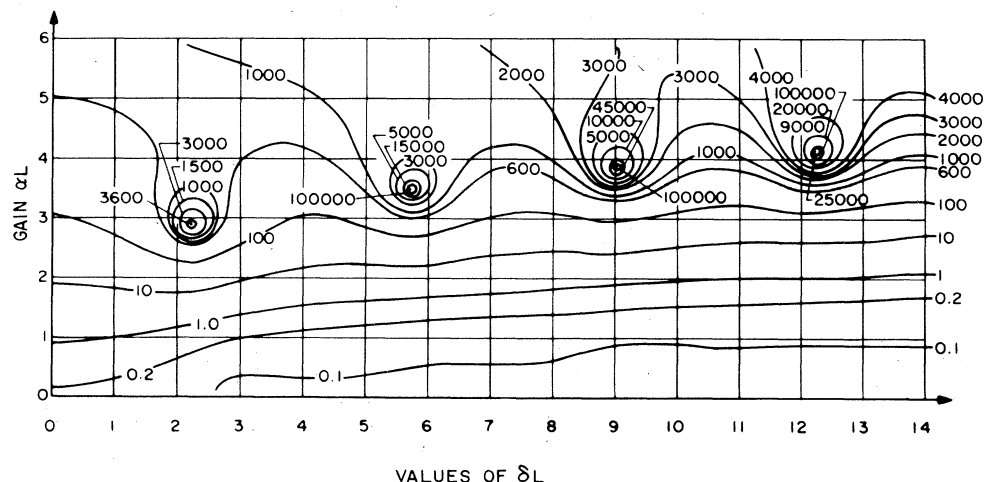
pumping power periodically in x , by using two oblique pumping beams which interfere with one another to produce a fringe pattern. A periodic gain is, however, difficult to achieve in the AlGaAs injection laser, since the diffusion length of the injected electrons is on the order of several microns and the period of gain modulation required in the AlGaAs laser is only 1200 Å for the first order of diffraction, and 3600 Å for the third order of diffraction. In this case, even if the electrons were to be injected according to a periodic pattern, they would tend to diffuse out of the pattern quickly. For a periodic gain modulation, the coupling constant κ will be imaginary. The waveguide may thus be considered as being periodically loaded with small shunt negative resistances. Since the wave reflected from a shunt resistance is not 90° out of phase with the wave that excites it, the DFB laser with periodic gain can be operated under the Bragg condition.

In an integrated optical circuit, the corrugated waveguide which forms the DFB laser is connected at both ends to a smooth waveguide. At the junctions, we expect the corrugation to taper off gradually. We have shown in Sec. III. A that when two smooth waveguides are connected through a tapered transition, no reflection will occur at the junction. We recall that normal modes deal with energy flows in the waveguide. It would then be interesting to know: will a normal mode of the corrugated waveguide, and thus the energy flow it represents, be reflected at a junction in which the corrugation tapers off gradually? This question must be answered, since the operation of the DFB laser depends upon such a reflection. We will analyze this situation using the wave solutions in normal modes derived earlier in Sec. IV. A. Figure 39 shows a forward wave $F(x, t)$ and a backward wave $G(x, t)$ in the corrugated section. According to Eq. (48), we have

$$F(x, t) = r_2 \exp\{i[\omega t - (|\gamma| + \beta_0)x]\} + \xi r_2 \exp\{i[\omega t - (|\gamma| - \beta_0)x]\},$$

$$G(x, t) = s_1 \exp\{i[\omega t + (|\gamma| + \beta_0)x]\} + \xi s_1 \exp\{i[\omega t + (|\gamma| - \beta_0)x]\}.$$

In the smooth waveguide at the right side, we have only



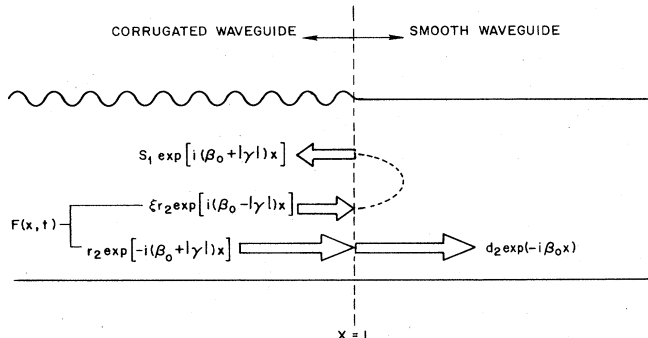


FIG. 39. The figure shows a corrugated waveguide connected to a smooth waveguide. It is possible to show that there will be a reflection of energy flow at the junction. The problem is analyzed in the text based on Floquet's theorem and normal mode analysis.

one forward wave propagating toward the right, since radiation is directed away from the laser. This wave may be described as

$$D(x, t) = d_2 e^{i(\omega t - \beta x)}, \quad (56)$$

which is, of course, a normal mode of the smooth waveguide. The arbitrary constants r_2 , s_1 , and d_2 must now be determined from the boundary conditions at the junction, $x=L$. If $|\gamma| \ll \beta$ and $\beta \approx \beta_0$, as we have assumed in our theory, the phase constant of the fundamental component in $F(x, t)$ will closely match that of $D(x, t)$. We thus would expect this component of $F(x, t)$ to propagate through the junction as $D(x, t)$, yielding $r_2 = d_2$. Furthermore, we find that the phase constant of the space harmonic in $F(x, t)$ matches that of the fundamental in $G(x, t)$; thus, $\xi r_2 = -s_1$. The ratio of $G(L, t)$ to $F(L, t)$ as determined by the boundary condition at $x=L$ is then approximately ξ . Therefore, part of the normal mode $F(x)$ will always be reflected according to the reflectivity ξ , when a corrugated waveguide is connected to a smooth waveguide regardless of whether the corrugation is terminated abruptly or tapered off gradually at the junction. Stated more specifically, a reflectionless tapered transition between a corrugated waveguide and a smooth waveguide simply does not exist. This is another important characteristic of the DFB structure, since AlGaAs DFB lasers are made by liquid phase epitaxy and the manner in which the corrugated section is joined into the smooth waveguide is difficult to control.

C. Al-Ga-As DFB and BR laser-diodes

AlGaAs double heterostructure (DH) diodes, with stripe geometry and cleaved ends, are the most advanced semiconductor lasers to date (Panish, 1975). These lasers have dimensions of typically $380 \mu\text{m} \times 15 \mu\text{m}$, requiring a few V and about 100 mA to operate. They have a projected lifetime of more than 10^5 h in continuous wave operation at room temperature, and are capable of generating over 10 mW coherent radiation. We have mentioned in the last section, once the two ends of a laser are cleaved, it is difficult to connect the diode into an optical circuit. In

integrated optics, therefore, we deal with DFB and BR lasers discussed in Sec. IV. B. At the beginning, both DFB and BR lasers had difficulties. The AlGaAs DFB laser requires complicated two-step growth process, since a grating must be formed on the active layer which has to be grown first, and then, additional layers have to be grown over the grating. Part of the corrugation could melt away during the second step of the growth and the grating thus formed is usually far from perfect, adding significant scattering loss to the optical cavity. In addition, chemical or ion etching used to fabricate the grating introduces interface nonradiative recombination centers which further degrade the efficiency of the laser. The fabrication of the AlGaAs BR laser is equally difficult. Although the BR laser can be grown in one step, the extra length of the active layer needed to form Bragg reflectors is not electrically pumped and can be very lossy. The problem is then that of fabricating Bragg reflectors very close to the gain region without affecting the injection and radiative recombination processes of the laser. Fortunately, these technical difficulties have gradually been solved in the past two years. As of today, both DFB and BR lasers have achieved room-temperature operation and have threshold currents approaching those of the cleaved lasers, although long lifetimes have not been demonstrated (Nakamura, 1973, 1974, 1975, 1975; Yen *et al.*, 1973; Scires *et al.*, 1974, 1975; Yang and Ballantyne, 1974; Wang, 1974; Reinhart *et al.*, 1975; Aiki *et al.*, 1975, 1976; Casey *et al.*, 1975; Streifer *et al.*, 1975; Tsang and Wang, 1976).

The DFB and BR lasers have the same heterostructures as the cleaved lasers. A typical DH structure consisting of four layers of different compositions is shown in Fig. 40. Starting from left to right with a heavily Sn-doped n-type GaAs substrate, the first layer is a $2.5-\mu\text{m}$ thick Sn-doped n-type $\text{Al}_{0.3}\text{Ga}_{0.7}\text{As}$ with a concentration of $1-4 \times 10^{18} \text{ cm}^{-3}$. The second layer is a $0.2-0.4 \mu\text{m}$ thick Si-doped p-type GaAs (a $10^{17}-10^{18} \text{ cm}^{-3}$ compensated active layer). These two layers form the p-n junction which is the heart of the laser. Next, we have a $1-2 \mu\text{m}$ thick Zn-doped p-type $\text{Al}_{0.3}\text{Ga}_{0.7}\text{As}$

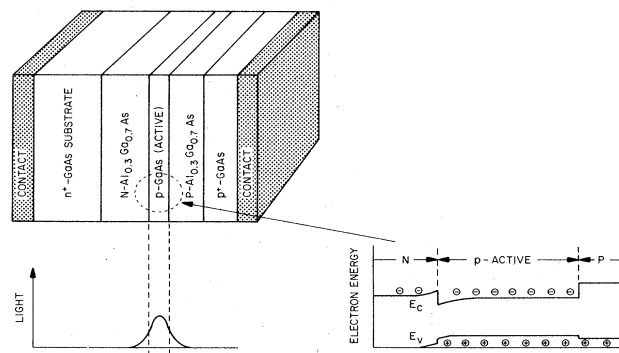


FIG. 40. The figure illustrates the double heterostructure used in lasers. Also shown in this figure are the potentials at the $N-p$ and $p-P$ junctions under a forward bias. These diagrams show the capability of the heterostructure to confine both the optical wave and the carriers to within the p -GaAs active layer.

($5-8 \times 10^{18} \text{ cm}^{-3}$). These three layers form the heterostructure. Finally, we have a $1-2\text{-}\mu\text{m}$ thick Ge-doped p^+ -type GaAs ($3-5 \times 10^{18} \text{ cm}^{-3}$) which is added simply to ease the formation of the Cr-Au contact needed for current injection. By applying a forward bias, electrons are injected across the $p-n$ junction into the second layer (p -GaAs) where laser action is achieved by recombination radiation. For this reason, this p -GaAs layer is called the active layer or active waveguide. It is convenient to use n and p to denote the n -type and p -type GaAs layers, and N_x and P_x to denote the n -type and p -type $\text{Al}_{0.3}\text{Ga}_{0.7}\text{As}$ layers. Figure 40 thus has an N_x-p-P_x-p structure, where $x=0.3$. A simplified potential diagram of the DH structure under a forward bias is also shown in this figure. GaAs has a direct energy bandgap of 1.43 eV, and $\text{Al}_{0.3}\text{Ga}_{0.7}\text{As}$ has one of 1.8 eV (Casey *et al.*, 1969). Recent work by Dingle *et al.* (1974) shows that the discontinuity in the potential diagram caused by the difference in energy gaps of $\text{Al}_{0.2}\text{Ga}_{0.8}\text{As}$ and GaAs, at the $p-P$ junction, is 85% in the conduction band and 15% in the valence band; thus electrons which are injected into the active layer are completely blocked at the $p-P$ junction by the potential discontinuity in the conduction band. Similarly, the discontinuity in the potential diagram at the $N-p$ junction in the valence band blocks holes from spreading over into the N layer. The heterostructure described above therefore serves the function of confining injected carriers to within a very thin active layer only $0.2-0.4 \mu\text{m}$ thick. This carrier confinement is very important since the minority-carrier diffusion lengths of GaAs are on the order of several microns for material doped in the $10^{17}-10^{18} \text{ cm}^{-3}$ range (Casey *et al.*, 1973), hence, without confinement, most of the carriers would be located outside the active layer. In addition to the carrier confinement, we recall that the refractive index of $\text{Al}_{0.3}\text{Ga}_{0.7}\text{As}$ is 3.48, and that of GaAs is 3.60. The $N-p-P$ heterostructure thus forms a perfect symmetrical waveguide which also confines light energy within the active layer. To show the advantages of the DH structure, we compare its performance with that of the homostructure in which there is little optical and carrier confinement. The threshold current density of the homostructure laser is $50-100 \text{ kA/cm}^2$ which is about 50 times that of the DH laser. The best DH lasers have a threshold current density less than 1 kA/cm^2 and an external differential quantum efficiency of 40–50% at room temperature.

During 1971 and 1972, DFB and BR dye lasers were constructed using a gelatin, polyurethane, or poly(methylmethacrylate) film doped with a dye called "rhodamine 6G" as the waveguide. The grating is either formed in the film by holographic technique or on the substrate by ion etching. These early efforts include the works of Kogelnik and Shank (1971), Kogelnik *et al.* (1971), Shank *et al.* (1971), Kaminow *et al.* (1971), Bjorkholm and Shank (1972), Bjorkholm *et al.* (1973), Schinke *et al.* (1972) and Zory (1973). Unfortunately, dye lasers cannot be used in optical circuits, since the dye bleaches easily, resulting in laser lifetimes of only a few minutes.

In 1973, laser action was observed for the first time in GaAs DFB structures by optical pumping (Nakamura *et al.*, 1973). In the following year, electrically ex-

cited DFB diode lasers were reported by Scifres *et al.* and also by Nakamura *et al.* In these lasers there were difficulties in grating fabrication and in "melt-back" problem. The reported experiments were performed at $80-100^\circ\text{K}$. Since the threshold current required for room-temperature operation is about five times that required at 80°K . The above lasers were not good enough to be operated at room temperature without causing excessive heating.

As early as 1972, Hayashi (Panish, 1976) proposed a more complex structure which would achieve so-called "separate confinement of carriers and optical wave". His structure is similar to the $N_x-N_y-p-P_y-P_x$ shown in Fig. 41. Here, the middle p -GaAs layer is the active layer. The neighboring N_y and P_y layers are $\text{Al}_{0.12}\text{Ga}_{0.88}\text{As}$. This material has a sufficiently large energy gap to confine the carriers in the p -GaAs layer, but does not have a sufficiently low refractive index to confine the optical wave. Instead, the optical wave is confined by the outer N_x and P_x layers which are made of $\text{Al}_{0.3}\text{Ga}_{0.7}\text{As}$. We recall that the refractive index of the AlGaAs system decreases with increasing Al concentration (Casey *et al.*, 1974). The $\text{Al}_{0.3}\text{Ga}_{0.7}\text{As}$ layers are able to confine the light wave, while $\text{Al}_{0.12}\text{Ga}_{0.88}\text{As}$ layers cannot. In this laser, N_y-p-N_y is the optical waveguide, where the carriers occupy only the middle part—the p layer. The original idea was that by confining the carriers to the middle part of the waveguide where the intensity of the optical wave is the largest, one might achieve a large efficiency. The idea turns out to be particularly attractive in the case of the DFB laser, since with separate confinement, one may form the corrugation on the P_x layer which is now remote from the active p -GaAs layer. Any damage done by the ion or chemical etching process thus will not affect the luminescence property of the laser. Indeed, in 1975, injection DFB-DH lasers using separate confinement

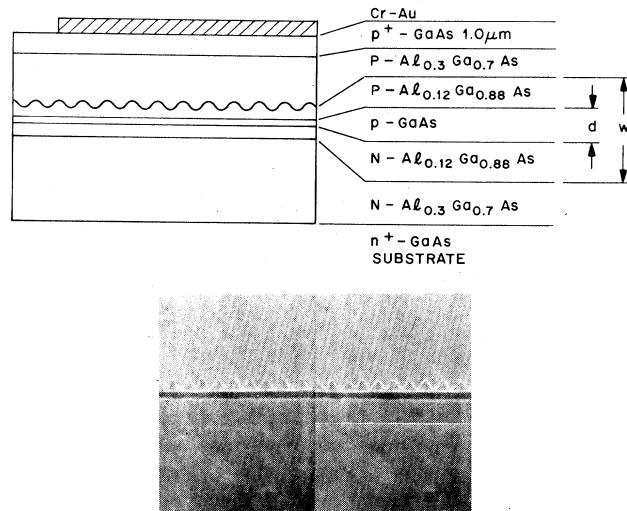


FIG. 41. The top figure shows an $N_x-N_y-p-P_y-P_x$ DFB structure which allows separate confinement of the optical wave and the carriers. The carriers are confined in the region d , which is the p -GaAs active layer. The optical wave is confined in the region w , which consists of the N_y , p , and P_y layers. The photograph below is a SEM micrograph of the structure (Ilegems, Casey, Somekh, and Panish, 1975).

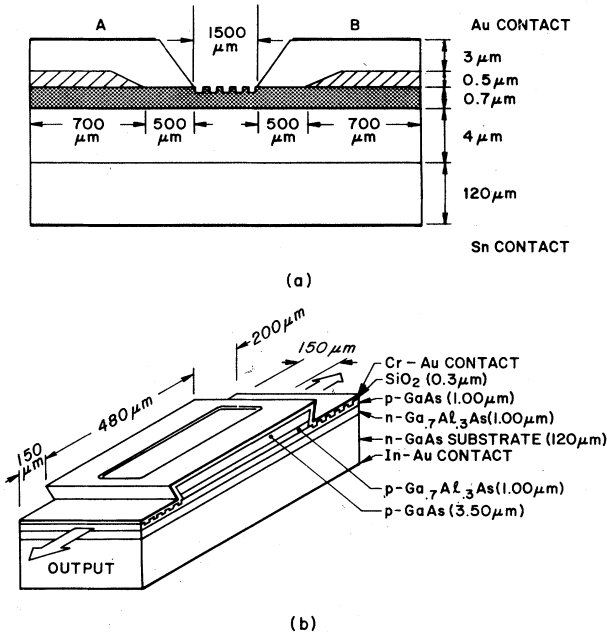


FIG. 42. Figures (a) and (b) show a Bragg-reflector laser constructed by Reinhart *et al.* (1975) and the one by Tsang and Wang (1976).

were operated at room temperature under pulsed conditions by Casey *et al.* (See Fig. 41), and in continuous wave by Nakamura *et al.* The efficiencies of these DFB lasers were quite comparable to those of cleaved lasers.

The BR lasers constructed by Reinhart *et al.* (1975) is shown in Fig. 42(a). The chip contains two BR lasers, *A* and *B*, formed side by side. The grating between the two heterostructures has a period of 3865 Å and diffraction of the third order is used for Bragg reflection. Consider the laser *A* specifically. The layer containing a tapered section is the active layer of the laser. Light generated in the active layer is reflected at the left by a cleaved surface. At the right, the light wave is coupled through the tapered section into a passive waveguide below, and there, the wave is reflected by a Bragg reflector. The tapered section is constructed by a technique developed by Logan which will be discussed later in Sec. IV. E. Since the grating is formed in the area remote from the gain region, and the part of the optical cavity associated with the passive waveguide is not lossy, the laser has a good efficiency achieving room temperature operation.

The BR laser reported by Tsang and Wang (1976) involves a structure shown in Fig. 42(b). In this laser, a heterostructure was first formed on the substrate by the usual liquid phase epitaxial techniques. The areas needed to form Bragg reflectors were then etched down to the *p*-GaAs active layer by using $H_2SO_4:H_2O_2:H_2O$ (1:8:8) as the etchant. Again, the third order gratings were used for Bragg reflectors and they had a period, $d = 3500$ Å and a depth, $h = 1000$ Å. After the gratings were made on the active layer by preferential etching (see Fig. 42(b)), the entire surface was covered by a layer of sputtered SiO_2 and a rectangular window 480 $\mu m \times 150$ μm was then opened for electric contact to the top *p*⁺-GaAs layer. The final BR laser diode was bonded to

a TO-5 transistor header as the heat sink. The laser was operated at 183 °K and had a threshold current 890 A/cm².

In 1975 and 1976, preferential etching and selective growth have become important techniques to GaAs. They have been used to form inverted ridge waveguides, embedded laser structures and mesa diode lasers. We will return to the discussion of the lasers and these techniques in Sec. IV. E.

D. Thin-film optical modulators, switches, and beam deflectors

In addition to the lasers used as light sources, other devices important in optical communication and signal processing are those to modulate, switch, deflect, and scan the light. In these devices, one varies the phase, polarization, or physical position of the light beam by applying the appropriate modulating electric, magnetic, or acoustic field. The materials used to perform these functions are electro-optic, magneto-optic, or acousto-optic single crystals. The devices to be discussed are thus in the form of electro-optic, magneto-optic, or acousto-optic waveguides, *p-n* junctions, heterostructures, or Schottky diodes. We will postpone the discussion of AlGaAs modulators until Sec. IV. E where, the subject of AlGaAs technology and monolithic integrated optical circuits will be brought into focus. We will confine the present discussion to devices made of ferroelectric $LiNbO_3$ and $LiTaO_3$, magneto-optic iron garnets, and II-VI compounds such as ZnO. The material $LiNbO_3$ has a linear electro-optic coefficient $r_{33} = 32 \times 10^{-12}$ m/V, and a photoelastic constant $p_{13} = 0.13$. Iron garnets such as $Y_3Ga_{0.75}Sc_{0.25}Fe_{3.75}O_{12}$ have a Faraday rotation constant of about 200°/cm. New materials $Gd_{1.5}Pr_{1.5}Fe_5O_{12}$ and $BiGd_2Fe_5O_{12}$, have Faraday rotation constants as large as 1125°/cm and 3400°/cm, respectively.

The performance of the modulator is measured by the merit constant, $\mu = p/\eta^2\Delta f$, which gives the electrical modulating power p required to achieve a given degree of modulation η over a bandwidth Δf . The merit constant depends on the laser wavelength, the refractive index, the device geometry, and the electro-optic, magneto-optic, or photoelastic constant. Consider an electro-optic modulator as an example, which has a cross-section of D^2 and a length L . The field E required to produce a given degree of modulation η is inversely proportional to the length L , while the electrical power required is directly proportional to the product of E^2 and the volume D^2L . The merit constant thus contains a geometric factor of D^2/L . In conventional bulk modulators, the size of the modulator is limited by the expansion of the light beam due to diffraction. Under this diffraction limit, it may be shown that $D^2/L = S^2(4\lambda_0/\pi n)$, where S is a safety factor, λ_0 is the laser wavelength in a vacuum, and n is the refractive index. For $\lambda_0 = 1.06 \mu m$ and with a phase modulation of $\eta = 1$ rad, we have for the best bulk electro-optic modulators, $D^2/L = 5.28 (\mu m)^2$, and $\mu = 10$ mW/MHz(rad)². By confining the light beam in a channel waveguide, one can, in principle, improve the geometric factor and thus the merit constant indefinitely by simply increasing the length of the

modulator. Indeed, a waveguide modulator with a merit constant as low as $\mu = 0.002 \text{ mW/MHz}(\text{rad})^2$ has already been demonstrated by Kaminow *et al.*, (1975). Because of this capability of concentrating both the optical wave and the modulating field in a very small space, waveguide modulators and switches are far more efficient than their bulk counterparts. These modulators and switches are also easy to fabricate and to operate, because of the planar geometry and since the electrodes may be evaporated directly onto the film.

Schemes for modulation, switching, and deflection of light appear in four basic forms: In form I, an applied modulating field causes the mode index of a waveguide to vary, thus altering the phase or the polarization of the light wave propagating in the waveguide. It is a straightforward phase or polarization modulation. Devices that fall into this category are electro-optic phase modulators and magneto-optic switches. In the form II, an acoustic wave or an electro-optic diffraction grating is used either to deflect a light beam according to the Bragg condition, or to diffract it into several different orders in the form of Raman-Nath type of diffraction. Electro-optic and acousto-optic deflectors belong to this scheme. The form III involves a directional coupler (or a branching waveguide) formed in an electro-optic material. A light wave launched in waveguide *A* of the coupler may remain in the same waveguide, or be switched into waveguide *B* according to the field applied to this coupler. We have already discussed briefly this type of device in Sec. III.E. The form IV is an electro-optic prism, which is capable of deflecting or scanning a light beam continuously from one direction to another over an angle of tens of degrees. We will discuss these four types of devices and their performances in detail below.

Between 1970 and 1972, good-quality electro-optic films other than III-V compounds were not available; most modulators were, and in fact they still are, made by diffusion. Waveguide electro-optic modulators other than *p-n* junction devices were first reported by Martin (Taylor *et al.*, 1972, Martin and Hall, 1972; Martin, 1973, 1975) by diffusing Se into CdS. A year later, a fast phase-modulator was discussed by Kaminow *et al.* (1973) by diffusing Li out of LiNbO₃. By that time, various methods of forming LiNbO₃ films were found to be successful, and a large number of electro-optic devices in various forms were reported (Kaminow *et al.*, 1973, 1974, 1975; Chen and Benson, 1974; Fukunski *et al.*, 1974; Noda *et al.*, 1975; Popuchon *et al.*, 1975; Tsai and Sannier, 1975; Uehara *et al.*, 1975; Webster and Zernike, 1975; Omachi and Noda, 1975; Tien *et al.*, 1975, Kaminow, 1975). We begin our discussion by singling out an electro-optic phase modulator, shown in Fig. 43(b), formed by Kaminow *et al.*, (1975), in Ti-diffused LiNbO₃. This modulator consists of a channel waveguide and two aluminum electrodes in a configuration where the electric vector of a TE wave excited in the waveguide, the *c* axis of the LiNbO₃ crystal, and the modulating field applied to the electrodes, are parallel to one another. It can easily be shown that a modulating electric field E_3 will produce a change in the refractive index of $\Delta n = \frac{1}{2} n_1^3 r_{33} E_3$, where r_{33} is the electro-optic coefficient. In response to this index change,

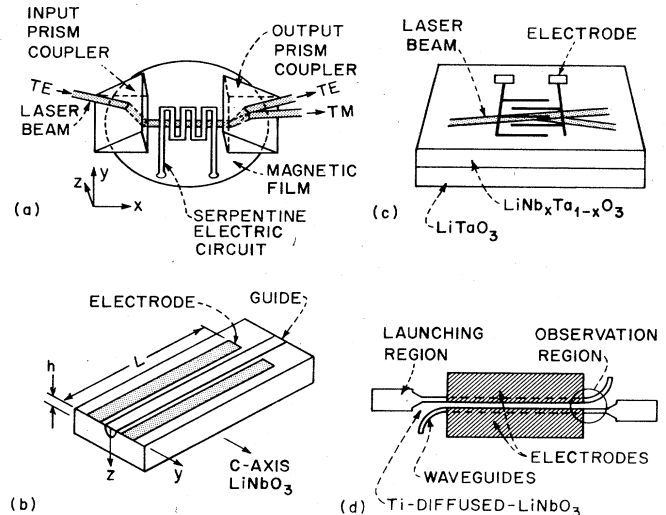


FIG. 43. Figures (a), (b), (c), and (d) show, respectively, a magneto-optic switch (Tien *et al.*, 1973, 1974), a Ti-diffused LiNbO₃ phase modulator, (Kaminow *et al.*, 1975), a Nb-diffused LiTaO₃ electro-optic deflector (Hammer and Philips, 1974), and a Ti-diffused LiNbO₃ directional-coupler switch (Popuchon *et al.*, 1975).

the light beam suffers a phase retardation of $\Delta\phi = 2\pi L \Delta n / \lambda_g$ in the waveguide. The channel waveguide is roughly 5-μm wide and 30-mm long and requires only 0.3 V to produce 1 rad of phase retardation. The merit factor of the modulator is 0.002 mW/MHz(rad)², a value which is better than that of the best bulk modulator by a factor of more than 5000.

Formation of waveguides by diffusing Ti into LiNbO₃ was first discussed by Schmidt and Kaminow (1974). The process has been used later in many devices; it increases the refractive index of the diffused layer by 0.04 for the extraordinary wave and 0.01 for the ordinary wave. A larger difference in refractive indices of the waveguide and substrate can be obtained by growing LiNbO₃ layers on LiTaO₃ substrates (Miyazawa, 1973; Tien *et al.*, 1974, Hammer and Philips, 1974; Ballman *et al.*, 1975; Miyazawa *et al.*, 1975; Kondo *et al.*, 1975). In this case, the refractive indices of the LiNbO₃ layer are 2.294 (ordinary) and 2.214 (extraordinary), and that of the LiTaO₃ substrate is 2.177 (ordinary and extraordinary).

The magneto-optic polarization switch reported by Tien *et al.*, (1972, 1973, 1974) is another example of the modulation scheme belonging to form I discussed above. It consists of a magnetic Y₃Ga_{0.75}Sc_{0.5}Fe_{3.75}O₁₂ film as an optical waveguide. The film was grown by the dipping method of liquid phase epitaxy on a Gd₃Ga₅O₁₂ substrate. In Fig. 43(a), the disk at the center is this magnetic film; the prism at the left was used to couple $\lambda = 1.15 \mu\text{m}$ laser light into the waveguide and the prism at the right coupled light out of the waveguide. Between the two prisms and deposited directly on the film is a serpentine electric circuit and the light wave propagated in the film from left to right underneath the circuit. Consider now, specifically, a TE wave excited in the waveguide. The TE wave has an electric field which lies in the plane of

the film. As the light wave propagates in the waveguide, its electric vector is rotated towards the normal of the film if the magnetization in the magneto-optic waveguide is in the direction of light wave propagation (x -direction). This process thus converts a TE wave into a TM wave. However, the process of Faraday rotation is not effective if the magnetization is normal to the direction of light wave propagation (that is, if the magnetization is in the y direction). Therefore, by rotating the magnetization in the $x-y$ plane of the film, one can switch the polarization of the light wave.

The motion of the magnetization is controlled by the current in the serpentine circuit. When the current is on, the magnetization is aligned parallel to the direction of wave propagation. When the current is off, the magnetization returns to the normal position because of the anisotropy of the crystal. The wave velocities of the TE and TM waves in the waveguide differ slightly. Thus, to insure a complete conversion between TE and TM waves, the period of the serpentine circuit must be designed such that the magnetization excited by the circuit forms a magnetic grating; then, the wave vector of the TM wave plus the grating vector will be exactly equal to the wave vector of the TE wave (see discussion in Sec. III. E for coupled waves).

The advantage of the waveguide magneto-optic switch over its bulk counterpart is that the demagnetization factor is zero in the plane of the film. To rotate the magnetization in this plane, it is then only necessary to overcome the anisotropy field which can be as small as 0.1 Oe. Indeed, the switch reported requires only a switching field on the order of 0.1 Oe, which is less than the Earth's magnetic field of 0.6 Oe. Using a larger switching field, the switch has been operated at speeds of up to 300 MHz.

We will next discuss the modulators of form II: acousto-optic and electro-optic deflectors. In the acousto-optic deflector, a periodic variation of the mode index is excited in the waveguide by a surface acoustic wave through the photoelastic constant. The magnitude of the index modulation is proportional to the square of the product of the photoelastic constant and the strain in the acoustic wave. This periodic variation of the index forms a grating which diffracts the light beam (see discussion in Sec. IV. A and IV. B). To maximize diffraction, the light beam should propagate in the direction nearly normal to the grating vector. Acousto-optic deflectors may be operated in two different modes. In the first mode known as the "Raman-Nath diffraction" [see Fig. 44(a)], the first-order diffracted light beam is displaced in the direction of the acoustic wave by a distance not quite enough to cross one acoustic wavelength. Then, the light beam will not be reflected sequentially at different grating planes, as described in a Bragg reflector. Instead, light will be diffracted into many orders simultaneously, at the angles θ_m given by

$$\theta_m = \arcsin(m\lambda_g/\Lambda), \quad m = 0, \pm 1, \pm 2, \dots, \quad (57)$$

where λ_g and Λ are, respectively, the wavelength of the light wave in the waveguide and that of the acoustic wave. Diffracted beams of different orders will have intensities according to

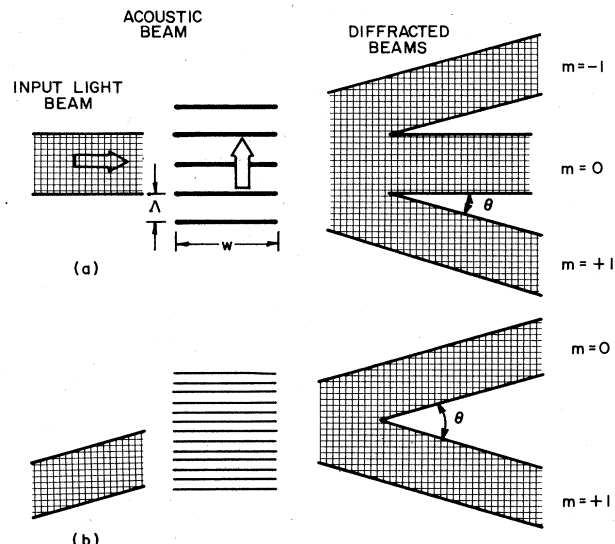


FIG. 44. The figures illustrate two types of acousto-optic diffraction: (a) the Raman-Nath diffraction and (b) the Bragg reflection.

$$I_m/I_0 = J_m^2(\eta), \quad (58)$$

where J_m is the m th Bessel function $\eta = 2\pi w\Delta n/\lambda_g$, Δn is the amplitude of the periodic index modulation, and w is the width of the acoustic beam. The second mode of operation is the usual Bragg reflection discussed in Secs. IV. A and IV. B, and in this case, the light beam intercepts many grating planes. One then observes only one diffracted beam which satisfies the Bragg condition [Fig. 44(b)].

The first waveguide acousto-optic beam-deflector was reported by Kuhn *et al.*, in 1970. In this deflector, a light beam was launched in a waveguide formed by sputtering a glass film 0.8- μm thick onto an α -quartz substrate. This beam was then diffracted by a surface acoustic wave excited in the same waveguide. A diffraction efficiency of 66% was obtained using 0.18 W of acoustic power at a frequency of 191 MHz. To produce this amount of acoustic power, 2.5 W of electric power were needed. Acousto-optic beam deflectors have also been reported by Ohmachi (1973) using an amorphous As_2S_3 film sputtered onto a LiNbO_3 substrate, and by Schmidt and Kaminow (1975) using a Ti-diffused LiNbO_3 waveguide. In the latter experiment, they used 50 mW electric power for 70% deflection of the light beam. The device was operated in the mode of Bragg reflection, having a bandwidth of about 50 MHz. The merit constant is about 1 mW/MHz. The advantage of acousto-optic beam deflectors is that one can control the intensities and angles of the diffracted beams independently by varying, respectively, the intensity and wavelength of the acoustic beam.

Of course, it is possible to replace the acoustic beam in the above deflector by an electro-optic grating. In this case, a set of interleaving positive and negative electrodes are deposited on an electro-optic waveguide and the periodic variation of the index is excited by the electric field from the electrodes through the electro-optic effect. A beam deflector in this form was built by Ham-

mer *et al.* (1972, 1973) and also by Hammer and Philips (1974). In the Hammer and Philips device shown in Fig. 43(c), they used a waveguide formed by diffusing Nb onto LiTaO₃ and obtained a diffraction efficiency of 80% by applying 5 V across the electrodes. The merit constant was $\mu = 0.2$ mW/MHz, a value which is lower than those of acousto-optic deflectors, but is still larger than the values obtainable in phase modulators.

The difficulty in the beam deflector, as compared with the phase modulator, is that a film waveguide, instead of a channel waveguide, must be used; consequently, the light beam is substantially wider, suffering a poor geometric factor. The modulators of form III involving directional couplers or branching waveguides are designed to remedy this situation. Figure 43(d) shows a directional coupler switch called "Cobra" reported by Papuchon *et al.* (1975). The directional coupler was formed in Ti-diffused LiNbO₃ and was designed such that a light wave applied, at the input end, to waveguide A will appear in waveguide B at the output end (see discussion in Sec. III. E). To accomplish this, the wave velocities in the two waveguides must be made to be identical—a condition known as "phase matching." By applying an electric field to the electrodes placed as shown in the figure, the refractive index in one waveguide may be increased while that in the other waveguide is decreased. This alters the wave velocities in the waveguides and has the effect of decoupling the two waveguides. A light beam launched in waveguide A would then remain in that waveguide. Therefore, as the voltage applied to the electrodes is switched on and off, the output light beam will be switched between waveguides A and B accordingly. A switch using branching waveguides and based on the principle of the Mach-Zehnder interferometer was reported by Ohmachi and Noda (1975) and also by Martin (1975). Still another directional coupler switch with stepped $\Delta\beta$ reversal has been discussed recently (Schmidt and Kogelnik, 1976; Kogelnik and Schmidt, 1976).

We have discussed in Sec. III. E that the coupling between two waveguides can be altered by control of either the coupling constant κ , or the indices of the two waveguides as required by the "phase matching." It can be shown that the driving voltage required to decouple two waveguides by spoiling the "phase-matching" condition is about two orders of magnitude smaller than that needed to control the coupling constant. For this reason, optical switches considered here are designed to control the relative phases of the waves in two waveguides which are either in the form of an interferometer or a directional coupler.

The modulators of form IV are designed to deflect or scan a light beam continuously from one direction to another in a waveguide. We thus ask whether there exists some form of refractive-index distribution, which can be excited by a set of simple electrodes through electro-optic effect, and which can be efficiently used to scan a light beam. The problem has been treated rather generally by Tien *et al.* (1974). The general equation for a light path in the $x-y$ plane where the refractive index varies as $n(x, y)$, is

$$\frac{d}{ds} n(x, y) \frac{d\rho}{ds} = \nabla n \quad (59)$$

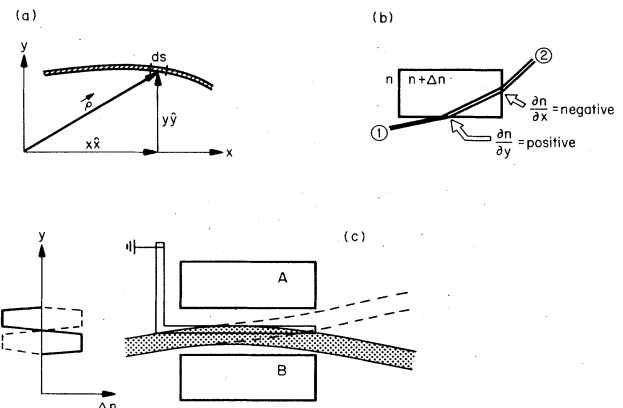


FIG. 45. We treat rather generally in the text light-wave propagation in the $x-y$ plane where the refractive index of the medium varies arbitrarily in x and y . Figure (a) shows the coordinate system used in the discussion. Here, ds is an element of the light path, and ρ is its position vector. Figure (b) shows the deflection of a light beam, as the beam starts in a medium of refractive index n and traverses through a rectangular area of refractive index $(n+\Delta n)$. Figure (c) illustrates an experimental arrangement used for scanning a light beam (Tien, Riva-Sanseverino, and Ballman, 1975).

Here, as shown in Fig. 45(a), ∇n is the gradient of $n(x, y)$, ds is an element of the light path, and ρ is the position vector of ds . Let the light beam initially be launched nearly parallel to the x axis. Then, $\tan\theta = dy/dx \approx \theta$ and the above equation reduces to

$$\Delta\theta = \theta_2 - \theta_1 = \int_{y_1}^{y_2} \frac{1}{n} \frac{1}{\tan\theta} \frac{\partial n}{\partial y} dy + \int_{x_1}^{x_2} \frac{1}{n} \tan\theta \left(-\frac{\partial n}{\partial x} \right) dx. \quad (60)$$

In this expression, $\Delta\theta$ is the deflection angle occurring in a light path from (x_1, y_1) to (x_2, y_2) , and θ_1 and θ_2 are, respectively, the entrance and exit angles. It is interesting to note that the first integral in Eq. (60) contains $\partial n/\partial y$ only and the second integral, $\partial n/\partial x$ only. Consider the deflection of a light beam which passes through a region of refractive index $(n+\Delta n)$ surrounded by a medium of refractive index n [Fig. 45(b)]. As the light beam enters the $(n+\Delta n)$ region, the refractive index along the light path increases. To optimize $\Delta\theta$ in Eq. (60), $\partial n/\partial x$ must be zero so that $\partial n/\partial y$ can be a maximum. Similarly, as the light beam leaves the $(n+\Delta n)$ region, the refractive index along the light path decreases, and we require $\partial n/\partial y = 0$ so that $\partial n/\partial x$ can be a maximum. An electrode configuration which fulfills these requirements is shown in Fig. 45(c). Using this structure, Tien *et al.* (1974) were able to scan a light beam continuously over 6° in a LiNbO₃ film waveguide which was grown epitaxially onto a LiTaO₃ substrate (Fig. 46). Another form of the light beam scanner which simulates an electro-optic prism has been studied by Kaminow (1975) and also by Tsai and Saunier (1975).

The modulators described above have sizes of a few millimeters. They are much larger than the diode lasers discussed in Sec. IV. C. This would limit the packing density of the optical circuit. We will continue in Sec. IV. E to discuss modulators made of AlGaAs $p-n$ junctions and heterostructures. Another way to modu-

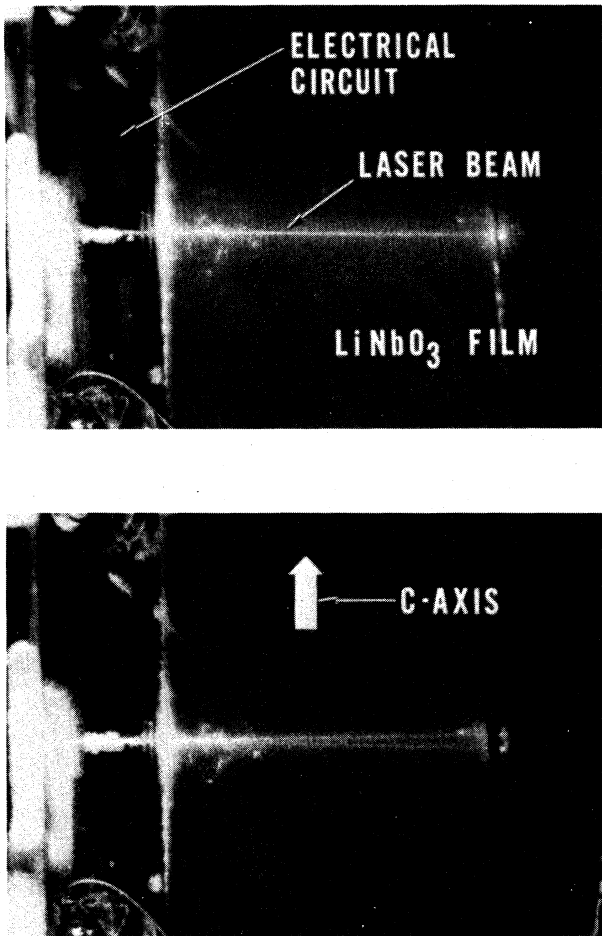


FIG. 46. The photographs show the operation of a LiNbO_3 light beam scanner. In the top photograph, the voltage on the circuit was zero, and in (b), an ac voltage was applied to the circuit. It was possible to scan a light beam in the LiNbO_3 waveguide over an angle of 6° covering roughly 10 resolvable beam spots (Tien, Riva-Sanseverino, and Ballman, 1975).

late the light is to pulse the laser directly. Lasers may be pulsed at speeds up to hundreds of MHz beyond which relaxation oscillation starts. We will discuss this problem too in Sec. IV. E.

E. (Al,Ga)As technology and monolithic integrated optical circuits

GaAs is a direct energy gap III-V semiconductor compound which can be easily doped both *p* and *n* type. At room temperature, it has an energy gap, $E_g = 1.424$ eV or $0.87 \mu\text{m}$. The effective masses of GaAs are 0.067 (electron), 0.45 (heavy hole) and $0.082 m_0$ (light hole). The room temperature mobilities are 5–8000 (electron) and $300 \text{ cm}^2/\text{V sec}$ (hole). The bandgap of the ternary compound $\text{Al}_x\text{Ga}_{1-x}\text{As}$ increases with x , and the transition from a direct to an indirect energy gap occurs at $E_g \approx 1.92$ eV or $x \approx 0.37$. In the range of the direct gap, E_g in electron volts varies as $1.424 + 1.142x + 0.504x^2$. The refractive index of this ternary decreases with x roughly according to $3.6 - 0.4x$. AlAs and GaAs have an identical

lattice constant $a_0 = 5.65 \text{ \AA}$ at the growth temperature 850°C and differ by only 0.1% at room temperature. Consequently, heterostructures such as $\text{Al}_x\text{Ga}_{1-x}\text{As}/\text{GaAs}/\text{Al}_x\text{Ga}_{1-x}\text{As}$ can be grown with little interfacial strain. The thermal expansion coefficients of AlAs and GaAs are, respectively, 5.2×10^{-6} and $5.8 \times 10^{-6}/^\circ\text{C}$. The material (Al, Ga)As has been used to form waveguides, directional couplers, modulators, lasers, and detectors. The (Al, Ga)As heterostructure lasers are the most advanced laser diodes available today. They can be grown either by liquid phase epitaxy or by molecular beam epitaxy. The laser emission is typically at $0.845 \mu\text{m}$. Because of the interest in these laser diodes (Al, Ga)As technology has been advanced rather rapidly. We will review in this section some of the innovative techniques and discuss their applications in integrated optics.

Waveguiding in GaAs *p-n* junctions (for example, Yariv and Leite, 1963; Bond *et al.*, 1963) and modulation of light in reversely biased junctions (for example, Nelson and Reinhart, 1964) were discussed in the sixties. Since the inception of integrated optics, Hall *et al.* (1970) formed waveguides by growing high resistivity GaAs on low resistivity GaAs substrates. The difference in carrier concentrations ($C_1 - C_0$) between the epitaxial layer and the substrate introduces a difference in refractive index ($n_1 - n_0$) as

$$n_1^2 - n_0^2 = (C_0 - C_1)e^2/m^*\omega^2 ,$$

where e and m^* are, respectively, the carrier charge and effective mass, and ω is the radian optical frequency. Similar waveguides may also be formed by bombarding a highly conductive substrate with protons of typical energy in the 300 000-eV range to form a highly compensated resistive layer (Garmire *et al.*, 1972). The best waveguides are, however, the $\text{Al}_y\text{Ga}_{1-y}\text{As}/\text{Al}_x\text{Ga}_{1-x}\text{As}/\text{Al}_z\text{Ga}_{1-z}\text{As}$ heterostructures where the refractive index difference between the waveguiding and cladding layers is approximately

$$n_1 - n_0 = 0.4(x - y).$$

Because of technical difficulties, early experiments to use these waveguides for various optical devices were only moderately successful. These experiments include Schottky junctions (Hall *et al.*, 1970) and directional couplers (Somekh *et al.*, 1972, 1973) for control of light, gratings for input and output couplings (Cheo, 1972), and parametric devices for nonlinear interaction (Anderson, 1972).

In an interesting paper published in 1970, Dobkin *et al.* reported formation of lasers and mirrors by wet etching. Later, Logan and Reinhart (1973) followed the same idea and etched (Al, Ga)As/GaAs/(Al, Ga)As heterolayers into $1-30 \mu\text{m}$ wide channel waveguides. The layers were grown by liquid phase epitaxy on the (100) face of a GaAs substrate, and the waveguides were along the $\langle 011 \rangle$ direction with two sides in the $\{111\}$ planes. Similar etched waveguides were also formed by Tracy *et al.* (1973) by molecular beam epitaxy. In these experiments, an anodization etching process was used. The process involved the formation of a surface oxide in a solution of 30% H_2O_2 (adjusted to $\text{pH} \approx 7.02$ by adding NH_4OH or H_3PO_4), and the crystal was etched as

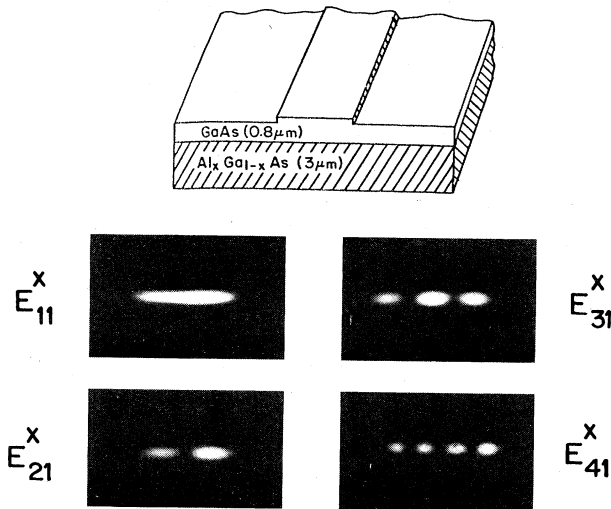


FIG. 47. The top figure shows a $(\text{Al}, \text{Ga})\text{As}$ rib waveguide constructed by Reinhart *et al.* (1974) using an anodization-etching process. The photographs below are mode patterns observed in this waveguide.

this surface oxide cracked away. Using the same etching process, Reinhart *et al.* (1974) reported a rib waveguide shown in Fig. 47. The waveguide-mode patterns observed in this waveguide are also shown in this figure. The waveguide consisted of $\text{GaAs}/\text{Al}_x\text{Ga}_{1-x}\text{As}$ heterolayers with a rib etched into the GaAs layer. It is interesting to note that, in such rib waveguides, light energy in the GaAs layer is confined in the region under the rib, which is only a few microns wide. From the potential-well model, it is easy to see that the portion of the waveguide under the rib forms a deeper potential well than those at the two sides. The light wave thus propagates within the center portion as though it were guided by the rib. Rib and channel waveguides have also been formed by vapor phase epitaxy (Blum *et al.*, 1974), by ion-milling (Garvin *et al.*, 1973), by diffusion (Garmire *et al.*, 1975), and by ion-implantation (Leonberger *et al.*, 1976; Auracher, 1976).

Following the work of etched waveguides, Comerford and Zory (1974) applied preferential etching techniques (Tarui *et al.*, 1970) to fabricate the V-groove diffraction gratings. The gratings were etched into the (100) surface of GaAs and the groove walls were along $A\{111\}$ crystallographic planes. In order to use a bromine-methanol etchant which could attack Shipley AZ positive resist, they had to form a 60% gold-40% palladium slotted mask for the etching process. Subsequently, Tsang and Wang (1976) formed better gratings by using an etchant consisting of 1 part of H_2SO_4 , 8 parts of (30%) H_2O_2 , and 40 parts of H_2O . This etchant may be used directly over Shipley AZ 1350 J photoresist and it takes only about 10 sec to etch a groove 1000-Å deep at room temperature. Figure 48 shows photographs of the gratings formed by this method. Tsang and Wang (1975) have also developed a "simultaneous exposure and development" method for forming better photoresist masks. Lately, we have also used a slow etchant in-

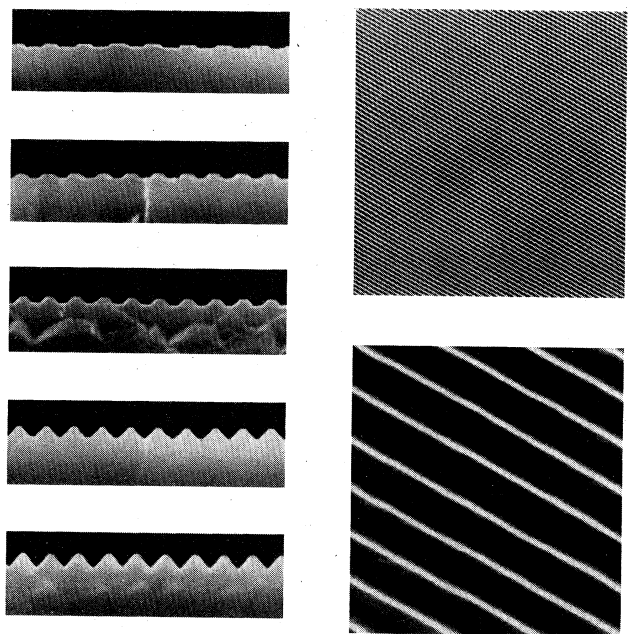


FIG. 48. The SEM photographs in this figure show the gratings formed by preferential etching in a $\text{H}_2\text{SO}_4-\text{H}_2\text{O}_2-\text{H}_2\text{O}$ system on a (100) surface of GaAs . The corrugations have a periodicity of about 5200 Å and are aligned along the [011] direction. The photographs at the left (from top to bottom) show the profiles of the gratings as the etching time was gradually increased, and those at the right are top views of the gratings (Tsang and Wang, 1976).

volving 10 parts of 50% citric acid mixed with 1 part of 30% H_2O_2 .

Although the properties of the DFB lasers are quite different from those of the cleaved lasers (Nakamura *et al.*, 1973, 1974, 1975; Shank *et al.*, 1974; Scifres *et al.*, 1974; Casey *et al.*, 1975; Hill and Watanabe, 1975), we expect that DFB and BR lasers can also be modulated by varying the injection current. Although selected cleaved lasers have been pulsed at a speed in the GHz range, transient phenomena such as spiking and damped relaxation oscillations often limit the operation (Rolden, 1967; McCumber, 1966; Paoli and Ripper, 1970; Boev, *et al.*, 1976; Palio, 1976; Dyment *et al.*, 1972; Lang and Kobayashi, 1975; Russer, 1975; Hillbrand and Russer, 1975). To remedy this situation, one could bias the laser slightly above the threshold so that the carrier density will not undergo large excursions. Alternatively, one could inject a coherent radiation into the laser to suppress the relaxation oscillation. The latter method is particularly interesting, since an integrated optical circuit containing two diode lasers can easily be built; one could then use one of the lasers for light injection.

Light emitting diodes (LEDs) can be used in integrated optics as amplifiers, modulators, and switches. One can also modulate a LED by modulating the injection current. In this case, the speed of the modulation is limited by the lifetime τ of the carriers. The carrier lifetime τ contains two parts, the radiative part τ_r and the nonradiative part τ_{nr} . Let the modulation band-

width and the internal quantum efficiency of the diode be, respectively, $\Delta\omega$ and η_i , we can write

$$1/\tau = 1/\tau_r + 1/\tau_{nr},$$

$$\eta_i = \tau/\tau_r,$$

and

$$\Delta\omega = 1/\tau.$$

Hence, for high quantum efficiency, one requires radiative recombination to dominate over nonradiative process, and for large modulation bandwidth, one should keep τ small (Lee, 1975; Ettenberg *et al.*, 1973; Zucker *et al.*, 1976; Namizaki *et al.*, 1974; Lin and Smith, 1975; Ozeki and Hara, 1976). For heavily doped diodes, τ_r is inversely proportional to the doping level. Using Ge as the dopant, (Al, Ga)As LEDs can be doped to a concentration larger than 10^{19} cm^{-3} , yielding a carrier lifetime of 1 to 2 nanosec or a modulation bandwidth over 500 MHz.

Although lasers and LEDs may be directly modulated as described above, more stable integrated optical circuits can be realized, if lasers are used as constant light sources and separate modulators and switches are provided for modulating the light. The electro-optic coefficient r_{41} in GaAs is 25 times smaller than the r_{33} of LiNbO₃, but the refractive index of GaAs is 1.6 times larger and the net electro-optic effect is only six times smaller in GaAs. When a *p-n* junction is reversely biased, a moderate voltage across the junction produces a large electric field in the depletion layer. The same situation exists in a back-biased Schottky barrier. Hence, light modulation by the linear electro-optic effect in *p-n* junctions and Schottky barriers can be very effective.

McKenna and Reinhart (1976) have shown that when an electric field is applied to a *p-n* junction in the [111] or [100] direction, only the phase of the light wave is modulated. In these cases, the two principal axes of the index ellipsoid are coplanar with the waveguiding layer. On the other hand, an electric field applied to the [110] direction will produce both phase and polarization modulations, and there will be a conversion between TE and TM modes. In the latter case, the junction diode in conjunction with a polarizer may be used as an intensity modulator. These phase and intensity modulators have been built in the (Al, Ga)As heterostructures with merit constants on the order of 0.1 to 0.2 mW/MHz (Reinhart *et al.*, 1972; McKenna and Reinhart, 1976).

The linear electro-optic effect in *p-n* junctions or Schottky barriers may also be used to control the phase-matching condition of a directional coupler. Such directional coupler switches have been built by Campbell, *et al.* (1975) in the form of two parallel metal-gap stripline waveguides, and by Leonberger (1976) in the form of *p+n-n+* junctions. The physics principle involved in these devices has already been discussed in Sec. IV. D.

In a monolithic integrated optical circuit, the wavelength of laser emission can be designed to be very close to the bandgap of the material used for modulators. A modulating electric field will shift the band-edge according to the Franz-Keldysh effect, and the light wave may be modulated in this way by the elec-

troabsorption. This type of modulation, however, requires a very sharp bandedge which is difficult to achieve. The problem has been discussed by Reinhart (1973), Dyment and Kapron (1976), and Stillman *et al.*, (1976).

The active layer in a double heterostructure diode laser is usually 0.1 to 0.4- μm thick. Due to diffraction, the output light beam from a diode laser expands very fast and typically, it has a divergence as much as 50° vertically and about 10° laterally. Several schemes have been presented for reducing the divergence of the exit beam. Early in 1973, Zory reported use of the corrugated surface in a DFB dye laser to couple light out of the waveguide. The output laser beam will then be coupled over the entire surface of the laser rather than through the cleaved end of the active layer and hence, the divergence of the beam will be reduced practically to zero. The problem has been subsequently investigated more in detail by Hill and Watanabe (1973). This type of laser is called "side-coupled" or "side-fire" laser. For this reason, the usual cleaved lasers are called "end-fire" lasers. The corrugated waveguides which serve this purpose are called "leaky" waveguides. (Al, Ga)As "side-fire" diode lasers have been built by Alferov *et al.* (1975) and also by Burnham *et al.* (1975).

Another idea to reduce divergence of the laser beam is the "twin-guide" laser introduced by Suematsu *et al.* (1975). They added to the usual heterostructure, another GaAs layer as the passive waveguide. Light generated in the active layer was coupled to the passive waveguide and then from this passive waveguide to the outside space. It was then possible to use a thin active layer for high efficiency of the laser and a thick passive waveguide to reduce divergence of the exit beam. Following the same idea, but for a better control of the exit beam, Burnham *et al.* (1975) used a corrugated passive waveguide in the twin-guide structure and obtained a beam divergence as small as $0.35^\circ \times 10^\circ$. A similar composite structure has also been constructed by Logan and Reinhart (1975) using a tapered-film coupler. We will discuss their work in more detail later.

Let a wave of phase constant β propagate in a corrugated waveguide with a grating vector $\mathbf{G} = 2\beta$. We have shown in Secs. IV. A and IV. B how the $m = -1$ diffraction order of the corrugation serves the functions of distributed feedback and Bragg reflection. In the (Al, Ga)As diode lasers, such corrugated waveguides have a period, $d = 1200 \text{ \AA}$. Interestingly, if we design a corrugated waveguide with $d = 2400 \text{ \AA}$, or $\mathbf{G} = \beta$, the $m = -2$ diffraction order will then serve the same functions of distributed feedback and Bragg reflection. It is also easy to see that, in this case, the $m = -1$ order will diffract the light wave out of the junction in the direction normal to the junction plane. A corrugated waveguide with $\mathbf{G} = \beta$ has thus one of the diffraction orders for feedback and another order for output coupling. A (Al, Ga)As DFB diode laser has been built utilizing this principle (Scifres *et al.*, 1975).

Interesting techniques have been developed by Logan *et al.* for forming tapered-film couplers and for forming epitaxial layers of "split composition." Figure 49 shows

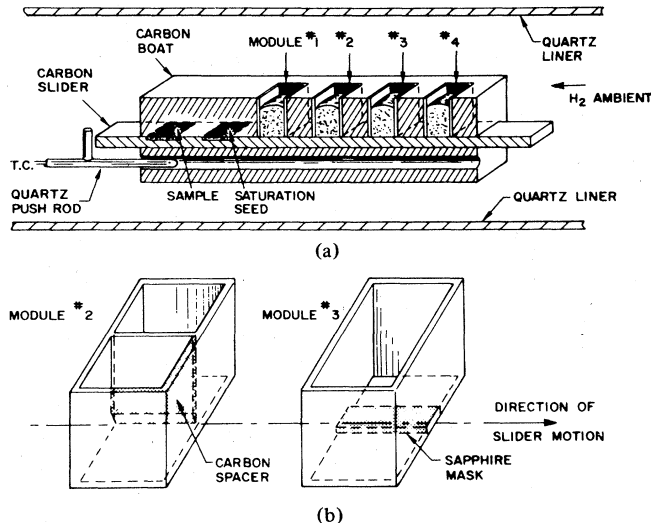


FIG. 49. A liquid-phase epitaxy apparatus used by Logan (Logan and Reinhart, 1975) to form tapered-film couplers and epitaxial layers of "split composition".

his liquid phase epitaxy apparatus (Logan and Reinhart, 1975). In this apparatus, a boat machined from dense carbon is situated in a quartz furnace liner. It contains four thin-walled modules fitted snugly into recesses of the boat. Melts of different compositions are placed in the four modules for growing different heterolayers. During the growth, a (100) oriented rectangular substrate sample is pushed successively under the saturated melts contained in the modules. At the same time the temperature of the furnace starting from 850°C drops at a rate of 0.2°C/min. The module No. 2 shown in Fig. 49(b) has a thin partition which divides the module into two compartments. This module may be used for two different purposes: (1) If different melts are placed in the two compartments, the layer grown has one composition under one compartment, another composition under the other compartment, and a smooth transition between. (2) If, however, the materials are the same in the two compartments, the carbon partition acts as a cooling fin, and the layer grown consists of two flat regions joined by a thicker region under the partition. The module number 3 shown in the same figure is used to grow tapered-film couplers. It contains a sapphire insulating mask at the bottom. Two uniform layer-segments will grow under the module in the areas not covered by the mask and these layer-segments terminate in smooth tapers, decreasing to zero thickness in distances of about 100 μm under the mask. Using the above apparatus, Logan and Reinhart constructed a twin-guide diode laser in which light from the active layer was coupled to the passive waveguide by a tapered-film coupler (1975). The thickness of the passive waveguide was not uniform and the light beam was coupled out at the thicker end to reduce the beam divergence. The BR laser (Reinhart et al., 1975) discussed in Sec. IV. C was also constructed in this apparatus. GaAs tapered-film couplers fabricated by this method and those formed by molecular beam epitaxy have been discussed in detail by Merz et al., (1975).

One discovered that it is not possible to grow (Al, Ga)As on silicon dioxide, silicon nitride, aluminum oxide, and oxidized (Al, Ga)As surfaces either by vapor phase epitaxy or by liquid phase epitaxy. For this reason, when one of the above materials is used as a mask over a GaAs substrate, the growth will take place only in the openings of the mask, but not on top of it. The technique is called "selective growth" and has been used to grow mesa structures for lasers, waveguides, and other optical components. However, this method does not apply to molecular beam epitaxy which is basically a vacuum deposition process. In the latter case, single crystal (Al, Ga)As will grow in the openings of the mask while the material deposited on top of the mask will be polycrystalline.

Using the selective vapor phase epitaxy technique described above, Blum et al. (1974) grew small mesa lasers over a SiO₂ mask on the [110] surface of a GaAs substrate. Operated at 77 K, these mesa lasers delivered a peak power up to a few tenths of a watt. Lately, Bellavance and Campbell (1976) reported similar mesa structures grown over a silicon nitride mask using selective growth of liquid phase epitaxy. Figure 50 shows a laser, a waveguide, and a Y divider grown by this method. Interestingly, the laser has the shape of an I bar. The two ends of the I bar, which form the laser cavity, are (100) and (100) crystalline planes and have grown vertical facets. In the circuit shown in Fig. 50, light was coupled from the laser to the waveguide and to the Y divider through these vertical facets. The I-bar laser had the usual heterostructure and has been operated at room temperature with a threshold current density of 7.5 kA/cm².

Instead of using the (110) substrate as described above, Samid et al. (1975) reported the liquid phase growth of (Al, Ga)As heterostructures through stripe openings in Al₂O₃ mask on a (100) GaAs substrate. The cross-section view of a grown structure is shown in Fig. 51. It is interesting to see that the growth overlays slightly over

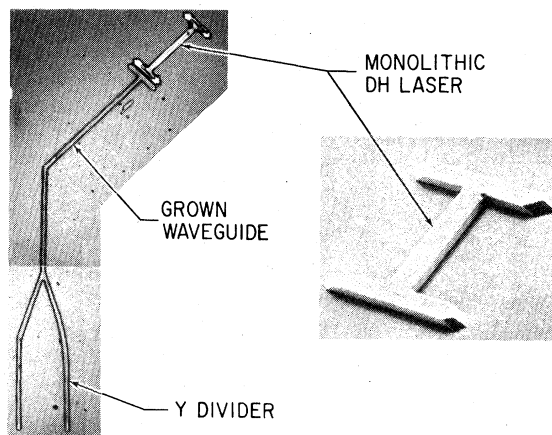


FIG. 50. An I-bar laser, a waveguide, and a Y divider shown in this figure were grown by liquid-phase epitaxy using a silicon nitride mask. Interestingly, these components had grown vertical facets at the two ends which were used for coupling light from one component to another (Bellavance and Campbell, 1976).

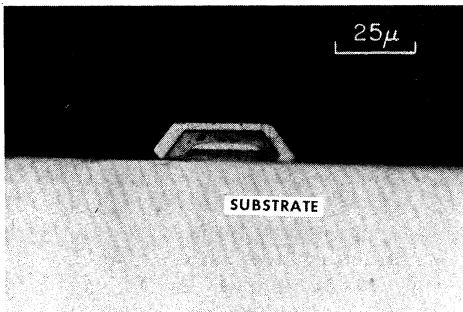


FIG. 51. The SEM photograph shows a cross section view of a mesa structure grown selectively through an opening in an Al_2O_3 mask on a (100) GaAs substrate. Interestingly, in this structure, the layers grown first were covered entirely by the layer grown later. For this reason, this technique is called "embedded epitaxy" (Samid *et al.* 1975).

the oxide surface. The stripes are perpendicular to (011) face and the two sides of the grown structure can be identified as (111) faces. It is also interesting to see that the layers which were grown first are completely covered by the layer grown later, and because of this phenomenon, they called this technique "embedded epitaxy."

In addition to the selective growth over a mask, it is also possible to grow heterostructures over preferentially etched channels by liquid phase epitaxy. The technique is called "etch and fill" by Botez *et al.* (1976). Earlier, Tarui *et al.* (1971) and Iida and Ito (1971) found that channels etched on the (100) surface of GaAs and perpendicular to the (011) face have V-shaped or trapezoidal cross sections, and those etched perpendicular to (011) face have cup-shaped cross sections. Figure 52 shows an inverted ridge waveguide formed by growing $\text{GaAs}/\text{Al}_{0.3}\text{Ga}_{0.7}\text{As}$ layers over a trapezoidal channel. As discussed earlier, this type of waveguide confines light waves within the channels and has excellent mode patterns (Tsang and Wang, 1976).

One of the difficulties in an integrated optical circuit is a large amount of the heat generated by the diode lasers. The current density in each laser must reach above the threshold in order to make it functional, which is in the range of 1 to 2 kA/cm^2 . Hence, to reduce the total current, and thus the heat generated in the circuit, one has to limit the area over which the current is injected. To fabricate a stripe-geometry laser, we usually bombard the laser chip by protons to make the material highly resistive, and leave, for current injection, only an area in the form of a thin stripe which is masked during the bombardment. The active area of the laser defined by this stripe geometry is typically $13\text{-}\mu\text{m}$ wide and $300\text{-}\mu\text{m}$ long, and such lasers take about 100 mA of the current to operate. There is a limit that one can reduce the width of the stripe. The diffusion lengths of the carriers are in the range of 2 to $10 \mu\text{m}$ for the material doped to a concentration of 10^{18} cm^{-3} . Even though we may restrict the current injection within a very narrow stripe, the carriers can diffuse out of the area quickly. Looking for other means to confine the carriers laterally, a breakthrough was made by Tsukada in 1974. He constructed a

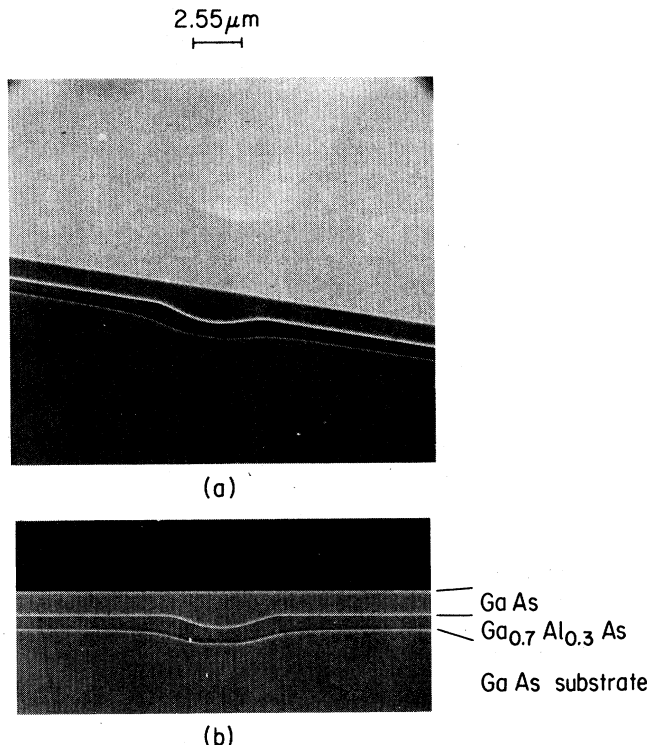


FIG. 52. SEM photographs of (a) the titled top view and (b) the side view of an inverted ridge waveguide fabricated by the "etch and fill" technique (Tsang and Wang, 1976).

"buried heterostructure" laser by the following process (see Fig. 53): (1) grow by liquid phase epitaxy (LPE), a usual $\text{Al}_x\text{Ga}_{1-x}\text{As}(N)/\text{GaAs}(p)/\text{Al}_x\text{Ga}_{1-x}\text{As}(P)$ laser structure on a GaAs substrate. (2) Etch the heterolayers formed above down to the substrate, leaving only a filament mesa standing. This filament laser structure could be less than $1\text{-}\mu\text{m}$ wide and $300\text{-}400\text{-}\mu\text{m}$ long. (3) Carry out a secondary growth by LPE to embed the entire filament mesa in $\text{Al}_y\text{Ga}_{1-y}\text{As}$, with $y > x$. (4) Cover the top surface by a layer of SiO_2 leaving only a window above the filament mesa for making electrical contact. (5) Skin diffusion of Zn in the filament area above the mesa to insure that the mesa has a $N-p-P$ structure. It is easy to see in this "buried heterostructure" laser that the carriers

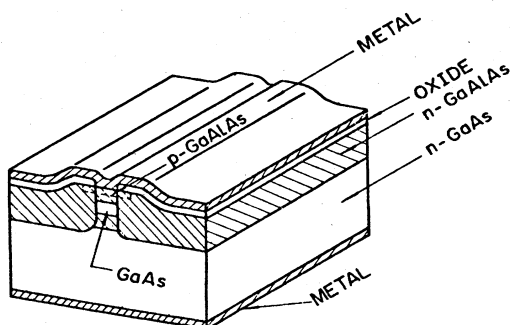


FIG. 53. A schematic drawing of the "buried heterostructure laser" fabricated by Tsukada (1974). The laser had a filament mesa structure at the center which was buried in AlGaAs for carrier confinement both vertically and laterally.

will be confined laterally in the mesa structure, since $\text{Al}_x\text{Ga}_{1-x}\text{As}$ which surrounds the structure has a higher energy gap and thus prevents the carriers to spread over. The mesa structure can then be made narrower than the diffusion length of the carriers. Tsukada's laser has been operated at room temperature with $J_{th} = 2.5 \text{ kA/cm}^2$ and for a total current of only 15 mA. This laser has also other advantages: The active region, being small, forms a single mode waveguide providing a more stable operation of the laser; it has also a nearly circular cross section and so, light from the laser can easily be coupled to an optical fiber. Similar buried structures have also been reported by Burnham and Scifres (1975) and by Lee and Cho (1976).

In principle, Tsukada's laser could be operated with an even smaller current, if some of the leakage current existing in the laser were eliminated. To attain a better lateral carrier confinement, one naturally thought of surrounding the filament mesa of Tsukada's laser by a reversely biased $p-n$ junction. Doing just that, Lee *et al.* (1976) formed a $p-N$ junction on a substrate, which will be reversely biased during the operation. They then etched a channel into this $p-N$ junction down to the substrate and subsequently grew a mesa structure into the channel. Based on the same concept, Burnham *et al.* (1976) formed an interesting "buried" DFB laser shown in Fig. 54. The laser has a $n-P$ junction for the active mesa region, and a $n-P-N-P$ junction for blocking the carriers as well as the pumping current from entering the surrounding area.

Another sticky problem in integrated optics is the loss in the circuit. There have been several independent measurements on the losses in $(\text{Al}, \text{Ga})\text{As}$ waveguides (Jensen *et al.*, 1975; Stillman *et al.*, 1976; Merz *et al.*, 1976). Merz *et al.* found that, at 1.165-eV (or 1.064- μm), the loss is dominated by free-carrier absorption for waveguides with impurity concentrations above $5 \times 10^{17} \text{ cm}^{-3}$. The loss is below 1 cm^{-1} (or 4.34 dB/cm) for relatively pure GaAs layers, and stays approximately constant in the energy range between 1.1 eV (or 1.12 μm) and 1.35 eV (or 0.89 μm). They also found that $\text{Al}_x\text{Ga}_{1-x}\text{As}$ layers have nearly the same amount of the losses as GaAs for x up to 0.1. Since the loss is lower in the 0.9- to 2.1- μm wavelength range than at

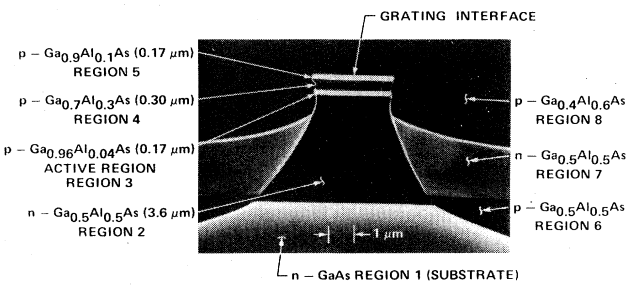


FIG. 54. The SEM photograph shows the cross section of a "buried" DFB laser constructed by Burnham *et al.* (1974). The laser has a $n-P$ junction for the active region at the center, and a $n-P-N-P$ structure in the surrounding area. The $n-P-N-P$ structure which is reversely biased during the operation, prevents the carriers and the pumping current from entering outside the active region.

0.85 μm , it is advisable to use long-wavelength lasers such as AlGaAsSb lasers in conjunction with $(\text{Al}, \text{Ga})\text{As}$ waveguides and modulators in integrated optical circuits.

It has become apparent that mesa etching and selective growth are powerful techniques to form integrated optical circuits. An integrated structure consisting of an $(\text{Al}, \text{Ga})\text{As}$ etched-mesa laser coupled to a high purity GaAs waveguide was reported by Hurwitz *et al.* (1975). Simple monolithic integrated optical circuits have also been demonstrated by Reinhart and Logan (1974; 1975). One of the circuits contained a $(\text{Al}, \text{Ga})\text{As}$ double heterostructure laser and a reversely biased electro-optic modulator. Light from the laser was coupled to the modulator by a tapered-film coupler in an arrangement similar to that shown in Fig. 42(a). The laser was operated at room temperature with $J_{th} = 8 \text{ kA/cm}^2$ and the modulator had a merit constant of $10 \mu\text{W/MHz}$ for 90% intensity modulation. The circuit was grown by liquid phase epitaxy in the apparatus shown in Fig. 49.

As of today, the most advanced integrated optical circuit was reported by Aiki *et al.* (1976). As shown in Fig. 55, the circuit contained six DFB diode lasers connected to six channel waveguides forming an integrated frequency multiplexing light source. The six DFB lasers had different grating periods so that they oscillated at wavelengths 20 \AA apart. The six waveguides were combined into a single output terminal which was ready to be coupled to an optical fiber. The lasers had a structure for separate optical and carrier confinement (see discussion in Sec. IV. C), and they were operated at room temperature with a differential quantum efficiency of 7 percent. Figure 56 shows how light from the laser was coupled to the waveguide. The coupling loss was about 30 percent. The loss in the waveguides including bends and confluence regions was measured to be about 5 cm^{-1} . The overall differential quantum efficiency of the circuit was 0.3 percent. The

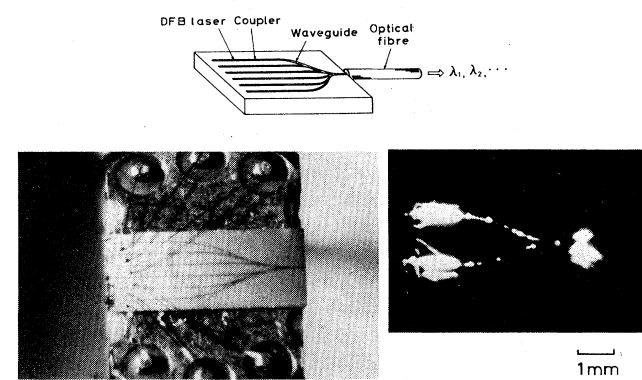


FIG. 55. The top figure is a schematic drawing of a monolithic integrated optical circuit reported by Aiki *et al.* (1976). The circuit contains six laser diodes connected to six channel waveguides forming a "frequency multiplexing light source." The figure at the lower left is a photograph of the circuit, and that at the lower right shows two of the six laser diodes being in operation. The circuit was fabricated by mesa-etching and two-step liquid-phase growth. It is the most advanced integrated optical circuit which has been reported so far.

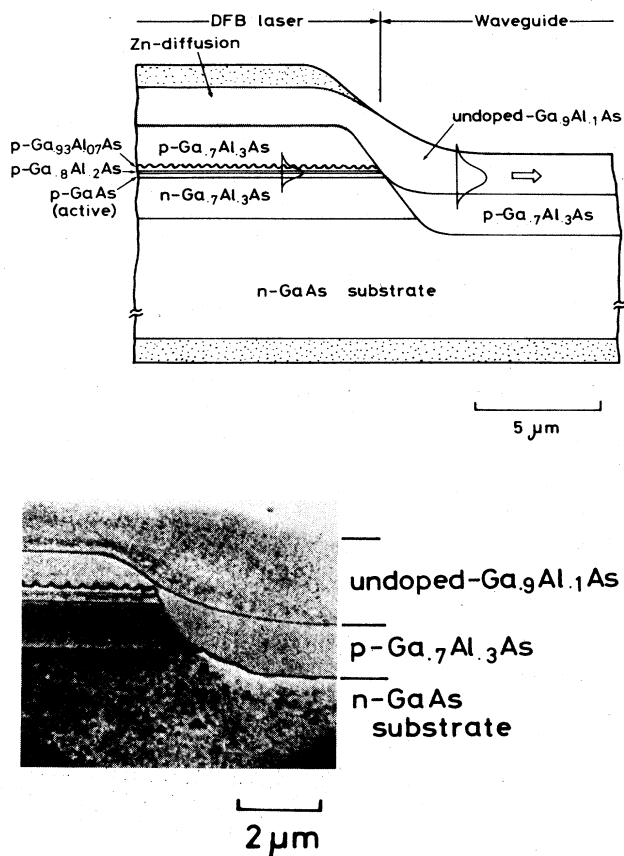


FIG. 56. The top schematic drawing and the lower SEM photograph show how light from a laser was coupled to a channel waveguide in the monolithic integrated optical circuit reported by Aiki *et al.* (1976).

circuit was formed by mesa etching and two-step liquid-phase growth process.

Although most of the devices and circuits described above were grown by liquid phase epitaxy, a relatively new technique, molecular beam epitaxy, has become competitive and even superior in many ways. For example, it can control the thickness of the layers accurate to a few molecular layers; the growth takes place without any chemical reaction; single crystalline layers may be grown on an existing structure without appreciably affecting it (see an excellent review paper by Cho and Arthur, 1975). In integrated optics, the molecular beam epitaxy has been used to form waveguides (Tracy *et al.*, 1973), tapered-film couplers (Merz *et al.*, 1975), lasers with separate confinement (Casey *et al.*, 1975), and those with buried structures (Lee and Cho, 1976).

V. CONCLUSIONS AND REMARKS

Most of the materials presented in this paper were collected from unpublished notes which the author has prepared for talks and lectures on various occasions. To limit the paper to a manageable size, field theories of channel waveguides, nonlinear optics in thin films,

methods of microfabrication and waveguide experiments at the wavelengths other than the near infrared, have not been included. An effort has been made to discuss every topic in very simple terms. To supplement the discussion, a fairly complete list of references is provided, which the reader should consult for further information.

The research in integrated optics discussed here, represents the efforts of about 100 scientists over the past six years. Integrated optics is a technology-oriented field; many of the experiments described here demand the most advanced technology and require close cooperation between physicists, electronics engineers, and material scientists. Miniaturization, batch-fabrication, multiplexing, and integration are the trends of modern technology. To make optical systems compatible with these trends, integrated optics seems to be the natural course to follow. To date, all needed *thin-film optical components* have been demonstrated and lend themselves ready for future development. Simple *integrated optical circuits* have also been realized showing promising results. There has also been an evolution in the concept of integrated optical circuits. Originally, we thought that a circuit should contain all sorts of optical components, and that the circuit is simply a miniaturized and integrated reproduction of what we have on an optical bench. Today, we look at the problem in a different light. We believe that a circuit should have a large number of components, but only two or three different kinds of components. In particular, laser diodes may be used to act as light sources, to be nonlinear elements, and to perform switching and logic functions. A circuit containing a large number of the laser diodes and waveguides is basically what we need for most of the applications. Moreover, laser diodes have smaller sizes than other components and such circuits will have a large packing density. Since waveguiding optical components and their integration offer new capabilities and also new limitations to the optical system, one has to explore new ideas and principles in circuit design to bring out the best in integrated optical circuits.

Undoubtedly, the major effort in the future will be focused on monolithic integrated optical circuits in the GaAs-related systems. The materials include binary, ternary, and quaternary compounds such as AlGaAs, AlGaAsP, GaSb, GaAsSb, AlGaAsSb, InAs, InGaAs, AlInGaAs, AlInAsSb, InP, and InGaAsP, and the substrates could be GaAs, GaSb, InAs, or InP. Mesa-etching, diffusion, selective growth, and formation of buried structures are powerful semiconductor technology; successful applications of these techniques by Aiki *et al.* (1976), Reinhart and Logan (1975), Hurwitz *et al.* (1975), Tsukada (1974, 1976), Burnham and Scifres (1975), Samid *et al.* (1975), Lee and Cho (1976), Bellavance and Campbell (1976), and Tsang and Wang (1975, 1976) to form either integrable components or integrated circuits, indicate that a medium-scale integration of optical circuits could be accomplished. On the other hand, problems that remain to be investigated are: heat dissipation of the circuit, losses in epitaxial layers, coupling between lasers and waveguides and between waveguides and optical fibers, life-

times and stability of the components and the circuit, crosstalk and electrical isolation between various components, and more importantly, integration of electronic and optical components in one chip. A great deal of engineering effort is needed before a practical circuit can be produced.

Integrated optics has always been a fascinating topic; it has caught the imagination of many and is both an art and a science. Over the past six years, the research is filled with interesting ideas and experiments which represent achievements in both physics and engineering. Examples are: *m*-line spectroscopy and its use for the study of new materials and new waveguide structures, distributed feedback and Bragg-reflector lasers and their room-temperature continuous-wave operation, thin-film prisms and lenses, various thin-film magneto-optic, electro-optic, and acousto-optic switches and modulators, and finally, tapered-film couplers and their use for light-guiding interconnections. Research in integrated optics has also far-reaching consequences in other related fields. It has greatly expanded studies in new optical materials, methods of epitaxy, and fabrication of submicron structures. It also offers new methods in experimental physics such as: concentration of a large amount of optical density in a waveguide for a long coherence distance, and easy observation and photography, under a powerful microscope, of experiments performed in thin-film optical waveguides.

Integrated optics adds a new dimension to modern electronics. It does not compete directly with the present microelectronics, but rather complements it. At present, the applications of integrated optics are confined to those areas where the manipulation of light is essential such as optical communication. Being immune from electrical interferences and signal jamming, integrated optical circuits have a unique advantage in military applications. Eventually, as smaller and cheaper circuits can be fabricated, we expect their applications will multiply.

The research activity in integrated optics can be gauged by the vast amount of publications it has produced. Between 1969 and 1976, there were about 400 publications in the United States alone. Most were published in *Applied Physics Letters*, *Applied Optics*, *Optics Communications*, and the *Bell System Technical Journal*. These publications can be divided under various topics as shown in Fig. 57. In the last three years, papers on diode lasers, modulators, switches, and waveguides, occupy about 9% of *Applied Physics Letters* indicating rapid progress made in these areas.

Since 1972, topical meetings on integrated optics were held in the United States every two years. Summaries of the papers presented in these meetings are printed in *Technical Digests*, which are still available from the Optical Society of America. The third topical meeting was held in January of 1976 in Salt Lake City, Utah. Remarkably, devices, techniques, and ideas reported in this paper have already reached a certain degree of sophistication. *Indeed integrated optics has already opened a new chapter in optical science. A great deal has been accomplished in the past six years, although much difficult technological development is still before us.*

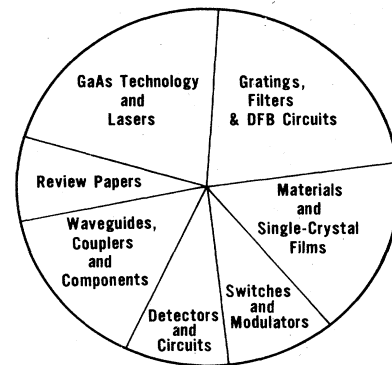


FIG. 57. Various topics published on integrated optics from 1969 to 1976.

ACKNOWLEDGMENTS

The author is very much indebted to my colleagues R. C. Miller, R. A. Logan, and F. K. Reinhart for valuable comments and suggestions. Based on their suggestions, the paper has been thoroughly revised. The author also wishes to thank M. Nakamura, A. Yariv, D. W. Bellavance, R. D. Burnham, and S. Wang for supplying photographs of their work as the illustrations. Special thanks should go to Mrs. L. Kohutich, for secretarial service and to my daughter, Julia J. W. Tien Stoeckenius for editing the final version of the manuscript.

REFERENCES

- Agrawal, V. K., Y. Miyazaki, and Y. Akao, 1975, "Waveguide Type Optical Modulator Using Kerr Magnetooptic Effect in Ni-Fe Films: Experimental Study," *Jap. J. Appl. Phys.* **14**, 1313.
- Aiki, K., M. Nakamura, and J. Umeda, 1976, "Frequency Multiplexing Light Source with Monolithically Integrated Distributed Feedback Diode Lasers," *Appl. Phys. Lett.* **29**, 506.
- Aiki, K., M. Nakamura, J. Umeda, A. Yariv, A. Katzir, and H. W. Yen, 1975, "GaAs-AlGaAs Distributed-Feedback Diode Lasers with Separate Optical and Carrier Confinement," *Appl. Phys. Lett.* **27**, 145.
- Alferov, Zh. I., V. M. Andreev, D. Z. Garbuzov, Yu. V. Zhilyaev, E. P. Morozov, E. L. Portnoi, and V. G. Trioifim, 1970, "Investigation of the Influence of the AlAs-GaAs Heterostructure Parameters on the Laser Threshold Current and the Realization of Continuous Emission at Room Temperature," *Fiz. Tekh. Poluprov.* **4**, 1826 [Sov. Phys.-Semicond. **4**, 1573 (1971)].
- Alferov, Zh. I., V. M. Andreev, S. A. Gurevich, R. F. Kazarinov, V. R. Larionov, M. N. Mizerov, and E. L. Portnoi, 1975, "Semiconductor Lasers with Light Output through the Diffraction Grating on the Surface of the Waveguide Laser," *IEEE J. Quantum Electron.* **11**, 449.
- Alferov, Zh. I., V. M. Andreev, V. I. Korol'kov, E. L. Portnoi, and D. N. Tret'yakov, 1968, "Injection Properties of n -Al_xGa_{1-x}As- p -GaAs Heterojunctions," *Fiz. Tekh. Poluprov.* **2**, 1016 [Sov. Phys.-Semicond. **2**, 843 (1969)].
- Alferov, Zh. I., S. A. Gurevich, R. F. Kazarinov, and R. V. Larionov, 1975, "Injection Heterolaser with Radiation Extracted through a Diffraction Grating," *Sov. Phys.-Semicond.* **8**, 1321.
- Anderson, D. B., 1972, "Waveguide Phase-Matched Parametric Interaction in GaAs," TuB5, Topical Meeting on Inte-

- grated Optics, Las Vegas, Nevada, 1972.
- Anderson, D. B., and J. T. Boyd, 1971, "Phase Matched Second Harmonic Generation in GaAs Thin Film Waveguides," *Appl. Phys. Lett.* **19**, 266.
- Andrews, R. A., 1971, "Optical Waveguides and Integrated Optics Technology," Naval Research Laboratory, Report 7291, August 20, 1971.
- Aoyagi, T., Y. Aoyagi, and S. Namba, 1976, "High Efficient Blazed Grating Couplers," Technical Digest, Topical Meeting on Integrated Optics, Salt Lake City, Utah, 1976; *Appl. Phys. Lett.* **29**, 303.
- Aoyagi, Y., and S. Nambu, 1974, "Laser Oscillation in Simple Corrugated Optical Waveguide," *Appl. Phys. Lett.* **24**, 537.
- Aoyagi, Y., and S. Namba, 1975, "Electron-Beam-Excited DFB Laser in CdS," *Appl. Phys. Lett.* **26**, 24.
- Arthur, J. R., 1968, "Interaction of Ga and As₂ Molecular Beams with GaAs Surfaces," *J. Appl. Phys.* **39**, 4032.
- Auracher, F., 1974, "Mode Order Converter," *Opt. Commun.* **11**, 187.
- Auracher, F., R. Th. Kersten, and H. Boroffka, 1976, "Directional Coupler for Integrated Optics," Topical Meeting on Integrated Optics, MD7, Salt Lake City, Utah, 1976.
- Auston, S., and F. T. Stone, 1976, "Periodic Structure in Photore sist," *Appl. Opt.* **15**, 1071; **15**, 2126.
- Ballman, A. A., H. Brown, P. K. Tien, and R. J. Martin, 1973, "The Growth of Single Crystalline Waveguiding Thin Films of Piezoelectric Silenites," *J. Cryst. Growth* **20**, 251.
- Ballman, A. A., H. Brown, P. K. Tien, and S. Riva-Sanseverino, 1975, "The Growth of LiNbO₃ Thin Films by Liquid Phase Epitaxial Techniques," *J. Cryst. Growth* **29**, 289.
- Ballman, A. A., H. Brown, P. K. Tien, and S. Riva-Sanseverino, 1975, "The Growth of Solid Solution LiNbO₃-LiTaO₃ Thin Films for Optical Waveguides," *J. Cryst. Growth* **30**, 37.
- Barnoski, M. K., 1973, *Introduction to Integrated Optics* (Plenum, New York).
- Barnoski, M. K., R. G. Hunsperger, and A. Lee, 1974, "Ion-Implanted GaAs Injection Laser," *Appl. Phys. Lett.* **24**, 627.
- Barnoski, M. K., R. G. Hunsperger, R. G. Wilson, and G. Tangonan, 1973, "Proton Implanted GaP Optical Waveguides," *J. Appl. Phys.* **44**, 1925.
- Batchman, T. E., and S. C. Rashigh, 1972, "Mode-Selective Properties of a Metal-Clad-Dielectric-Slab Waveguide for Integrated Optics," *IEEE J. Quantum Electron.* **QE-8**, 848.
- Bechmann, P., and A. Spizzichino, 1963, *International Series of Monographs on Electromagnetic Waves* (Oxford, New York), Chap. 5.
- Bellavance, D. W., and J. C. Campbell, 1976, "Room Temperature Mesa Lasers Grown by Selective Liquid Phase Epitaxy," *Appl. Phys. Lett.* **29**, 162.
- Bjorkholm, J. W., and C. V. Shank, 1972, "Distributed Feedback Lasers in Optical Waveguides," *IEEE J. Quantum Electron.* **QE-8**, 833.
- Bjorkholm, J. E., T. P. Sosnowski, and C. V. Shank, 1973, "Distributed Feedback Lasers in Optical Waveguides Deposited on Anisotropic Substrates," *Appl. Phys. Lett.* **22**, 132.
- Bjorklund, G. C., L. F. Mollenauer, and W. J. Tomlinson, 1976, "Distributed Feedback Color Center Lasers in the 2.5-3.0 μm Region," *Appl. Phys. Lett.* **29**, 116.
- Blum, F. A., 1975, "Integrated Optics Mirror Microwave Concept," *Microwaves*, Part I, p. 54, April; Part II, p. 56, May, 1975.
- Blum, F. A., K. L. Lawley, F. H. Doerbeck, and W. C. Holton, 1974, "Monolithic GaAs Injection Mesa Lasers with Grown Optical Facets," *Appl. Phys. Lett.* **25**, 620.
- Blum, F. A., K. L. Lawley, and W. C. Holton, 1974, "Optically Pumped Grown GaAs Mesa Surface Laser," *Appl. Phys. Lett.* **24**, 430.
- Blum, F. A., K. L. Lawley, and W. C. Holton, 1975, "Monolithic Ga_{1-x}In_xAs Mesa Lasers with Grown Optical Facets," *Appl. Phys. Lett.* **46**, 2605.
- Blum, F. A., D. W. Shaw, and W. C. Holton, 1974, in "Optical Striplines for Integrated Optical Circuits in Epitaxial GaAs," *Appl. Phys. Lett.* **25**, 116.
- Boers, P. M., M. T. Vlaardingerbroek, and M. Danielson, 1975, "Dynamic Behavior of Semiconductor Lasers," *Electron. Lett.* **11**, 206.
- Bond, W. L., B. G. Cohn, R. C. C. Leite, and A. Yariv, 1963, "Observation of the Dielectric Waveguide Mode of Light Propagation in p-n Junctions," *Appl. Phys. Lett.* **2**, 57.
- Born, M., and E. Wolf, 1970, *Principles of Optics* (Pergamon, New York), p. 49, Eq. (60).
- Botez, D., L. Figueira, and S. Wang, 1976, "Optically Pumped GaAs-Ga_{1-x}Al_xAs Ring Laser Fabricated by Liquid Phase Epitaxy over Chemically Etched Channels," paper II-A-1, p. 4, Conference Abstract, Device Research Conference, Salt Lake City, Utah, June 21-23, 1976.
- Botez, D., L. Figueira, and S. Wang, 1976, "Optically Pumped GaAs-Ga_{1-x}Al_xAs Half-Ring Laser Fabricated by Liquid-Phase Epitaxy over Chemically Etched Channels," *Appl. Phys. Lett.* **29**, 502.
- Botez, D., W. T. Tsang, and S. Wang, 1976, "Growth Characteristics of GaAs-Ga_{1-x}Al_xAs Structures Fabricated by Liquid-Phase Epitaxy over Preferentially Etched Channels," *Appl. Phys. Lett.* **28**, 234.
- Bovin, L. P., 1974, "Thin-Film Laser to Fiber Coupler," *Appl. Opt.* **13**, 391.
- Broers, A. N., W. W. Molzen, J. J. Cuomo, and N. D. Wittels, 1976, "Electron Beam Fabrication of 80 Å Metal Structures," *Appl. Phys. Lett.* **29**, 596.
- Burnham, R. D., and D. R. Scifres, 1975, "Etched Buried Heterostructure GaAs/GaAlAs Injection Lasers," *Appl. Phys. Lett.* **27**, 510.
- Burnham, R. D., D. R. Scifres, and W. Streifer, 1975, "Low Divergence Beams from Grating Coupled Composite Guide Heterostructure GaAlAs Diode Lasers," *Appl. Phys. Lett.* **26**, 644.
- Burnham, R. D., D. R. Scifres, and W. Streifer, 1975, "Highly Collimated Laser Beams from Distributed Feedback Lasers," *J. Opt. Soc. Am.* **65**, 225.
- Burnham, R. D., D. R. Scifres, and W. Streifer, 1975, "Single-Heterostructure Distributed Feedback GaAs Diode Lasers," *IEEE J. Quantum Electron.* **QE-11**, 439.
- Burnham, R. D., D. R. Scifres, and W. Streifer, 1975, "Striped Substrate Double Heterostructure Lasers," *IEEE J. Quantum Electron.* **QE-11**, 418.
- Burnham, R. D., D. R. Scifres, and W. Streifer, 1976, "Distributed Feedback Buried Heterostructure Diode Lasers," *Appl. Phys. Lett.* **29**, 287.
- Burns, W. K., A. B. Lee, and A. F. Milton, 1977, "Active Branching Waveguide Modulator," *Appl. Phys. Lett.*, to be published.
- Burns, W. K., and A. F. Milton, 1975, "Mode Conversion in Planar-Dielectric Separating Waveguides," *IEEE J. Quantum Electron.* **QE-11**, 32.
- Burns, W. K., A. F. Milton, A. B. Lee, and E. J. West, 1976, "Optical Modal Evolution 3-dB Coupler," *Appl. Opt.* **15**, 1053.
- Burns, W. K., A. F. Milton, and A. B. Lee, "Optical Waveguide Parabolic Coupling Horns," *Appl. Phys. Lett.* (to be published).
- Burns, W. K., and J. Warner, 1974, "Mode Dispersion in Uniaxial Optical Waveguides," *J. Opt. Soc. Am.* **64**, 4.
- Burns, W. K., and J. Warner, 1974, "Mode Dispersion in Uniaxial Optical Waveguides," *J. Opt. Soc. Am.* **64**, 441.
- Butler, J. K., C. S. Wang, and J. C. Campbell, 1976, "Mode Characteristics of Optical Stripline Waveguides," *J. Appl. Phys.* **47**, 4033.
- Campbell, J. C., F. A. Blum, and D. W. Shaw, 1975, "GaAs Electrooptic Channel Waveguide Modulator," *Appl. Phys. Lett.* **26**, 640.
- Campbell, J. C., F. A. Blum, D. W. Shaw, and K. L. Lawley, 1975, "GaAs Electrooptic Directional-Coupler Switch," *Appl.*

- Phys. Lett. **27**, 202.
- Carruthers, J. R., I. P. Kaminow, and L. W. Stulz, 1974, "Diffusion Kinetics and Optical Waveguiding Properties of Out-Diffused Layers in Lithium Tantalate," Appl. Opt. **13**, 2333.
- Casey, H. C., Jr., A. Y. Cho, and P. A. Barnes, 1975, "Application of Molecular Beam Layers to Heterostructure Lasers," IEEE J. Quantum Electron. **QE-11**, 467.
- Casey, H. C., Jr., B. I. Miller, and E. Pinkas, 1973, "Variation of Minority-Carrier Diffusion Length with Carrier Concentration in GaAs Liquid-Phase Epitaxial Layers," J. Appl. Phys. **44**, 1281.
- Casey, H. C., Jr., and M. B. Panish, 1969, "Composition Dependence of the $\text{Ga}_{1-x}\text{Al}_x\text{As}$ Direct and Indirect Energy Gaps," J. Appl. Phys. **40**, 4910.
- Casey, H. C., Jr., D. D. Sell, and M. B. Panish, 1974, "Refractive Index of $\text{Al}_x\text{Ga}_{1-x}\text{As}$ between 1.2 and 1.8 eV," Appl. Phys. Lett. **24**, 63.
- Casey, H. C., Jr., S. Somekh, and M. Illegems, 1975, "Room-Temperature Operation of Low-Threshold Separate-Confinement Heterostructure Injection Laser with Distributed Feedback," Appl. Phys. Lett. **27**, 142.
- Chandross, E. A., C. A. Pryde, and W. J. Tomlinson, 1974, "Photolocking—A New Technique for Fabricating Optical Waveguide Circuits," in OSA Tech. Digest, Integrated Optics (New Orleans, La.), paper ThA5-1, January, 1974.
- Chang, L. L., and A. Koma, 1976, "Interdiffusion between AlAs and GaAs," Appl. Phys. Lett. **29**, 138.
- Chang, M. S., 1974, "Tolerance to the Phase-Matching Condition for the Integrated Acoustooptical Filter," Appl. Opt. **13**, 1867.
- Chang, M. S., P. Burlamachhi, C. Hu, and J. R. Whinnery, 1972, "Light Amplification in a Thin Film," Appl. Phys. Lett. **20**.
- Chang, W. S. C., 1971, "Acoustooptical Deflections in Thin Films," IEEE J. Quantum Electron. (Corresp.), **QE-7**, 167.
- Chang, W. S. C., 1973, "Periodic Structures and Their Application in Integrated Optics," IEEE Trans. Microwave Theory Tech. **21**, 775.
- Chang, W. S. C., 1975, "Integrated Optics at 10.6 μm Wavelength," IEEE Trans. Microwave Theory Tech. **23**, 31.
- Chang, W. S. C., M. W. Muller, and F. J. Rosenbaum, 1974, *Integrated Optics Vol. 2: Laser Applications* (Academic, New York).
- Chen, Bor-Uei, and C. L. Tang, 1976, "Nd-Glass Thin-Film Waveguide: An Active Medium for Nd Thin-Film Laser," Appl. Phys. Lett. **28**, 435.
- Chen, F. S., 1970, "Modulators for Optical Communications," Proc. IEEE (Special Issue on Optical Communication) **58**, 1440.
- Chen, F. S., and W. W. Benson, 1974, "A Lithium Niobate Light Modulator for Optical Communications," Proc. IEEE (Lett.) **62**, 133.
- Cheo, P. K., 1972, "Excitation and Modulation of 10.6 μm Guided Waves in GaAs Epitaxial Thin Film," TuB3, Topical Meeting on Integrated Optics, Las Vegas, Nevada, 1972.
- Cheo, P. K., 1973, "Pulse Amplitude Modulation of CO_2 Laser in an Electrooptic Thin-Film Waveguide," Appl. Phys. Lett. **22**, 241.
- Cheo, P. K., 1973, "Electrooptic Properties of Reverse-Biased GaAs Epitaxial Thin Films at 10.6 μm ," Appl. Phys. Lett. **23**, 439.
- Cheo, P. K., J. M. Berak, W. Oshinsky, and J. L. Swindal, 1973, "Optical Waveguide Structures for CO_2 Lasers," Appl. Opt. **12**, 500.
- Cheo, P. K., and M. Gilden, 1976, "High Power Integrated Optic IR Modulator at Microwave Frequencies," Appl. Phys. Lett. **28**, 626.
- Chin, G. Y., A. A. Ballman, P. K. Tien, and S. Riva-Sanseverino, 1975, "Diffusion Kinetics and Optical Quality in LiNbO_3 - LiTaO_3 Optical Waveguides," Appl. Phys. Lett. **26**, 637.
- Chinn, S. R., 1973, "Effect of Mirror Reflectivity in a Distributed Feedback Laser," IEEE J. Quantum Electron. **QE-9**, 574.
- Chinn, S. R., and D. L. Kelley, 1974, "Analysis of the Transmission, Reflection and Noise Properties of Distributed Feedback Amplifiers," Opt. Commun. **10**, 123.
- Cho, A. Y., 1971, "Film Deposition by Molecular-Beam Techniques," J. Vac. Sci. Tech. **8**, S31.
- Cho, A. Y., and J. R. Arthur, 1975, "Molecular Beam Epitaxy," Prog. Solid State Chem. **10**, Part 3, 157.
- Cho, A. Y., and W. C. Ballamy, 1975, "GaAs Planar Technology by Molecular Beam Epitaxy (MBE)," J. Appl. Phys. **46**, 783.
- Cho, A. Y., and H. C. Casey, Jr., 1974, "GaAs- $\text{Al}_x\text{Ga}_{1-x}\text{As}$ Double Heterostructure Lasers Prepared by Molecular-Beam Epitaxy," Appl. Phys. Lett. **25**, 288.
- Cho, A. Y., R. W. Dixon, H. C. Casey, Jr., and R. L. Hartman, 1976, "Continuous Operation of GaAs- $\text{Al}_x\text{Ga}_{1-x}\text{As}$ Double Heterostructure Lasers Prepared by Molecular-Beam Epitaxy," Appl. Phys. Lett. **28**, 501.
- Cho, A. Y., M. B. Panish, and I. Hayashi, 1971, "Molecular Beam Epitaxy of GaAs, $\text{Al}_x\text{Ga}_{1-x}$ and GaP," in *Proceedings of the Symposium on Gallium Arsenide and Related Compounds*, Aachen, Germany, 1970 (Institute of Physics, London), pp. 18-29.
- Cho, A. Y., and F. K. Reinhart, 1972, "Growth of Three-Dimensional Dielectric Waveguides for Integrated Optics by Molecular Beam Epitaxy," Appl. Phys. Lett. **21**, 355.
- Chown, M., A. R. Goodwin, D. F. Lovelace, G. H. B. Thompson, and P. R. Selway, 1973, "Direct Modulation of Double Heterostructure Lasers at Rates up to 1 Gbit/s," Electron. Lett. **9**, 34.
- Chu, R. S., and T. Tamir, 1970, "Guided Wave Theory of Light Diffraction by Acoustic Microwaves," IEEE Trans. Microwave Theory Tech. **18**, 486.
- Collin, R. E., 1960, *Field Theory of Guided Waves* (McGraw-Hill, New York).
- Comerford, L., and D. Zory, 1974, "Selectively Etched Diffraction Gratings in GaAs," Appl. Phys. Lett. **25**, 208.
- Conwell, E. M., 1973, "Modes in Optical Waveguides Formed by Diffusion," Appl. Phys. Lett. **23**, 328.
- Conwell, E. M., 1976, "Integrated Optics," Phys. Today **29**, May 1976, p. 48.
- Cordero, R. F., and S. Wang, 1974, "Threshold Condition for Thin-Film Distributed Feedback Lasers," Appl. Phys. Lett. **24**, 474.
- Cordero, R. F., and S. Wang, 1976, "Sputtered-Etched Ta_2O_5 Corrugation Gratings for DFB Lasers," Wave Electronics **1**, 355.
- Dabby, F. W., and A. Kestenbaum, 1974, "Forward Scattering in Periodic Waveguide," OSA Tech. Digest, Integrated Optics (New Orleans, La.), paper T4B3-1, Jan., 1974.
- Dabby, F. W., A. Kestenbaum, and V. C. Paek, 1972, "Periodic Dielectric Waveguides," Opt. Commun. **6**, 125.
- Dabby, F. W., M. A. Saifi, and A. Kestenbaum, 1973, "High Frequency Cut-off Periodic Dielectric Waveguides," Appl. Phys. Lett. **22**, 190.
- Dakss, M. L., L. Kuhn, P. F. Heidrich, and B. A. Scott, 1970, "Grating Couplers for Efficient Excitation of Optical Guided Waves in Thin Films," Appl. Phys. Lett. **16**, 523.
- Dalgoutte, D. G., 1973, "A High Efficiency Thin Grating Coupler for Integrated Optics," Opt. Commun. **8**, 124.
- Dalgoutte, D. G., R. B. Smith, G. Achutaramayya, and J. H. Harris, 1975, "Externally Mounted Fibers for Integrated Optics Interconnections," Appl. Opt. **14**, 1860.
- DeBarros, M. A. R. P., and M. G. F. Wilson, 1972, "High Speed Electrooptic Diffraction Modulator for Baseband Operation," Proc. Inst. Electr. Eng. Lond. **119**, 807.
- DeWames, R. E., and W. F. Hall, 1973, "Conditions in Distributed Feedback Waveguides," Appl. Phys. Lett. **23**, 28.
- Dingle, R., W. Wiegmann, and C. H. Henry, 1974, "Quantum States of Confined Carriers in Very Thin $\text{Al}_x\text{Ga}_{1-x}\text{As}$ - $\text{Al}_x\text{Ga}_{1-x}\text{As}$ Heterostructures," Phys. Rev. Lett. **33**, 827.
- Dixon, R. W., F. R. Nash, R. L. Hartman, and R. T. Hepple-

- white, 1976, "Improved Light-Output Linearity in Stripe-Geometry Double-Heterostructure (Al, Ga) As Lasers," *Appl. Phys. Lett.* **29**, 372.
- Dobkin, A. S., V. V. Kokorev, G. A. Lapitskaya, A. A. Pleskov, O. N. Prozorov, L. A. Rivkin, G. A. Sulharev, V. S. Shil'dyaev, and D. H. Yakubovich, 1970, Sov. Phys.—Semi-cond. **4**, 515.
- Dymant, J. C., L. A. D'Asaro, and J. C. North, 1971, "Optical and Electrical Properties of Proton Bombarded *p*-type GaAs," *Bull. Am. Phys. Soc.* **16**, 329.
- Dymant, J. C., L. A. D'Asaro, J. C. North, B. I. Miller, and J. E. Ripper, 1972, "Proton-Bombardment Formation of Stripe-Geometry Heterostructure Lasers for 300 °K CW Operation," *Proc. IEEE (Lett.)* **60**, 726.
- Dymant, J. C., and F. P. Kapron, 1976, "Extinction Ratio Limitation in GaAlAs Electroabsorption Light Modulators," *J. Appl. Phys.* **47**, 1523.
- Dymant, J. C., J. E. Ripper, and T. D. Lee, 1972, "Measurement and Interpretation of Long Spontaneous Lifetimes In DH Lasers," *J. Appl. Phys.* **43**, 452.
- Elachi, C., and C. Yeh, 1973, "Periodic Structures in Integrated Optics," *J. Appl. Phys.* **44**, 3146.
- Ettenberg, M., and H. Kressel, 1976, "Interfacial Recombination at (Al, Ga)As/GaAs Heterojunction Structures," *J. Appl. Phys.* **47**, 1538.
- Ettenberg, M., H. Kressel, and S. L. Gilbert, 1973, "Minority Carrier Diffusion Length and Recombination Lifetime in GaAs:Ge Prepared by Liquid Phase Epitaxy," *J. Appl. Phys.* **44**, 827.
- Evtuhov, V., and A. Yariv, 1975, "GaAs and GaAlAs Devices for Integrated Optics," *IEEE Trans. Microwave Theory Tech.* **23**, 44.
- Felsen, L. B., and S. Y. Shin, 1975, "Rays, Beams, and Modes Pertaining to the Excitation of Dielectric Waveguides," *IEEE Trans. Microwave Theory Tech.* **23**, 150.
- Flanders, D. C., H. Kogelnik, R. V. Schmidt, and C. V. Shank, 1974, "Grating Filters for Thin-Film Optical Waveguides," *Appl. Phys. Lett.* **24**, 194.
- Fox, A. J., and T. M. Bruton, 1975, "Electrooptic Effects in the Optically Active Compounds Bi₁₂TiO₂₀ and Bi₄₀Ga₂O₆₃," *Appl. Phys. Lett.* **27**, 360.
- Fukunishi, S., N. Uchida, S. Miyazawa, and J. Noda, 1974, "Electrooptic Modulation of Optical Guided Wave in LiNbO₃ Thin Film Fabricated by EGM Method," *Appl. Phys. Lett.* **24**, 424.
- Furuta, H., H. Noda, and A. Ihaya, 1974, "Optical Directional Coupler Consisting of Optical Stripline" in OSA Tech. Digest, Integrated Optics (New Orleans, La.), paper WB4-1, January, 1974.
- Furuta, H., H. Noda, and A. Ihaya, 1974, "Novel Optical Waveguide for Integrated Optics," *Appl. Opt.* **13**, 322.
- Gandrud, W. B., 1971, "Reduced Modulator Drive-Power Requirements for 10.6-μ Guided Waves," *IEEE J. Quantum Electron. (Corresp.) QE-7*, 580.
- Garmire, E., 1973, "Optical Waveguides in Single Layers of Ga_{1-x}Al_xAs Grown on GaAs Substrates," *Appl. Phys. Lett.* **23**, 403.
- Garmire, E., D. F. Lovelace, and H. B. Tompson, 1975, "Diffused Two-Dimensional Optical Waveguides in GaAs," *Appl. Phys. Lett.* **26**, 329.
- Garmire, E., H. Stoll, A. Yariv, and R. E. Hunsperger, 1972, "Optical Waveguiding in Proton-Implanted GaAs," *Appl. Phys. Lett.* **21**, 87.
- Garvin, H. L., E. Garmire, S. Somekh, H. Stoll, and A. Yariv, 1973, "Ion Beam Micromachining of Integrated Optics Components," *Appl. Opt.* **12**, 455.
- Gedeon, A., 1974, "The Effective Thickness of Optical Waveguides in Tunable Directional Couplers," *J. Opt. Soc. Amer.* **64**, 615.
- Gfeller, F. R., 1974, "Acoustooptic Scanner," presented at the Integrated Optics Meeting, New Orleans, La., 1974.
- Gfeller, F. R., and C. W. Pitt, 1972, "Collinear Acoustooptic Deflection in Thin Films," *Electron. Lett.* **8**, 549.
- Ghizoni, C. C., B. U. Chen, and C. L. Tang, 1976, "Theory and Experiments on Grating Couplers for Thin-Film Waveguides," *IEEE J. Quantum Electron.* **QE-12**, 69.
- Giallorenzi, T. G., and A. F. Milton, 1974, "Acoustooptic Beam Deflection in Multimode Optical Waveguide," *J. Appl. Phys.* **45**, 4.
- Giallorenzi, T. G., and J. P. Sheridan, 1975, "Light Scattering in Nematic Liquid Crystal Waveguides," *J. Appl. Phys.* **46**, 1271.
- Giallorenzi, T. G., and J. P. Sheridan, 1976, "Light Scattering from Smectic Liquid Crystal Waveguides," *J. Appl. Phys.* (to be published).
- Giallorenzi, T. G., E. J. West, R. Kirk, R. Ginter, and R. A. Andrews, 1973, "Optical Waveguides Formed by Thermal Migration of Ions in Glass," *Appl. Opt.* **12**, 1240.
- Gia Russo, D. P., and J. H. Harris, 1971, "Electrooptic Modulation in a Thin-Film Waveguide," *Appl. Opt.* **10**, 2786.
- Gia Russo, D. P., and C. S. Kumar, 1973, "Sputtered Ferroelectric Thin-Film Electrooptic Modulator," *Appl. Phys. Lett.* **23**, 229.
- Goell, J. E., 1969, "A Circular-Harmonic Computer Analysis of Rectangular Dielectric Waveguides," *Bell Syst. Tech. J.* **48**, 2133.
- Goell, J. E., 1973, "Electron-Resist Fabrication of Bends and Couplers for Integrated Optical Circuits," *Appl. Opt.* **12**, 729.
- Goell, J. E., 1973, "Barium Silicate Films for Integrated Optical Circuits," *Appl. Opt.* **12**, 737.
- Goell, J. E., and R. D. Standley, 1969, "Sputtered Glass Waveguides for Integrated Optical Circuits," *Bell Syst. Tech. J.* **48**, 3445.
- Goell, J. E., and R. D. Standley, 1970, "Integrated Optical Circuits," *Proc. IEEE* **58**, 1504.
- Goell, J. E., R. D. Standley, and T. Li, 1970, "Optical Waveguides Bring Laser Communication Closer," *Electronics* **60**, August 31, 1970.
- Gossard, A. C., P. M. Potroff, W. Weigmann, R. Dingle, and A. Savage, 1976, "Epitaxial Structure with Alternate-Atomic-Layer Composition Modulation," *Appl. Phys. Lett.* **29**, 323.
- Hall, D., A. Yariv, and E. Garmire, 1970, "Optical Guiding and Electrooptic Modulation in GaAs Epitaxial Layers," *Opt. Commun.* **1**, 403.
- Hall, D., A. Yariv, and E. Garmire, 1970, "Observation of Propagation Cut-off and Its Control in Thin Optical Waveguides," *Appl. Phys. Lett.* **17**, 127.
- Hammer, J. M., R. A. Bartolini, A. Miller, and C. C. Neil, 1976, "Optical Grating Coupling between Low Index Fibers and High Index Film Waveguides," *Appl. Phys. Lett.* **28**, 192.
- Hammer, J. M., D. J. Chanin, and M. T. Duffy, 1973, "Fast Electrooptic Waveguide Deflector Modulator," *Appl. Phys. Lett.* **23**, 1973.
- Hammer, J. M., D. J. Chanin, M. T. Duffy, and J. P. Wittke, 1972, "Low Loss Epitaxial ZnO Optical Waveguides," *Appl. Phys. Lett.* **21**, 358.
- Hammer, J. M., and W. Philips, 1974, "Low-Loss Single-Mode Optical Waveguides and Efficient High-Speed Modulators of LiNb_xTa_{1-x}O₃ on LiTaO₃," *Appl. Phys. Lett.* **24**, 545.
- Handa, K., S. T. Peng, and T. Tamir, 1975, "Improved Perturbation Analysis of Dielectric Gratings," *Appl. Phys.* **5**, 325.
- Harper, J., and E. Spiller, 1975, "High Resolution Lenses for Optical Waveguides," Second Topical Meeting on Integrated Optics, New Orleans (1974, a report of this meeting in *Appl. Opt.* **14**, 573).
- Harris, J. H., and R. Shubert, 1969, URSI Conference Abstracts, Washington, D. C., April, 1969.
- Harris, J. H., and R. Shubert, 1971, "Variable Tunneling Excitation of Optical Surface Waves," *IEEE Trans. Microwave Theory Tech.* **19**, 269.
- Harris, J. H., R. Shubert, and J. N. Polky, 1970, "Beam Coupling to Films," *J. Opt. Soc. Am.* **60**, 1007.

- Harris, J. H., R. K. Winn, and D. G. Dalgoutte, 1972, "Theory and Design of Periodic Couplers," *Appl. Opt.* **11**, 2234.
- Haus, H. A., 1976, "Gain Saturation in Distributed Feedback Lasers," to be published.
- Haus, H. A., and R. V. Schmidt, 1976, "Approximate Analysis of Optical Waveguide Grating Coupling Coefficients," to be published.
- Haus, H. A., and C. V. Shank, 1976, "Antisymmetric Taper of Distributed Feedback Laser," to be published.
- Hayashi, I., and M. B. Panish, 1970, "GaAs-Ga_xAl_{1-x}As Heterostructure Injection Lasers which Exhibit Low Thresholds at Room Temperature," *J. Appl. Phys.* **41**, 150.
- Hayashi, I., M. B. Panish, P. W. Foy, and S. Sumski, 1970, "Junction Lasers which Operate Continuously at Room Temperature," *Appl. Phys. Lett.* **17**, 109.
- Hensler, D. H., J. D. Cuthbert, R. J. Martin, and P. K. Tien, 1971, "Optical Propagation in Sheet and Pattern Generated Films in Ta₂O₅," *Appl. Opt.* **10**, 1037.
- Hepner, G., B. Desormiere, and J. P. Castera, 1975, "Magnetooptic Effect in Garnet Film Waveguides," *Appl. Opt.* **14**, 1479.
- Hill, K. O., 1974, "A Periodic Distributed Parameter Waveguide for Integrated Optics," *Appl. Opt.* **13**, 1853.
- Hill, K. O., and A. Watanabe, 1972, "A Distributed Feedback Side-Coupler Laser," *Opt. Commun.* **5**, 389.
- Hill, K. O., and A. Watanabe, 1973, "Distributed-Feedback Side Coupled Laser; Passive Core Corrugated-Waveguide Laser," *Appl. Opt.* **12**, 430.
- Hill, K. O., and A. Watanabe, 1975, "Envelope Gain Structure in Distributed-Feedback Lasers," *Appl. Opt.* **14**, 950.
- Hillbrand, H., and P. Russer, 1972, "Large Signal PCM Behavior of Injection Lasers with Coherent Irradiation into One of Its Oscillating Modes," *Electron. Lett.* **11**, 372.
- Hocker, G. B., and W. K. Burns, 1975, "Modes in Diffused Optical Waveguides of Arbitrary Index Profile," *IEEE J. Quantum Electron.* **QE-11**, 6.
- Hondros, D., and P. Debye, 1910, "Elektromagnetische Wellen an dielektrischen Drähten," *Ann. Phys. (Leipz.)* **32**, 465.
- Hope, L. L., 1972, "Theory of Optical Grating Couplers," *Opt. Commun.* **5**, 179.
- Horowitz, B. R., and T. Tamir, 1971, "Lateral Displacement of a Light Beam at a Dielectric Interface," *J. Opt. Soc. Am.* **61**, 594.
- Houghton, A. J., and P. D. Townsend, 1976, "Optical Waveguides Formed by Low-Energy Electron Irradiation of Silica," *Appl. Phys. Lett.* **29**, 565.
- Hsieh, J. J., 1976, "Room-Temperature Operation of GaInAsP/InP Double Heterostructure Diode Lasers Emitting at 1.1 μm," *Appl. Phys. Lett.* **28**, 283.
- Hsu, H. P., and A. F. Milton, "Single Mode Coupling between Fibers and Channel Waveguides," *IEEE J. Quantum Electron.* (to be published).
- Hu, Chenming, and John R. Whinnery, 1974, "Field-Realigned Nematic-Liquid-Crystal Optical Waveguides," *IEEE J. Quantum Electron.* **QE-10**, 556.
- Hu, Chenming, and John R. Whinnery, 1974, "Losses of a Nematic-Liquid-Crystal Optical Waveguide," *J. Opt. Soc. Am.* **64**, 1424.
- Hu, Chenming, John R. Whinnery, and N. M. Amer, 1974, "Optical Deflection in Thin-Film Nematic-Liquid-Crystal Waveguides," *IEEE J. Quantum Electron.* **QE-10**, 218.
- Hu, Chenming, Y. S. Kwon, and J. R. Whinnery, "Liquid Crystal Waveguides for Integrated Optics," special issue on Integrated Optics of *IEEE J. Quantum Electron.*, submitted October, 1976.
- Hurwitz, C. E., J. A. Rossi, J. J. Hsieh, and C. M. Wolfe, 1975, "Integrated GaAs-AlGaAs Double-Heterostructure Lasers," *Appl. Phys. Lett.* **27**, 241.
- Ihaya, A., H. Furuta, and H. Noda, 1972, "Thin-Film Optical Directional Coupler," *Proc. IEEE* **60**, 470.
- Iida, S., and K. Ito, 1971, "Selective Etching of Gallium Arsenide Crystals in H₂SO₄-H₂O₂-H₂O System," *J. Electrochem. Soc.* **118**, 769.
- Logansen, L. V., 1962, "Theory of Resonant Electromagnetic Systems that Use Total Intuned Reflection," *Sov. Phys.-Tech. Phys.* **7**, 295.
- Ishitani, A., and M. Kimura, 1976, "Single Crystal Sr₂Nb₂O₇ Film Optical Waveguide Deposited by rf Sputtering," *Appl. Phys. Lett.* **29**, 289.
- Izawa, T., and H. Nakagome, 1972, "Optical Waveguide Formed by Electrically Induced Migration of Ions in Glass Plates," *Appl. Phys. Lett.* **21**, 584.
- Jensen, S. M., M. K. Barnoski, R. G. Hunsberger, and G. S. Kamath, 1975, "Low-Loss Optical Waveguides in Single Layer of Ga_{1-x}Al_xAs," *Appl. Phys. Lett.* **46**, 3547.
- Joyce, W. B., R. W. Dixon, and R. L. Hartman, 1976, "Statistical Characterization of the Lifetimes of Continuously Operated (Al, Ga)As Double-Heterostructure Lasers," *Appl. Phys. Lett.* **28**, 684.
- Kaminow, I. P., 1974, *An Introduction to Electrooptic Devices* (Academic, New York).
- Kaminow, I. P., 1975, "Optical Waveguide Modulators," *IEEE Trans. Microwave Theory Tech.* **23**, 57.
- Kaminow, I. P., and J. R. Carruthers, 1973, "Optical Waveguiding Layers in LiNbO₃ on LiTaO₃," *Appl. Phys. Lett.* **22**, 326.
- Kaminow, I. P., J. R. Carruthers, E. H. Turner, and L. W. Stulz, 1973, "Thin-Film LiNbO₃ Electrooptic Light Modulator," *Appl. Phys. Lett.* **22**, 540.
- Kaminow, I. P., W. L. Mammel, and H. P. Weber, 1974, "Metal-Clad Waveguides: Analytical and Experimental Study," *Appl. Opt.* **13**, 396.
- Kaminow, I. P., V. Ramaswamy, R. V. Schmidt, and E. H. Turner, 1974, "LiNbO₃ Ridge Waveguide Modulator," *Appl. Phys. Lett.* **24**, 622.
- Kaminow, I. P., and L. W. Stulz, 1975, "A Planar Electrooptic Prism Switch," *IEEE J. Quantum Electron.* **QE-11**, 633.
- Kaminow, I. P., L. W. Stulz, and E. H. Turner, 1975, "Efficient Strip Waveguide Modulator," *Appl. Phys. Lett.* **27**, 555.
- Kaminow, I. P., and E. H. Turner, 1966, "Electrooptic Light Modulators," *Proc. IEEE (A Special Joint Issue on Optical Electronics with Applied Optics, the Optical Society of America)* **54**, 1374.
- Kaminow, I. P., H. P. Weber, and E. A. Chandross, 1971, "Poly(Methyl Methacrylate) Dye Lasers with Internal Diffraction Grating Resonator," *Appl. Phys. Lett.* **18**, 497.
- Kappeny, N. S., and J. J. Burke, 1973, *Optical Waveguides* (Academic, New York).
- Kapron, F. P., D. B. Keck, and R. D. Maurer, 1970, "Radiation Losses in Glass Optical Waveguides," *Appl. Phys. Lett.* **17**, 423.
- Katzir, A., A. Yariv, H. W. Yen, M. Nakamura, K. Aiki, and J. Umeda, 1975, "Corrugated Laser Structures," *J. Vac. Sci. Tech.* **12**, 865.
- Kawabe, M., H. Kotani, K. Masuda, and S. Namba, 1975, "Heterostructure CdS_{1-x}Se_x-CdS Surface Lasers for Integrated Optics," *Appl. Phys. Lett.* **26**, 46.
- Kawakami, S., M. Miyagi, and S. Nishida, 1975, "Bending Losses of Dielectric Slab Optical Waveguides with Double or Multiple Claddings: Theory," *Appl. Opt.* **14**, 2588.
- Kawakami, T., and K. Sugiyama, 1973, "Selective Liquid Phase Epitaxy of AlGaAs," *Jap. J. Appl. Phys.* **12**, 1808.
- Keck, D. B., R. D. Maurer, and P. C. Schultz, 1973, "On the Ultimate Limit of Attenuation in Glass Optical Waveguides," *Appl. Phys. Lett.* **22**, 307.
- Kendall, D. L., 1975, "On Etching Very Narrow Grooves in Silicon," *Appl. Phys. Lett.* **26**, 195.
- Kermisch, D., 1969, "Nonuniform Sinusoidally Modulated Dielectric Gratings," *J. Opt. Soc. Amer.* **59**, 1409.
- Keune, D. L., N. Holonyak, R. D. Burnham, P. D. Dapkus, and R. D. Dupuis, 1970, "Thin Semiconductor Laser to Thin Platelet Optical Coupler," *Appl. Phys. Lett.* **16**, 18.
- Klein, W. R., and B. D. Cook, 1967, "Unified Approach to

- Ultrasonic Light Diffraction," IEEE Trans. Sonics Ultrason. **SU-14**, 123.
- Kleinknecht, H. D., and A. E. Widmer, 1974, "(GaAl)P Optical Waveguide Modulators Fabricated by Liquid Phase Epitaxy," Integrated Optics Meeting, New Orleans, La., 1974.
- Kogelnik, H., 1975, "An Introduction to Integrated Optics," IEEE Trans. Microwave Theory Tech. **23**, 2.
- Kogelnik, H., 1976, "Filter Response of Nonuniform Periodic Structures," Bell Syst. Tech. J. **55**, 109.
- Kogelnik, H., and V. Ramaswamy, 1974, "Scaling Rules for Thin-Film Optical Waveguides," Appl. Opt. **13**, 1857.
- Kogelnik, H., and R. V. Schmidt, 1976, "Switched Directional Couplers with Alternating $\Delta\beta$," IEEE J. Quantum Electron. **QE-12**, 396.
- Kogelnik, H., and C. V. Shank, 1971, "Stimulated Emission in a Periodic Structure," Appl. Phys. Lett. **18**, 152.
- Kogelnik, H., and C. V. Shank, 1972, "Coupled Wave Theory Distributed Feedback Lasers," J. Appl. Phys. **43**, 2327.
- Kogelnik, H., C. V. Shank, and J. R. Bjorkholm, 1973, "Hybrid Scattering in Periodic Waveguides," Appl. Phys. Lett. **22**, 135.
- Kogelnik, H., and T. Sosnowski, 1970, "Holographic Thin-Film Couplers," Bell Syst. Tech. J. **49**, 1602.
- Kogelnik, H., and H. P. Weber, 1974, "Rays, Stored Energy, and Power Flow in Dielectric Waveguides," J. Opt. Soc. Am. **64**, 174.
- Kondo, S., S. Miyazawa, S. Fushimi, and K. Sugii, 1975, "Liquid Phase-Epitaxial Growth of Single Crystal LiNbO_3 Thin Film," Appl. Phys. Lett. **26**, 489.
- Kozaki, S., and Y. Mushike, 1975, "Total Reflection of a Gaussian Beam from an Inhomogeneous Medium," J. Appl. Phys. **46**, 4098.
- Kressel, H., and H. Nelson, 1969, "Close Confinement Gallium Arsenide PN Junction Lasers with Reduced Optical Loss at Room Temperature," RCA Rev. (Radio Corp. Am.) **30**, 106.
- Kuester, E. F., and D. C. Chang, 1975, "Propagation, Attenuation and Dispersion Characteristics of Inhomogeneous Dielectric Slab Waveguides," IEEE Trans. Microwave Theory Tech. **23**, 98.
- Kuhn, L., M. L. Dakss, P. F. Heidrich, and B. A. Scott, 1970, "Deflection of an Optical Guided Wave by a Surface Acoustic Wave," Appl. Phys. Lett. **6**, 265.
- Kuhn, L., P. F. Heidrich, and E. G. Lean, 1971, "Optical Guided Wave Mode Conversion by an Acoustic Surface Wave," Appl. Phys. Lett. **19**, 428.
- Kurazono, S., K. Iwasaki, and N. Kumagi, 1972, "A New Optical Modulator Consisting of Coupled Optical Waveguides," J. Inst. Electr. Commun. Eng. Jpn. **55C**, 103.
- Lang, R., and K. Kobayashi, 1975, "Suppression of the Relaxation Oscillation in the Modulated Output of Semiconductor Lasers," IEEE J. Quantum Electron. **QE-12**, 194.
- Lee, C. P., I. Samid, A. Gover, and A. Yariv, 1976, "Low-Threshold Room-Temperature Embedded Heterostructure Lasers," Appl. Phys. Lett. **29**, 365.
- Lee, T. P., 1975, "Effect of Junction Capacitance on the Rise Time of LEDs and on the Turn-on Delay of Injection Lasers," Bell Syst. Tech. J. **54**, 53.
- Lee, T. P., C. A. Burrus, B. I. Miller, and R. A. Logan, 1975, " $\text{Al}_x\text{Ga}_{1-x}\text{As}$ Double-Heterostructure Rib-Waveguide Injection Laser," IEEE J. Quantum Electron. **QE-11**, 432.
- Lee, T. P., and A. Y. Cho, 1976, "Single-Transverse-Mode Injection Lasers with Embedded Stripe Layer Grown by Molecular Beam Epitaxy," presented at the Topical Meeting on Integrated Optics, Optical Society of America, Salt Lake City, Utah, January 1976.
- Lee, T. P., and A. Y. Cho, 1976, "Single Transverse-Mode Injection Lasers with Embedded Stripe Layer Grown by Molecular Beam Epitaxy," Appl. Phys. Lett. **29**, 164.
- Lee, T. P., and A. G. Dentai, 1976, "Design Criteria for GaAs-AlGaAs High-Radiance LEDs for Optical Fiber Communication Systems," to be published.
- Lee, T. P., and T. J. B. Serra, 1976, "Characteristics of Injection Locking of Self-Pulsing in AlGaAs DH Junction Laser," IEEE J. Quantum Electron. **QE-12**, 368.
- Lee, Y. K., and S. Wang, 1974, "Tantalum Oxide Light Guide on Lithium Tantalate," Appl. Phys. Lett. **25**, 164.
- Lee, Y. K., and S. Wang, 1976, "Electrooptic Guided-to-Unguided Mode Converter," IEEE J. Quantum Electron. **QE-12**, 273.
- Lee, Y. K., and S. Wang, 1976, "Theoretical and Experimental Studies of Electrooptic Bragg-Deflection Modulators," Appl. Opt. **15**, 1565.
- Leonberger, F. J., J. P. Donnelly, and C. O. Bozler, 1976, "Low-Loss GaAs $p^n n^+$ Three-Dimensional Optical Waveguides," Appl. Phys. Lett. **28**, 616.
- Leonberger, F. J., J. P. Donnelly, and C. O. Bozler, 1976, "GaAs $p^n n^+$ Directional-Coupler Switch," Appl. Phys. Lett. **29**, 652.
- Liu, Y. S., and D. A. Smith, 1975, "The Frequency Response of an Amplitude-Modulated GaAs Luminescence Diode," Proc. IEEE **63**, 542.
- Logan, R. A., 1976, "Integrated Optical Circuits Grown by Liquid Phase Epitaxy," Technical Digest, Topical Meeting on Integrated Optics, Salt Lake City, Utah, 1976.
- Logan, R. A., and F. K. Reinhart, 1973, "Optical Waveguides in GaAs-AlGaAs Epitaxial Layers," J. Appl. Phys. **44**, 4172.
- Logan, R. A., and F. K. Reinhart, 1975, "Integrated GaAs-AlGaAs Double-Heterostructure Laser with Independently Controlled Optical Output Divergence," IEEE J. Quantum Electron. **QE-11**, 461.
- Lotsch, H. K. V., 1968, "Reflection and Refraction of a Beam of Light at a Plane Interface," J. Opt. Soc. Am. **58**, 551.
- Lotspeich, J. F., 1975, "Explicit General Eigenvale Solutions for Dielectric Slab Waveguides," Appl. Opt. **14**, 327.
- Louisell, W. H., 1960, *Coupled Mode and Parametric Electronics* (Wiley, New York).
- Mahlein, H. F., R. Overbacher, and W. Rauscher, 1975, "An Integrated Optical TE-TM Mode Splitter," Appl. Phys. **7**, 15.
- Marcatili, E. A. J., 1969, "Dielectric Rectangular Waveguides and Directional Couplers for Integrated Optics," Bell Syst. Tech. J. **48**, 2071.
- Marcatili, E. A. J., 1969, "Bends in Optical Dielectric Guides," Bell Syst. Tech. J. **48**, 2103.
- Marcuse, D., 1969, "Radiation Loss of Dielectric Waveguides in Terms of the Power Spectrum of the Wall Distortion Function," Bell Syst. Tech. J. **48**, 3233.
- Marcuse, D., 1969, "Mode Conversion by Surface Imperfection of a Dielectric Slab Waveguide," Bell Syst. Tech. J. **48**, 3187.
- Marcuse, D., 1970, "Radiation Losses of Tapered Dielectric Waveguides," Bell Syst. Tech. J. **49**, 273.
- Marcuse, D., 1971, "Crosstalk by Scattering in Slab Waveguides," Bell Syst. Tech. J. **50**, 1817.
- Marcuse, D., 1971, "The Coupling of Degenerate Modes in Parallel Dielectric Waveguides," Bell Syst. Tech. J. **50**, 1791.
- Marcuse, D., 1971, *Light Transmission Optics* (Van Nostrand, Reinhold, New York).
- Marcuse, D., 1972, "Hollow Dielectric Periodic Waveguides for Distributed Feedback Lasers," IEEE J. Quantum Electron. **QE-8**, 661.
- Marcuse, D., 1972, "Power Distribution and Radiation Losses in Multimode Dielectric Slab Waveguides," Bell Syst. Tech. J. **51**, 429.
- Marcuse, D., 1973, *Integrated Optics* (IEEE, New York).
- Marcuse, D., 1973, "Coupling Coefficients for Imperfect Asymmetric Slab Waveguides," Bell Syst. Tech. J. **52**, 63.
- Marcuse, D., 1974, *Theory of Dielectric Optical Waveguides* (Academic, New York).
- Marcuse, D., 1975, "Electrooptic Coupling between TE and TM Modes in Anisotropic Slabs," IEEE J. Quantum Electron. **QE-9**, 759.
- Marcuvitz, N., 1948, *Waveguide Handbook* (McGraw-Hill, New York).
- Martin, W. E., 1973, "Waveguide Electrooptic Modulation in II-VI Compounds," J. Appl. Phys. **44**, 3703.

- Martin, W. E., 1975, "Refractive Index Profile Optimization in Diffused Graded Index Lenses," *Appl. Opt.* **14**, 2427.
- Martin, W. E., 1975, "A New Waveguide Switch/Modulator for Integrated Optics," *Appl. Phys. Lett.* **26**, 562.
- Martin, W. E., and D. B. Hall, 1972, "Optical Waveguides by Diffusion in II-VI Compounds," *Appl. Phys. Lett.* **21**, 325.
- Matsuura, M., and K. O. Hill, 1974, "Optical Waveguide Band-Rejection Filters: Design," *Appl. Opt.* **13**, 2886.
- Matsuura, M., K. O. Hill, and A. Watanabe, 1975, "Optical Waveguide Filters Synthesis," *J. Opt. Soc. Am.* **65**, 804.
- Maxwell-Garnett, J. C., 1904, "Color in Metal Glasses and Films," *Philos. Trans. R. Soc. Lond.* **A202**, 3852.
- Maxwell-Garnett, J. C., 1906, "Color in Metal Glasses and Films," *Philos. Trans. R. Soc. Lond.* **A205**, 237.
- McCumber, D. E., 1966, "Intensity Fluctuations in the Output of CW Laser Oscillations I," *Phys. Rev.* **141**, 306.
- McFee, J. H., R. E. Nahory, M. A. Pollack, and R. A. Logan, 1973, "Beam Deflection and Amplitude Modulation of 10.6 μm Guided Waves by Free-Carrier Injection in GaAs-AlGaAs Heterostructures," *Appl. Phys. Lett.* **23**, 571.
- McKenna, J., 1967, "The Excitation of Planar Dielectric Waveguides at p-n Junctions, I," *Bell Syst. Tech. J.* **46**, 1491.
- McKenna, J., and F. K. Reinhart, 1976, "The Double Heterostructure GaAs-Al_xGa_{1-x}As (110) p-n Junction Diode Modulator," *J. Appl. Phys.* **47**, 2069.
- McLachlan, M. W., 1947, *Theory and Application of Mathieu Functions* (Clarendon, Oxford).
- McLevige, W. V., T. Itoh, and R. Mittra, 1975, "New Waveguide Structures for Millimeter-Wave and Optical Integrated Circuits," *IEEE Trans. Microwave Theory Tech.* **23**, 788.
- McMurray, J. A., and C. R. Stanley, 1976, "Taper Coupling between 7059-glass and CdS Films and Phase Modulation in the Composite Waveguide Structure," *Appl. Phys. Lett.* **28**, 126.
- Melngailis, I., 1975, "GaAs-Based Integrated Optical Circuits," in *Proceedings of the Technical Program, Electrooptical Systems Design Conference-1975*, International Laser Exposition, Anaheim, California, Nov. 11-13, 1975 (Industrial and Scientific Conference Management, Inc., Chicago), p. 453.
- Merz, J. L., Logan, R. A., Wiegmann, W., and Gossard, A. C., 1975, "Taper Couplers for GaAs-Al_xGa_{1-x}As Waveguide Layers Produced by Liquid Phase and Molecular Beam Epitaxy," *Appl. Phys. Lett.* **26**, 337.
- Merz, J. L., and A. Y. Cho, 1976, "Low Loss Al_xGa_{1-x}As Waveguides Grown by Molecular Beam Epitaxy," presented at the Topical Meeting on Integrated Optics, Optical Society of America, Salt Lake City, Utah, January 1976.
- Merz, J. L., and R. A. Logan, 1976, "GaAs Double Heterostructure Lasers Fabricated by Wet Chemical Etching," *Appl. Phys.* **47**, 3503.
- Merz, J. L., R. A. Logan, and A. M. Sergent, 1976, "Loss Measurements in GaAs-Dielectric Waveguides," *Appl. Phys. Lett.* **47**, 1436.
- Midwinter, J. E., 1970, "Evanescent Field Coupling into a Thin-Film Waveguide," *IEEE J. Quant. Electron.* **QE-6**, 583.
- Mikami, O., and J. Noda, 1976, "Phase Tuning in Optical Directional Coupler," *Appl. Phys. Lett.* **29**, 555.
- Miller, S. E., 1969, "Integrated Optics: An Introduction," *Bell Syst. Tech. J.* **48**, 2059.
- Miller, S. E., 1972, "A Survey of Integrated Optics," *IEEE J. Quantum Electron.* **QE-8**, Part 2, 199.
- Miller, S. E., E. A. J. Marcatili, and T. Li, 1973, "Research toward Optical Fiber Transmission System," *Proc. IEEE* **61**, 1703.
- Milton, A. F., and W. K. Burns, 1975, "Tapered Velocity Couplers for Integrated Optics: Design," *Appl. Opt.* **14**, 1207.
- Minakata, M., J. Noda, and N. Uchida, 1975, "LiNb_xTa_{1-x}O₃ Optical Waveguiding Layer in LiTaO₃ Fabricated by Diffusion of LiNb_x Sputtered Film," *Appl. Phys. Lett.* **26**, 395.
- Miyazawa, S., 1973, "Growth of LiNbO₃ Single Crystal Film for Optical Waveguides," *Appl. Phys. Lett.* **23**, 198.
- Miyazawa, S., S. Fushimi, and S. Kundo, 1975, "Optical Waveguide of LiNbO₃ Thin Film Grown by Liquid Phase Epitaxy," *Appl. Phys. Lett.* **26**, 8.
- Mollenauer, L. F., W. J. Tomlinson, and G. C. Bjorklund, 1977, "Piecewise Interferometric Generation of Precision Grating," to be published.
- Nahory, R. E., M. A. Pollack, E. D. Beebe, J. C. DeWinter, and R. W. Dixon, 1976, "Continuous Operation of 1.0 μm-Wavelength GaAs_{1-x}Sb_x/Al_yGa_{1-y}As_{1-x}Sb_x Double Heterostructure Injection Lasers at Room Temperature," *Appl. Phys. Lett.* **28**, 19.
- Nakamura, M., K. Aiki, J. Umeda, A. Yariv, H. W. Yen, and T. Morikawa, 1974, "Liquid Phase Epitaxy of GaAlAs on GaAs Substrates with Fine Surface Corrugations," *Appl. Phys. Lett.* **24**, 466.
- Nakamura, M., K. Aiki, J. Umeda, A. Yariv, H. W. Yen, and T. Morikawa, 1974, "GaAs-Ga_{1-x}Al_xAs Double-Heterostructure Distributed Feedback Diode Lasers," *Appl. Phys. Lett.* **25**, 487.
- Nakamura, M., K. Aiki, J. Umeda, and A. Yariv, 1975, "CW Operation of Distributed-Feedback GaAs-GaAlAs Diode Laser at Temperatures up to 300 °K," *Appl. Phys. Lett.* **27**, 403.
- Nakamura, M., K. Aiki, J. Umeda, A. Katzir, A. Yariv, and H. W. Yen, 1975, "GaAs-GaAlAs Double-Heterostructure Injection Lasers with Distributed Feedback," *IEEE J. Quantum Electron.* **QE-11**, 436.
- Nakamura, M., A. Yariv, H. W. Yen, S. Somekh, and H. L. Garvin, 1973, "Optically Pumped GaAs Surface Laser with Corrugation Feedback," *Appl. Phys. Lett.* **22**, 515.
- Nakamura, M., H. W. Yen, A. Yariv, E. Garmire, and S. Somekh, 1973, "Laser Oscillation in Epitaxial GaAs Waveguide with Corrugation Feedback," *Appl. Phys. Lett.* **23**, 224.
- Namizaki, H., M. Nagano, and S. Nakahara, 1974, "Frequency Response of Ga_{1-x}Al_xAs Light Emitting Diodes," *IEEE Trans. Electron Devices* **ED-21**, 688.
- Nelson, A. R., D. H. McMahon, and R. L. Gravel, 1976, "Electrooptic Channel Waveguide Modulator for Multimode Fibers," *Appl. Phys. Lett.* **28**, 321.
- Nelson, D. F., and R. K. Reinhart, 1964, "Light Modulation by the Electrooptic Effect in Reverse-Biased GaP Junctions," *Appl. Phys. Lett.* **5**, 148.
- Neviere, M., M. Cadilhac, and R. Petit, 1973, "Application of Conformal Mapping to the Diffraction of Electromagnetic Waves by a Grating," *IEEE Trans. Antennas Propag.* **AP-21**, 37.
- Neviere, M., R. Petit, and M. Cadilhac, 1973, "About the Theory of Optical Grating Coupler Waveguide System," *Opt. Commun.* **8**, 113.
- Noda, J., T. Saku, and N. Uchida, 1974, "Fabrication of Optical Waveguiding Layer in LiTaO₃ by Cu Diffusion," *Appl. Phys. Lett.* **25**, 308.
- Noda, J., N. Uchida, M. Minhata, T. Saku, S. Saito, and Y. Ohmachi, 1975, "Electrooptic Intensity Modulation in LiTaO₃ Ridge Waveguide," *Appl. Phys. Lett.* **26**, 298.
- Noda, J., N. Uchida, S. Saito, T. Saku, and M. Minaka, 1975, "Electrooptic Amplitude Modulation Using Three-Dimensional LiNbO₃ Waveguide Fabricated by TiO₂ Diffusion," *Appl. Phys. Lett.* **27**, 19.
- Norman, S. L., 1971, "A Look at Optical Integrated Circuits," *Electrooptical Systems Design* **3**, 22.
- Ogawa, K., W. S. C. Chang, B. L. Sopori, and F. J. Rosenbaum, 1973, "A Theoretical Analysis of Etched Grating Couplers for Integrated Optics," *IEEE J. Quantum Electron.* **QE-9**, 20.
- Ohmachi, Y., 1973, "Acoustooptical Light Diffraction in Thin Films," *J. Appl. Phys.* **44**, 3928.
- Ohmachi, Y., 1973, "Acoustooptic TE₀-TM₀ Mode Conversion in a Thin Film of Amorphous Tellurium Dioxide," *Electron. Lett.* **9**, 539.
- Ohmachi, Y., and J. Noda, 1975, "Electrooptic Light Modulator with Branching Ridge Waveguide," *Appl. Phys. Lett.* **27**, 544.
- Okuda, M., K. Murata, and K. Oonaka, 1976, "Optimum De-

- sign of a Distributed Bragg-Reflector Laser with Optical Loss in the Corrugated Waveguide," *Opt. Commun.* **16**, 30.
- Olsen, G. H., and V. S. Ban, 1976, "Use of Thin Carbon Films for Selective Chemical Etching and Epitaxial Deposition of III-V Semiconductors," *Appl. Phys. Lett.* **28**, 734.
- Osterberg, H., and L. G. Smith, 1964, "Transmission of Optical Energy along Surfaces," Parts I and II, *J. Opt. Soc. Am.* **54**, 1073.
- Ostrowsky, D. B., and A. Jacques, 1971, "Formation of Optical Waveguides in Photoresist Films," *Appl. Phys. Lett.* **18**, 556.
- Ostrowsky, D. B., R. Poirier, L. M. Reiber, and C. Deverdun, 1973, "Integrated Optical Photodetector," *Appl. Phys. Lett.* **22**, 463.
- Otto, A., 1968, "Excitation of Nonradiative Plasma Waves in Silver by the Method of Frustrated Total Reflection," *Z. Phys.* **216**, 398.
- Otto, A., and W. Sohler, 1971, "Modification of the Told Reflection Modes in a Dielectric Film by One Metal Boundary," *Opt. Commun.* **3**, 254.
- Ozeki, T., and E. H. Hara, 1976, "Measurement of Nonlinear Distortion in Light-Emitting Diodes," *Electron. Lett.* **12**, 78.
- Panish, M. B., 1975, "Heterostructure Injection Lasers," *IEEE Trans. Microwave Theory Tech.* **23**, 20.
- Panish, M. B., 1976, "Heterostructure Injection Lasers," *Proc. IEEE* **64**, 1512.
- Panish, M. B., I. Hayashi, and S. Sumski, 1969, "A Technique for the Preparation of Low-Threshold Room-Temperature GaAs Laser Diode Structures," *IEEE J. Quantum Electron. (Corresp.) QE-5*, 210.
- Paoli, T. L., and J. E. Ripper, 1969, "Coupled Longitudinal Mode Pulsing in Semiconductor Lasers," *Phys. Rev. Lett.* **22**, 1085.
- Paoli, T. L., and J. E. Ripper, 1969 and 1970, "Direct Modulation of Semiconductor Lasers," *Proc. IEEE* **58**, 1457 and *Appl. Phys. Lett.* **15**, 105.
- Paoli, T. L., J. E. Ripper, A. C. Morosini, and N. B. Patel, 1975, "Suppression of Intensity Self-Pulsations in CW Junction Lasers by Frequency Selective Optical Feedback," *IEEE J. Quantum Electron.* **11**, Part II, 525.
- Papuchon, M., Y. Combemale, X. Mathieu, D. B. Ostrowsky, L. Reiber, A. M. Roy, B. Sejourne, and M. Werner, 1975, "Electrically Switched Optical Directional Coupler: Cobra," *Appl. Phys. Lett.* **27**, 289.
- Peng, S. T., H. L. Bertoni, and T. Tamir, 1974, "Analysis of Periodic Thin-Film Structures with Rectangular Profile," *Opt. Commun.* **10**, 91.
- Peng, S. T., and T. Tamir, 1975, "TM-Mode Perturbation Analysis of Dielectric Gratings," *Appl. Phys.* **7**, 35.
- Peng, S. T., T. Tamir, and H. L. Bertoni, 1975, "Theory of Periodic Dielectric Waveguides," *IEEE Trans. Microwave Theory Tech.* **23**, 123.
- Pierce, J. R., 1954, "Coupling of Modes of Propagation," *J. Appl. Phys.* **25**, 179.
- Pole, R. V., E. M. Conwell, H. Kogelnik, P. K. Tien, J. R. Whinnery, A. Yariv, and A. J. DeMaria, 1975, "Integrated Optics—A Report on the Second OSA Topical Meeting," *Appl. Opt.* **14**, 569.
- Pole, R. V., S. E. Miller, J. H. Harris, and P. K. Tien, 1972, "Integrated Optics and Guided Waves—A Report of the Topical Meeting," *Appl. Opt.* **11**, 1675.
- Polley, J. N., and J. H. Harris, 1972, "Electrooptic Thin-Film Modulator," *Appl. Phys. Lett.* **21**, 307.
- Pollack, M. A., and R. E. Nahory, 1976, "CW Double Heterostructure LED and Laser Sources for the 1 μm Wavelength Region," presented at Topical Meeting on Integrated Optics, Optical Society of America, Salt Lake City, January, 1976.
- Quinn, D. J., J. M. Berak, and D. E. Cullen, 1975, "Growth and Optical Properties of Films Sputtered from Neodymium Pentaphosphate," *J. Appl. Phys.* **46**, 3866.
- Ralston, R. W., J. N. Walpole, T. C. Harman, and I. Melnagailis, 1975, "Double Heterostructure $\text{Pb}_{1-x}\text{Sn}_x\text{Te}$ Waveguides at 10.6 μm ," *Appl. Phys. Lett.* **26**, 64.
- Rand, M. J., and R. D. Standley, 1972, "Silicon Oxynitride Films on Fused Silica for Optical Waveguides," *Appl. Opt.* **11**, 2482.
- Ranganath, T. R., W. T. Tsang, and S. Wang, 1975, "Tapered Edge Ridge Waveguide for Integrated Optics," *Appl. Opt.* **14**, 1847.
- Ranganath, T. R., and S. Wang, 1976, "An Efficient Amplitude Modulator Using Diffused Ti-LiNbO_3 Branched Ridge Waveguides," paper IIA-6, p. 6, Conference Abstract, Device Research Conference, Salt Lake City, Utah, June 21-23, 1976.
- Ramaswamy, V., 1972, "Epitaxial Electrooptic Mixed-Crystal $(\text{NH}_\alpha)_x\text{K}_{1-x}\text{H}_2\text{PO}_4$ Film Waveguide," *Appl. Phys. Lett.* **21**, 183.
- Ramaswamy, V., and R. D. Standley, 1975, "Growth Strains and Losses in Nb-Diffused LiTaO_3 Optical Film Waveguides," *Appl. Phys. Lett.* **26**, 10.
- Rawson, E. G., R. E. Norton, R. D. Burnham, and D. R. Sci- fress, 1975, "A Striped Substrate, Double-Heterostructure Source for Optical Communication," in *Proceedings of the European Conference on Optical Fibre Communication*, London, September, 1975, pp. 108-110.
- Rayleigh, Lord, 1896, *The Theory of Sound* (MacMillan, London) 3rd edition.
- Rayleigh, Lord, 1907, "On the Light Dispersion from Fine Lines Ruled upon Reflecting Surfaces or Transmitted by Very Narrow Slits," *Philos. Mag.* **14**, 350.
- Rayleigh, Lord, 1907, "On the Dynamical Theory of Gratings," *Proc. R. Soc. Lond. A* **79**, 399.
- Reinhart, F. K., 1968, "Reversed Biased Gallium Phosphide Diodes as High Frequency Light Modulators," *J. Appl. Phys.* **39**, 3426.
- Reinhart, F. K., 1972, "Electro-absorption in $\text{Al}_x\text{Ga}_{1-x}\text{As}-\text{Al}_x\text{Ga}_{1-x}\text{As}$ Double Heterostructures," *Appl. Phys. Lett.* **22**, 372.
- Reinhart, F. K., and R. A. Logan, 1973, "Interfacial Stress of $\text{Al}_x\text{Ga}_{1-x}\text{As}-\text{GaAs}$ Layer Structures," *J. Appl. Phys.* **44**, 3171.
- Reinhart, F. K., and R. A. Logan, 1974, "Monolithically Integrated AlGaAs Double Heterostructure Optical Components," *Appl. Phys. Lett.* **25**, 622.
- Reinhart, F. K., and R. A. Logan, 1975, "Integrated Electro-optic Intracavity Frequency Modulation of Double Heterostructure Injection Laser," *Appl. Phys. Lett.* **27**, 532.
- Reinhart, F. K., and R. A. Logan, 1975, "GaAs-AlGaAs Double Heterostructure Lasers with Taper Coupled Passive Waveguides," *Appl. Phys. Lett.* **26**, 516.
- Reinhart, F. K., R. A. Logan, and T. P. Lee, 1974, "Transmission Properties of Rib Waveguides Formed by Anodization of Epitaxial GaAs on $\text{Al}_x\text{Ga}_{1-x}\text{As}$ Layers," *Appl. Phys. Lett.* **24**, 270.
- Reinhart, F. K., R. A. Logan, and C. V. Shank, 1975, "GaAs- $\text{Al}_x\text{Ga}_{1-x}\text{As}$ Injection Lasers with Distributed Bragg Reflectors," *Appl. Phys. Lett.* **27**, 45.
- Reinhart, F. K., and B. I. Miller, 1972, "Efficient GaAs- $\text{Al}_x\text{Ga}_{1-x}\text{As}$ Double-Heterostructure Light Modulators," *Appl. Phys. Lett.* **20**, 36.
- Reinhart, F. K., D. F. Nelson, and J. McKenna, 1969, "Electrooptic and Waveguide Properties of Reversed Biased Gal- lium Phosphide $p-n$ Junctions," *Phys. Rev.* **177**, 1208.
- Reinhart, F. K., W. R. Sinclair, and R. A. Logan, 1976, "Single Heterostructure $\text{Al}_x\text{Ga}_{1-x}\text{As}$ Phase Modulator with SnO_2 -doped In_2O_3 Cladding Layer," *Appl. Phys. Lett.* **29**, 21.
- Reisinger, A., 1973, "Attenuation Properties of Optical Waveguides with a Metal Boundary," *Appl. Phys. Lett.* **23**, 237.
- Reisinger, A., 1973, "Characteristics of Optical Guided Modes in Lossy Waveguides," *Appl. Opt.* **12**, 1015.
- Renard, R. H., 1964, "Total Reflection: A New Evaluation of the Goos-Häenchen Shift," *J. Opt. Soc. Am.* **54**, 1900.
- Righini, G. C., V. Russo, S. Sattini, and G. Toraldo di Francia, 1972, "Thin-Film Geodesic Lens," *Appl. Opt.* **11**, 1442.

- Rigrod, W. W., 1974, "Diffraction Efficiency of Non-Sinusoidal Bragg Reflection Gratings," *J. Opt. Soc. Am.* **64**, 97.
- Rigrod, W. W., and D. Marcuse, 1976, "Radiation Loss Coefficients of Asymmetric Dielectric Waveguides with Shallow Sinusoidal Corrugations," *IEEE J. Quantum Electron.* **QE-12**, 673.
- Ripper, J. E., and T. L. Paoli, 1971, "Optical Self Pulsing of Junction Lasers Operating Continuously at Room Temperature," *Appl. Phys. Lett.* **18**, 466.
- Roldan, R., 1967, "Spike in the Light Output of Room Temperature GaAs Junction Lasers," *Appl. Phys. Lett.* **11**, 346.
- Rossi, J. A., D. L. Deume, N. Holonyak, Jr., P. D. Dupuis, and R. D. Burnham, 1970, "Threshold Requirements and Carrier Interaction Effects in GaAs Platelet Lasers (77°K)," *J. Appl. Phys.* **41**, 312.
- Russer, P., 1975, "Modulation Behavior of Injected Lasers with Coherent Irradiation into Their Oscillating Mode," *Arch. Elektrotech. Übertrag.* **29**, 231.
- Russer, P., and S. Schulz, 1973, "Direkte Modulation Eines Doppel-Heterostruktur Lasers Mit Einer Bitrate Von 2.3 Gbit/s," *Arch. Elektrotech. Übertragung* **27**, 193.
- Sakuda, K., and A. Yariv, 1973, "Analysis of Optical Propagation in a Corrugated Dielectric Waveguide," *Opt. Commun.* **8**, 1.
- Samid, I., C. P. Lee, A. Gover, and A. Yariv, 1975, "Embedded Heterostructure Epitaxy: A Technique for Two-Dimensional Thin-Film Definition," *Appl. Phys. Lett.* **27**, 405.
- Schicketanz, D., 1975, "Large-Signal Modulation of GaAs Laser Diodes," *Siemens Forsch. U. Entwickl. Ber.* **4**, 325.
- Schineller, E. R., R. P. Flam, and D. W. Wilmot, 1968, "Optical Waveguides Formed by Proton Irradiation of Fused Silica," *J. Opt. Soc. Am.* **58**, 1171.
- Schinke, D. P., R. G. Smith, E. G. Spencer, and M. F. Galvin, 1972, "Thin Film Distributed Feedback Lasers Fabricated by Ion Milling," *Appl. Phys. Lett.* **21**, 494.
- Schmidt, R. V., 1976, "Acoustooptic Interactions between Guided Optical Waves and Acoustic Surface Waves," *IEEE Trans. Sonics Ultrason.* **SU-23**, 22.
- Schmidt, R. V., and L. L. Buhl, 1976, "An Experimental Integrated Optical 4 × 4 Switching Network," to be published in *Electron. Lett.*
- Schmidt, R. V., D. C. Flanders, C. V. Shank, and R. D. Standley, 1974, "Narrow Band Grating Filters for Thin-Film Optical Waveguides," *Appl. Phys. Lett.* **25**, 651.
- Schmidt, R. V., and I. P. Kaminow, 1974, "Metal-Diffused Optical Waveguides in LiNbO₃," *Appl. Phys. Lett.* **25**, 458.
- Schmidt, R. V., and I. P. Kaminow, 1975, "Acoustooptic Bragg Deflection in LiNbO₃ Ti-Diffused Waveguides," *IEEE J. Quantum Electron. (Corresp.)* **QE-11**, 57.
- Schmidt, R. V., I. P. Kaminow, and J. R. Carruthers, 1973, "Acoustooptic Diffraction of Guided Optical Waves in LiNbO₃," *Appl. Phys. Lett.* **23**, 417.
- Schmidt, R. V., and H. Kogelnik, 1976, "Electrooptically Switched Couplers with Stepped Δβ Reversal Using Ti-Diffused LiNbO₃ Waveguides," *Appl. Phys. Lett.* **28**, 503.
- Scifres, D. R., R. D. Burnham, and W. Streifer, 1974, "Distributed Feedback Single Heterojunction GaAs Diode Laser," *Appl. Phys. Lett.* **25**, 203.
- Scifres, D. R., R. D. Burnham, and W. Streifer, 1974, "A Distributed Feedback Single Heterojunction Diode Laser," *IEEE J. Quantum Electron.* **QE-10**, 790.
- Scifres, D. R., R. D. Burnham, and W. Streifer, 1975, "Application of High Resolution Photolithography to Integrated Optics," in *Proceedings of Micro-Photofabrication Conference*, Palo Alto, California, February, 1975.
- Scifres, D. R., R. D. Burnham, and W. Streifer, 1975, "GaAs/GaAlAs Heterostructure Distributed Feedback Lasers," in *Proceedings of the IEEE Conference on Active Semiconductor Devices for Microwaves and Integrated Optics*, Cornell University, 1975, pp. 47–56.
- Scifres, D. R., R. D. Burnham, and W. Streifer, 1975, "Highly Collimated Laser Beams for Electrically Pumped SH GaAs/GaAlAs Distributed Feedback Lasers," *Appl. Phys. Lett.* **26**, 48.
- Scifres, D. R., R. D. Burnham, and W. Streifer, 1975, "Output Coupling and Distributed Feedback Utilizing Substrate Corrugations in Double-Heterostructure GaAs Lasers," *Appl. Phys. Lett.* **27**, 295.
- Scifres, D. R., R. D. Burnham, and W. Streifer, 1975, "Longitudinal and Radiation Modes in GaAs Single Heterojunction Distributed Feedback Injection Lasers," *IEEE Trans. Electron Devices* **ED-22**, 609.
- Scifres, D. R., R. D. Burnham, and W. Streifer, 1976, "Distributed Feedback GaAs/GaAlAs Diode Lasers," *Proc. Soc. Photo-Optical Instrumentation Engineers (issue on Fibers and Integrated Optics)* **77**, 44.
- Scifres, D. R., R. D. Burnham, and W. Streifer, 1976, "Grating Coupled GaAs/GaAlAs Ring Laser," *Integrated Optics Technical Digest WC5*, Salt Lake City, January, 1976.
- Scifres, D. R., R. D. Burnham, and W. Streifer, 1976, "Grating-Coupled GaAs Single-Heterostructure Ring Laser," *Appl. Phys. Lett.* **28**, 681.
- Scifres, D. R., W. Streifer, and R. D. Burnham, 1976, "Leaky Wave Room-Temperature Double Heterostructure GaAs:GaAlAs Diode Laser," *Appl. Phys. Lett.* **29**, 23.
- Scifres, D. R., R. D. Burnham, W. Streifer, J. Tramontana, and A. Alimonda, 1975, "Distributed Feedback with GaAs Semiconductor Diode Lasers," *Industrial Research*, Sept. 1975, p. 62.
- Shah, M. L., 1975, "Optical Waveguide in LiNbO₃ by Ion Exchange Techniques," *Appl. Phys. Lett.* **26**, 652.
- Shah, M., J. D. Crow, and S. Wang, 1972, "Optical-Waveguide Mode Conversion Experiments," *Appl. Phys. Lett.* **20**, 66.
- Shah, M., J. D. Crow, and S. Wang, 1972, "Optical-Waveguide Mode-Conversion Experiments and Further Development of the Theory of Propagation in Waveguides with Gyrotropic and Anisotropic Substrates," paper MB2 (1–4), *Digest of Technical Papers, Topical Meeting on Integrated Optics, Optical Society of America*, Las Vegas, Nevada, February 7–9, 1972.
- Shank, C. V., J. E. Bjorkholm, and H. Kogelnik, 1971, "Tunable Distributed Feedback Dye Lasers," *Appl. Phys. Lett.* **18**, 395.
- Shank, C. V., and R. V. Schmidt, 1973, "Optical Technique for Producing 0.1 μ Periodic Surface Structure," *Appl. Phys. Lett.* **23**, 154.
- Shank, C. V., R. V. Schmidt, and B. I. Miller, 1974, "Double Heterostructure GaAs Distributed Feedback Laser," *Appl. Phys. Lett.* **25**, 200.
- Sheem, S., 1974, "Drawn Pitch Threads as Masks for Micro-fabrication," *Appl. Opt. (letter)* **13**, 1757.
- Sheem, S., 1975, "Three Dimensional Curved Surface for Integrated Optics," *Appl. Opt.* **14**, 1854.
- Sheem, S., and J. R. Whinnery, 1974, "Guiding by Single Curved Boundaries in Integrated Optics," *Wave Electronics* **1**, 61.
- Sheem, S., and J. R. Whinnery, 1975, "Modes of a Curved Surface Waveguide for Integrated Optics," *Wave Electronics* **1**, 105.
- Sheridan, J. P., J. M. Schmur, and T. G. Ciallorenzi, 1973, "Electrooptic Switching in Low Loss Liquid Crystal Waveguides," *Appl. Phys. Lett.* **33**, 350.
- Shubert, R., 1974, "Theory of Optical-Waveguide Distributed Lasers with Nonuniform Gain and Coupling," *J. Appl. Phys.* **45**, 209.
- Shubert, R., and J. H. Harris, 1968, "Optical Surface Waves on Thin Films and Their Application to Integrated Data Processors," *IEEE Trans. Microwave Theory Tech.* **16**, 1048.
- Shubert, R., and J. H. Harris, 1970, "Optical Guide-Wave Focusing, Diffraction," *J. Opt. Soc. Am.* **61**, 154.
- Shuskus, A. J., T. M. Reeder, and E. L. Paradis, 1974, "Rf-Sputtered Aluminum Nitride Films on Sapphire," *Appl. Phys. Lett.* **24**, 155.
- Somekh, S., H. C. Casey, and M. Illegems, 1977, "Preparation

- of High-Aspect Ratio Periodic Corrugations by Plasma and Ion Etching," to be published.
- Somekh, S., H. C. Casey, Jr., and M. Illegems, 1976, "Dry Processing of High Resolution and High Aspect Ratio Structures in GaAs/Al_xGa_{1-x}As for Integrated Optics," unpublished.
- Somekh, S., E. Garmire, and A. Yariv, 1973, "Channel Optical Waveguide Directional Couplers," *Appl. Phys. Lett.* **22**, 46.
- Somekh, S., E. Garmire, A. Yariv, H. L. Garvin, and R. G. Hunsperger, 1974, "Channel Optical Waveguides and Directional Couplers in GaAs," *Appl. Opt.* **13**, 327.
- Somekh, S., and A. Yariv, 1972, "Phase Matching by Periodic Modulation of the Nonlinear Properties," *Opt. Commun.* **6**, 301.
- Spears, D. L., A. J. Strauss, S. R. Chinn, I. Melngailis, and p. Vohl, 1976, "CdTe Waveguide Devices and HgCdTe Epitaxial Layers for Integrated Optics," *Integrated Optics (Technical Digest of the Topical Meeting on Integrated Optics, January 12-14, 1976, Salt Lake City, Utah)*, Opt. Soc. of Am., Paper TuD3.
- Spears, D. L., A. J. Strauss, I. Melngailis, and J. L. Ryan, 1974, "Low-Loss Waveguides at 10.6 μm Produced by High-Energy Proton Bombardment of CdTe," *Digest of Technical Papers, Topical Meeting on Integrated Optics, January 21-24, 1974, New Orleans, La. (Opt. Soc. Am.)*, paper ThA10.
- Standley, R. D., W. M. Gibson, and T. D. Rogers, 1972, "Properties of Ion Bombarded Quartz for Integrated Optics," *Appl. Opt.* **11**, 1313.
- Standley, R. D., and V. Ramaswamy, 1974, "Nb-Diffused LiTaO₃ Optical Waveguides: Planar and Embedded Strip Guides," *Appl. Phys. Lett.* **25**, 711.
- Standley, R. D., and V. Ramaswamy, 1976, "A New Method for Measuring Parallel Waveguide Directional Coupler Parameters," *Topical Meeting on Integrated Optics MD8, Salt Lake City, Utah*, 1976.
- Steinberg, R., and T. G. Giallorenzi, 1976, "Performance Limitations Imposed on Optical Waveguide Switches/Modulators by Polarization," *Appl. Opt.*, to be published.
- Stepke, E. T., 1975, "Integrated Optics Electro Optics," *Systems Design* **5**, 18.
- Stillman, G. E., C. M. Wolfe, and I. Melngailis, 1974, "Monolithic Integrated In_xGa_{1-x}As Schottky Barrier Waveguide Detector," *Digest of Technical Papers, Topical Meeting on Integrated Optics, January 21-24, 1974, New Orleans, La. (Opt. Soc. Am.)*, paper MA9.
- Stillman, G. E., C. M. Wolfe, and I. Melngailis, 1974, "Monolithic Integrated In_xGa_{1-x}As Schottky-Barrier Waveguide Photodetector," *Appl. Phys. Lett.* **25**, 36.
- Stillman, G. E., C. M. Wolfe, C. O. Bozler, and J. A. Rossi, 1976, "Electroabsorption in GaAs and its Application to Waveguide Detectors and Modulators," *Appl. Phys. Lett.* **28**, 544.
- Stillman, G. E., C. M. Wolfe, J. A. Rossi, and H. Heckscher, 1976, "Low-Loss High-Purity GaAs Waveguides for Monolithic Integrated Optical Circuits at GaAs Laser Wavelengths," *Appl. Phys. Lett.* **28**, 197.
- Stoll, H., and A. Yariv, 1973, "Coupled Mode Analysis of Periodic Dielectric Waveguide," *Opt. Commun.* **8**, 5.
- Stoll, H., A. Yariv, R. G. Hunsperger, and G. L. Tangonan, 1973, "Proton-Implanted Optical Waveguides Detector in GaAs," *Appl. Phys. Lett.* **23**, 664.
- Streifer, W., R. D. Burnham, and D. R. Scifres, 1975, "Coupling Coefficients and Propagation Constants in Guided Wave Distributed Feedback Lasers," *J. Appl. Phys.* **46**, 946.
- Streifer, W., R. D. Burnham, and D. R. Scifres, 1975, "Effect of External Reflectors on Longitudinal Modes of Distributed Feedback Lasers," *IEEE J. Quantum Electron.* **QE-11**, 154.
- Streifer, W., R. D. Burnham, and D. R. Scifres, 1976, "Analysis of Grating-Coupled Radiation in GaAs:GaAlAs Lasers and Waveguides-II: Blazing Effects," *IEEE J. Quantum Electron.* **QE-12**, 494.
- Streifer, W., R. D. Burnham, and D. R. Scifres, 1976, "Substrate Radiation Losses in GaAs Heterostructure Lasers," *IEEE J. Quantum Electron.* **QE-12**, 177.
- Streifer, W., R. D. Burnham, and D. R. Scifres, 1976, "Grating Coupled Output Beams from Distributed Feedback Diode Lasers," in *Proceedings of the Technical Programs on Electro-Optical Systems Design*, 221-226.
- Streifer, W., R. D. Burnham, and D. R. Scifres, 1976, "Analysis of Grating-Coupled Radiation in GaAs:GaAlAs Lasers and Waveguides I and II," *IEEE J. Quantum Electron.* **12**, 422 (I) and 495 (II).
- Streifer, W., D. R. Scifres, and R. D. Burnham, 1975, "Longitudinal Modes in Distributed Feedback Lasers with External Reflectors," *J. Appl. Phys.* **46**, 247.
- Streifer, W., D. R. Scifres, and R. D. Burnham, 1975, "Coupling Coefficients for Distributed Feedback Single and Double Heterostructure Diode Lasers," *IEEE J. Quantum Electron.* **QE-11**, 867.
- Streifer, W., D. R. Scifres, and R. D. Burnham, 1976, "TM Mode Coupling Coefficients in Guided Wave Distributed Feedback Lasers," *IEEE J. Quantum Electron.* **QE-12**, 74.
- Suematsu, Y., 1975, "The Progress of Integrated Optics in Japan," *IEEE Trans. Microwave Theory Tech.* **23**, 16.
- Suematsu, Y., and K. Furuya, 1975, "Quasi-Guided Modes and Related Losses in Optical Dielectric Waveguides with External High Index Surroundings," *IEEE Trans. Microwave Theory Tech.* **23**, 170.
- Suematsu, Y., M. Hakuta, K. Furuya, K. Chiba, and R. Hasumi, 1972, "Fundamental Transverse Electric Field (TE₀) Mode Selection for Thin-Film Asymmetric Light Guide," *Appl. Phys. Lett.* **21**, 291.
- Suematsu, Y., Y. Sasaki, K. Furuya, K. Shibata, and S. Ibusukuro, 1973, "Optical Second Harmonic Generation Due to Guided Wave Structure Consisting of Quartz and Glass Film," *IEEE J. Quantum Electron.* **QE-10**, Part II, 222.
- Suematsu, Y., M. Yamada, and K. Hayashi, 1975, "A Multi-Hetero-AlGaAs Laser with Integrated Twin Guide," *Proc. IEEE* **63**, 208.
- Suematsu, Y., M. Yamada, and I. Hayashi, 1975, "Integrated Twin Guide AlGaAs Laser with Multiheterostructures," *IEEE J. Quantum Electron.* **QE-11**, Part II, 457.
- Takada, S., M. Ohnishi, H. Hayakawa, and M. Mikoshiba, 1974, "Optical Waveguides of Single Crystal LiNbO₃ Film Deposited by rf Sputtering," *Appl. Phys. Lett.* **24**, 490.
- Takamo, T., and J. Hamasaki, 1972, "Propagating Modes of a Metal-Clad Dielectric-Slab Waveguide for Integrated Optics," *IEEE J. Quantum Electron.* **QE-8**, 206.
- Tamir, T., 1972, "Inhomogeneous Wave Types at Planar Interfaces," *Optik (Stuttg.)* **36**, 209.
- Tamir, T., and H. L. Bertoni, 1971, "Lateral Displacement of Optical Beams at Multilayered and Periodic Structures," *J. Opt. Soc. Am.* **61**, 1397.
- Tamir, T., and A. A. Oliner, 1969, "Role of the Lateral Wave in Total Reflection of Light," *J. Opt. Soc. Am.* **59**, 942.
- Tarui, Y., Y. Komiya, and Y. Harada, 1971, "Preferential Etching and Etched GaAs Profile," *J. Electrochem. Soc. Jpn.* **118**, 118.
- Taylor, H. E., W. E. Martin, D. B. Hall, and V. M. Smiley, 1972, "Fabrication of Single Crystal Semiconductor Optical Waveguides by Solid-State Diffusion," *Appl. Phys. Lett.* **21**, 95.
- Taylor, H. F., 1973, "Frequency Selective Coupling in Parallel Dielectric Waveguides," *Opt. Commun.* **8**, 421.
- Taylor, H. F., and A. Yariv, 1974, "Guided Wave Optics," *Proc. IEEE* **62**, 1044.
- Tien, P. K., 1958, "Parametric Amplification and Frequency Mixing in Propagating Circuits," *J. Appl. Phys.* **29**, 1347.
- Tien, P. K., 1971, "Light Waves in Thin Films and Integrated Optics," *Appl. Opt.* **10**, 2395.
- Tien, P. K., 1974, "Integrated Optics," *Sci. Am.* **230**, 28.
- Tien, P. K., 1974, "Integrated Optics—Present and Future," *J. Jap. Soc. Appl. Phys., Suppl.* **43**, 119.
- Tien, P. K., 1976, "Low-Loss Junctions between the Dielec-

- tric and Metal-Clad Optical Waveguides and the Maxwell-Garnet Theory," Topical Meeting on Integrated Optics, Salt Lake City, Utah, MC3.
- Tien, P. K., and A. A. Ballman, 1975, "Research in Optical Films for the Application of Integrated Optics," *J. Vac. Sci. Technol.* **12**, 892.
- Tien, P. K., J. P. Gordon, and J. R. Whinnery, 1965, "Focusing of a Light Beam of Gaussian Field Distribution in Continuous and Periodic Lens-Like Media," *Proc. IEEE* **53**, 129.
- Tien, P. K., and R. J. Martin, 1971, "Experiments in Light Waves in a Thin, Tapered Film and a New Light-Wave Coupler," *Appl. Phys. Lett.* **18**, 398.
- Tien, P. K., R. J. Martin, S. L. Blank, S. H. Wemple, and L. J. Varnerin, 1972, "Optical Waveguides of Single Crystal Garnet Films," *Appl. Phys. Lett.* **21**, 207.
- Tien, P. K., R. J. Martin, and S. Riva-Sanseverino, 1975, "Novel Metal-Clad Optical Components and Method of Forming High-Index Substrate for Forming Integrated Optical Circuits," *Appl. Phys. Lett.* **27**, 251.
- Tien, P. K., R. J. Martin, and G. Smolinsky, 1973, "Formation of Light-Guiding Interconnections in an Integrated Optical Circuit by Composite Tapered-Film Coupling," *Appl. Opt.* **12**, 1909.
- Tien, P. K., R. J. Martin, R. Wolfe, R. C. LeCraw, and S. L. Blank, 1972, "Switching and Modulation of Light in Magneto-optic Waveguides of Garnet Films," *Appl. Phys. Lett.* **21**, 394.
- Tien, P. K., S. Riva-Sanseverino, and A. A. Ballman, 1974, "Light Beam Scanning and Deflection of Epitaxial LiNbO_3 Electrooptic Waveguides," *Appl. Phys. Lett.* **25**, 563.
- Tien, P. K., S. Riva-Sanseverino, R. J. Martin, and A. A. Ballman, 1974, "Optical Waveguide Modes in Single Crystalline LiNbO_3 - LiTaO_3 Solid Solution Films," *Appl. Phys. Lett.* **24**, 503.
- Tien, P. K. S. Riva-Sanseverino, R. J. Martin, and G. Smolinsky, 1974, "Two-Layered Construction of Integrated Optical Circuits and Formation of Thin-Film Prisms, Lenses and Reflectors," *Appl. Phys. Lett.* **24**, 547.
- Tien, P. K., D. P. Schinke, and S. L. Blank, 1974, "Magneto-optics and Motion of the Magnetization in a Film Waveguide Optical Switch," *J. Appl. Phys.* **45**, 3059.
- Tien, P. K., G. Smolinsky, and R. J. Martin, 1972, "Thin Organosilicon Films for Integrated Optics," *Appl. Opt.* **11**, 637.
- Tien, P. K., G. Smolinsky, and R. J. Martin, 1975, "Radiation Fields of a Tapered Film and a Novel Film-to-Fiber Coupler," *IEEE Trans. Microwave Theory Tech.* **23**, 79.
- Tien, P. K., and R. Ulrich, 1970, "Theory of Prism-Film Coupler and Thin-Film Light Guides," *J. Opt. Soc. Am.* **60**, 1325.
- Tien, P. K., R. Ulrich, and R. J. Martin, 1969, "Modes of Propagating Light Waves in Thin Deposited Semiconductor Films," *Appl. Phys. Lett.* **14**, 291.
- Tien, P. K., R. Ulrich, and R. J. Martin, 1969, "Prism-Film Coupler and Thin-Film Prism and Lens," Research Conference on Electron Devices, Rochester, New York.
- Tien, P. K., R. Ulrich, and R. J. Martin, 1970, "Optical Second Harmonic Generation in Form of Coherent Cerenkov Radiation from a Thin-Film Waveguide," *Appl. Phys. Lett.* **17**, 447.
- Tomlinson, W. J., and H. P. Weber, 1975, "Optical Directional Couplers and Grating Couplers Using a New High Resolution Photolocking Material," *Appl. Phys. Lett.* **26**, 303.
- Tracy, T. C., W. Wiegman, R. A. Logan, and F. K. Reinhart, 1973, "Three Dimensional Light Guides in Single-Crystal $\text{GaAs-Al}_x\text{Ga}_{1-x}\text{As}$," *Appl. Phys. Lett.* **22**, 511.
- Tsai, C. S., and P. Saunier, 1975, "Ultrafast Guided-Light Beam Deflection/Switching and Modulation Using Simulated Electrooptic Prism Structures in LiNbO_3 Waveguides," *Appl. Phys. Lett.* **27**, 248.
- Tsang, W. T., C. C. Tseng, and S. Wang, 1975, "Optical Waveguides Fabricated by Preferential Etching," *Appl. Opt.* **14**, 1200.
- Tsang, W. T., and S. Wang, 1974, "Simultaneous Exposure and Development Technique for Making Gratings on Positive Photoresist," *Appl. Phys. Lett.* **24**, 196.
- Tsang, W. T., and S. Wang, 1974, "Grating Masks Suitable for Ion-Beam Machining and Chemical Etching," *Appl. Phys. Lett.* **25**, 415.
- Tsang, W. T., and S. Wang, 1975, "A Thin-Film Ring Distributed Feedback Laser," *J. Appl. Phys.* **46**, 838.
- Tsang, W. T., and S. Wang, 1975, "Preferentially Etched Diffraction Gratings in Silicon," *J. Appl. Phys.* **46**, 2163.
- Tsang, W. T., and S. Wang, 1975, "Microfabrication Using Laser Beam Interferometric Technique Coupled with Simultaneous Exposure and Development Method," presented at 13th Symposium on Electron, Ion, and Photon Beam Technology, Colorado Springs, May 21-23, 1975.
- Tsang, W. T., and S. Wang, 1975, "Experimental Studies of Photoresist Gratings," *Wave Electronics* **1**, 85.
- Tsang, W. T., and S. Wang, 1975, "Microfabrication of Two-Dimensional Periodic Arrays by Laser Beam Interferometric Technique," *Appl. Phys. Lett.* **27**, 79.
- Tsang, W. T., and S. Wang, 1975, "Microfabrication Using Laser Beam Interferometric Technique Coupled with Simultaneous Exposure and Development Method," *J. Vac. Sci. Technol.* **12**, 1336.
- Tsang, W. T., and S. Wang, 1975, "Thin-Film Beam Splitter and Reflector for Guided Optical Waves," *Appl. Phys. Lett.* **27**, 588.
- Tsang, W. T., and S. Wang, 1976, "Profile and Groove-Depth Control in GaAs Diffraction Gratings Fabricated by Preferential Chemical Etching in $\text{H}_2\text{SO}_4-\text{H}_2\text{O}_2-\text{H}_2\text{O}$ System," *Appl. Phys. Lett.* **28**, 44.
- Tsang, W. T., and S. Wang, 1976, "Lateral Optical Confinement in $\text{GaAs}-\text{Ga}_{0.7}\text{Al}_{0.3}\text{As}$ Heterostructure Waveguide Fabricated by Liquid-Phase Epitaxy over Preferentially Etched Channels," paper MA2 Technical Digest, Integrated Optics Meeting, Salt Lake City, Utah, January 12-14, 1976.
- Tsang, W. T., and S. Wang, 1976, "GaAs-Ga_{1-x}Al_xAs Double-Heterostructure Injection Lasers with Distributed Bragg Reflectors," *Appl. Phys. Lett.* **28**, 596.
- Tsang, W. T., and S. Wang, 1976, "Mode Properties of GaAs-Ga_{1-x}Al_xAs Heterostructure Inverted Ridge Optical Waveguides," *Appl. Phys. Lett.* **28**, 665.
- Tsang, W. T., and S. Wang, 1976, "GaAs-Ga_{1-x}Al_xAs Double-Heterostructure Injection Lasers with Distributed Bragg Reflectors," paper E3, p. 38, Conference Digest, 9th International Conference on Quantum Electronics, Amsterdam, The Netherlands, June 14-18, 1976.
- Tseng, C. C., D. Botez, and S. Wang, 1975, "Optical Bends and Rings Fabricated by Preferential Etching," *Appl. Phys. Lett.* **26**, 699.
- Tseng, C. C., D. Botez, and S. Wang, 1976, "Optically Pumped Epitaxial GaAs Waveguide Lasers with Distributed Bragg Reflectors," *IEEE J. Quantum Electron.* **QE-12**, 549.
- Tseng, C. C., W. T. Tsang, and S. Wang, 1975, "A Thin-Film Prism as a Beam Separator for Multimode Guided Waves in Integrated Optics," *Opt. Commun.* **13**, 342.
- Tseng, C. C., and S. Wang, 1975, "Integrated Grating-Type Schottky-Barrier Photodetector with Optical Channel Waveguide," *Appl. Phys. Lett.* **26**, 632.
- Tsukada, T., 1974, "GaAs-Ga_{1-x}Al_xAs Buried-Heterostructure Injection Lasers," *J. Appl. Phys.* **45**, 4899.
- Tsukada, T., 1976, "Liquid Phase Epitaxial Growth of Ga_{1-x}Al_xAs on the Side and Top Surfaces of Air-Exposed Ga_{1-y}Al_yAs," *Appl. Phys. Lett.* **28**, 697.
- Tsukada, T., R. Ito, H. Nakashima, and O. Nakada, 1973, "Mesa-Stripe-Geometry Double-Heterostructure Injection Lasers," *IEEE J. Quantum Electron.* **QE-9**, 356.
- Turner, J. J., B. Chen, L. Yang, J. M. Ballantyne, and C. L. Tang, 1973, "Grating for Integrated Optics Fabricated by Electron-Microscope," *Appl. Phys. Lett.* **23**, 333.
- Uchida, N., 1973, "Calculation of Diffraction Efficiency in Hologram Gratings Attenuated along the Direction Perpen-

- dicular to the Grating Vector," *J. Opt. Soc. Am.* **63**, 280.
- Uchida, N., and N. Niizeki, 1973, "Acoustooptic Deflection Materials and Techniques," *Proc. IEEE* **61**, 1073.
- Uehara, S., T. Izawa, and H. Nakagome, 1974, "Optical Waveguide Polarizer," *Appl. Opt.* **13**, 1753.
- Uehara, S., K. Takamoto, S. Matsuo, and Y. Yamauchi, 1975, "Optical Intensity Modulator with Three-Dimensional Waveguide," *Appl. Phys. Lett.* **26**, 296.
- Uesugi, N., and T. Kimura, 1976, "Efficient Second-Harmonic Generation in Three-Dimensional LiNbO₃ Optical Waveguide," *Appl. Phys. Lett.* **29**, 572.
- Ulrich, R., 1970, "Theory of Prism-Film Coupler by Plane Wave Analysis," *J. Opt. Soc. Am.* **60**, 1337.
- Ulrich, R., 1971, "Optimum Excitation of Optical Surface Waves," *J. Opt. Soc. Am.* **61**, 1467.
- Ulrich, R., 1973, "Efficiency of Optical Grating Coupler," *J. Opt. Soc. Am.* **63**, 1419.
- Ulrich, R., and R. J. Martin, 1971, "Geometric Optics in Thin-Film Light Guides," *Appl. Opt.* **9**, 2077.
- Ulrich, R., and R. Torge, 1973, "Measurement of Thin Film Parameters with a Prism Coupler," *Appl. Opt.* **12**, 2901.
- Ulrich, R., and H. P. Weber, 1972, "Solution-Deposited Thin Films as Passive and Active Light-Guides," *Appl. Opt.* **11**, 428.
- Ulrich, R., H. P. Weber, E. A. Chandross, W. J. Tomlinson, and E. A. Franke, 1972, "Embossed Optical Waveguides," *Appl. Phys. Lett.* **20**, 213.
- Van der Ziel, J. P., R. Dingle, R. C. Miller, W. Wiegmann, and W. A. Nordland, Jr., 1975, "Laser Oscillation from Quantum States in Very Thin GaAs-Al_{0.2}Ga_{0.8}As Multilayer Structure," *Appl. Phys. Lett.* **26**, 463.
- Van der Ziel, J. P., and M. Illegems, 1976, "Optical Second Harmonic Generation in Periodic Multilayer GaAs-Al_{0.3}Ga_{0.7}As Structures," *Appl. Phys. Lett.* **28**, 437.
- Verber, M., D. E. Vahey, and V. E. Wood, 1976, "Focal Properties of Geodesic Waveguide Lenses," *Appl. Phys. Lett.* **28**, 514.
- Walpole, J. N., A. R. Calawa, T. C. Harman, and S. H. Groves, 1976, "Double-Heterostructure PbSnTe Lasers by Molecular Beam Epitaxy with CW Operation at 114 °K," *Appl. Phys. Lett.* **28**, 552.
- Walpole, J. N., A. R. Calawa, S. R. Chinn, S. H. Groves, and T. C. Harman, 1976, "Distributed Feedback Pb_{1-x}Sn_xTe Double-Heterostructure Lasers," *Appl. Phys. Lett.* **29**, 307.
- Wang, S., 1972, "Proposal of Periodic Layered Structures for Distributed Lasers," *Digest of Technical Papers, VII International Quantum Electronics Conference, Montreal, Canada, May 8-11, 1972*, p. 29.
- Wang, S., 1974, "Principles of Distributed Feedback (DFB) and Distributed Bragg-Reflector (DBR) Lasers," paper TuB4 (1-4), *Digest of Technical Papers, Topical Meeting on Integrated Optics, Optical Society of America, New Orleans, La., January 21-24, 1974*.
- Wang, S., 1974, "Principles of Distributed Feedback and Distributed Bragg-Reflector Lasers," *J. Quantum Electron.* **QE-10**, 413.
- Wang, S., 1974, "Thin-Film Bragg Lasers for Integrated Optics," *Wave Electronics* **1**, 31.
- Wang, S., 1975, "Energy Velocity and Effective Gain in Distributed Feedback Lasers," *Appl. Phys. Lett.* **26**, 89.
- Want, S., R. F. Cordero, and C. C. Tseng, 1974, "Analysis of Distributed Feedback and Distributed Bragg-Reflector Laser Structures by Method of Multiple Reflections," *J. Appl. Phys.* **45**, 3975.
- Wang, S., J. D. Crow, and M. Shah, 1971, "Studies of Magneto-optic Effects for Thin-Film Optical-Waveguide Applications," *IEEE Trans. Magn.* **MAG-7**, 385.
- Wang, S., J. D. Crow, and M. Shah, 1971, "Thin-Film Optical-Waveguide Mode Converters Using Gyrotropic and Anisotropic Substrates," *Appl. Phys. Lett.* **19**, 187.
- Wang, S., J. D. Crow, S. L. Wong, and M. Shah, 1973, "Eigen-Mode Analysis of Wave propagation in Optical Waveguides Deposited on Gyrotropic and Anisotropic Substrates," *J. Appl. Phys.* **44**, 3232.
- Wang, S., M. Shah, and J. D. Crow, 1972, "Wave propagation in Thin-Film Optical Waveguides Using Gyrotropic and Anisotropic Materials as Substrates," *IEEE J. Quantum Electron.* **QE-8**, 212.
- Wang, S., M. Shah, and J. D. Crow, 1972, "Studies of the Use of Gyrotropic and Anisotropic Materials for Mode Conversion in Thin-Film Optical Waveguide Applications," *J. Appl. Phys.* **43**, 1861.
- Wang, S., and S. Sheem, 1973, "Two-Dimensional Distributed-Feedback Lasers and Their Applications," presented at Mid-Winter Solid-State Research Conference, Newport Beach, California, Jan. 22-26, 1973.
- Wang, S., and S. Sheem, 1973, "Two-Dimensional Distributed-Feedback Lasers and Their Applications," *Appl. Phys. Lett.* **22**, 460.
- Wang, S., and W. T. Tsang, 1974, "Analysis of Ring Distributed Feedback Lasers," *J. Appl. Phys.* **45**, 3978.
- Warner, J., 1973, "Faraday Optical Isolator/Gyrator Design in Planar Dielectric Waveguide Form," *IEEE Trans. Microwave Theory Tech.* **21**, 12.
- Warner, J., 1974, "Excitation of Hybrid Modes in Magneto-optical Waveguides," *Appl. Opt.* **13**, 1001.
- Warner, J., 1975, "Nonreciprocal Magneto-optic Waveguides," *IEEE Trans. Microwave Theory Tech.* **23**, 70.
- Weber, H. P., F. A. Dunn, and W. N. Leibolt, 1973, "Loss Measurements in Thin-Film Optical Waveguides," *Appl. Opt.* **12**, 755.
- Weber, H. P., R. Ulrich, E. A. Chandross, and W. J. Tomlinson, 1972, "Light-Guiding Structures of Photoresist Films," *Appl. Phys. Lett.* **20**, 143.
- Webster, J. C., and F. Zernike, 1975, "Push-Pull Thin-Film Optical Modulator," *Appl. Phys. Lett.* **26**, 465.
- Wei, D. T. Y., W. W. Lee, and L. R. Bloom, 1973, "Quartz Optical Waveguide by Ion Implantation," *Appl. Phys. Lett.* **22**, 5.
- Wei, D. T. Y., W. W. Lee, and L. R. Bloom, 1975, "Large Refractive Index Change Induced by Ion Implantation in Lithium Niobate," *Appl. Phys. Lett.* **25**, 329.
- Wei, J., S. J. Ingrey, W. D. Westwood, and S. Kos, 1976, "Accurate Phase Matching in Sputtered Birefringent Ta₂O₅N_x Waveguides," *Appl. Phys. Lett.* **28**, 317.
- Weller, J. F., and T. G. Giallorenzi, 1975, "Effects of Thin Film Overlays in Indiffused Waveguides," *Appl. Opt.* **14**, 2329.
- Wemple, S. H., J. R. Dillon, Jr., L. G. Van Uitert, and W. H. Grodkiewicz, 1973, "Iron Garnet Crystals for Magneto-optic Light Modulators at 1.06 μm," *Appl. Phys. Lett.* **22**, 331.
- Westwood, W. D., and S. J. Ingrey, 1975, "Sputtered ZnO Optical Waveguides," *Wave Electronics* **1**, 139.
- Wilson, L. O., and F. K. Reinhart, 1974, "Phase Modulation Nonlinearity of Double-Heterostructure p-n Junction Diode Light Modulators," *J. Appl. Phys.* **45**, 2219.
- Wilson, M. G. F., and G. A. Teh, 1973, "Improved Tolerance in Optical Directional Couplers," *Electron. Lett.* **9**, 453.
- Wilson, M. G. F., and G. A. Teh, 1975, "Tapered Directional Coupler," *IEEE Trans. Microwave Theory Tech.* **23**, 85.
- Winn, R. K., and J. H. Harris, 1975, "Coupling from Multi-mode to Single Mode Linear Waveguides Using Horn-Shaped Structures," *IEEE Trans. Microwave Theory Tech.* **23**, 92.
- Wittke, J. P., 1972, "Thin-Film Lasers," *RCA Rev. (Radio Corp. Am.)* **33**, 674.
- Wolfe, C. M., G. E. Stillman, and I. Melngailis, 1974, "Epitaxial Growth of In_xGa_{1-x}As Waveguide Detectors for Integrated Optics," *J. Electrochem. Soc.* **121**, 1507.
- Wolfe, C. M., G. E. Stillman, and I. Melngailis, 1974, "Epitaxial Growth of InGaAs-GaAs for Integrated Optics," in *Digest of Technical Papers, Topical Meeting on Integrated Optics, Jan. 21-24, 1974, New Orleans, La. (Opt. Soc. Am.)*, paper MA8.
- Wright, S., and M. G. F. Wilson, 1973, "New Form of Electrooptic Deflector," *Electron. Lett.* **9**, 169.

- Yajima, H., 1973, "Dielectric Thin-Film Optical Branching Waveguides," *Appl. Phys. Lett.* **22**, 647.
- Yamamoto, Y., T. Kamiya, and H. Yanai, 1975, "Propagation Characteristics of a Partial Metal-Clad Optical Guide: Metal-Clad Optical stripline," *Appl. Opt.* **14**, 322.
- Yamanouchi, K., K. Higuchi, and H. F. Budd, 1976, "TE-TM Mode Conversion by Interaction between Elastic Surface Waves and a Laser Beam on a Metal-Diffused Optical Waveguide," *Appl. Phys. Lett.* **28**, 75.
- Yanai, H., M. Yano, and T. Kamiya, 1975, "Direct Modulation of a DH Laser Using a Schottky-Barrier-Gate Gunn Effect Digital Device," *IEEE J. Quantum Electron.* **11**, Part II, 519.
- Yang, L., and J. M. Ballantyne, 1974, "Epitaxial Growth over Optical Grating on GaAs," *Appl. Phys. Lett.* **25**, 67.
- Yariv, A., 1958, "On the Coupling Coefficients in the Coupled Mode Theory," *Proc. IRE* **46**, 1956.
- Yariv, A., 1972, "Components for Integrated Optics," *Laser Focus* **40**, Dec.
- Yariv, A., 1973, "Coupled Mode Theory for Guided Wave Optics," *IEEE J. Quantum Electron.* **QE-9**, 919.
- Yariv, A., 1974, "Active Integrated Optics," in *Proceedings of the 1971 Esfahan Conference on Pure and Applied Physics* (Wiley, New York).
- Yariv, A., 1976, "Three-Dimensional Pictorial Transmission in Optical Fibers," *Appl. Phys. Lett.* **28**, 88.
- Yariv, A., 1976, "On Transmission and Recovery of Three-Dimensional Image Information in Optical Waveguides," *J. Opt. Soc. Am.* **66**, 301.
- Yariv, A., and W. M. Caton, 1974, "Frequency, Intensity and Field Fluctuations in Laser Oscillators," *IEEE J. Quantum Electron.* **QE-10**, 509.
- Yariv, A., and A. Gover, 1975, "Equivalence of the Coupled-Mode and Floquet-Bloch Formalisms in Periodic Optical Waveguides," *Appl. Phys. Lett.* **26**, 537.
- Yariv, A., and R. C. C. Leite, 1963, "Dielectric-Waveguide Mode of Light Propagation in *p-n* Junction," *Appl. Phys. Lett.* **2**, 55.
- Yariv, A., and H. W. Yen, 1974, "Bragg Amplification and Oscillation in Periodic Optical Media," *Opt. Commun.* **10**, 120.
- Yen, H. W., M. Nakamura, E. Garmire, S. Somekh, and A. Yariv, 1973, "Optically Pumped GaAs Waveguide Lasers with a Fundamental 0.1 μ Corrugation Feedback," *Opt. Commun.* **9**, 35.
- Yen, H. W., W. Ng, I. Samid, and A. Yariv, 1976, "GaAs Distributed Bragg Reflector Lasers," *Opt. Commun.* **17**, 213.
- Zemon, S., R. R. Alfano, S. L. Shapiro, and E. Conwell, 1972, "High Power Effects in Nonlinear Optical Waveguides," *Appl. Phys. Lett.* **21**, 327.
- Zory, P. S., 1972, "Leaky Wave Thin Film Laser," *Integrated Optics Conference—Digest of Technical Papers*, Las Vegas, Nevada, 1972.
- Zory, P., 1973, "Laser Oscillation in Corrugated Optical Waveguides," *Appl. Phys. Lett.* **22**, 125.
- Zory, P. S., 1976, "Corrugated Grating Coupled Devices and Coupling Coefficients," *Integrated Optics Conference—Digest of Technical Papers*, Opt. Soc. Am.
- Zory, P. S., 1976, "Grating Coupled Diode Lasers," in *Proceedings of the 1976 Electrooptics/Laser Conference*, to be published.
- Zory, P. S., and L. D. Comerford, 1975, "Grating Coupled Double-Heterostructure AlGaAs Diode Lasers," *IEEE J. Quantum Electron.* **11**, 451.
- Zucker, J., R. B. Lauer, and J. Schlafer, 1976, "Response Time of Ge-Doped (AlGa)As-GaAs Double Heterostructure LED's," *J. Appl. Phys.* **47**, 2082.

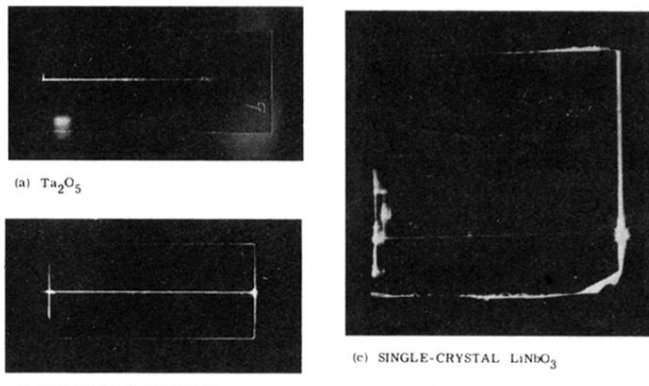


FIG. 1. Photographs (a), (b), and (c) show light wave propagation observed in a Ta_2O_5 , a vinyltrimethylsilane, and a single-crystal LiNbO_3 film waveguide. The losses in these waveguides are 1, 0.1, and 1 dB/cm, respectively.

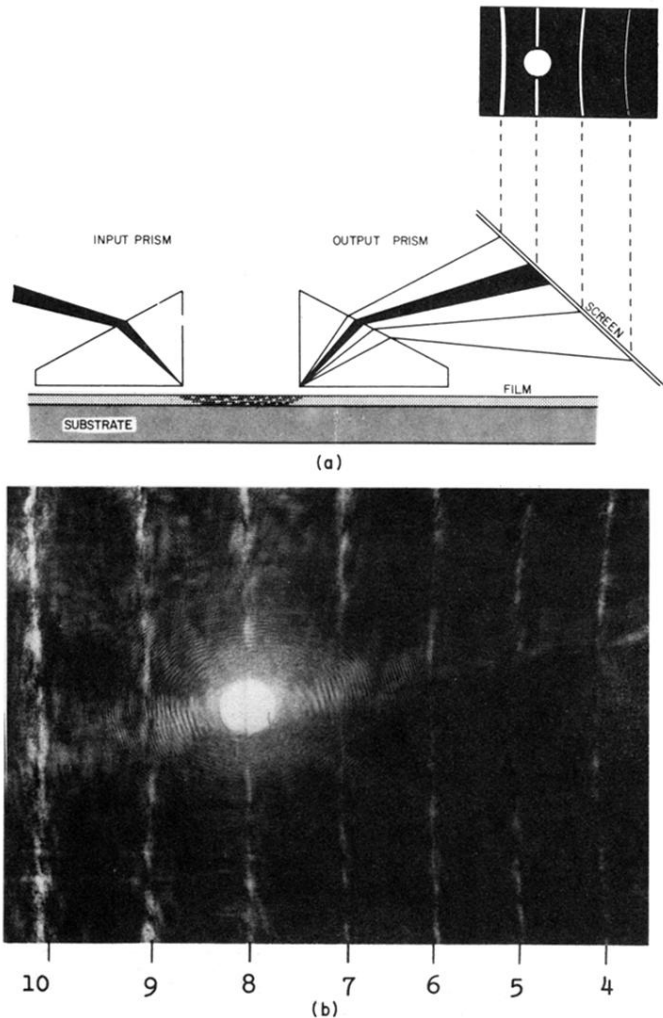


FIG. 12. (a) illustrates the experimental arrangement used in observing m lines, and (b) is a photograph of the m lines observed in a ZnO/glass waveguide. Each m line shown in this photograph represents one waveguide mode. The numbers at the bottom of this photograph indicate the orders of the modes (Tien, Ulrich, and Martin, 1969).

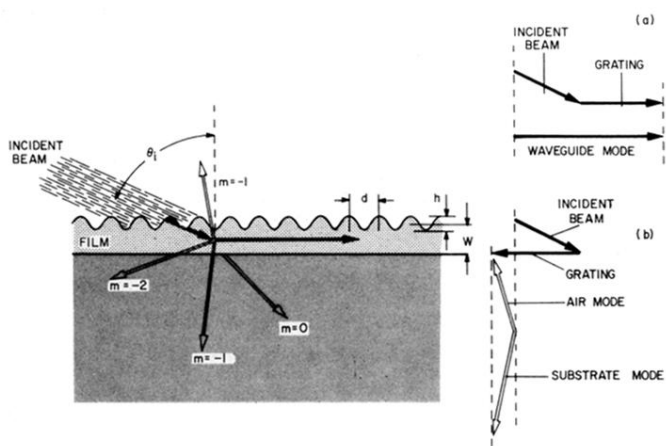


FIG. 13. The figure at the left shows how a grating can diffract an incident wave into many orders. A zigzag wave and thus a "waveguide" mode is excited in a waveguide only if one of the diffraction orders is in phase with the zigzag wave. The diagram in (a) shows the vector relation required for such a grating coupler. On the other hand, other diffraction orders of the grating could match the phases of the "substrate" or "airspace" modes and thus introduce losses to the coupling by diverting part of the incident energy into radiations in substrate or air-space.

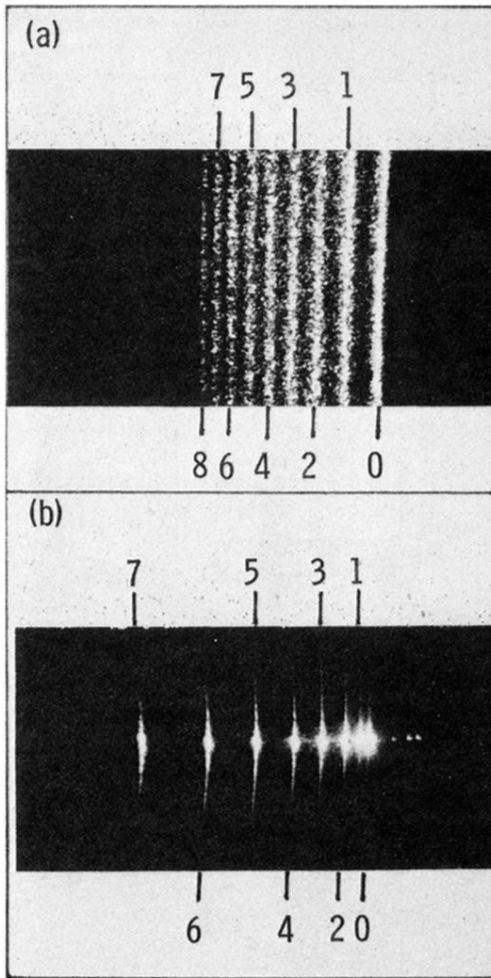


FIG. 15. The photographs in this figure show the m lines observed in (a) a "graded" waveguide, and (b) a "uniform" waveguide, and the numbers indicate orders of the waveguide modes. Interestingly, the spacings of the m lines in a "graded" waveguide decrease with the mode order, m , whereas those of a "uniform" waveguide increase with m . (Tien, Riva-Sanseverino, Martin, Ballman, and Brown, 1974).

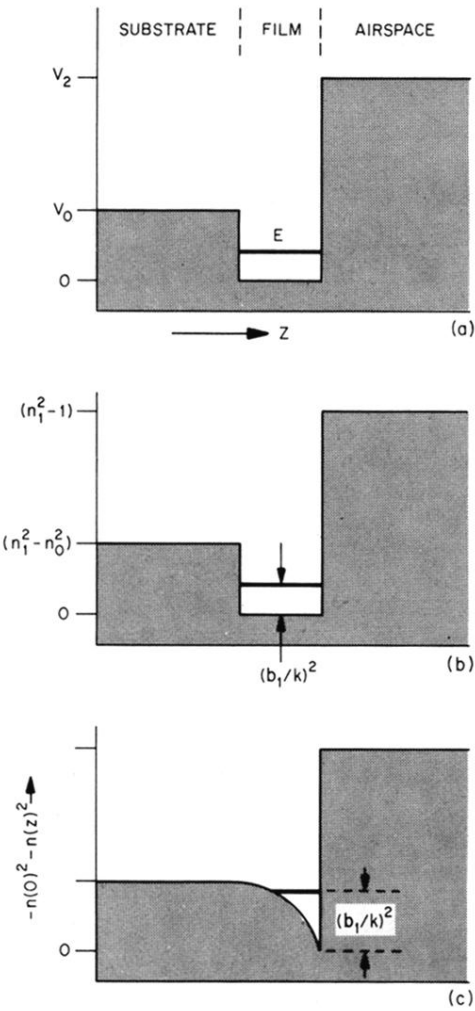


FIG. 16. As far as the field distribution is considered, a light wave in a waveguide may be analyzed as an electron trapped in a potential well. The diagram in (a) shows the usual potential energy distribution and an energy level E of an electron in a square potential well. The diagrams in (b) and (c) show, respectively, the similar distributions of $n^2(0)-n^2(z)$ in a "uniform" and a "graded" waveguide. Using this model, the eigenvalue of the waveguide mode corresponds to the energy level of the electron.

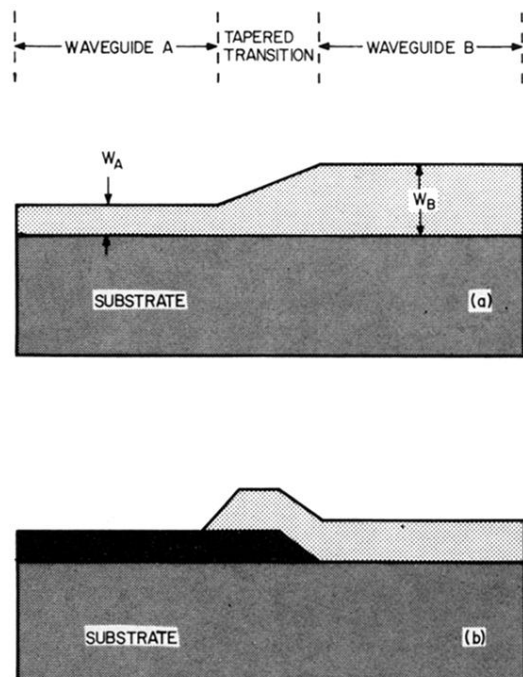


FIG. 17. The schematic drawings in this figure show examples of tapered transitions: In (a), a tapered transition joins smoothly two waveguides of different thicknesses, and in (b), the transition is formed by overlapping the ends of two waveguides. A tapered transition should have a structure which varies slowly in space as compared with the optical wavelength, and which must have a refractive index larger than the substrate.

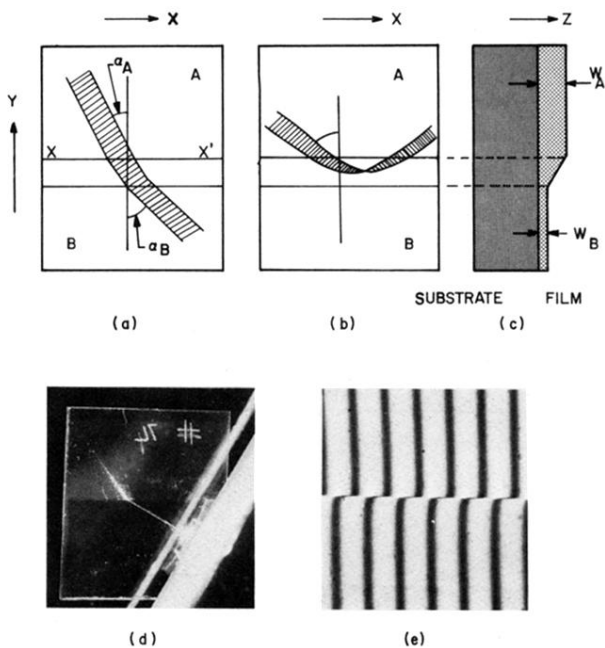


FIG. 18. The diagrams (a) and (b) illustrate refraction and total reflection of light observed between two film-waveguides, *A* and *B*. The side view of the waveguides used in this observation is shown in (c). In the experiment discussed in the text, a ZnS/glass waveguide was used for *A* and a polystyrene/glass waveguide for *B*. A photograph of the experimental observation is shown in (d). The photograph in (e) was taken under a Leitz interference microscope. The large shift in the interference fringes observed in this photograph at the junction of the waveguides *A* and *B* indicates that the two waveguides have widely different mode indices (P. K. Tien, and R. J. Martin, unpublished work).

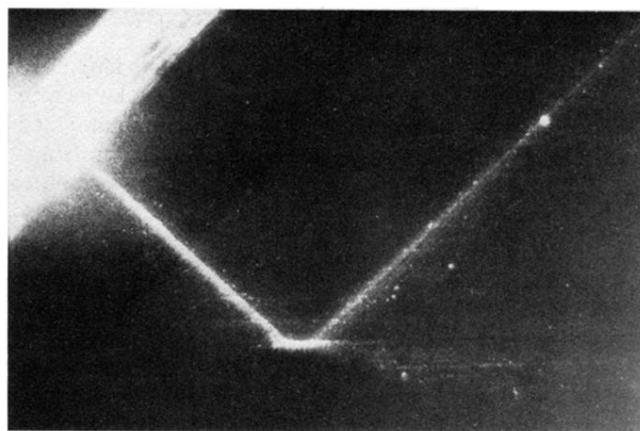


FIG. 19. The photograph shows an unusually large Goos-Häenchen's shift observed at the tapered edge of a film waveguide. In this photograph, the fine dark horizontal line is the tapered edge of the film, at which, the light wave shown is totally reflected (P. K. Tien and R. J. Martin, unpublished work).

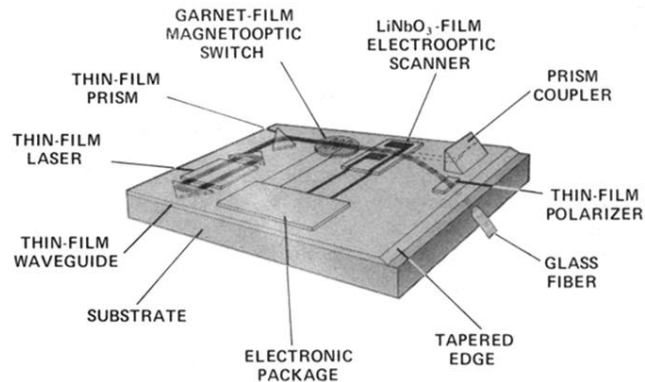


FIG. 2. Historically, we thought an integrated optical circuit should contain all sorts of optical devices such as the one shown above. The devices are made of thin films and they are interconnected by thin-film waveguides. However, as integrated optics developed, we realized that such circuits are difficult to fabricate. We now believe that a circuit should have only two or three different kinds of devices, although we can have a large number of them in each kind. For example, a circuit containing a large number of laser diodes and waveguides can satisfy most of our needs.

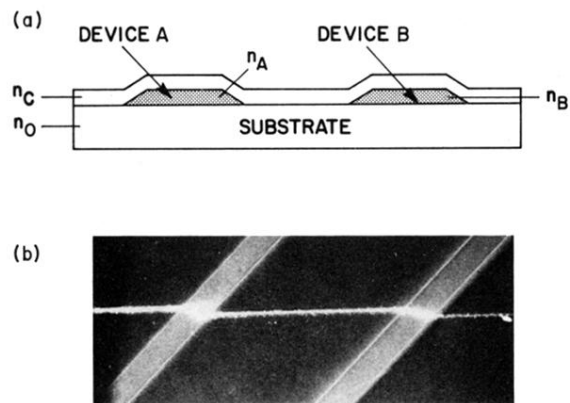


FIG. 20. The diagram in (a) illustrates two-layered construction. In this method, one first forms devices *A* and *B* on a substrate, which are then covered by film *C*. In the experiment described in the text, devices *A* and *B* are the two diagonal ZnS strips shown in the photograph in (b). The light wave propagated, from left to right, in the following order: first in film *C*, next in ZnS strip, then in film *C* again, in the second ZnS strip, and finally in Film *C*. In this case, film *C* is used for the interconnection between *A* and *B* as well as their input and output terminals (Tien, Riva-Sanseverino, Martin, and Smolinsky, 1974).

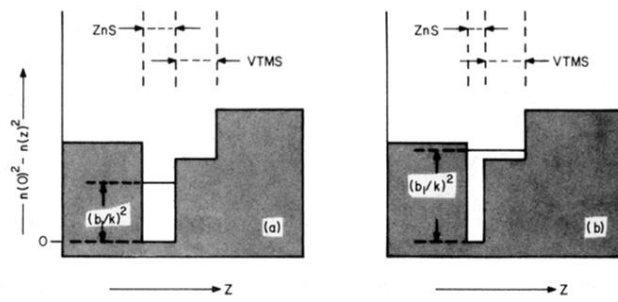


FIG. 21. The composite waveguide discussed in the text has two light-guiding films, a VTMS film and a ZnS film. Such a waveguide may be analyzed as two potential wells standing side by side. The diagram in (a) shows the case that the light wave is completely trapped in the ZnS film, whereas the diagram in (b) corresponds to the case that the light energy spreads over evenly in both films.

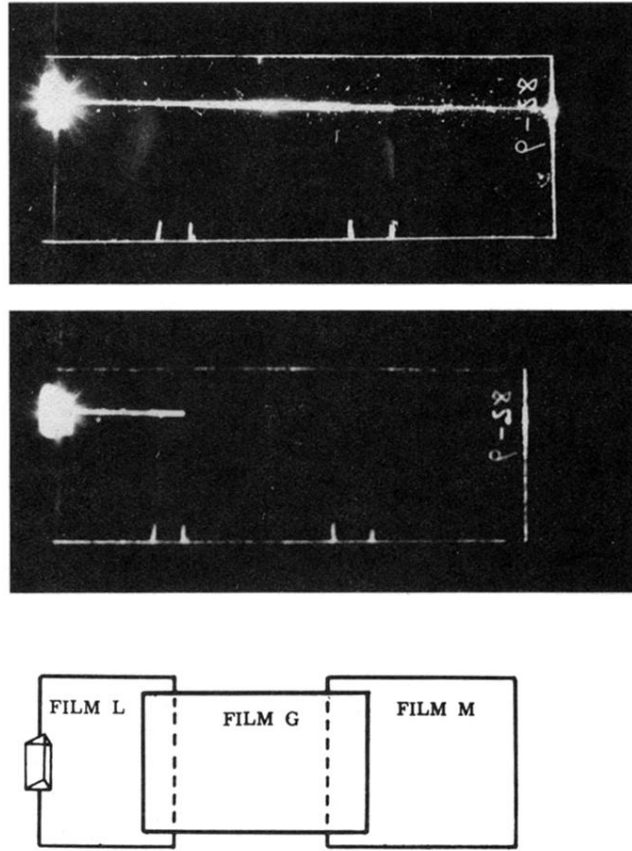


FIG. 23. The two top photographs were taken in an experiment used to demonstrate the interconnection method illustrated in Fig. 22. The bottom diagram shows the arrangement of films L , G , and M used in this experiment. Both films L and M can carry TE $m=0$ and $m=1$ modes, but the TE $m=1$ mode is cut-off in film G . The top photograph shows that a light wave excited in film L in the TE $m=0$ mode proceeded smoothly from L to G and to M indicating that this method of interconnection worked perfectly. In the lower photograph, the light beam stopped abruptly at film G , indicating that there was no mode conversion in the tapered transition. Otherwise, the converted light would have gone through and would have appeared as a faint beam in G and M . (Tien, Martin, and Smolinsky, 1973).

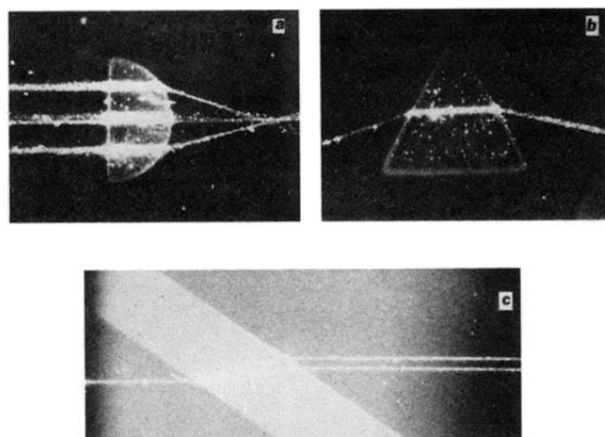


FIG. 24. Photographs in (a), (b), and (c) show, respectively, a thin-film lens, a thin-film prism, and a thin-film polarizer made in two-layered construction (Tien, Riva-Sanseverino, Martin, and Smolinsky, 1974).

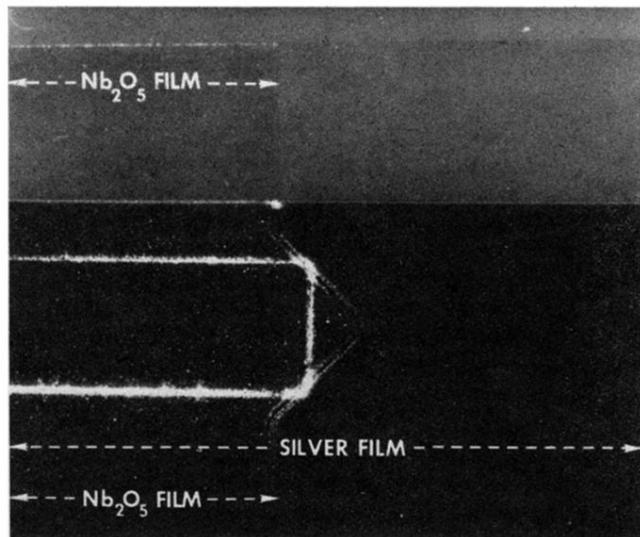


FIG. 25. The advantage of the metal-clad optical components is that they can be formed on any substrate. The above photograph shows a thin-film corner-reflector which has the structure of a silver-clad Nb_2O_5 waveguide (Tien, Martin, and Riva-Sanseverino, 1975).

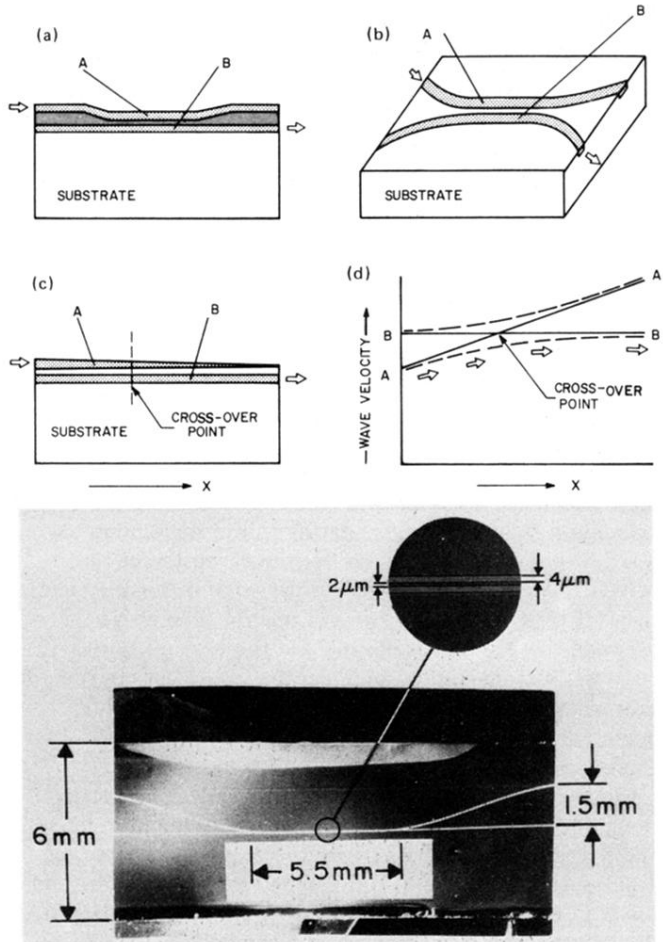


FIG. 26. Figures (a) and (b) illustrate directional couplers made from film-waveguides and from channel waveguides. Figures (c) and (d) show the tapered-velocity coupler discussed in the text. We have plotted, in (d), wave velocities of the two wave guides *A* and *B*, versus distance, *x*, along the waveguides. The dashed curves are the true velocities in the coupler, and the solid curves are the wave velocities, if the two waveguides are not coupled. The arrows indicate that a wave fed into waveguide *A* will be coupled to waveguide *B* in this coupler. Figure (e) is a photograph of a directional coupler made of two channel waveguides, each 4- μm wide. In the coupling region, the spacing between the two waveguides is 2 μm . This directional coupler was made by R. D. Standley and V. Ramaswamy by diffusing Ti into LiNbO_3 (1976).

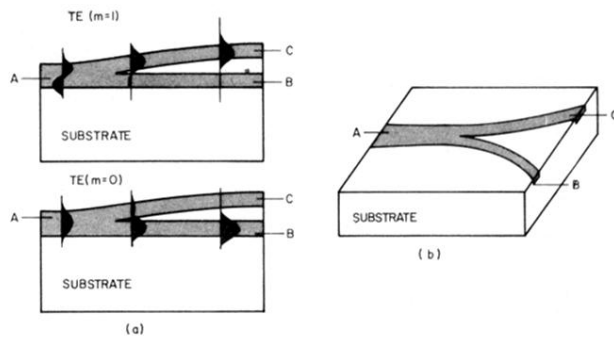


FIG. 27. The figures (a) and (b) illustrate a branching waveguide made from film waveguides, and from channel waveguides, respectively. In (a), we show that a TE $m=1$ mode excited at the input terminal A will be directed to the upper branch C , while a TE $m=0$ mode will be directed to the lower branch B . The operation of the branching waveguide depends upon the field distribution and the wave velocities of the input and branch waveguides at the branching point.

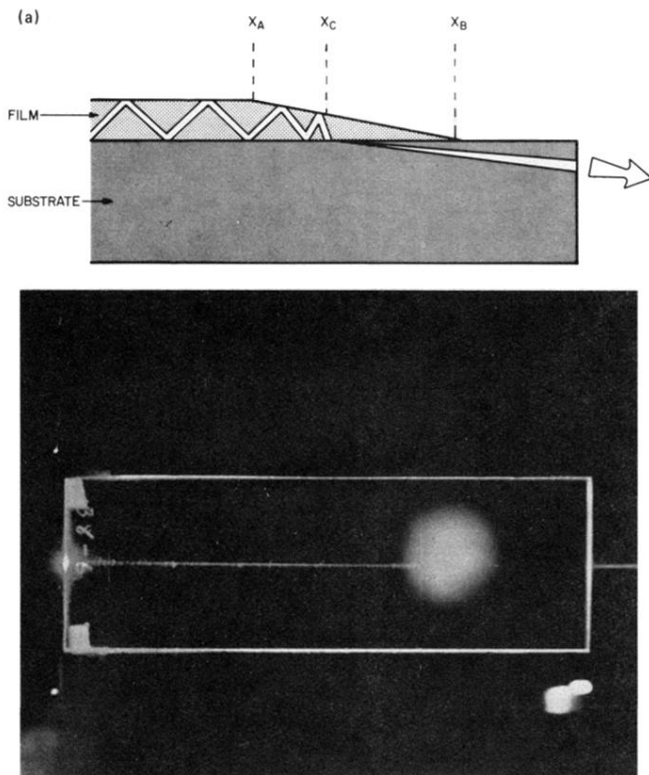


FIG. 28. To explain physics of the tapered film coupler, we should look at the up-down motion of the zigzag wave in the $x-z$ plane of the coupler. In (a), we show that a zigzag wave enters into the tapered edge of the film ($X_A \rightarrow X_B$). The zigzag angle of the wave becomes smaller and smaller, and eventually, at point X_c , the angle becomes smaller than the critical angle at the film-substrate interface. The light wave then can no longer be totally reflected at the interface, and instead, enters into the substrate. The photograph in (b) shows an experimental demonstration of the coupler. A light beam in a ZnS film was coupled into a glass substrate at a tapered edge and then through the substrate entered into outside space. Note that the glass substrate did not scatter the light; the light beam became totally invisible, once it entered into the substrate. The circular spot light shown near the center of this photograph was used in order to make the tapered edge of the film visible (Tien and Martin, 1970).

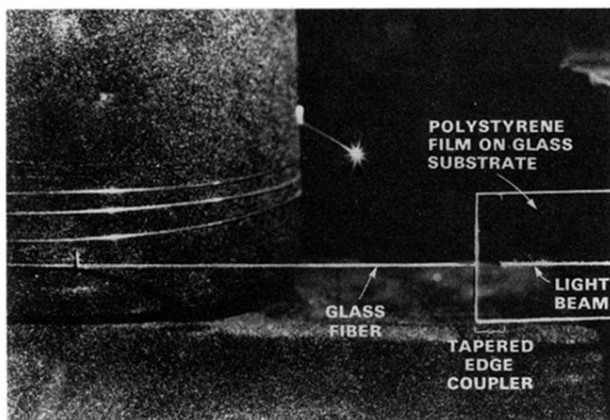


FIG. 29. In the experiment shown in the above photograph, a light beam in a polystyrene/glass waveguide was coupled into the substrate through a tapered edge of the film. The radiation in the substrate was then intercepted by a glass fiber. This film to fiber coupler had a coupling efficiency better than 90% (Tien, Smolinsky, and Martin, 1975).

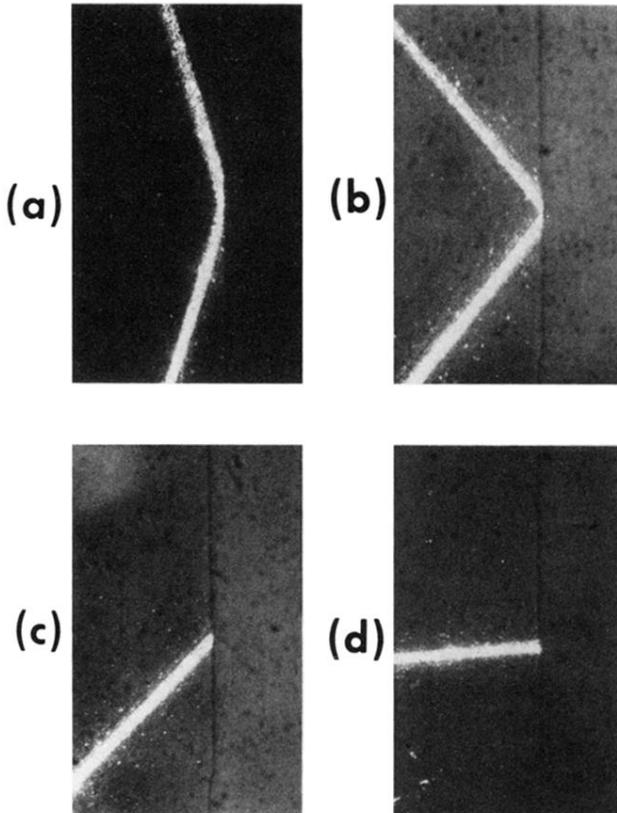


FIG. 30. A series of photographs shows experiments of refraction and reflection of light at a tapered edge of a ZnS/glass waveguide. The tapered edge appears in these photographs as a dark vertical line. In the area at the left of this edge, there was a uniform ZnS film, and at the right of this edge, it was a bare glass substrate surface. We are showing here the light paths in the $x-y$ plane of the film. The light wave was launched in the waveguide from left to right toward the tapered edge. It may be seen that the light beam was either totally reflected as in (a) and (b) or refracted into the substrate as in (c) and (d). Of course, the light beam became invisible inside the substrate which did not scatter the light. The incident angle α_i in the plane of the film was 75° , 53° , 47° , and 3° , respectively, in (a), (b), (c), and (d). The critical angle at the ZnS/glass interface was 49.5° (Tien and Martin, 1970).

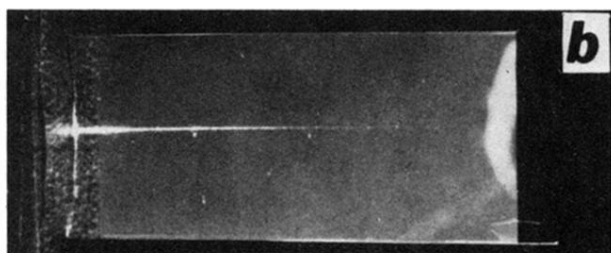
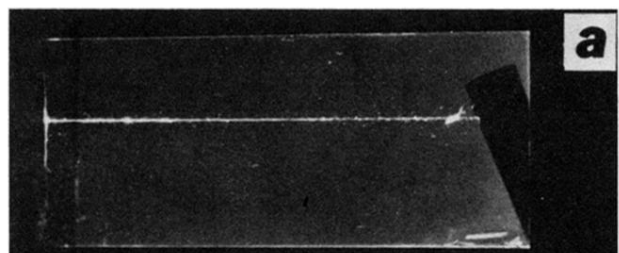


FIG. 31. Photographs (a) and (b) show light wave propagation in a silver-clad and in an aluminum-clad polystyrene waveguide. In such photographs, a short light path means a large loss in the waveguide (Tien, Martin, and Riva-Sanseverino, 1975).

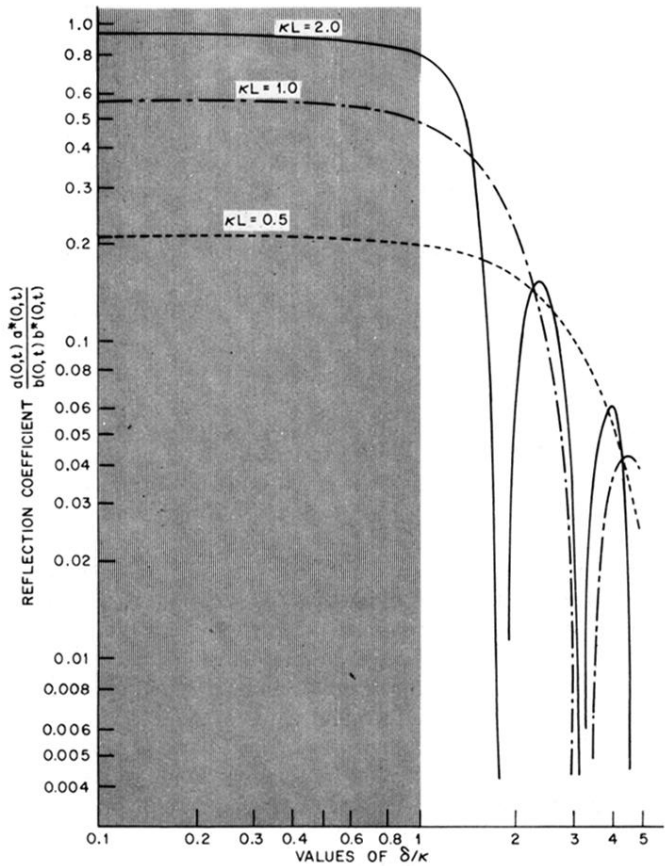


FIG. 34. In a corrugated waveguide, the reflection is maximum at the Bragg condition. The above diagram shows how the reflection coefficient varies as we move away from this condition. The curves are plotted versus δ/k for $\kappa L = 0.5, 1.0$, and 2.0 , where κ is the coupling constant, and δ is the deviation (in phase constant) from the Bragg condition. The shaded area is the stop band.

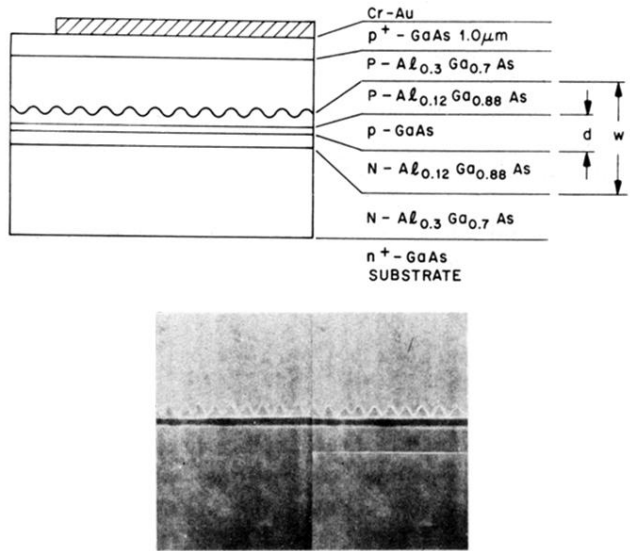


FIG. 41. The top figure shows an $N_x-N_y-p-P_y-P_x$ DFB structure which allows separate confinement of the optical wave and the carriers. The carriers are confined in the region d , which is the p -GaAs active layer. The optical wave is confined in the region W , which consists of the N_y , p , and P_y layers. The photograph below is a SEM micrograph of the structure (Ilegems, Casey, Somekh, and Panish, 1975).

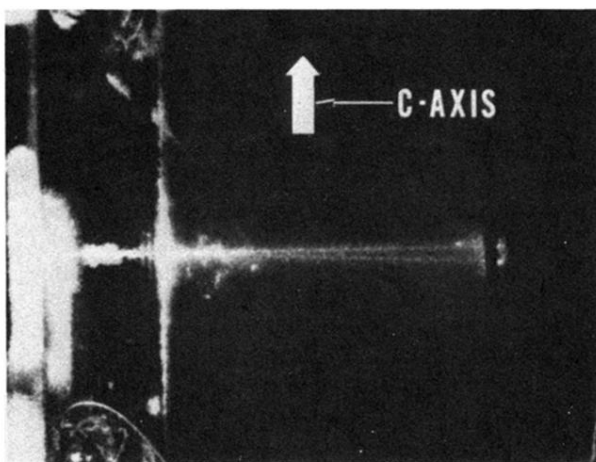
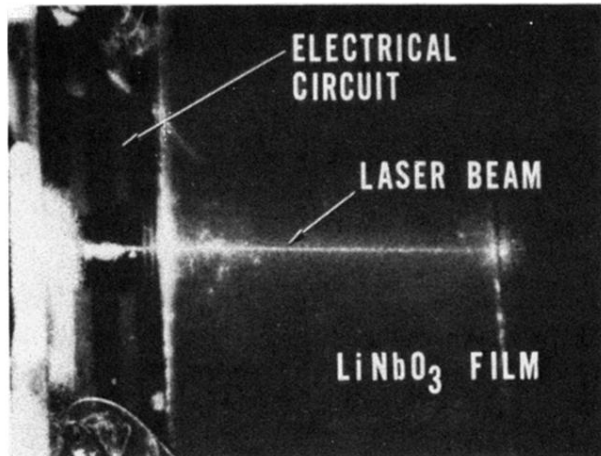


FIG. 46. The photographs show the operation of a LiNbO_3 light beam scanner. In the top photograph, the voltage on the circuit was zero, and in (b), an ac voltage was applied to the circuit. It was possible to scan a light beam in the LiNbO_3 waveguide over an angle of 6° covering roughly 10 resolvable beam spots (Tien, Riva-Sanseverino, and Ballman, 1975).

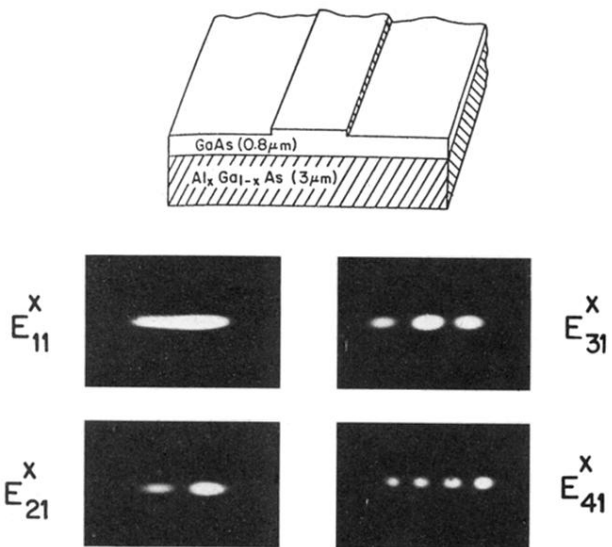


FIG. 47. The top figure shows a (Al, Ga)As rib waveguide constructed by Reinhart *et al.* (1974) using an anodization-etching process. The photographs below are mode patterns observed in this waveguide.

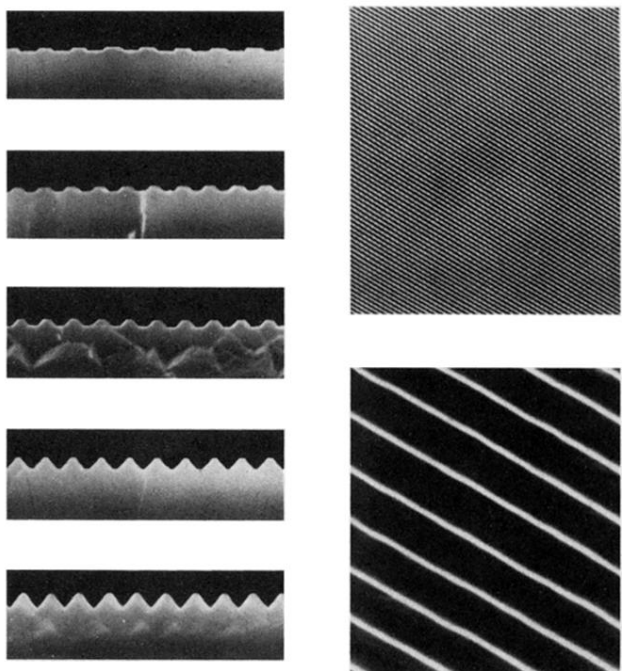


FIG. 48. The SEM photographs in this figure show the gratings formed by preferential etching in a $\text{H}_2\text{SO}_4-\text{H}_2\text{O}_2-\text{H}_2\text{O}$ system on a (100) surface of GaAs. The corrugations have a periodicity of about 5200 Å and are aligned along the $[0\bar{1}\bar{1}]$ direction. The photographs at the left (from top to bottom) show the profiles of the gratings as the etching time was gradually increased, and those at the right are top views of the gratings (Tsang and Wang, 1976).

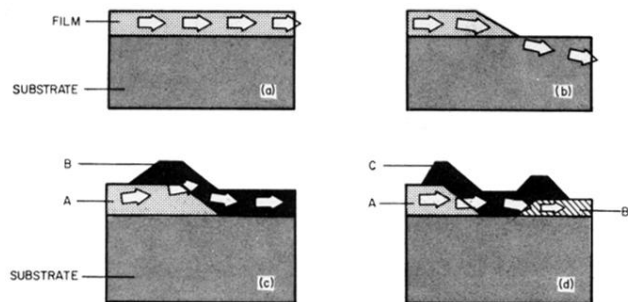


FIG. 5. It is possible to explain light wave propagation in (a) a film waveguide; (b) a tapered-film light-wave coupler; (c) a junction between two waveguides and (d) an interconnection C between devices A and B by a simple rule of refractive index.

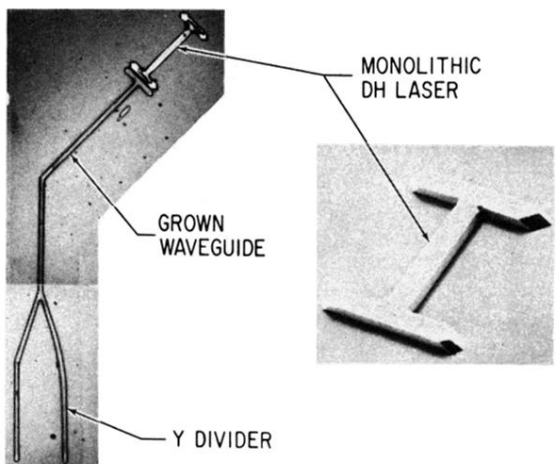


FIG. 50. An *I*-bar laser, a waveguide, and a *Y* divider shown in this figure were grown by liquid-phase epitaxy using a silicon nitride mask. Interestingly, these components had grown vertical facets at the two ends which were used for coupling light from one component to another (Bellavance and Campbell, 1976).

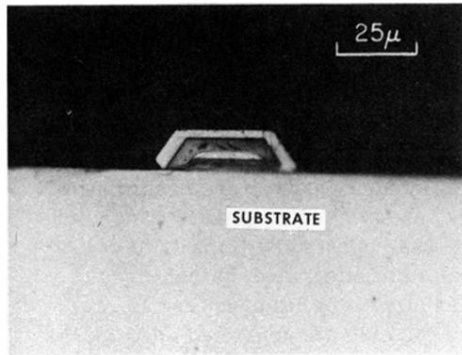


FIG. 51. The SEM photograph shows a cross section view of a mesa structure grown selectively through an opening in an Al_2O_3 mask on a (100) GaAs substrate. Interestingly, in this structure, the layers grown first were covered entirely by the layer grown later. For this reason, this technique is called "embedded epitaxy" (Samid *et al.* 1975).

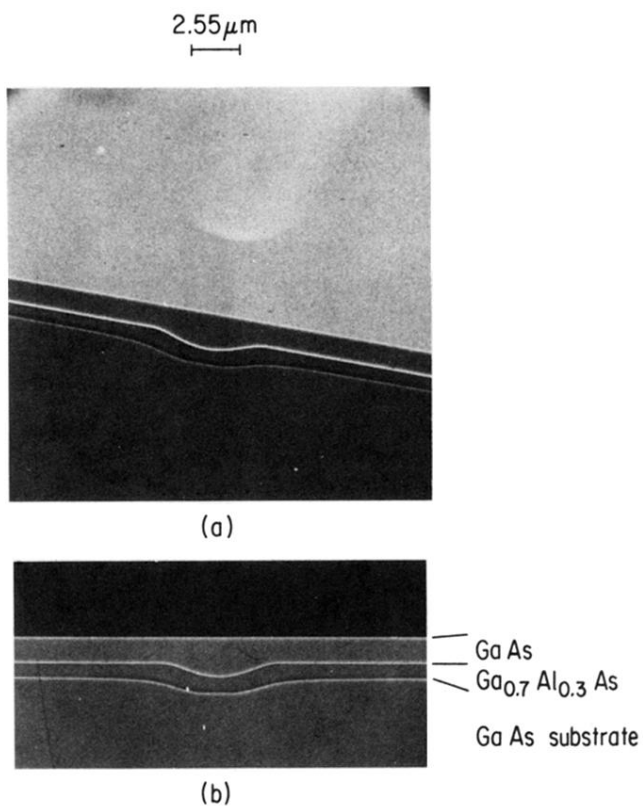


FIG. 52. SEM photographs of (a) the titled top view and (b) the side view of an inverted ridge waveguide fabricated by the "etch and fill" technique (Tsang and Wang, 1976).

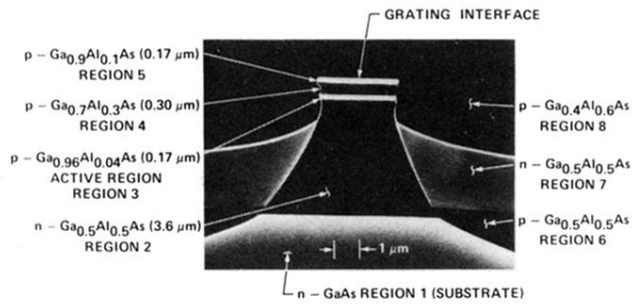


FIG. 54. The SEM photograph shows the cross section of a "buried" DFB laser constructed by Burnham *et al.* (1974). The laser has a $n-P$ junction for the active region at the center, and a $n-P-N-P$ structure in the surrounding area. The $n-P-N-P$ structure which is reversely biased during the operation, prevents the carriers and the pumping current from entering outside the active region.

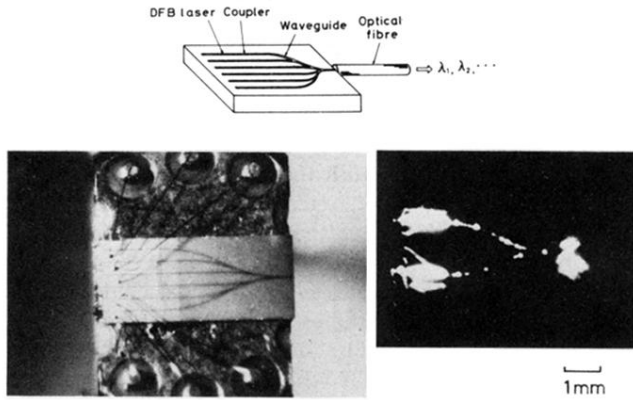


FIG. 55. The top figure is a schematic drawing of a monolithic integrated optical circuit reported by Aiki *et al.* (1976). The circuit contains six laser diodes connected to six channel waveguides forming a "frequency multiplexing light source." The figure at the lower left is a photograph of the circuit, and that at the lower right shows two of the six laser diodes being in operation. The circuit was fabricated by mesa-etching and two-step liquid-phase growth. It is the most advanced integrated optical circuit which has been reported so far.

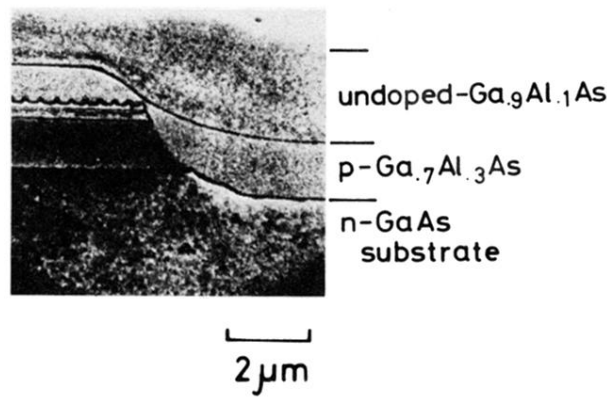
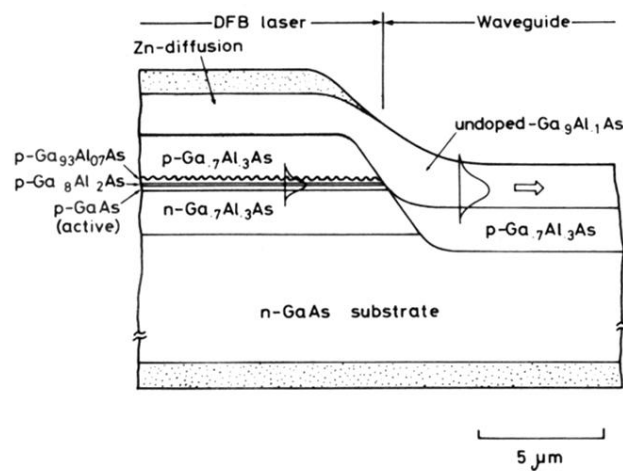


FIG. 56. The top schematic drawing and the lower SEM photograph show how light from a laser was coupled to a channel waveguide in the monolithic integrated optical circuit reported by Aiki *et al.* (1976).

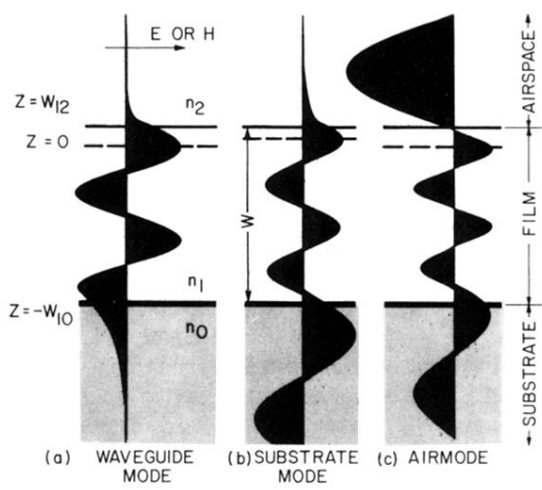


FIG. 6. Electric field distribution of a TE wave in (a) a "wave-guide" mode; (b) a "substrate" mode; and (c) an "airspace" mode.

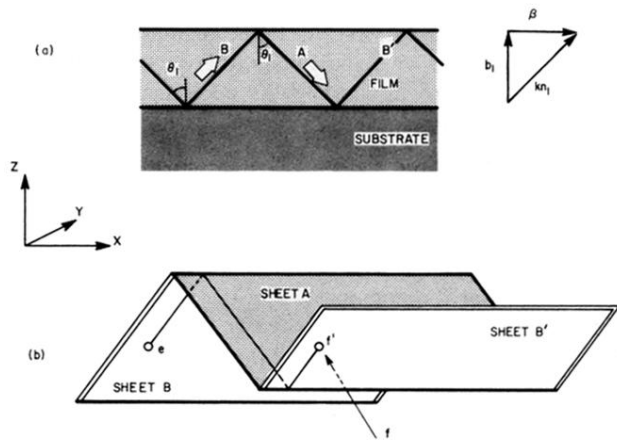


FIG. 7. In the zigzag-wave model, we use rays B, A, B', \dots , to represent waves in a waveguide. Hence, the zigzag ray shown in (a) is equivalent to the plane wave shown in (b). We can visualize, in this model, a sheet of the plane wave B which folds into sheet A at the upper film boundary, then into sheet B' at the lower film boundary and so on.